Modeling of mountain snow and ice water resources at the human-environment system interface

Doctoral thesis

submitted to the
Faculty of Geo- and Atmospheric Sciences
of the
University of Innsbruck

in partial fulfillment of the requirements for the degree of
Doctor of Philosophy

by
Florian Hanzer

Supervised by
Prof. Ulrich Strasser

June 2017

Abstract

Snow and ice water resources stored in the mountain regions of the world are of enormous importance for a variety of affected socioeconomic sectors, two very prominent examples being hydropower and winter tourism. While hydropower operations are dependent on the amount of winter precipitation falling as snow and the timing of the generation of snow and ice meltwater contributing to the reservoirs, the winter tourism sector is reliant on both natural snowfall and adequate conditions for producing technical snow. Hydrological model simulations allow to assess the amount and distribution of mountain water resources stored as snow and ice and their short- to long-term changes. However, when applied in coupled human-environment systems, an integrative perspective is required, i. e., the interactions between water and people must be considered.

This thesis aims at the physically based modeling of snow and ice resources in coupled human-environment systems in mountain regions. A conceptual framework defining interfaces between quantitative numerical model calculations and socioeconomic qualities lays the foundation for several modeling case studies addressing the socioeconomic systems winter tourism and hydropower in two regions of the Austrian Alps. For these studies, the fully distributed hydroclimatological model AMUNDSEN is applied.

To simulate snowmaking operations, two approaches for technical snow production are implemented in the model: one simple method which is easily transferable and applicable on the regional scale, and one very detailed approach which explicitly takes snowmaking infrastructure including technical and environmental constraints as well as human-environment interactions in terms of snow production strategies into account. Both of these approaches are applied in the Schladming region – the former to assess the effects of climate change on both natural and artificial snow conditions in the region, and the latter to simulate real-world snowmaking operations for a single ski area. The results of these studies demonstrate the skill of the coupled model in translating quantitative to qualitative data (in the form of socioeconomic in-

dicators such as the length of the ski season) and vice versa (in the form of rules when and where to produce snow).

Future hydropower potential is simulated for the glacierized region of the Ötztal Alps. A novel, generically applicable concept for systematically validating environmental models is developed and utilized to validate the model setup for past conditions. Subsequently, the impacts of 21st century climate change on snow, glaciers, and hydrological regimes in the region are investigated using state-of-the-art climate projections. The results indicate strongly receding glaciers and declining runoff volumes throughout the century, accompanied by considerable shifts in runoff regimes, and provide a basis for future hydropower management and planning in the area.

Zusammenfassung

Die in den Gebirgsregionen der Erde als Schnee und Eis gespeicherten Wasserressourcen sind von enormer Wichtigkeit für eine Reihe betroffener sozioökonomischer Bereiche. Zwei prominente Beispiele dafür sind die Wasserkraftproduktion sowie der Wintertourismus. Während die Wasserkraftproduktion aus Speicherkraftwerken von der Menge des festen Winterniederschlags sowie dem zeitlichen Ablauf der daraus folgenden Schnee- und Eisschmelze abhängt, ist der Wintertourismussektor sowohl von natürlichem Schneefall als auch von adäquaten Bedingungen zur Produktion technischen Schnees abhängig. Hydrologische Modellsimulationen erlauben die Abschätzung der Menge und räumlichen Verteilung der im Gebirge gespeicherten Schnee- und Eisressourcen sowie deren Veränderung in kurz- bis langfristigen Zeitskalen. Bei der Anwendung solcher Modelle in gekoppelten Mensch-Umwelt-Systemen ist jedoch eine integrative Perspektive notwendig, d. h. die Interaktionen zwischen Wasser und der Gesellschaft müssen berücksichtigt werden.

Diese Arbeit beschäftigt sich mit der physikalisch basierten Modellierung der Schnee- und Eisressourcen in gekoppelten Mensch-Umwelt-Systemen in Gebirgsregionen. Ein konzeptuelles Framework, welches Schnittstellen zwischen quantitativen numerischen Modellergebnissen und qualitativen sozioökonomischen Informationen definiert, stellt die Grundlage für mehrere Untersuchungen dar, die die sozioökonomischen Bereiche Wintertourismus und Wasserkraft in zwei Regionen der Österreichischen Alpen adressieren. Für diese Untersuchungen wird das vollverteilte hydroklimatologische Modell AMUNDEN angewendet.

Zur Simulation der technischen Beschneiung werden zwei Ansätze zur Schneeproduktion im Modell implementiert: ein einfacher Ansatz, welcher leicht übertragbar auf verschiedene Skigebiete ist und sich für die Anwendung auf der regionalen Skala eignet, und ein sehr detaillierter Ansatz, welcher explizit die im Skigebiet vorhandene Beschneiungsinfrastruktur sowie lokale Beschneiungsstrategien berücksichtigt. Beide dieser Ansätze werden in der Region Schladming angewendet. Während der einfachere Ansatz verwendet wird, um Klimawandelauswirkungen auf Natur- und Kun-

stschneebedingungen in der Region abzuschätzen, werden mittels des detaillierten Ansatzes die Infrastruktur und die Beschneiungspraktiken eines einzelnen Skigebiet in der Region abgebildet. Die Ergebnisse dieser Studien zeigen, dass das gekoppelte System in der Lage ist sowohl quantitative in qualitative Informationen (in der Form von sozioökonomischen Indikatoren wie der Länge der Skisaison) als auch umgekehrt (in der Form von Beschneiungsstrategien und Managementpraktiken) zu übersetzen.

Die Simulation des zukünftigen Wasserkraftpotentials wird für das vergletscherte Gebiet der Ötztaler Alpen durchgeführt. Ein neues, allgemein anwendbares Konzept zur systematischen Validierung von Umweltmodellen wird entwickelt und verwendet, um das Modellsetup für vergangene Bedingungen zu validieren. Anschließend werden die Auswirkungen des Klimawandels im 21. Jahrhunderts auf die Schneedecke, die Gletscher und die hydrologischen Regime in der Region mittels aktueller Klimaprojektionen analysiert. Die Ergebnisse, die sich stark zurückziehende Gletscher und verringerte Abflussmengen in Kombination mit deutlichen Verschiebungen in den Abflussregimen bis zum Ende des Jahrhunderts zeigen, stellen eine Basis für zukünftiges Management und Planung von Wasserkraftanlagen in der Region dar.

Acknowledgements

First and foremost I wish to express my gratitude to my supervisor Ulrich Strasser for his continuous support, motivation and encouragement throughout the years. For the confidence he placed in me, his expertise, and his enthusiasm for our common research interests I am sincerely thankful. All of this contributed greatly to this work.

A very special thanks also goes to Thomas Marke and Kristian Förster for the many inspiring discussions and the excellent and fun collaboration on many exciting topics, which I very much enjoyed.

Many thanks go to Matthias Huttenlau and Katrin Schneider for their support and contribution to providing a very pleasant working environment at alpS.

I also would like to thank Daniel Günther, Elisabeth Mair, Paul Schattan, Marcel Siegmann, Jan Schmieder, Benjamin Winter, and all other colleagues from the AHC team at the University of Innsbruck and from alpS for the always very pleasant working environment and many fruitful discussions.

The work presented in this thesis is based on my work on the projects CC-Snow, CC-Snow II, MUSICALS, MUSICALS II, hiSNOW, and HydroGeM3. Thanks to all the people who collaborated with me in these projects and who contributed to the papers that make up this thesis!

Finally, my greatest appreciation goes to my family, above all my wife Karin and my daughter Mariella for their unconditional support and patience throughout the last years. Thank you for everything!

Contents

List of Figures

List of Tables

Chapter 1

Introduction

1.1 Motivation

The mountain regions of the world are often referred to as "water towers" due to their vital role in providing freshwater to the forelands. As mountains form a natural barrier in the landscape, incoming air masses are forced to rise and cool down, triggering cloud formation and precipitation. Consequently, mountain regions feature significantly higher precipitation amounts compared to the forelands and contribute disproportionally high runoff amounts (Kaser et al., 2010; Meybeck et al., 2009; Viviroli et al., 2007; Viviroli et al., 2003). Hence, mountain water resources also have an enormous socioeconomic importance. Water is often the dominant or even only useful natural resource in mountainous areas (Wehren et al., 2010a), serving various vital societal purposes such as being used for drinking water supply, agriculture, irrigation, or energy supply.

Considerable parts of the winter precipitation amounts in mountain areas are temporarily stored in the form of snow, either being released as meltwater during spring and summer or stored for longer periods of time as firn or glacier ice. Approximately one sixth of the world's population lives in regions where the annual runoff is dominated by snow or glacier melt (Barnett et al., 2005). In the Alps, snow and glaciers are of particular importance for a range of economic sectors, two very prominent examples being hydropower and winter tourism. In Switzerland and Austria for example, 50–75 % of the total annual energy production are generated by hydropower (Lehner

et al., 2005; Wehren et al., 2010b). Major parts of this electricity are generated by storage power plants, which are used both for satisfying short-term demands during peak hours and for satisfying the generally higher electricity demands during winter by collecting snow and ice meltwater during spring and summer (Schaefli et al., 2007).

The winter tourism sector is naturally highly dependent on snow conditions. Besides the obvious reliance on natural snowfall required for winter sports activities, the importance of snowmaking has steadily increased over the past decades. While the first large-scale snowmaking systems in the Alps were installed as a reaction to a series of particularly snow-scarce winters during the mid-1980s (Jong, 2011; Pröbstl, 2006; Teich et al., 2007), the usage of snowmaking has enormously gained in importance since then. In Austria, being the country with the largest share of snowmaking facilities in the Alps (SBS, 2016), snowmaking coverage today amounts to approximately 70 % of the total slope area (WKO, 2016). This development is however far from being only an adaptation measure to declining natural snow amounts and rising temperatures. Rather, the widespread use of snowmaking nowadays is motivated by a variety of reasons such as mitigating the natural climate variability in terms of snowfall and temperature fluctuations, prolonging the ski season with respect to both the start and the end date while ensuring a continuous period of guaranteed snow reliability in between, and optimizing slope grooming operations in order to provide perfect "skiing highways" without bumps or icy or dirty parts (Dawson and Scott, 2013; Mayer et al., 2007; Pröbstl, 2006). However, snowmaking is also subject to both environmental and economical constraints. Certain air temperature and humidity conditions are a prerequisite in order for snowmaking to be efficient or possible at all, and large amounts of water and electricity are required for snowmaking operations. This translates into considerable costs – for an average mid-sized Austrian ski area for example, snowmaking costs amount to approximately 25 % of the annual turnover, with the shares of variable (water, electricity, gasoline, personell) and fixed (infrastructure) costs of snowmaking operations being approx. 20 and 80 %, respectively (M. Rothleitner, pers. comm., 2017).

Current and future climate change is expected to significantly alter the snow and ice resources stored in mountain regions. In the Alps, which have shown to be particularly vulnerable to climate change in the past (e. g., Beniston, 2005; Gobiet et al., 2014), further rising temperatures are expected to result in larger amounts of precipitation falling as rain instead of snow, a delayed onset of the snow-covered period, and an earlier onset of snowmelt (e. g., Frei et al., 2017; Gobiet et al., 2014; Marty et al., 2017). While a tendency of shifting precipitation amounts from summer towards winter is

projected by most climate models, this effect will likely not compensate for the rising temperatures except possibly in the very highest elevated regions (e. g., Schmucki et al., 2015b). As a consequence of less snow accumulation and accelerated melting, the European mountain glaciers will continue to lose substantial parts of their volume and area throughout the 21st century, resulting in a total glacier volume reduction in the Alps of 65–100 % by 2100 (depending on the considered emission scenario) according to several global-scale studies (Bliss et al., 2014; Huss and Hock, 2015; Marzeion et al., 2012; Radić et al., 2013).

These climatic changes will also impact the socioeconomic systems dependent on the mountain snow and ice resources. The runoff regimes of snow- and ice melt-dominated Alpine catchments will undergo significant changes: meltwater contribution of the seasonal snow cover will be reduced, resulting in increased winter low flows, declining summer runoff, and shifts of the peak flows towards earlier periods of the year (Barnett et al., 2005; Horton et al., 2006; Stewart, 2009). In glacierized regions, annual runoff might increase initially as glacier melt increases due to rising temperatures, whereas at some point a moment of "peak water" will be reached as a consequence of reduced glacier areas that are potentially available for melt, followed by an eventual decrease of total runoff (and hence reservoir inflow) volumes. Besides this overall decrease in annual inflow, the seasonal shifts in runoff – especially the strongly decreasing ice melt runoff volumes during summer – might force hydropower operators to adapt their management rules (e. g., Clarvis et al., 2014; Finger et al., 2012; Schaefli et al., 2007). In the winter tourism sector, decreasing natural snow amounts will lead to an increase in snowmaking demand, which will however be challenged by generally less favorable snowmaking conditions and shorter windows with optimal snowmaking conditions due to rising temperatures. Hence, considerable investments in snowmaking infrastructure (larger reservoirs, higher-capacity pumping and pipe systems, additional snow guns) will be required along with higher running costs due to increased energy and water consumption.

Robust model-based assessments about the amount and distribution of mountain water resources in coupled human-environment systems and their future evolution in short- to long-term time scales are hence of vital interest for both the scientific community and stakeholders of potentially affected socioeconomic sectors. In the scientific community, it is however increasingly recognized that especially for long-term predictions of hydrologic systems the human-environment system, i. e., the interactions and feedbacks between water and people, cannot be neglected but rather an integrative, inter- and transdisciplinary perspective is required. The recently established field

of socio-hydrology (Sivapalan et al., 2012) addresses such considerations. As part of the current IAHS Scientific Decade 2013–2022 "Panta Rhei" (Montanari et al., 2013), which aims at investigating change in hydrology and society, socio-hydrology seeks to understand the co-evolution of coupled human and water systems. With regard to hydropower management for example, the decision when water is stored or released is based not only on physical parameters but also depending on economic, ecologic, and legal factors and regulations and their interactions. Similarly, in ski areas snow is not always produced when the conditions allow it, but the decision when and where to produce snow is based on the interplay of many factors such as snow demand, the planned season opening and closing dates, the time of day, legal regulations, or the weather forecast.

This thesis focuses on the physically based modeling of snow and ice resources in mountain regions while presenting interfaces to and interactions with affected socioeconomic systems. An integrative framework is presented, which addresses the question on how to translate the quantitative output from the numerical model into socioeconomic qualities and vice versa, as well as how to systematically validate environmental models and the simulated key variables. Based on concrete case studies addressing the socioeconomic systems winter tourism and hydropower, a hydroclimatological model (AMUNDSEN) is then applied in two regions of the Austrian Alps for detailed simulations of snow and ice water resources under present and climate change conditions.

1.2 Modeling of mountain water resources

Klemeš (1990) has prominently described the modeling of mountain hydrology as the "ultimate challenge" of hydrological modeling, mainly due to the higher complexity of the involved processes, the difficulties in observing them, and their limited areal representativeness. The involved processes in snow-hydrological and glacio-hydrological modeling include, but are not limited to (Pomeroy et al., 1998; Strasser, 2008): snow accumulation (increasing precipitation with elevation, precipitation phase determination), short- and longwave radiative fluxes, canopy interception and sublimation, snow redistribution due to wind and gravitational forces, snow sublimation, snow metamorphosis (albedo aging, densification), energy and mass fluxes within the snowpack, turbulent exchange, glacier flow, and runoff concentration and routing. Not all of these processes are explicitly accounted for by all models – depending on the model and the application, usually some of the processes are considered only

by simple parameterizations or entirely neglected.

Generally, it can be distinguished between conceptual and physically based models. Conceptual models often use simple transfer functions to translate input data (e. g., meteorological data) to the desired output variables (e. g., runoff). They tend to be comparatively parsimonious both in terms of input data and the number of parameters, however as the parameters often have no direct physical meaning their values usually have to be determined by calibration, i. e., by tuning them until the model produces the desired output. As conceptual models are usually calibrated to optimize results for a certain period of time, their performance under changing conditions (e. g., climate change) is uncertain. With physically based models on the contrary, it is aimed to explicitly simulate individual processes by following the laws of physics such as conservation of energy, mass, and momentum. In a fully physically based model, all parameters have a physical interpretation and can, in principle, be derived from field measurements. In reality however, every physically based model necessarily includes simplifications of the considered processes to some degree, hence in practice the classification of models into conceptual or physically based comprises a continuum rather than a dichotomy.

Perhaps the most important distinction between different types of snow- and glacio-hydrological models is the approach used for snow and ice melt calculation. The simplest approach is the temperature index method (e. g., Rango and Martinec, 1995), which assumes melt rates to be linearly dependent on (positive) air temperature, essentially exploiting the fact that the most important heat sources relevant for determining snowmelt (longwave radiation, shortwave radiation, and sensible heat fluxes) are strongly correlated with air temperature (Ohmura, 2001). As this approach requires only air temperature in daily – or even monthly (e. g., Bock et al., 2016; Förster et al., 2016b) – resolution as meteorological forcing, it is very parsimonious both with respect to the number of required variables and the temporal and spatial resolution (the latter due to the comparatively easy spatial interpolation of air temperature), and hence especially suited for the application in data-sparse regions (Hock, 2003). However, the degree-day factors relating temperature to melt have to be determined by calibration, and their transferability in space and time is uncertain. Hence, their application in climate change scenario simulations is questionable. Extensions of this approach, so-called enhanced temperature index (ETI) methods, have hence been developed which for example also take incoming and/or reflected shortwave radiation into account for melt calculation (e. g., Hock, 2003; Pellicciotti et al., 2005). These models represent hybrids between the classical temperature index and the energy balance

models. Finally, the most physically based approach for ablation modeling is solving the full snow surface energy balance, by implementing parameterizations for net short- and longwave radiation, sensible and latent heat, advective energy, and soil heat fluxes (e. g., Ferguson, 1999; Strasser, 2008). Under the premise of appropriate forcing these models tend to perform best at the point scale, however the regionalization of the individual energy balance components for the application in distributed mode remains a challenge.

Another distinction between snow models can be made based on the representation of the internal snowpack structure. One class of models treats the snowpack as a single bulk layer, i. e., does not perform any vertical subdivision of the snowpack and uses empirical assumptions for calculating the temperature inside the snowpack and at its surface. On the other end of the spectrum are models which explicitly account for snowpack layering, microstructure, and metamorphism in a most detailed manner, e. g., Crocus (Vionnet et al., 2012), SNOWPACK (Lehning et al., 2002), or SNTHERM (Jordan, 1991). An additional class of models with intermediate complexity (e. g., Best et al., 2011; Essery, 2015; Shrestha et al., 2010) discretizes the snowpack in a fixed, small number of layers (typically 2–5) and applies parameterizations for internal snowpack processes.

Hence, for a given application it is essential to choose the right model for the right purpose (Strasser, 2008). Conceptual approaches such as temperature index models are particularly suited for the application in data-sparse regions, but are also commonly used for operational purposes such as short-term flood forecasting, where accurate predictions for a given target variable (e. g., snowmelt) are more important than process understanding. In this respect, these models – due to being calibrated – often perform better than more complex approaches (even if they might be right for the wrong reasons – see, e. g., Beven (1989), Kirchner (2006), and Klemeš (1982)). Energy balance models on the other hand are especially suited for long-term simulations (where the assumed stationarity of the calibration parameters might not hold true) and for applications aiming at understanding the interactions and feedbacks between individual processes.

For the simulation studies presented in this thesis, the hydroclimatological model AMUNDSEN (Strasser, 2008) is applied. AMUNDSEN is a fully distributed modeling system that includes process descriptions of varying complexity and physical basis, in terms of snowmelt calculation for example ranging from simple temperature index calculations on daily time steps, over an ETI approach operating on hourly time scales (Pellicciotti et al., 2005) and a one-layer energy balance approach (Strasser, 2008) up to

a coupled mode with a multi-layer snowpack model (Essery, 2015). AMUNDSEN has been specifically designed for the application in high mountain regions and as such aims at adequately quantifying the spatial heterogeneity of the mountain snow and ice cover while maximizing transferability and minimizing the need for calibration. It is explicitly applicable for long-term water balance simulations (years to decades), incorporating model components that aim at avoiding model artifacts and minimizing possible drift due to accumulated errors. Details on the model functionality and the considered processes can be found in chapters 3–6.

1.3 Thesis outline

The thesis is composed of five self-contained chapters, which are framed by the introductory chapter and a concluding chapter presenting a synthesis of the work and an outlook of potential future research. In the following, a short description of the contents of the main chapters is given.

Chapter 2 – Coupled component modelling for inter- and transdisciplinary climate change impact research: Dimensions of integration and examples of interface design
This chapter, which has been published in *Environmental Modelling & Software* (Strasser et al., 2014), presents the methodological framework of coupled component modeling, which provides formalized interfaces for linking scientific fields in inter- and transdisciplinary research projects. Using the example of a case study for investigation of climate change impacts on future snow conditions, economy of skiing, and regional tourism structure in Austrian ski areas, the process of building an integrative model by developing and defining the interfaces that connect the disciplinary models is explained. Furthermore, it is advocated for a "joint development" process in inter- and transdisciplinary research projects in the sense of that the integration process itself should be considered a result of the project, and that the model should be jointly developed and applied in a recursive process, thereby discovering additional aspects of the research object or reformulating the research questions. Finally, it is emphasized that the integration of stakeholder perspectives in the research process is required in order to improve case understanding and create acceptance for solutions provided as research outcomes. The interface tools developed in this chapter – *variables*, *indicators*, and *thresholds* – set the basis on which the results of the subsequent chapters are presented on.

Chapter 3 – Scenarios of Future Snow Conditions in Styria (Austrian Alps)
In this chapter, published in *Journal of Hydrometeorology* (Marke et al., 2015), climate change impacts on natural and artificial (i. e., including snowmaking) snow conditions are investigated for the Schladming region. An ensemble of four statistically downscaled and bias-corrected GCM-RCM realizations of the SRES A1B scenario is used to drive AMUNDSEN for a region encompassing the ski areas in the Schladming region and the period 1961–2050. A pragmatic top-down approach for simulating technical snow production is introduced, which relies on basic assumptions on snowmaking efficiency and requires little input data (at the very least, only the slope locations and the total number of snow guns per ski area). Results are evaluated on the basis of various indicators (number of snow cover days, snow cover duration, ski season length, snowmaking hours). Maximum decreases of > 25 snow cover days and > 35 days of ski season length are projected until 2050, with the largest decreases in medium elevations. The total number of simulated actual snowmaking hours shows no significant negative trend in the future, however rising temperatures cause a shift towards more unfavorable snowmaking conditions (i. e., less snow is be produced in the same amount of time).

Chapter 4 – Distributed, explicit modeling of technical snow production for a ski area in the Schladming region (Austrian Alps)
This chapter, published in *Cold Regions Science and Technology* (Hanzer et al., 2014), builds on the pragmatic snowmaking approach introduced in chapter 3. While the latter is, due to its simplicity and limited input data requirements, particularly suited for regional-scale applications (i. e., with several ski areas involved), it relies on several assumptions which often might not be applicable for detailed analyses of snowmaking operations in individual ski areas. In this chapter, an entirely new approach is presented, which considers snowmaking operations in a bottom-up rather than a top-down way. Specifically, it allows to consider individual snow guns, their technical specifications, and their locations along the ski slopes. The snow guns can act independently of each other and produce snow depending on the local snowmaking conditions and snow demand on the slopes. Additionally, limitations of the ski area infrastructure are considered, most importantly in terms of water availability and pumping capacity. This allows the simulation of snowmaking operations and ski area management in – until then – unprecedented level of detail and causality in terms of process interactions. As an example application, snowmaking operations are simulated for a ski area in the Schladming region. Comparison of actual recorded and

simulated daily snowmaking hours and water consumption rates for historical conditions reveal a high model skill in reproducing real-world snowmaking operations.

Chapter 5 – Multilevel spatiotemporal validation of snow/ice mass balance and runoff modeling in glacierized catchments
This chapter has been published in *The Cryosphere* (Hanzer et al., 2016) and describes the setup of AMUNDSEN for the study region of the Ötztal Alps (Austria) while introducing several new model components. As an attempt to systematically address the validation of the model and its coupled components for historical conditions, a validation concept based on the observation scale of support, spacing, and extent is introduced. Eight independent validation data sets are embedded in this framework, thereby allowing a systematic, independent, complete, and redundant model validation. The results indicate a high overall model skill and illustrate the benefits of this concept, which can serve as a guideline for systematically validating the coupled components in integrated snow-hydrological and glacio-hydrological models.

Chapter 6 – Projected cryospheric and hydrological impacts of 21st century climate change in the Ötztal Alps (Austria) simulated using a physically based approach
This chapter builds on the former one and describes the application of the AMUNDSEN model setup for the Ötztal Alps for scenario conditions (until 2100). In order to enable realistic glacier geometries in the long-term simulations, a glacier retreat parameterization (Δh approach) is added to the model. A set of in total 31 statistically downscaled and bias-corrected EURO-CORDEX climate scenarios for the emission scenarios RCP2.6, RCP4.5, and RCP8.5 is then used as meteorological forcing data for the AMUNDSEN simulations. The results indicate strong decreases in snow amounts until the end of the century with the exception of very high elevations, strongly retreating glaciers with almost complete deglacierization in the RCP8.5 scenario, and changing runoff regimes with large decreases during summer and a shift of the runoff peak from July towards June.

1.4 Study areas

Figure 1.1 shows the locations of the considered study areas within Austria including their area and elevation range. The winter tourism related modeling studies are conducted for the Schladming region, a major Austrian winter sports region in the province of Styria. The investigation of climate change impacts on future natural and

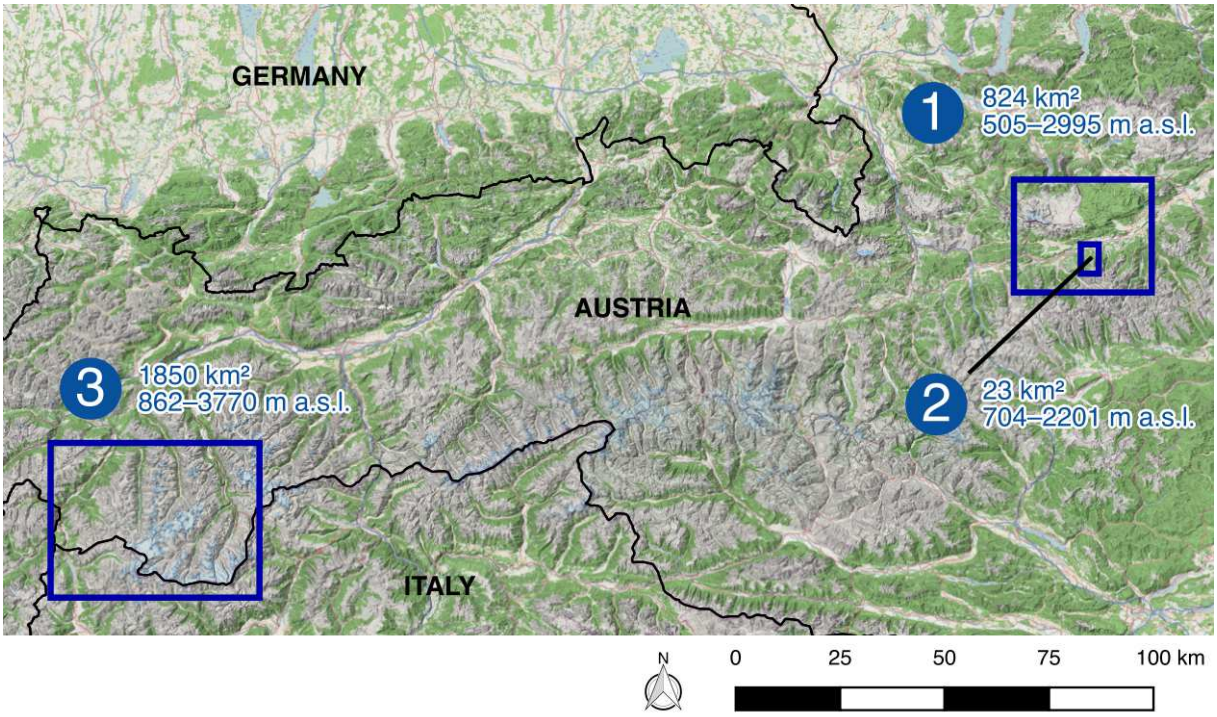

Figure 1.1: Map showing the locations of the three study areas considered for the hydroclimatological simulations presented in this thesis. Simulations for study area 1 (greater Schladming region) are carried out in chapter 3, for study area 2 (individual ski area in the Schladming region) in chapter 4, and for study area 3 (Ötztal Alps) in chapters 5 and 6.

artificial snow conditions (chapter 3) is carried out for region 1 in fig. 1.1, a 824 km^2 large area encompassing all eight ski resorts of the Schladming region, while the detailed case study on the explicit simulation of snowmaking operations (chapter 4) is carried out for one of these ski areas (region 2 in fig. 1.1). The hydropower-related studies (chapters 5 and 6) are carried out for an 1850 km^2 large area encompassing the glacierized mountain range of the Ötztal Alps within the western Austrian province of Tyrol, covering an almost 3000 m elevation range (region 3 in fig. 1.1). More detailed information on the individual study areas is found in the individual chapters.

Chapter 2

Coupled component modelling for inter- and transdisciplinary climate change impact research: Dimensions of integration and examples of interface design

Ulrich Strasser, Ulli Vilsmaier, Franz Prettenthaler, Thomas Marke, Robert Steiger, Andrea Damm, **Florian Hanzer**, Renate A. I. Wilcke, Johann Stötter

Published in *Environmental Modelling & Software* (Volume 60, October 2014, Pages 180–187, doi: 10.1016/j.envsoft.2014.06.014).

My contribution to this article: participating in the joint implementation and recursive modeling process as part of the "task force" within the CC-Snow projects, co-developing the interface tools, and implementing them in the AMUNDSEN model.

Abstract

In environmental research the importance of interfaces between the traditional knowledge fields in natural and social sciences is increasingly recognized. In coupled component modelling, the process of developing interface designs can support the communicative, social and cognitive integration between representatives of different knowledge fields. The task of integration is thereby not merely an additive procedure but has to be considered as important part of the research process. In our application, the development of a coupled component model facilitated an integrative assessment of the impact of climate change on snow conditions and skiing tourism in a typical Austrian ski resort. We elaborate the integration on two abstraction levels, a theoretical one and an applied one related to the case study. Other than model output, results presented here relate to the inter- and transdisciplinary development of the coupled component model and its interface design. We show how scientists from various disciplines and representatives from diverse societal fields jointly design interface tools. We identify joint model development – taking into consideration the different dimensions of integration – and recursive modelling as keys for successful inter- and transdisciplinary integration. Such integrative interface science can provide new insights which go beyond the sum of what can be learned from its disciplinary components.

2.1 Introduction

The orientation in science towards complex environmental phenomena has raised new challenges for researchers from various fields. These phenomena are typically characterized by dynamic interactions between humans and ecosystems. While historically environmental change has been investigated from the view of single disciplines, its complexity requires interdisciplinary research efforts. We understand interdisciplinary environmental research – after Roy et al. (2013) – as "research that involves scholars from different disciplines collaborating to develop terminology, research approaches, methodologies, or theories that are integrated across multiple disciplines". Such research requires the joint development of appropriate models and interface tools aiming at integrating quantitative and qualitative knowledge (Kalaugher et al., 2013; Kelly Letcher et al., 2013; Kragt et al., 2013).

The task of integration is further complicated when addressing societal challenges which call for transformation. Strong societal embedding of research processes becomes important in order to gain a better understanding by integrating different types of knowledge, achieved in professional practice or everyday life (e. g., Vos et al., 2013),

and to foster action-orientation to create transformative potential in the course of the research process (Hirsch Hadorn et al., 2010; Lang et al., 2012). Environmental literacy therefore requires an integrated, holistic view on the environment (Ostrom, 2008; Scholz, 2011). Transdisciplinary research teams consist of both, scientists from different disciplines and representatives of the non-scientific society, and as such enable a co-production of knowledge (Jasanoff, 2004; Pohl et al., 2010). The inter- and transdisciplinary dimension of the research addressed in this paper is the process of communicative, social and cognitive integration between scientists and non-scientific actors (Bergmann et al., 2012).

Today, the need for interdisciplinary research is widely acknowledged (e. g., Frodemann, 2010; Vasbinder et al., 2010a) and transdisciplinary approaches are currently increasing in environmental and sustainability science (Lang et al., 2012; Scholz, 2011). It is recognized that measures suggested by researchers to decision-makers are generally a weak motivation for true sustainable change (Smit and Wandel, 2006). Thus, modes of research that foster the linkage between knowledge production and societal transformation are promising alternatives to more traditional research that focuses only on scientific knowledge production. However, integrative inter- and transdisciplinary research approaches are still far from being consolidated. For many research groups it remains a major challenge, and success in real integration often fails (Jahn et al., 2012; Roy et al., 2013).

Tackling the scientific and societal challenge of climate change – particularly with regard to modelling climatic change impacts – is a paradigmatic example for the need of inter- and transdisciplinary research. When modelling climate change impact phenomena, coupling disciplinary model components via appropriate interface tools is required for passing quantitative and qualitative measures. Such integration is further complicated because the model components are context and research question specific, and requires the consideration of values which are economically, ecologically and socially anchored. Such knowledge produced can directly link to the perceptions, assumptions, challenges and questions which decision or policy makers have. Both, the grasping of the complexity of the phenomenon (Hirsch Hadorn, 2008) as well as the impact of modelling results improve when climate change impact modelling is realized in an inter- and transdisciplinary way.

Here, the coupled model has a double role: It is the basis for and the aim of the integration process. Thus, integration is not just an outcome, but a process in its nature (Jakeman and Letcher, 2003; Kelly Letcher et al., 2013). Where research on climate change impacts is based on integrated modelling, the joint model development and in-

terface design are hence core elements of integration. Such integration can be regarded as a mutual learning and negotiation process where understanding continuously develops, often unpredictably, and it is highly dependent on how it is organized. One major characteristic of such coupling processes is recursivity: the outcome of a certain model run can stimulate the repetition of the numerical experiment with modified settings. Similarly, in the development of the modelling concept, recursivity can be very important in continuously improving the models quality.

Integration has also become a widely claimed quality in environmental modelling. Kelly Letcher et al. (2013) distinguish the five types of integration: (i) integrated treatment of issues, (ii) integration with stakeholders, (iii) integration of disciplines, (iv) integration of processes and (v) integration of scales of consideration. Also Kragt et al. (2013) present challenges of integrated research and modelling of environmental systems, focussing on the modellers role in structuring integrated research projects. They choose the differentiation between technology integration, knowledge integration and team integration. In inter- and transdisciplinary research integration is a major challenge (Bammer, 2013; Bergmann et al., 2012; Roy et al., 2013; Stokols et al., 2013) and has to be addressed in a differentiated manner to be appropriately structured and enabled.

In this article we address the challenge of the integration process in inter- and transdisciplinary modelling, focussing on joint development of interfaces between the model components. We therefore distinguish the three dimensions communicative, social and cognitive, and we show how interface tools can serve both, the integration process itself as well as the integrative modelling. The paper first addresses integration and interface design on a theoretical level, and then shows how it was realized in a specific case study. We discuss how heterogeneous research groups can create a joint language and understanding of diverse perspectives and methodologies that lead to the development of a coupled component model and interface design. Particular attention is paid to the importance of a systematic development of the interfaces to ensure the required consistency and traceability (Giupponi et al., 2013). We then exemplarily outline the application of our coupled component model studying the impacts of climate change on future snow conditions, economy of skiing and regional tourism structure as developed in the two-stage CC-Snow project[a]. With respect to the interface tools of the coupled model – *variables*, *indicators* and *thresholds* – we make an attempt to formalize their functionality in the integration process. We describe how

[a]CC-Snow: Effects of Climate Change on Future Snow Conditions in Tyrol and Styria (Austrian Climate Research Programme, K09AC0K00038) CC-Snow II: Effects of Future Snow Conditions on Tourism and Economy in Tyrol and Styria (Austrian Climate Research Programme, K10 AC0K00049).

the interface tools support appropriate routing and modification of different types of information across the scientific disciplines in the model. Finally, the potential benefits and challenges of inter- and transdisciplinary research are discussed, with a particular focus on the framework conditions required for integrative research.

2.2 Dimensions and tools for integration

In contrast to disciplinary modelling, where one single person or a homogeneous research team can derive models from theoretical disciplinary backgrounds, the development of models in inter- and transdisciplinary research is a central part of the research process itself (Kelly Letcher et al., 2013). The research object is constituted only due to the integration of diverse perspectives and the identification of objectives and goals of the involved parties. The effort of integration varies according to the distance between the knowledge fields, whether they are closely related or widely separated in terms of cultures of cognition and practices. It further depends on the size and the respective heterogeneity of the involved parties. In our case study, the CC-Snow project, we are referring to a research consortium that consisted of several disciplinary research teams from the fields of climatology, hydrology, tourism economy and regional tourism, each having a sub-project leader and research assistants on both the pre- and post-doc level and stakeholders from skiing area management, regional development, tourism management and local administration/policy.

In the following, we outline the different dimensions of integration on a theoretical level. We then show how inter- and transdisciplinary modelling can be initiated, leading to a modelling concept. We will present different integration methods, emphasizing their double role in the integration process and the implementation of the model. As we are referring to a sequential process, we describe and discuss the different aspects in a chronological order from the constitution of the research team to the consolidation and application of the model.

In distinguishing between communicative, social and cognitive dimensions of integration we follow Bergmann et al. (2012). The authors refer to *communicative integration* as the "differentiating and linking of different linguistic expressions and communicative practices" aimed at developing "a common discursive practice in which mutual understanding and communication is possible" (ibid.: 45). This includes the clarification of common terms and, if necessary, the creation of new ones. *Social integration* addresses the need for differentiating and correlating the interests and activities of involved parties, as well as the clarification of roles and the building of teams

and leadership. It further includes organizational aspects which provide practical conditions for integration. *Cognitive integration* relates to the differentiation and linkage of different knowledge bases, to create mutual understanding with respect to theoretical concepts and methods applied in the disciplines involved.

These dimensions are addressed separately to improve the structure and organization of the integration process. In practice, they are strongly overlapping. In particular during the phase of team-building, the process of differentiating and linking of the diverse practices and concepts is of substantial importance (Muhar et al., 2006).

A promising framework to structure and organize the overall integration process and to create space for social integration is to establish boards of integration (often called task force) which are established at the beginning of inter- and transdisciplinary research projects. They consist of representatives of the sub-groups or involved knowledge fields. These representatives have to be fully involved in the disciplinary research process or respective knowledge fields. Task force members define and negotiate roles and responsibilities of the involved parties, formulate objectives and agreements and communicate results to the rest of the research consortium. Members of such boards of integration are key persons in developing interface designs and require the ability and willingness to (i) learn in order to enable cognitive integration when dealing with other research practices and modes of thought, and to (ii) disclose their disciplinary research strategies, policies related to the research project, and data bases. Integration work requires experienced researchers, but to additionally involve early-stage researchers provides valuable learning opportunities. For organizational establishment and team cooperation, methods of managing inter- and transdisciplinary research consortia can be applied (e. g. Defila et al., 2006; Vasbinder et al., 2010b).

These boards of integration are the space where communicative and cognitive integration takes place. In the following we present a way to initiate communicative integration that seamlessly leads to cognitive integration.

To get inter- and transdisciplinary teams started, mutual presentation of the research and knowledge fields, including general background information on the discipline/subdiscipline/societal field and the outline of the particular interest are required. While many professionals, in particular scientists, are usually familiar with presenting their work, the identification of key concepts and terms usually does not form part of their everyday practice. This step has a self-reflective component which helps to characterize ones' own field of professional activity and to identify its boundaries, the latter being a prerequisite for developing interfaces. Conceptual work starts with identi-

fying important terms within the knowledge fields, followed by a clustering and/or hierarchical ordering to describe their relations and roles. This very simple task is helpful as a starting point to systematically explore interfaces of the respective fields by identifying overlapping or relating concepts (Bergmann et al., 2012). The analysis of key concepts aims at unfolding the meanings and the theoretical foundations of terms frequently used in the respective field. Concepts are the material of which theories are built of. Therefore, cognitive integration has to start with conceptual work. Both, key concepts with importance for a single discipline as well as jointly identified overlapping concepts have to be addressed in this step. As many concepts can be interpreted in multiple ways and are, at the same time, used in every day communication, it is important to carefully explore their theoretical constitution in order to avoid misleading assumptions of apparently mutual understanding (Bergmann et al., 2012; Kragt et al., 2013). Furthermore, it is important to be aware of the double role of key concepts in inter- and transdisciplinary research, taking into consideration their delimiting and connecting potential (Klein, 2000). In this sense, concept work is a basis for the framing of the joint research object and accordingly, the building of a modelling concept. For example, when it comes to jointly develop and formulate variables and indicators as interface tools for the modelling, it is important to generate a mutually shared and seamless understanding of the data semantics (Kragt et al., 2013).

By interface tools we refer to instruments with a twofold function: First, they facilitate the combination of the model components, aggregation and/or reduction of numerical data and the expression of jointly negotiated values. As such they transmit/route information across the model components and enable linking and transforming of quantitative information into qualities. Technical implementation of the interface tools can be supported by integration frameworks such as OpenMI (*Open Modelling Interface*; Bulatewicz et al., 2013; Moore and Tindall, 2005), or by means of formalized languages such as UML (*Unified Modelling Language*; Booch et al., 1999). A prominent example for the latter in environmental modelling is the Global Change Decision Support System DANUBIA (Barth et al., 2004; Barthel, 2011). Second, the interface tools can be regarded as intermediaries between theoretical and empirical descriptions of the issue of concern (Morgan and Morrison, 1999), linking disciplinary based theoretical knowledge to the specific case which is reflected in the interface design. They allow for combining the case specific (idiographic) with the theoretical (nomothetic) dimensions of the according research question (Krohn, 2010).

Figure 2.1 shows a general scheme of knowledge fields, integration methods, interface tools and the outcomes of inter- and transdisciplinary component modelling.

The arrows indicate the double role of the interface tools. The development of the modelling concept guides the communicative, social and cognitive integration, while its technical implementation and application facilitates the overall research task. The three interface tools have specific roles and functions. *Variables* enable the framing of the joint research object in the course of the building of the model and play an important role for creating a joint understanding of the case. In our application, variables have the function to link continuous system states. Their signification and value – here: time series of quantitative physical measures – remain the same when passing from one model component to the other (e.g., a meteorological variable like air temperature passing from the climate model to the snow model). *Indicators* are reduced system states derived by aggregation of variables that abstract dynamics by transforming them into patterns which have to be negotiated in the inter- or transdisciplinary research team and deepen the joint understanding of the phenomenon of concern. As such, indicators can be regarded as hybrids of system states and values. In the course of developing the model their role is to structure the negotiation process. Indicators like e.g., the future ski season length in our case study, are key elements for measuring, explaining, visualizing, comparing and communicating results between the research groups, the stakeholders and the broader public. Finally, *thresholds* indicate critical system states. As such they help negotiate values. Thresholds identify outcomes from the modelling which are of interest for stakeholders (a prominent example of a threshold in our case study would be the amount of water required for sufficient technical snow production).

Integration, as described so far, is far from being a linear process. In the course of integration in environmental research, mutual learning can lead to discover additional aspects of the research object or even to a reformulation of research questions. Thus, the adaptation or modification of formerly defined steps is not a failure *per se*. On the contrary, it can reflect the further development of the system understanding. Though not predictable in its details, a stepwise, recursive learning process can represent the main scientific advance and benefit. For inter- and transdisciplinary climate change impact modelling it is important to acknowledge its recursive character, both, in its development and implementation. Recursive modelling is generated through the continuous development of the modelling concept, and consecutive model application.

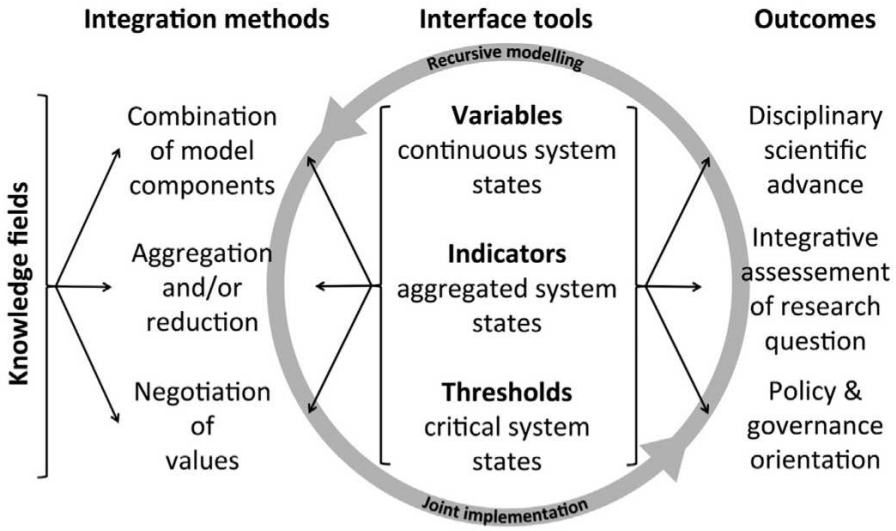

Figure 2.1: Interface design for coupled, inter- and transdisciplinary component modelling with knowledge fields, integration methods, interface tools and outcomes. The circle indicates recursive modelling and joint implementation through the continuous development of the modelling concept, and consecutive model application.

2.3 Building an integrative tool

To investigate the impact of climate change on future snow conditions, economy of skiing and regional tourism structure in the CC-Snow project, interface tools were developed for the respective model components (Strasser et al., 2011b). The interface tools connect the climate signal with the natural and technical snow (production) conditions and the economically motivated decisions of the skiing area operators. The interfaces were jointly developed by scientists and the decision makers responsible for the skiing industry and the regional tourism development. The knowledge of climate scientists, snow hydrologists, economists and tourism researchers and finally, stakeholders was brought together by the *CC-Snow task force* to develop the interfaces between the disciplinary model components. Figure 2.2 shows the complexity of the coupled system that was finally agreed upon, comprising the coupled component model, the stakeholders from the study area, and data. The component model permits the linkage between (i) potential future climate change (Marke et al., 2015), (ii) respective snow cover evolution, conditions for technical snow production and its efficiency, water and energy consumption (Hanzer et al., 2014), (iii) future economic conditions for skiing area operation (Damm et al., 2014) and finally, (iv) consequences for the regional tourism structure (Steiger et al., 2012). Arrows indicate the direction in which information is transported.

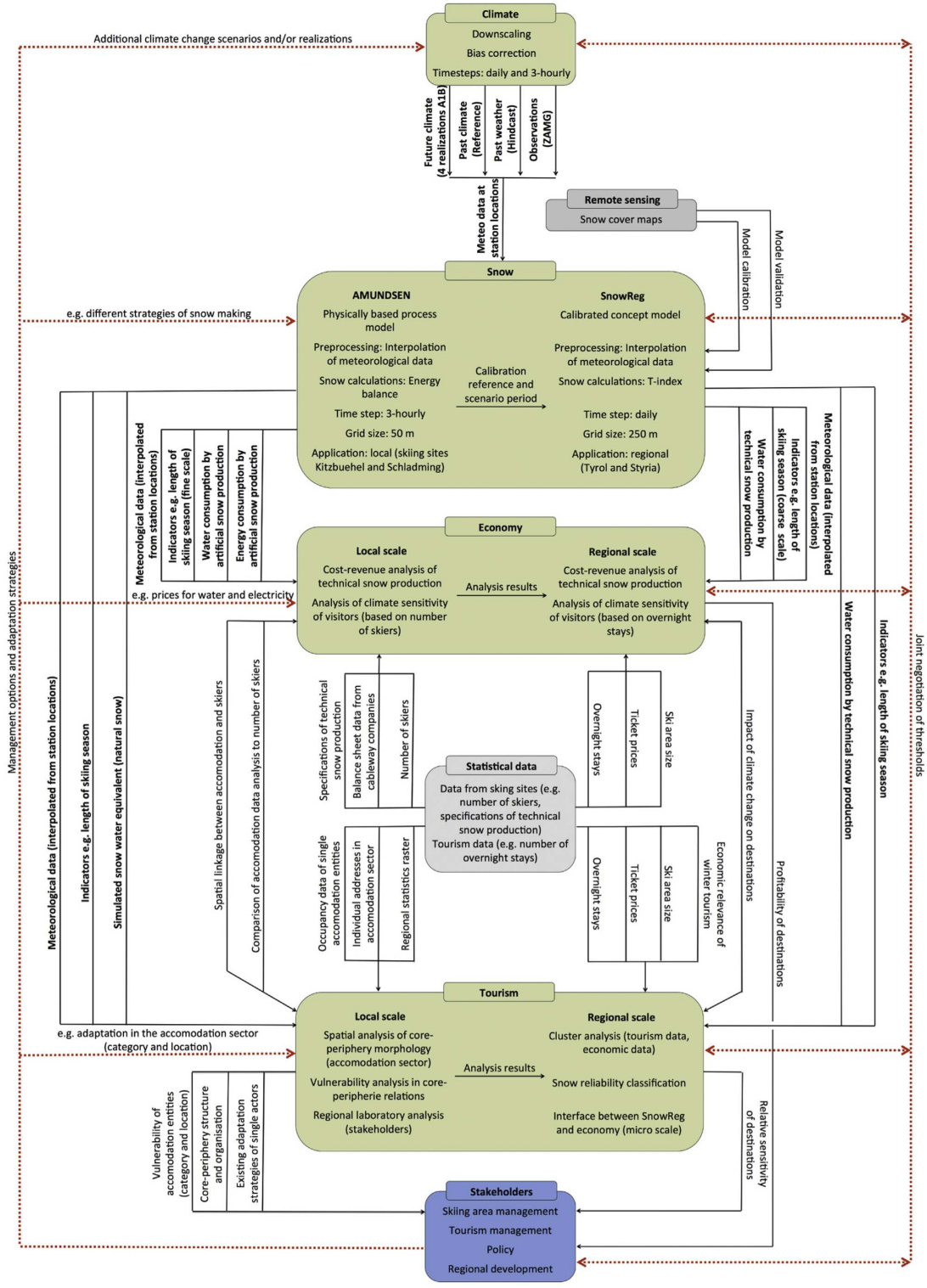

Figure 2.2: Case-specific coupled component modelling of the effects of climate change on future snow conditions, economy of skiing and tourism: the example of CC-Snow. The figure comprises (i) model components from knowledge fields (*green*), (ii) stakeholders from the study area (*blue*), and (iii) data (*grey*). Black arrows indicate the interconnections within the investigated natural and socio-economic system, the flow of data and information, and the manifold interfaces between the model components. Variables and indicators passed between model components are indicated in bold. The integration of non-scientific knowledge (*red lines*) comprises the negotiation of values to be implemented as thresholds into the model components (*right*), and the development of management options and/or climate change adaptation strategies by means of recursive modelling (*left*).

To combine the climate model with the local scale snow model ("AMUNDSEN" in fig. 2.2), a classical *variable* coupling was implemented: the results provided by the downscaling of the climate model output (meteorological variables) are directly used as input for the snow modelling. As both models use the same temporal resolution (3 h) no temporal aggregation or disaggregation is applied. Here, *designing the interface* was reduced to select the variables that are required as input by the local snow model, and the units to be used. Being quantitative physical measures, the character of variables remains unchanged in the snow modelling; the output is again a time series of quantities with a physical meaning. Hence, coupled modelling by means of variables provides a process-oriented and analytical, continuous description of system states. At this step still no transition between scientific cultures or from quantitative to qualitative measures is undertaken.

For the case of the coupling between the climate model and the regional scale snow model ("SnowReg" in fig. 2.2), the general coupling technique remains similar, but only a reduced set of variables is required: whereas AMUNDSEN is a physically based model with detailed process description (Strasser, 2008), SnowReg is a degree-day model only using daily values of temperature and precipitation as proxies to describe snow accumulation and the melting process (Ragg et al., 2011). Due to the reduced computational cost, degree-day models were applied for larger areas or longer time series and calibrated using satellite data derived snow cover maps. Similarly the statistical data, these are externally provided and not part of the model component coupling described here.

Future natural and technical snow conditions are used as input for the economic modelling. Daily visitor numbers are calculated using a regression analysis derived from historical conditions (for which visitor numbers are known, provided by the skiing resort operator). The regression uses the following variables as input: total snow depth on the piste (i.e., both natural and technical snow), snow- and rainfall, mean temperature, wind speed, global radiation, day of the week, public holiday yes/no, and skiing operation yes/no. Except the calendar dates which are tracked inside the economic model, these variables are directly passed by the local scale snow model (connecting arrows between the *Snow* and the and the *Economy* boxes in fig. 2.2), enabling for the first time a prognostic calculation of daily visitor numbers for a skiing area under conditions of future climate change including the production of technical snow (Damm et al., 2014). This coupling is again an example for direct variable passing, however, other than at the climate/snow interface, here a transition from a natural science assessment to a socio-economic application has been undertaken.

At the regional scale, such model coupling is not possible. Whereas at the local scale detailed information of skiing area operators could be utilized, no such model input was available for regions with many skiing areas which are operated by different managers with idiosyncratic management strategies. At the regional scale the model SnowReg was used to produce *indicators* which give an integrated, temporally aggregated picture of means and trends to describe the future conditions of skiing tourism in a changing climate (Ragg et al., 2011; Steiger et al., 2012).

As with variables, indicators are spatially distributed and enable a translation from quantitative information (physical and proxy variables describing the snow conditions) to qualitative information (application-oriented measures, jointly defined with the stakeholders in the skiing area). As general transferable measures indicators provide a picture of the skiing area and regional system state that could be communicated to the local tourism managers, policy makers, or to the public at large. The indicator definition process represented the transition from disciplinary perspectives on the natural, technical and social processes and phenomena to an integrated and holistic human–environment system perspective. In the CC-Snow project, the list of indicators jointly defined for that purpose included, e.g., date of ski opening (natural and technical snow), hours of technical snow production, date of ski closing (natural and technical snow), days with white winter landscape, season length (natural and technical snow), operation time and events of heavy snowfall. The indicators are used for the economic analysis of skiing at the regional scale, and for an estimation of the climate sensitivity of the visitors. In addition the indicators also represented inputs in the future regional tourism structure assessment for a changing climate (see fig. 2.2). Development and definition of the indicators started in the beginning of the project, acknowledging the importance of initializing the inter- and transdisciplinary process before the disciplinary research work itself begins (Kragt et al., 2013).

Finally, we made use of the *threshold* interface mechanism as the third tool in our coupled component modelling. Thresholds are local warnings that indicate model variables that have exceeded certain critical values, here mostly related to skiing conditions. A simple but prominent example for a typical threshold in winter tourism research is the "100 day rule": This rule states that a ski area is snow reliable if ski operation can be maintained for at least 100 days in 7 out of 10 seasons (Abegg et al., 2007). The CC-Snow thresholds were jointly negotiated between the stakeholders and the scientists, and directly implemented in the model components (see fig. 2.2).

In table 2.1, the three types of interface tools variables, indicators and threshold as used in CC-Snow are compared to each other with their main characteristics both

in their specific, and in a more general meaning: With respect to temporal resolution, all three interface tools are different: whereas variables were passed with the 3 h resolution of the modelling, indicators were measures comprising one winter season. Thresholds were single dates when something significant had happened (i.e., poor snow conditions forcing the end of the winter skiing season). Spatial resolution was the fully distributed modelling raster for variables and indicators, i.e. the results could be illustrated by means of maps. Thresholds were related to the local skiing area only. The quantitative numerical nature of the system was conserved for the variables, whereas indicators and thresholds were used to link the quantitative measures in the system with their qualitative evaluation, i.e. the view of the stakeholders. In a more general context, our interface types could be characterized as: (i) variables were process-oriented, analytical and disciplinary, whereas (ii) indicators were descriptive, application-oriented more general, transferable hybrids, and finally, (iii) thresholds were system-dependent, actor oriented warning signals.

Table 2.1: Characteristics of the three types of coupled component modelling interface tools for integration in CC-Snow.

Variables	Indicators	Thresholds
Continuous system states	Aggregated system states	Critical system states
Time series with modeltemporal resolution	Temporally aggregated means and trends	Single dates with modeltemporal resolution
Spatially distributed	Spatially distributed	Local
Quantitative → quantitative	Quantitative → qualitative	Quantitative → qualitative
Process-oriented	Descriptive	System dependent
Analytical	Application-oriented	Actor-oriented
Provide disciplinary data information	Provide general, transferable measures	Provide warning signals

These tools were crucial for a successful interface design in the project with respect to a seamless routing of the climate change signal through the physical science processes, to the socio-economic analysis, and thereby reflecting the societal perspective on the interaction between humans and ecosystems.

2.4 Potential and challenges

In the following we outline potential benefits and challenges experienced in the process of building the coupled component model, and we discuss framework conditions required for inter- and transdisciplinary research. Thereby we focus on resources, funding policies and inter- and transdisciplinary training programs.

Creating conditions for inter- and transdisciplinary research on climate change impact research has been presented as a major challenge of *integration*. Diverse disciplinary-based research is required in order to address complex research questions related to sustainable adaptation to changing future snow conditions in regions with a high vulnerability due to their economic dependency on winter tourism. Further, the integration of stakeholder perspectives in the research process is required to improve the particular case understanding and to create acceptance for solutions provided as research outcomes. Joint development of the component model, taking into consideration the different dimensions of integration, and the recursive modelling approach proved to be the key for successful inter- and transdisciplinary modelling. The overall potential of this approach lies in the possibility to provide socially and scientifically robust knowledge for societal transformation.

However, the chosen process of integration creates a series of challenges which can benefit from the systematization of the integration approaches. The constitution of a *task force* can be helpful in ensuring successful research processes. The establishment of a cooperative team requires building trust, distributing roles and responsibilities, and formulating agreements (*social integration*), skills which have to develop constantly (Muhar et al., 2006). The finding of a common language has been experienced as a prerequisite to enable joint research (*communicative integration*), but it is generally underestimated in its importance. One of the many reasons for this underestimation is that many concepts applied in research are at the same time used in everyday communication where they are weakly structured but commonly applied (Klein, 2000). The failure in inter- and transdisciplinary research is often rooted in a lack of conceptual work at an early stage of the research process (Bergmann et al., 2012). To elaborate interface tools (*cognitive integration*), a profound mutual understanding regarding the different theoretical concepts, characteristics and methods applied in the diverse knowledge fields is a major challenge. It requires intellectual openness and a strong cooperativeness when dealing with other research practices and modes of thought. Likewise, a self-reflective attitude is necessary when it comes to identify the boundaries of one's own knowledge field. The identification of boundaries is an important prerequisite for integrative research (i.e., the *interface design* process).

Other challenges originate in the formal organization and conditions of research projects. Many funding instruments do not provide resources for a stepwise design of a research project including a preceding inter- and transdisciplinary knowledge integration processes, and the joint elaboration of tailored interfaces for numerical analyses. Task force work to foster a seemless knowledge integration to enable an appro-

priate research strategy might be seen as unimportant, uninteresting, or too expensive – by reviewers, principal investigators, and the scientists who consider the task force work as inefficient. Similar is the situation with respect to research niches, review culture and publication strategies – it is much easier to become integrated in a certain community with a traditional background and known players and rules. Finally, the field of inter- and transdisciplinary knowledge integration is still in its infancy with respect to our educational programmes, and only few examples exist where it is at least partially included (e. g., Blöschl et al., 2012). This makes it even more important to let students participate in inter- and transdisciplinary scientific projects.

2.5 Conclusion and outlook

Inter- and transdisciplinary research approaches represent a fundamental prerequisite for tackling the inherent complexity linked to the investigation of environmental phenomena and the need for sustainable societal transformation. The call for inter- and transdisciplinary environmental research has come from many disciplines, and large international research networks have been initiated (e.g., Earth System Science Partnership, International Geosphere-Biosphere Programme, International Human Dimensions Programme on Global Environmental Change, Future Earth). Still, true integration remains a challenge.

This paper has presented an example for the development of a coupled component model applied for the assessment of climate change effects on snow and skiing conditions in an Austrian ski resort, including the associated impacts on the economy of skiing and tourism structure. The design of the model coupling by means of interface tools is the result of an integration process, and the modelling concept. The flow of information through the various model components representing different knowledge fields as well as the translation of quantitative model results to qualitative information through the interfaces has been systematically structured and described. These interfaces serve as methodological framework to foster the inter- and transdisciplinary research process. The different types of interfaces presented in this paper function as a concept to enable and stimulate such inter- and transdisciplinary integration processes. As demonstrated, the integration – by a coupling of model components and the development of the respective model interfaces – is not merely an additive procedure but should be considered as important component of the entire research process, to be initiated in the beginning of a research project. Moreover, the building of a well structured inter- and transdisciplinary research team and the joint generation of a

mutual understanding in terms of objectives of the research activity, key concepts and theoretical foundations is a demanding process that requires openness, cooperativeness and the willing participation of all involved researchers. This joint development process, including recursive modelling for mutual learning, is the prerequisite to a successful design, and application of models that produce results which support the understanding and transformation of a concrete case.

Researchers and funding organisations should accept that the development process for inter- and transdisciplinary research is key for subsequent scientific advances and societal transformations with regard to environmental and sustainability concerns. Tackling integration is an important research process itself, and cannot be provided in the proposal writing stage of a project. The time and personal resources to be invested prior to the disciplinary project work should be accounted for in the temporal and financial planning. However, this calls for the funding organisations to be willing to provide financial support for the development of such integrative project concepts, or even better, to request such structures in proposal calls.

Acknowledgements

We gratefully acknowledge the valuable contributions of the CC-Snow sub-project leaders Andreas Gobiet and Karl Steininger (Wegener Center for Climate and Global Change, University of Graz, Austria), Hans-Jörg Ragg and Hannes Kleindienst (GRID-IT Innsbruck, Austria) and various colleagues and stakeholders from the study sites who contributed to the CC-Snow project. We acknowledge David Abson (Leuphana University Lüneburg, Germany) for proofreading the second version of the manuscript. Both stages of the project have been funded by the Austrian Climate and Energy Fund (Austrian Climate Research Program, grant nr. K09AC0K00038/K10AC0K00049). The availability of the resulting model itself is governed by the respective institutions where it has been developed (please contact the corresponding author for further information on the conditions of its use).

Publication of this paper has been supported by the University of Innsbruck (Austria).

Chapter 3

Scenarios of Future Snow Conditions in Styria (Austrian Alps)

Thomas Marke, Ulrich Strasser, **Florian Hanzer**, Johann Stötter, Renate A. I. Wilcke, Andreas Gobiet

Published in *Journal of Hydrometeorology* (Volume 16, February 2015, Pages 261–277, doi: 10.1175/JHM-D-14-0035.1).

My contribution to this article: implementing the snow layering and densification scheme in the AMUNDSEN model as well as the interface to the RCM data, setting up the model for the study site, performing the model runs, producing most of the plots, analyzing the model results, and writing section 2 of the article.

Scenarios of Future Snow Conditions in Styria (Austrian Alps)

THOMAS MARKE, ULRICH STRASSER, FLORIAN HANZER, AND JOHANN STÖTTER

Institute of Geography, University of Innsbruck, Innsbruck, Austria

RENATE ANNA IRMA WILCKE AND ANDREAS GOBIET

Wegener Center for Climate and Global Change, Graz, Austria

(Manuscript received 11 February 2014, in final form 18 July 2014)

ABSTRACT

A hydrometeorological model chain is applied to investigate climate change effects on natural and artificial snow conditions in the Schladming region in Styria (Austria). Four dynamically refined realizations of the IPCC A1B scenario covering the warm/cold and wet/dry bandwidth of projected changes in temperature and precipitation in the winter half-year are statistically downscaled and bias corrected prior to their application as input for a physically based, distributed energy-balance snow model. However, owing to the poor skills in the reproduction of past climate and snow conditions in the considered region, one realization had to be removed from the selection to avoid biases in the results of the climate change impact analysis. The model's capabilities in the simulation of natural and artificial snow conditions are evaluated and changes in snow conditions are addressed by comparing the number of snow cover days, the length of the ski season, and the amounts of technically produced snow as simulated for the past and the future. The results for natural snow conditions indicate decreases in the number of snow cover days and the ski season length of up to >25 and >35 days, respectively. The highest decrease in the calculated ski season length has been found for elevations between 1600 and 2700 m MSL, with an average decrease rate of ~2.6 days decade^{-1}. For the exemplary ski site considered, the ski season length simulated for natural snow conditions decreases from >50 days at present to ~40 days in the 2050s. Technical snow production allows the season to be prolonged by ~80 days and hence allows ski season lengths of ~120 days until the end of the scenario period in 2050.

1. Introduction

Mountain ecosystems are known to be particularly vulnerable to climate change (EEA 2012). To investigate climate change effects in Alpine regions, scenario simulations represent suitable tools in a wide range of applications (Mauser and Ludwig 2002), the modeling of future climate and natural snow cover being important examples (Liston 2004; Strasser 2008; Strasser and Marke 2010). Investigating potential changes in the spatial and temporal evolution of the Alpine (natural) snow cover seems particularly important as the temporal storage of water in the snowpack and the related water release in spring affect soil moisture conditions and evapotranspiration, as well as runoff generation, timing, and magnitude (Kane et al. 1991; Hinzman et al. 1996; Marsh 1999; Luce et al. 1998). In Alpine headwatersheds, snow distributions further play a crucial role for water availability in downstream regions, where water is utilized in a domestic, industrial, or agricultural context.

From a socioeconomic view, snow availability and reliability represent prerequisites for snow-related sport activities and hence are key factors for Alpine winter tourism (EEA 2012). According to Elsasser and Messerli (2001), this dependence of the tourism sector on snow availability in Alpine areas has even increased over the past several years.

The complex topographic conditions in mountain regions make both the generation of future climate scenarios [here by regional climate models (RCMs)] and the adequate representation of all processes that determine snow accumulation and ablation exceptionally demanding (Blöschl 1999; Cline et al. 1998). Nonetheless,

Corresponding author address: Thomas Marke, Institute of Geography, University of Innsbruck, Innrain 52f, 6020 Innsbruck, Austria.
E-mail: thomas.marke@uibk.ac.at

DOI: 10.1175/JHM-D-14-0035.1

the generation of scenarios of future snow conditions, including natural snow conditions and technical snow production, is highly desirable.

Considering the simulation of climate conditions, present-generation RCMs provide raster resolutions of 50–10 km (e.g., Christensen and Christensen 2007; Loibl et al. 2007; Hewitt and Griggs 2004). Owing to the remaining gap between the spatial resolution of RCMs ($\geq 10^4$ m) and that of impact models operating at the land surface (10^1–10^3 m), the application of statistical downscaling techniques still represents a prerequisite for scenario simulations with hydrometeorological model chains (Marke 2008; Marke et al. 2011a,b). Wilby and Wigley (1997) and Fowler et al. (2007) provide an extensive review on different downscaling techniques and their performance in the view of hydrological modeling. Most statistical methods are comparatively inexpensive in terms of computational costs, which can be a major advantage in many applications. They further bring the benefit that biases in terms of deviations from observed climatological conditions can be corrected in the downscaling process (Marke et al. 2011b). However, many empirical methods only produce data valid in a climatological sense, owing to their very design. Often it is most desirable to develop downscaling methods that allow for application and comparison to observations at shorter (i.e., from daily to hourly) time scales, particularly in hydrological studies.

For mountain (natural) snow cover modeling, a lot of scientific effort has been put into the discussion of which type of model to use for what purpose (Klemes 1990; WMO 1986). Simple and computationally inexpensive temperature-index models have proven to be suitable for snowmelt modeling, sometimes even outperforming the more complex energy-balance models at the catchment scale (Hock 2003). Requiring only near-surface air temperature and precipitation as meteorological forcings, these models have little demand on meteorological input and can be applied in a wide range of geographic regions and climatic settings. As the applied melt factors vary in space and time and are often calibrated to best possibly reproduce observed melt rates, index models are limited in spatial and temporal transferability. This somehow limits their applicability in climate change impact studies (Hock 2003; Warscher et al. 2013). Moreover, calculating snowmelt on the basis of temperature only, classic temperature index models are not able to reproduce spatial variability induced by topographic effects like orographic shading, slope, and aspect (Hock 2003). Naturally, these effects can be decisive in mountainous terrain where steep gradients in meteorological variables (e.g., global radiation) exist over short distances because of complex topographic conditions. Deterministic (process oriented) snow cover models like the energy- and mass-balance model ISNOBAL (Marks 1988), Snow Thermal Model (SNTHERM) (Jordan 1991), or SnowModel (Liston and Elder 2006a) describe the physics of most important surface processes (e.g., turbulent and radiative fluxes in the boundary layer) and, hence, are considered transferable in space and time. Such models explicitly calculate the energy balance of a snow surface, a snowpack, or sometimes even for different snow layers for every model time step from minutes to hours. Hence, they are demanding in terms of meteorological input variables as well as computational resources. A more comprehensive overview of distributed snow modeling and snow process modeling in different applications is given by Kirnbauer et al. (1994), Fierz et al. (2003), and Marsh (1999). Besides a calculation of natural snow conditions, the production of technical snow, which represents one of the most important climate change adaptation measures in Alpine ski areas (Abegg et al. 2008; Wolfsegger et al. 2008), needs to be considered in numerical models as soon as climate change impacts on Alpine winter tourism are intended to be investigated. While approaches for the simulation of technical snow have been developed in the past (Steiger 2010; Schmidt et al. 2012; Scott et al. 2003; Formayer et al. 2009), these models are point based or semidistributed (in altitudinal bands) and often merely provide the potential for snow production. To the knowledge of the authors, no models currently exist that explicitly quantify technical snow production in a physically based, spatially distributed simulation of the mountain snow cover.

This study presents the results of the projects CC-Snow and CC-Snow II (funded by the Climate and Energy Fund of the Austrian Climate Research Programme; see www.cc-snow.at for details on the projects), where improved future climate scenario simulations have been utilized in combination with a physically based, energy-balance snow model to determine the effect of climate change on future natural and artificial snow conditions in the Austrian Alps. In this paper, results are shown for the Schladming region (Styria, Austria; see Fig. 1). The study site represents a typical Austrian winter destination and host of the ski world championships in 2013 (www.schladming2013.at). The main research questions to be addressed exemplarily for the Schladming region are as follows:

- How does the natural snow cover change in response to climate change?
- How is the ski season length in the ski areas affected by these changes in the natural snow cover?
- To what extent can technical snow production help to compensate decreases in the ski season length in the ski areas?

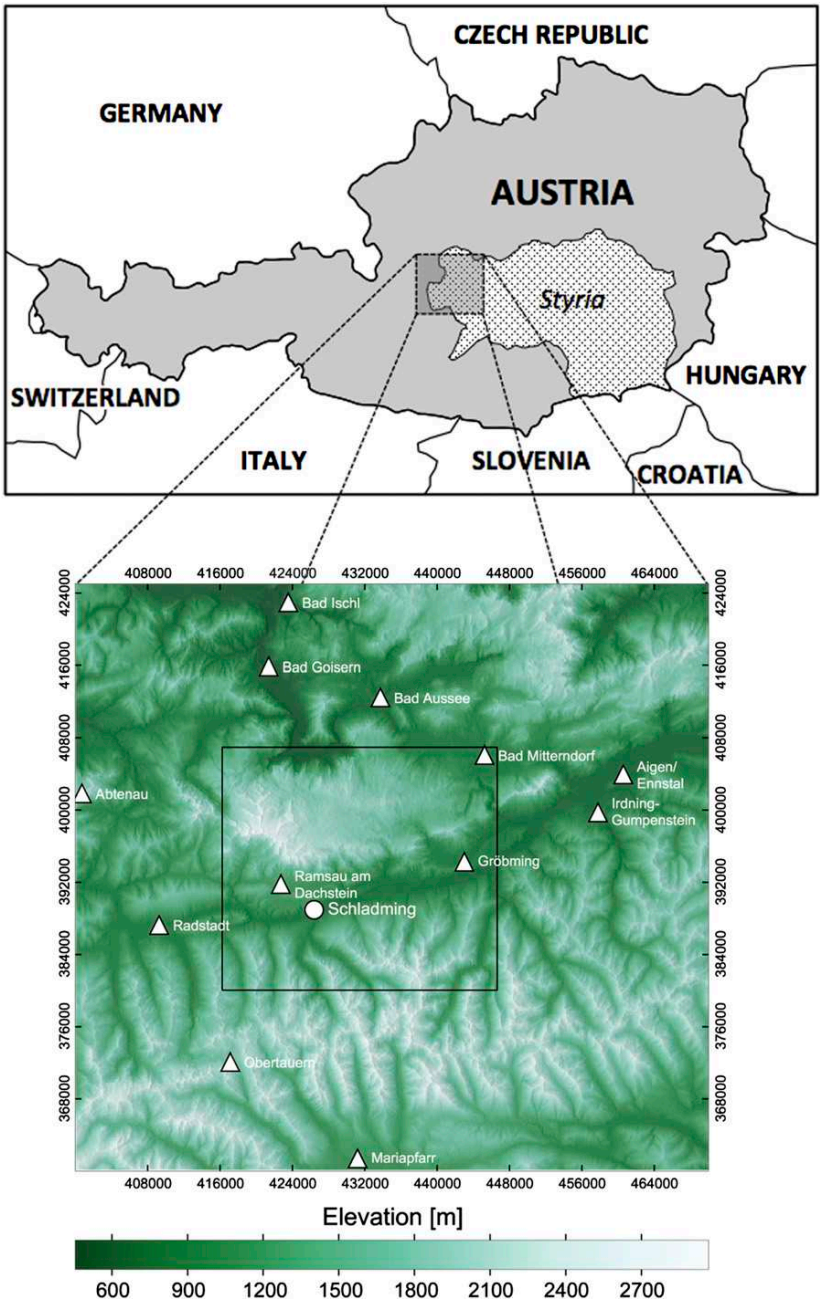

FIG. 1. Study site of the Schladming region in the province of Styria (dotted square) in Austria. The triangles indicate the location of meteorological stations, and the community of Schladming is marked with a circle. While simulations have only been carried out for the inner part (black rectangle), meteorological stations in the outer frame have additionally been considered in the interpolation of meteorological data. The numbers framing the digital elevation model represent grid coordinates [m; coordinate reference system Militärgeographischen Institutes (MGI)/Austria Lambert].

To answer these questions, a pragmatic approach for the simulation of technical snow production has been developed and integrated in a distributed, physically based snow model. The applied snow model has specifically been developed for the simulation of snow conditions in high mountain regions. As the model does not include calibrated components but applies physically based descriptions of the processes that determine the temporal and spatial variability of the snow cover in the complex topography of the Alps (e.g., the simulation of short- and longwave radiative fluxes including consideration of orographic shadows and cloudiness as well as multiple and terrain reflections), the model is considered transferable in time and hence is particularly suited for scenario simulations. Four realizations of the Intergovernmental Panel on Climate Change (IPCC) A1B scenario (Nakicenovic and Swart 2000) have been selected, downscaled, bias corrected, and used as input for the snow model to simulate past and potential future snow conditions with a focus on the number of days with snow cover as well as the ski season length and the amount of technically produced snow (for a schematic overview of the workflow, see Fig. 2). Please note that due to unsatisfying performance in the reproduction of past climate conditions in the study site, one combination of a global and a regional climate model (HadCM2Q16 provided by C4I) has been removed from the selection of realizations.

For the downscaling and bias correction of RCM data, an empirical statistical method, quantile mapping (Themeßl et al. 2011) has been applied. This state-of-the-art approach allows for the application and interpretation of RCM simulations at high temporal resolution (subdaily values) and is computationally efficient. Changes in future snow conditions are addressed for the whole study domain of the Schladming region in the case of natural snow conditions and for an exemplary ski area in the Schladming region considering natural snow as well as technically produced snow. Thereby, two approaches are followed for the analysis of changes in snow conditions:

- The mean snow conditions for a reference period (1971–2000) are compared to those of a scenario period (2021–50). This approach is particularly suited to analyze and illustrate changes in the spatial distribution of snow conditions.
- A continuous evolution of snow conditions is provided and analyzed for the years 1961–2050. This approach is particularly suited to analyze and illustrate the temporal evolution of snow conditions. It is applied in context with area means only, but allows the analysis of trends in the time series.

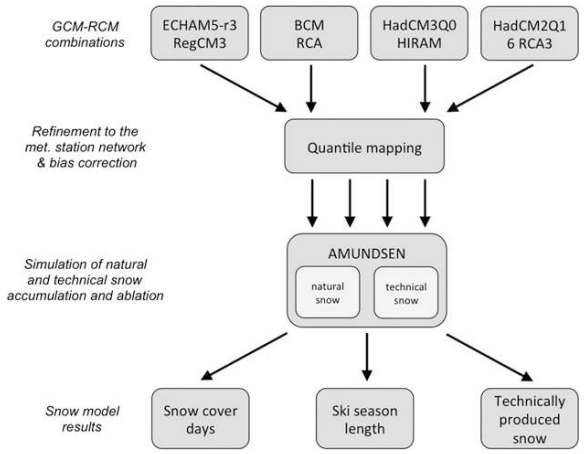

FIG. 2. Schematic overview of the work flow in the present study, including downscaling and bias correction of four RCM realizations of the IPCC A1B scenario and provision of the resulting data as input for the simulation of natural and technical snow with the snow model AMUNDSEN.

The names and locations of the ski areas are not provided to ensure the anonymity of the cooperating ski areas. The snow scenarios presented in this paper represent a basis for further investigations of climate change effects on winter tourism and economy in the Schladming region as carried out as part of the follow-up project CC-Snow II.

2. Methods

a. The snow model AMUNDSEN

In the present study the modular, physically based Alpine Multiscale Numerical Distributed Simulation Engine (AMUNDSEN) (Strasser 2008) is applied for the simulation of the mountain snow cover. The model has been designed to specifically address the requirements of snow modeling in mountain regions under climate change conditions (Strasser et al. 2004, 2008; Strasser 2008). The functionality of the model includes several interpolation routines for scattered meteorological measurements (Strasser 2008; Marke 2008); rapid computation of topographic parameters from a digital elevation model (Strasser 2008); simulation of short- and longwave radiation including topographic (e.g., shadows) and cloud effects (Corripio 2003; Greuell et al. 1997); parameterization of snow albedo depending on snow age and temperature (Rohrer 1992); determination of snowmelt based on an energy-balance approach (Strasser et al. 2008); modeling of the forest snow processes of interception, sublimation, and melt unload according to Liston and Elder (2006a), including the effect of the trees on the micrometeorological

conditions at the ground (Strasser et al. 2008); and simulation of wind-induced snow transport as well as gravitational redistribution of snow (Gruber 2007). To transform snow water equivalent (SWE) to snow depth, an approach for the calculation of snow density has recently been implemented into the model. Thereby, it distinguishes between two types of snow layers, herein called new snow (representing freshly fallen snow) and old snow. The density of freshly fallen snow ρ_{ns} (kg m^{-3}) is calculated as a function of 2-m air temperature T_a (°C) (Anderson 1976):

$$\rho_{ns} = \begin{cases} 50, & T_a \leq -15°C \\ 50 + 1.7(T_a + 15)^{1.5}, & T_a > -15°C. \end{cases} \quad (1)$$

Snow densification is calculated following Anderson (1976) and Jordan (1991), taking into account the effects of compaction and metamorphism. The densification rate due to destructive metamorphism, which is primarily important during the initial phase of rapid settling of freshly fallen snow, is calculated using the relationship

$$\frac{d\rho_s}{dt} = \rho_s[c_4 e^{-c_5(T^* - T_s)} c_6], \quad (2)$$

with ρ_s being the respective layer's (new snow or old snow) density, $T^* = 0°C$, $c_4 = 0.01\,m^{-1}\,h$, $c_5 = 0.04°C^{-1}$,

$$c_6 = \begin{cases} e^{-c_7(\rho_s - \rho_d)}, & \rho_s > \rho_d \\ 1, & \rho_s \leq \rho_d, \end{cases} \quad (3)$$

$c_7 = 0.046\,m^3\,kg^{-1}$, and $\rho_d = 150\,kg\,m^{-3}$. Densification owing to compaction, that is, caused by the weight of the overlying snow layers, is calculated as

$$\frac{d\rho_s}{dt} = \rho_s[c_1 W^* e^{-c_2(T^* - T_s)} e^{-c_3\rho_s}], \quad (4)$$

with W^* (kg m^{-2}) being the load of snow water equivalent (snow in the layer above and 50% of the snow in the current layer), $c_1 = 0.01\,m^{-1}\,h$ (new snow), $c_1 = 0.001\,m^{-1}\,h$ (old snow), $c_2 = 0.08°C^{-1}$, and $c_3 = 0.021\,m^3\,kg^{-1}$. The new snow layer is converted to old snow when reaching a density of 200 kg m^{-3}.

For the simulation of snow conditions in the Schladming region, a spatial resolution of $50 \times 50\,m^2$ is chosen out of the following reasons. On the one hand, it can be assumed that, at that spatial resolution, the main atmosphere–snow surface interaction processes that force the evolution and distribution of the snow cover can be realistically reproduced; this includes the provision of meteorological forcing, for example, a proper conversion and distribution of downscaled RCM output, and the explicit modeling of topographic effects. On the other hand this spatial resolution in combination with the size of the model domain ($\sim 30 \times 27\,km^2$) results in a manageable number of model grid cells and ensures acceptable computing time even for long-term scenario simulations. Analogously, temporal resolution was set to 3 h to minimize computational costs while still allowing the capture of the diurnal course of global radiation, which represents the most important energy source for snowmelt. To avoid small-scale variations in modeled snow cover induced by different vegetation types (which might be subject to change in the future), the influence of vegetation on micrometeorological conditions on the ground (e.g., lower values of temperature and global radiation inside the forest canopy) and the associated effect on snow accumulation and ablation have not been considered in the model runs presented in this study. For further details on the different model algorithms, refer to Strasser (2008) and Strasser et al. (2011).

b. *Technical snow production*

A pragmatic approach for technical snow production has been developed that utilizes data (e.g., location of the ski slopes and number and technical specification of onsite snow guns) and information on the local snow production practice as provided by the managers of the ski areas in the model domain. Required input data for the snowmaking module are the locations of the ski slopes as well as the total number of snow guns for the ski area and the maximum water flow for the entire ski area in cubic meters per hour (as determined by the pumping capacity of the snowmaking infrastructure).

The maximum snow production per snow gun $P_{max_{gun}}$(m^3 h^{-1}) is calculated as a function of wet-bulb temperature T_w (°C) as proposed by Olefs et al. (2010):

$$P_{max_{gun}} = -4.83 T_w + 3.94. \quad (5)$$

This relation was derived as an average of state-of-the-art fan guns by several manufacturers and is valid for wet-bulb temperatures between −14° and −2°C and a technical snow density of 400 kg m^{-3}.

In each model time step, using the condition $T_w \leq -2°C$, all slope pixels where snowmaking is possible are first selected. Then, given the mean number of snow guns per square meter,

$$N_{mean} = \frac{N_{guns}}{A_{slope}}, \quad (6)$$

a maximum snow production amount for the entire ski area is calculated by

$$P_{\max_{\text{total}}} = N_{\text{mean}} A_{\text{snowmaking}} P_{\max_{\text{gun}}}, \quad (7)$$

with $A_{\text{snowmaking}}$ (m^2) as the total area of the selected snowmaking pixels and $P_{\max_{\text{gun}}}$ as Eq. (5) evaluated with the mean wet-bulb temperature of the selected pixels. In a subsequent processing step, $P_{\max_{\text{total}}}$ is converted to a water equivalent value using the assumed technical snow density of $400\,\text{kg}\,\text{m}^{-3}$ and is additionally constrained by the maximum water throughflow rate of the snow guns and by the onsite demand for technical snow. The resulting snow amount is distributed equally over the selected slope pixels.

Following the guidelines of the local practitioners, snow demand is not a limiting factor from 1 November (start of the snow production season) to 15 December. Hence, in this period of time, the maximum possible amount of snow is produced (only limited by the meteorological conditions and technical restrictions). From 16 December until the end of the snow production season on 28 February, the model maintains a minimum snow depth of 0.6 m on the slopes, as suggested by Scott et al. (2007). Combining natural snow accumulation with the simulated technical snow production allows the total snow water equivalent on the ski slopes to be calculated.

This approach assumes the snow guns to be equally distributed over the ski slope, which does not necessarily reflect the conditions at the ski sites. However, its modest requirements in terms of input data make it comparatively easily transferable to other ski areas. A more complex approach that allows one to specify the exact position and type for every snow gun and also considers limited water availability due to reservoir capacities has already been developed (Hanzer et al. 2014).

c. *Processing of meteorological data*

Meteorological input data for the snow model in the current study are sourced from meteorological station data recorded by the Austrian Central Institute for Meteorology and Geodynamics (ZAMG) and the Austrian Hydrographical Service as well as from publicly available RCM simulations (http://ensemblesrt3.dmi.dk). While station data were used in the framework of validation runs only, RCM data were applied for validation of the coupled model system and for scenario simulations. Thereby, the RCMs were driven by different lateral boundary conditions for evaluation of the model chain [European Centre for Medium-Range Weather Forecasts (ECMWF) 40-yr Re-Analysis (ERA-40) (Uppala et al. 2005)] and for the generation of climate conditions for a reference and a scenario period [global climate model (GCM) output]. As all IPCC emission scenarios show nearly the same warming behavior until 2050 (Prein et al. 2011), we selected four realizations of the popular A1B scenario out of the ENSEMBLES database (van der Linden and Mitchell 2009) that reasonably span the warm/cold and wet/dry bandwidth of temperature and precipitation changes in the winter half-year (see Fig. 3). While Fig. 3 shows the climate change signals of temperature and precipitation for the whole province of Styria, Table 1 gives an overview of the selected model combinations and the climate change signals in the Schladming region. As Table 1 shows, the selection includes little warming with dry conditions (ICTP run), little warming with humid conditions (SMHI run), average warming with humid conditions (METNO run), and strong warming with dry conditions (C4I run). As the C4I-HadCM2Q16 (ERA-40 driven) run has shown a weak representation of spatial and temporal structure for past and present climate for the topographically complex area of the Alps, it has to be doubted that the model run delivers robust information on future climate conditions in the considered region. The HadCM2Q16 GCM–RCM combination provided by C4I has therefore been excluded from the selection of realizations considered in the climate change impact analysis.

Prior to an application as input for the snow model, the meteorological data (precipitation amount, 2-m air temperature, relative humidity, 10-m wind speed, and global radiation) were bias corrected and downscaled to the station locations illustrated in Fig. 1 (triangles) using the empirical statistical approach of quantile mapping (Themeßl et al. 2011, 2012). The method generates daily correction functions by comparing observed to calculated climate conditions for a historical period (here 1971–2000) and applies the resulting correction functions on RCM simulations for both historical and scenario periods (Wilcke et al. 2013). The downscaled and bias-corrected daily RCM data are later disaggregated using the 3-hourly diurnal cycle of the raw RCM data.

Nešpor and Sevruk (1999) and Frei and Schär (1998) show the undercatch in observed precipitation, especially in winter and higher altitudes. This undercatch translates to underestimated snow depths in first modeling experiments using hourly station data as meteorological input for the snow model. Therefore, an elevation-based precipitation correction function has been developed. This has been done by comparing simulated snow depth and multiyear snow depth measurements at 55 snow gauges in Austria, resulting in a correction term of approximately $+12\%\,(100\,\text{m})^{-1}$ for solid precipitation. Regardless of the origin of the

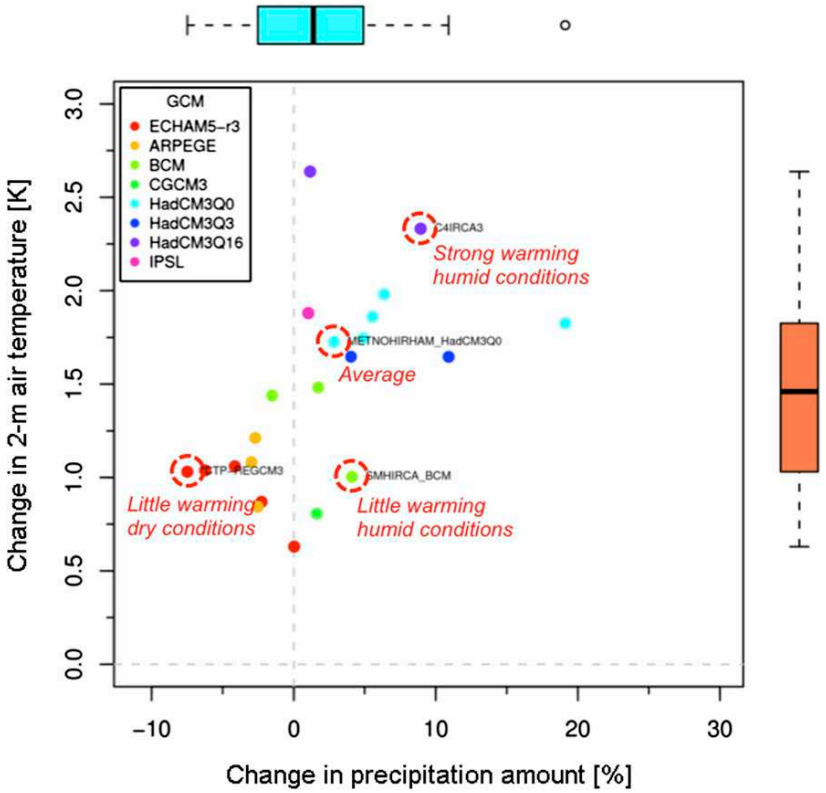

FIG. 3. Climate change signal of the different realizations of the A1B scenario as provided by the ENSEMBLES project for the whole province of Styria and the winter half-year (November–April). The change signal has been calculated by comparing the simulations for the period 1971–2000 to 2021–50; dashed circles mark the realizations considered in this study.

meteorological data, a meteorological preprocessor in AMUNDSEN is used to spatially interpolate the point information from the station locations to the model domain for every model time step of 3 h. In case of temperature and precipitation, topographic corrections are carried out by applying monthly temperature lapse rates and elevation adjustment factors, respectively, as described in detail by Marke (2008). Snow and rain are then distinguished using a wet-bulb temperature threshold of 2°C. Humidity is regionalized by first converting from relative humidity to dewpoint temperature, and then applying dewpoint temperature lapse rates for

TABLE 1. The four realizations of the A1B scenario selected for this study. The change signal has been calculated on the basis of RCM raw data for the winter half-year (November–April) by comparing the periods 1971–2000 and 2021–50 and considering all RCM raster elements with center coordinates in the Schladming region.

Institution	GCM	RCM	Temp change (K)	Precipitation change (%)
Abdus Salam International Centre for Theoretical Physics (ICTP)	ECHAM5-r3	Regional Climate Model, version 3 (RegCM3)	+1.0	−4.5
Swedish Meteorological and Hydrological Institute (SMHI)	Bergen Climate Model (BCM)	Rossby Center Regional Atmospheric Model (RCA)	+1.1	+2.0
Norwegian Meteorological Institute (METNO)	Hadley Centre Coupled Model, version 3, Q0 (HadCM3Q0)	High Resolution Atmospheric Model (HiRAM)	+1.7	+4.0
Community Climate Change Consortium for Ireland (C4I)	Hadley Centre Coupled Model, version 2, Q16 (HadCM2Q16)	Rossby Center Regional Atmospheric Model 3 (RCA3)	+2.6	+6.5

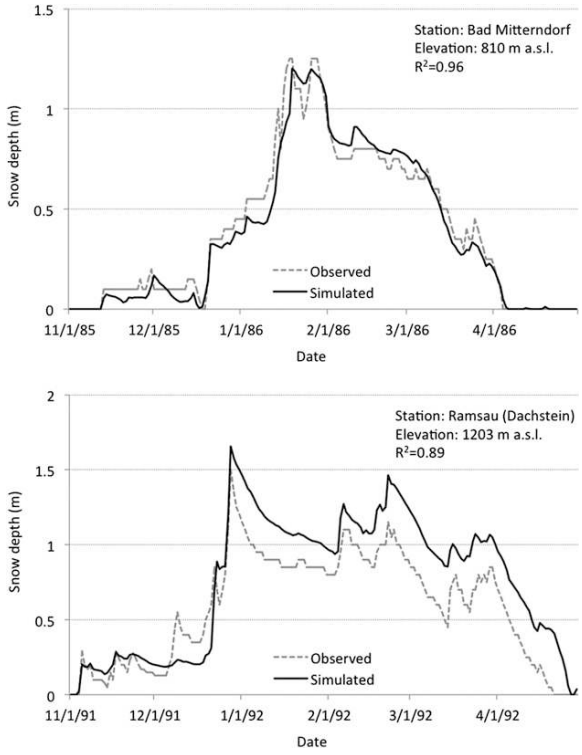

FIG. 4. Comparison of simulated and observed snow depth at stations (top) Bad Mitterndorf (1985/86) and (bottom) Ramsau am Dachstein (1991/92).

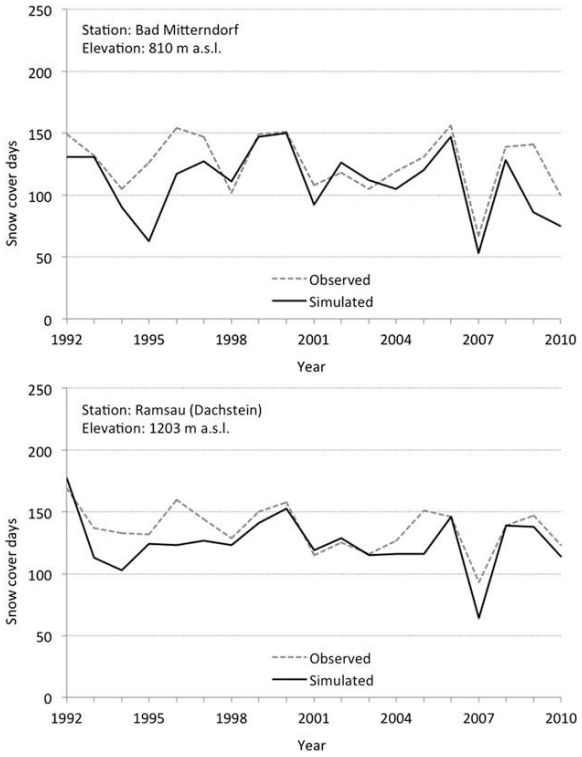

FIG. 5. Comparison of simulated and observed number of snow cover days (1992–2010) at stations (top) Bad Mitterndorf and (bottom) Ramsau am Dachstein.

altitudinal corrections, before a reconversion to relative humidity is carried out (see Marke 2008). The latter is necessary as relative humidity shows a nonlinear temperature dependence, while dewpoint temperature decreases linearly with increasing terrain elevation (Liston and Elder 2006b). Wind speed is corrected for terrain elevation using a linear regression function derived from the station data for a given model time step (see Strasser 2008). Global radiation is spatially distributed by inverting a cloud factor from global radiation at the station locations, which is later used to reduce simulated potential direct and diffuse solar radiation separately. Within the calculation of global radiation, topographic slope, aspect, as well as orographic shadowing and multiple reflection from clouds and surrounding snow covered slopes are taken into account (Strasser 2008).

3. Results

a. *Model validation*

The model chain has been validated by using station recordings as meteorological input for the snow model and comparing modeled snow depths to snow measurements at different stations of the ZAMG station network in a first step. Such validation on the basis of simulated snow depth is quite demanding, as the correct reproduction of snow depth requires both an accurate simulation of snow water equivalent and a precise estimate of actual snow density. Figure 4 shows the model performance exemplarily for the stations Bad Mitterndorf (810 m MSL) and Ramsau am Dachstein (1203 m MSL). As the evaluation at Bad Mitterndorf shows, the snow model is capable of reproducing observed snow depths with good accuracy, which is indicated by the degree of accordance between the two lines as well as by the coefficient of determination (R^2 = 0.96). While the coefficient of determination is high in the case of station Ramsau am Dachstein as well (R^2 = 0.89), a certain overestimation can be observed that sets in late December 1991 and persists until the end of the season. It should, however, be kept in mind that such deviations can be the result of single rainfall events, which might have been misinterpreted by the model as snowfall.

As the number of snow cover days (defined as days with SWE values >1 mm) will serve as an indicator for the analysis of changes in future snow conditions in a later section of this study, Fig. 5 gives an overview of

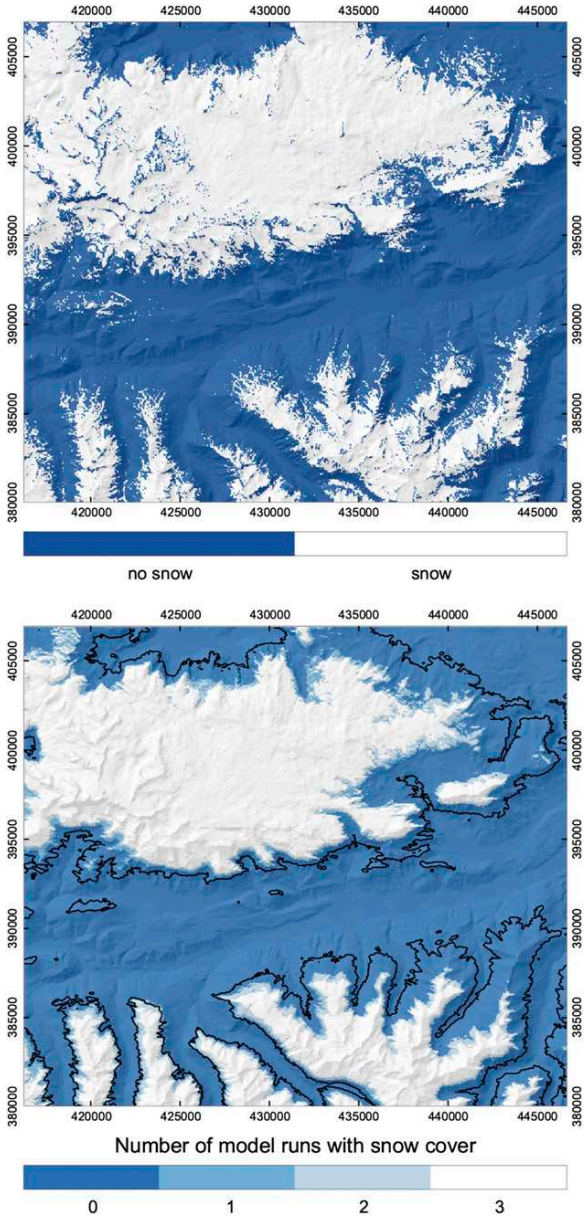

FIG. 6. Comparison of (top) remotely sensed and (bottom) calculated snow distributions for 26 April 2000. Black contours (bottom) indicate the snow distribution obtained by driving the snow model with station data, while the white to blue colors represent the number of RCM-driven model runs (including the ICTP, SMHI, and METNO runs) that have predicted the presence of snow for each raster cell of $50 \times 50\,m^2$. The numbers framing the two plots represent grid coordinates (m; coordinate reference system MGI/Austria Lambert).

model performance in terms of an accurate reproduction of observed number of snow cover days at the two station locations. While considerable deviations between the observed and simulated number of snow cover days exist for single years, particularly in the case of station Bad Mitterndorf (>50 days in 1995), the general dimensions at both stations are reasonably reproduced over climatological periods. Existing deviations between simulations and observations can at least partly be traced back to errors in the applied precipitation input data, which consists of hourly observations aggregated to 3-hourly values prior to model application. In the case of station Bad Mitterndorf, a comparison of observed hourly precipitation to observed daily precipitation at the same station (not shown here) revealed an underestimation of annual precipitation $O(35\%)$ in the hourly data for the year 1995. As this bias in precipitation recordings affects the simulations with station observations as meteorological input only, it does not compromise the results achieved with downscaled RCM simulations and hence does not induce biases in the climate change impact analysis.

To analyze the model's capabilities in the reproduction of snow patterns in the model domain, calculated snow distributions have been compared to remotely sensed snow distributions [classified *Landsat-7* Enhanced Thematic Mapper Plus (ETM+) images using the normalized difference snow index (NDSI) (Hall et al. 1995) for the snow/no snow classification] in a second validation step. Thresholds for the snow classification were NDSI > 0.4 and SWE > 1 mm. Besides the application of station data as drivers for the snow model, RCM hindcast simulations have been included in the validation procedure illustrated in Fig. 6. The term "hindcast" thereby describes a model setup in which the RCMs are driven by observed climate conditions (reanalysis data) at the boundaries of the model domains to evaluate their performance under best possible boundary conditions. This allows one to isolate the effect that results from substituting station data with RCM simulations. As Fig. 6 (bottom) shows, driven with station data (black contour), AMUNDSEN allows simulation of the actual snow distribution with good accuracy with only a slight tendency to overestimate snow cover toward lower elevations. The analysis of the different RCM-driven model runs, excluding the C4I run (white to blue colors in Fig. 6, bottom), reveals that snow distributions in the higher elevated parts of the study region are well reproduced using RCM hindcast data as input for the snow model, whereas the results in the midelevated parts of the Schladming region differ from the remotely sensed data and the station data–driven model run.

Table 2 gives a more comprehensive overview of the performance of the coupled model system for the different hindcast runs based on the efficiency criteria $F^{\langle 1\rangle}$, $F^{\langle 2\rangle}$, and $F^{\langle 3\rangle}$ (Aronica et al. 2002):

TABLE 2. Model performance obtained by comparing remotely sensed and simulated snow distributions for 26 April 2000.

	Model run		
	$F^{\langle 1\rangle}$	$F^{\langle 2\rangle}$	$F^{\langle 3\rangle}$
Station run	0.826	0.710	0.670
C4I	0.678	0.291	0.338
ICTP	0.839	0.672	0.860
METNO	0.854	0.707	0.932
SMHI	0.823	0.628	0.756

$$F^{\langle 1\rangle} = \frac{\sum_{i=1}^{n} P_i^{D_0M_0} + \sum_{i=1}^{n} P_i^{D_1M_1}}{n}, \tag{8}$$

$$F^{\langle 2\rangle} = \frac{\sum_i P_i^{D_1M_1}}{\sum_i P_i^{D_1M_1} + \sum_i P_i^{D_1M_0} + \sum_i P_i^{D_0M_1}}, \quad \text{and} \tag{9}$$

$$F^{\langle 3\rangle} = 1 - \frac{\left|\sum_i P_i^{D_0M_1} - \sum_i P_i^{D_1M_0}\right|}{\sum_i P_i^{D_1M_1} + \sum_i P_i^{D_1M_0}}, \tag{10}$$

where $P_i^{D_1M_1}$ takes a value of 1 for a pixel i where both data (D) and model (M) are classified as snow covered, $P_i^{D_0M_0}$ is where both are snow-free, and $P_i^{D_0M_1}$ and $P_i^{D_1M_0}$ are where one is snow covered and the other is snow-free. As the performance of the different RCM-driven model runs can be separately analyzed by means of Table 2, the C4I run has not been excluded here. All three measures have a maximum value of 1, corresponding to a perfect fit between observations and model. Regarding $F^{\langle 1\rangle}$, which is the fraction of pixels correctly classified by the model, all RCM-driven runs except the C4I run show a comparable or even slightly higher performance than the station data–driven run. For $F^{\langle 2\rangle}$, which is the fraction of correctly classified pixels among the set of pixels that are classified as snow covered in either the observations or the simulations, the station run and the METNO run show the best performance. The METNO run also shows the highest $F^{\langle 3\rangle}$ value, which is a measure of how close the total observed and the total simulated snow-covered area match.

The simulation of technical snow has been validated for an exemplary ski area in the Schladming region, where information on actual snowmaking hours and season length has been provided by the operators of the ski area. From a modeling perspective, the indicator ski season length has been defined in the CC-Snow projects as the number of days between the ski opening (SWE > 120 mm after 1 November for at least 5 consecutive days) and the ski closing (SWE < 80 mm for at least 10 consecutive days between the opening and 30 April). Figure 7 shows calculated snowmaking hours for the period 1986–2011, as calculated on the basis of interpolated meteorological station recordings in comparison to observed snowmaking hours. As can be seen, the validation suffers from a lack of available observations (blue line). Taking a closer look at the winter seasons 2009/10 and 2010/11, the daily number of snowmaking hours seem to be well reproduced for the 2009/10 season, while a distinct overestimation can be observed in December 2010/11. The latter can be explained by the extraordinarily cold preseason (October–December) in 2010, which led to optimal conditions for snow production. While in reality, perfect snow conditions had been achieved until early December and production had been reduced accordingly, the model approach still produced as much snow as possible, as defined by the implemented set of management rules received from the local practitioners (see section 2b). Considering the model's capability to reproduce observed ski season lengths, Fig. 8 shows that the general dimension of ski season length is well reproduced by the model (red line),

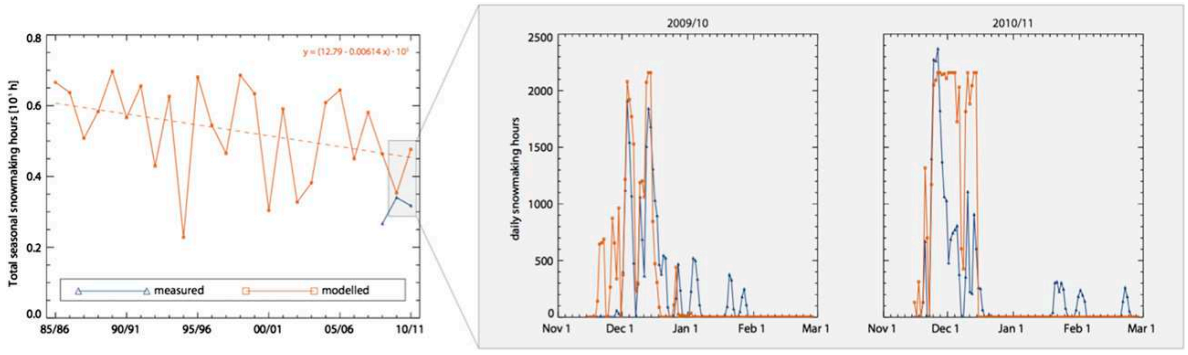

FIG. 7. Snowmaking hours (1985–2011) simulated on the basis of meteorological station recordings in comparison to available observations.

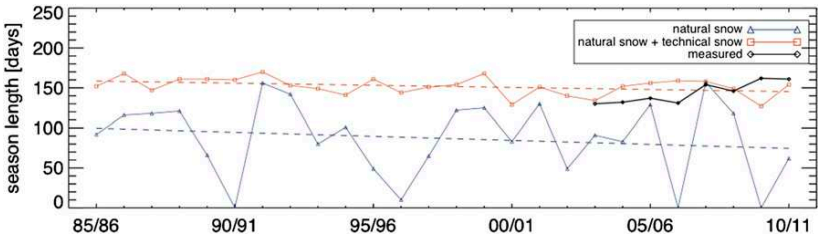

FIG. 8. Ski season length (1985–2011) simulated on the basis of meteorological station recordings in comparison to available observations.

although deviations O(5–30 days) can be observed. Here, it has to be kept in mind that the pragmatic approach for snow production assumes the current number and technology for the snow guns, which might not reflect the actual conditions in the ski areas in the past. Particularly distinct is the strong variability of the ski season length calculated for natural snow conditions only (blue line in Fig. 8), which clearly illustrates the general necessity for technical snow production in the considered ski area.

b. Scenario results

As the capabilities of the coupled model system with respect to the reproduction of snow conditions in the study region could be successfully demonstrated in the previous paragraphs, the change in snow conditions calculated on the basis of three different realizations of the A1B scenario will be discussed in the following. Here, the RCMs are driven by GCM-simulated climate data at the boundaries of the model domain (Europe), which includes the changes in atmospheric greenhouse gas concentrations as defined for the A1B scenario. Figure 9 (top) shows the mean number of snow cover days in the winter season (November–April) for the reference period 1971–2000 as simulated on the basis of three GCM–RCM realizations. Naturally, the number of days with snow cover is highest in the summit regions (snow cover over all 6 considered months) and lowest in the lower elevated valleys (2 months of snow cover). While the results of all realizations agree in the higher elevated parts of the study region (see circles indicating the standard deviation of the model runs), a certain spread between the realizations can be observed that is highest in the lower elevations of the valleys. The decrease in the mean number of snow cover days (1971–2000 versus 2021–50) displayed in Fig. 9 (bottom) with <5 days is lowest in the higher elevated parts and increases with decreasing terrain elevation to 25–30 days in part of the midelevated regions. In the lower elevations of the valleys, the decrease with <25 days is less distinct as a result of the frequent occurrence of temperature inversions. Again, differences between the realizations are comparatively small in the summit regions, whereas larger differences exist in lower elevations. An important question to be addressed is whether there is a significant tendency for the shortening of the snow cover period to occur at the beginning or at the end of the winter season. To answer this question, changes in the snow cover period have been analyzed separately for the different realizations and different elevation belts. As Fig. 10 clearly indicates, it largely depends on the realization of whether the shortening of the snow covered period is located at the beginning or at the end of the winter season—this holds true over the whole range of altitudes. Analogously to Fig. 9, Fig. 11 shows the mean ski season length (1971–2000) and the change in the mean season length (1971–2000 versus 2021–50) for the Schladming region. Other than the number of snow cover days, the indicator ski season length describes whether snow conditions allow skiing in the ski areas and hence provides tourism-relevant information on whether the ski areas could be continuously opened or not. As observed for the number of snow cover days, ski season length is highest in the summit regions (180 days) and lowest in the valleys (close to 0). The decrease in the ski season length ranges from a few days in the valleys to over 35 days in the midelevations to <5 days in the higher elevated parts (see Fig. 11, bottom). In the case of ski season length, it is the short season length in the reference run that limits the potential for decrease in the lower elevations and valleys in the scenario period. While skiing is possible in these elevations in the reference period for single years, the meteorological conditions provided by all considered RCMs do not allow skiing in the scenario period, leading to a spread between the different realizations of close to 0.

The temporal evolution of the mean ski season length and the mean development in different elevation ranges are illustrated for the Schladming region in Fig. 12. While no significant trend can be observed in the average of all model runs until 2000, a distinct decrease of $\sim$2.6 days decade^{-1} manifests over the total period from 1961 to 2050 (see Fig. 12, top). Considering changes of the ski season length over the range of altitudes in the study area, the snow model runs with application of most

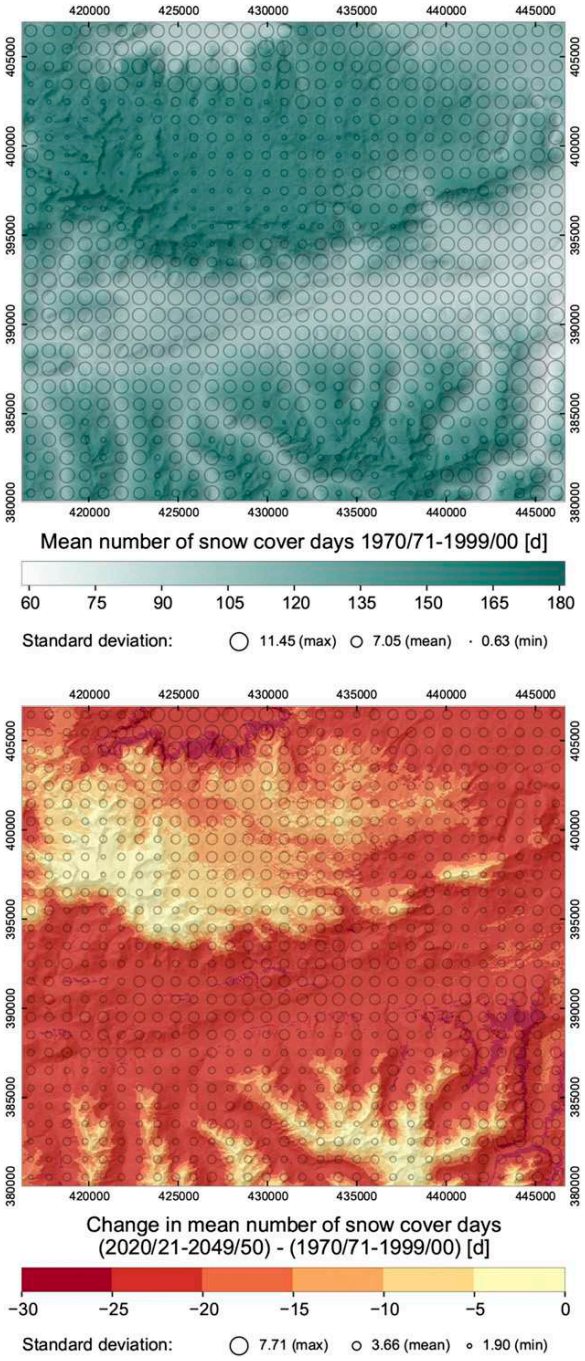

FIG. 9. (top) Mean number of snow cover days (November–April) for the reference period (1971–2000) as simulated with AMUNDSEN on the basis of three realizations (including the ICTP, SMHI, and METNO runs) and (bottom) change in snow cover days (1971–2000 vs 2021–50) in the Schladming region. The numbers framing the two plots represent grid coordinates (m; coordinate reference system MGI/Austria Lambert).

GCM–RCM combinations describe a most severe decrease of 30–40 days in elevations between 1600 and 2700 m MSL. While the moderate values of ski season length simulated for the reference period in elevations below 1600 m MSL somehow limit the potential for decrease and hence lead to comparatively small absolute decreases in these elevations, above 2700 m MSL it is the naturally low temperatures in combination with increasing winter precipitation that attenuate the decrease in ski season length.

Figures 9–12 provide a good overview of changes in natural snow conditions in the study area; however, the analysis of climate change impacts in the Austrian ski areas requires a closer look at the local conditions at the ski slopes as well as the consideration of technical snow production. To do so, the described pragmatic snowmaking approach has been applied for the simulation of snow production in an exemplary ski area in the Schladming region. The temporal evolution of actual seasonal snow production hours, produced snow amounts, and the ski season length calculated for natural snow conditions only, as well as for natural and technical snow, are illustrated in Fig. 13. Snowmaking hours show almost no trend over the period 1961–2050, which suggests that technical snow is produced over almost the same number of hours in the past and the future. However, considering the amount of technically produced snow (Fig. 13, middle), a certain decrease unfolds from the line plot. As the efficiency of snow production is calculated as a function of wet-bulb temperature [see Eq. (5)], and hence depends on air humidity and air temperature, our results suggest that snow production can be expected to become less efficient in the future. The temporal evolution of the ski season length calculated on the basis of natural snow (black line) in Fig. 13 (bottom) indicates a decrease of the ski season length for the considered ski area from >50 days at present to ~40 days in the 2050s in the case of natural snow. Making use of technical snow production (red line), the ski season can be prolonged by ~80 days, resulting in a reduction of the ski season length from ~140 days at present to ~120 days at the end of the scenario period. Please note that technical snow is produced assuming today's snow production infrastructure (canon number and technical specifications). This has to be taken into account when interpreting the results for the past (no/less technical snow production with less advanced technical equipment) and the future (technical advances not considered).

4. Discussion and conclusions

A hydrometeorological model chain has been applied to generate scenarios of future natural and artificial snow conditions for a study site in Styria (Austria). To

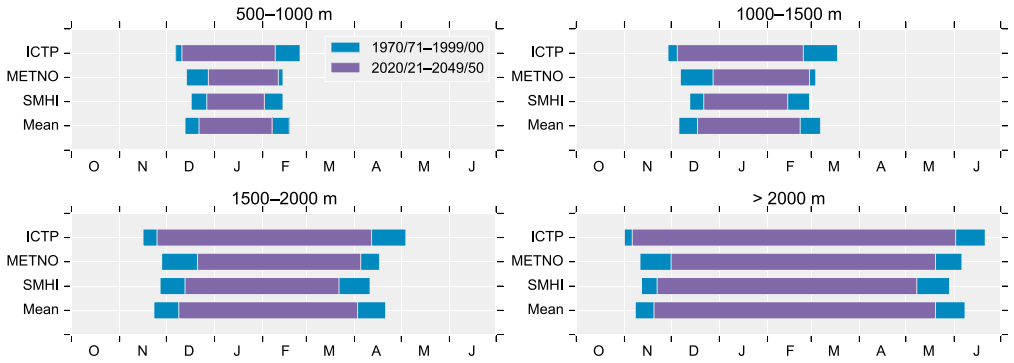

FIG. 10. Change in the length of the snow-covered period (longest period with SWE values above 1 mm) for different elevation belts according to the three realizations of the A1B scenario (including the ICTP, SMHI, and METNO runs).

cover a wide range of potential future climate conditions, four realizations of the A1B scenario have been statistically refined to the location of various meteorological stations in the study region. However, owing to the poor skills in the reproduction of past climate and snow conditions in the considered region, one realization had to be removed from the selection to avoid biases in the climate change impact analysis. Since the applied physically based snow model has originally been designed for the simulation of natural snow conditions, a pragmatic approach has been developed for the simulation of technical snow production. Following a comprehensive validation at both the point and regional scale, the snow model has been utilized to spatially interpolate the downscaled and bias-corrected RCM data and to calculate snow distributions for the period 1961–2050. Considering natural snow conditions in the Schladming region, the comparison of the scenario results (2021–50) to those for a reference period (1971–2000) has revealed severe decreases in the number of snow cover days and the ski season length of up to >25 and >35 days, respectively. Both indicators show most severe decreases in midelevations, which corresponds to the findings of other studies (e.g., Formayer et al. 2009; Steiger 2010). In the case of the indicator ski season length, the analysis of changes in different elevation belts has shown highest decreases O(40 days) in elevations between 1600 and 2700 m, with a mean decrease rate of ~2.6 days decade^{-1} as the average over all elevations and realizations. With respect to a tendency of the shortening of the snow cover period to occur at the beginning or at the end of the winter season, a large spread between the different realizations has been observed with no significant tendency toward the beginning or end of the winter season in the average of all model runs. Applying the presented snow production approach in an exemplary ski area in the Schladming region, the number of hours used for snow production, the amount of technically produced snow, and the resulting ski season length have been calculated. While no significant trend could be found in the number of actual snowmaking hours, a decrease in produced snow amounts could be extracted from the scenario results. Based on these results, it can be concluded that technical snow production might become less effective in the future. In the exemplary ski area considered, the season length calculated for natural snow conditions decreases by ~3.2 days decade^{-1}, which leads to a reduction from >50 days at present to ~40 days in the 2050s. The decrease rate is only slightly higher including technical snow production (~4.1 days decade^{-1}); however, snow production prolongs the season by ~80 days, still allowing a ski season length of ~120 days in the considered area in 2050. Please note that these findings are based on an approach that makes several assumptions that might not reflect the actual conditions on the ski slopes. While snow guns are assumed to be equally distributed over the slopes, in reality, lower-elevated parts often show higher snow gun densities than the (with respect to natural snow conditions favored) summit regions. Moreover, number and technical specifications (e.g., efficiency, water and energy consumption, and maximum water throughflow rates) of the snow guns reflect present-day conditions and average characteristics of present-generation technical instrumentation, respectively. Even if technical snow would have been as intensively produced in the past as it is today, technical infrastructure would have been less advanced; both of these restrictions suggest that, although not detectable owing to a lack of observations, snow production calculated for the early reference period is overestimated. On the other hand, the technical advances that can be expected for the coming decades (e.g., higher efficiency, less water and energy consumption, and snow production

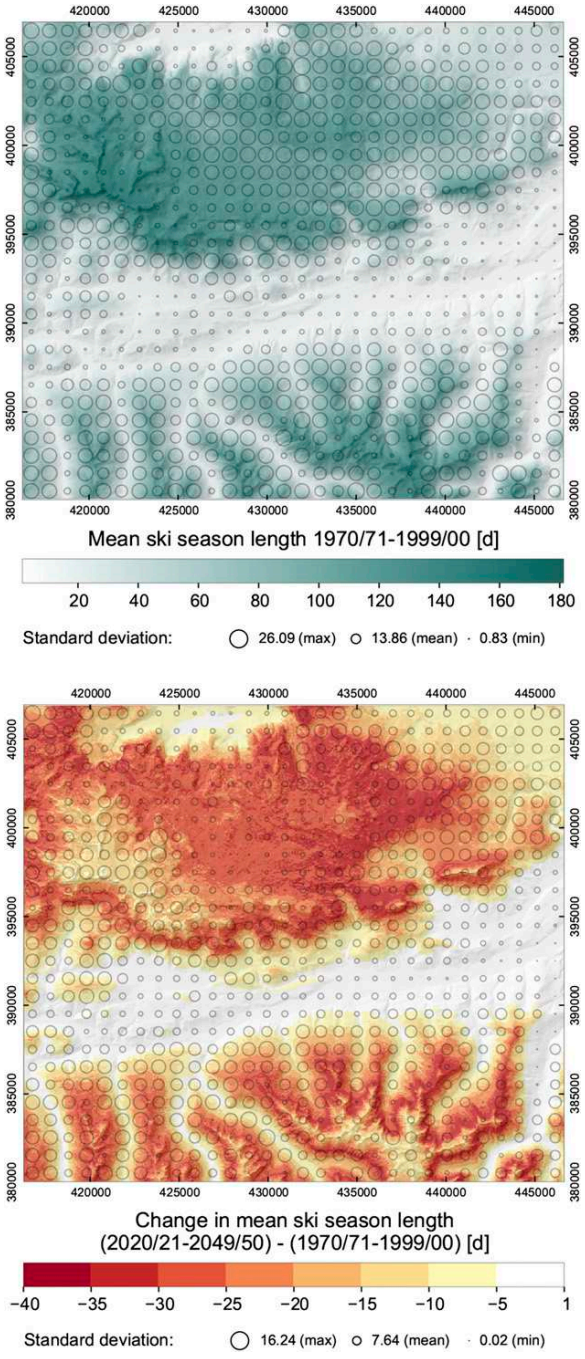

FIG. 11. (top) Ski season length in the Schladming region simulated on the basis of the three realizations (including the ICTP, SMHI, and METNO runs) and (bottom) change in ski season length. The numbers framing the two plots represent grid coordinates (m; coordinate reference system MGI/Austria Lambert).

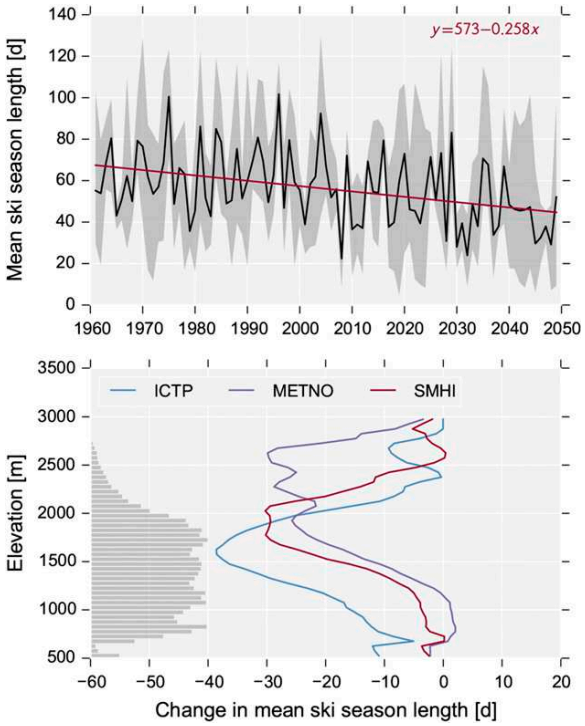

FIG. 12. (top) Temporal evolution of the ski season length simulated on the basis of the three realizations (including the ICTP, SMHI, and METNO runs) and (bottom) elevation dependence of the change signal. The black line and the dark gray area (top) represent the average of all model runs and the minimum and maximum within the realizations, respectively. The gray bars (bottom) show the relative size of the respective elevation classes.

at higher temperatures) have not been considered in the scenario simulations—this might result in an underestimation of technical snow production in the simulations for the future. Of course, the management rules implemented in the model also induce uncertainties and might be subject to change in the future. Finally, it has to be remarked that the present study does consider the pumping capacities of snow-making infrastructure in the ski areas, but it assumes future water availability for technical snow production to be unlimited. While Austria does not suffer water scarcity at present, future water availability and demand will regulate to what extent these conditions remain unchanged. At present, water for snow production in the considered ski area is provided by storage ponds (which are filled by precipitation throughout the year) as well as by extracting water from local rivers. Considering the slight decrease in future water consumption for snow production (Fig. 13, middle) in combination with potentially increasing annual precipitation in the region (Prettenthaler 2009), water availability from ponds can be expected to remain more or less

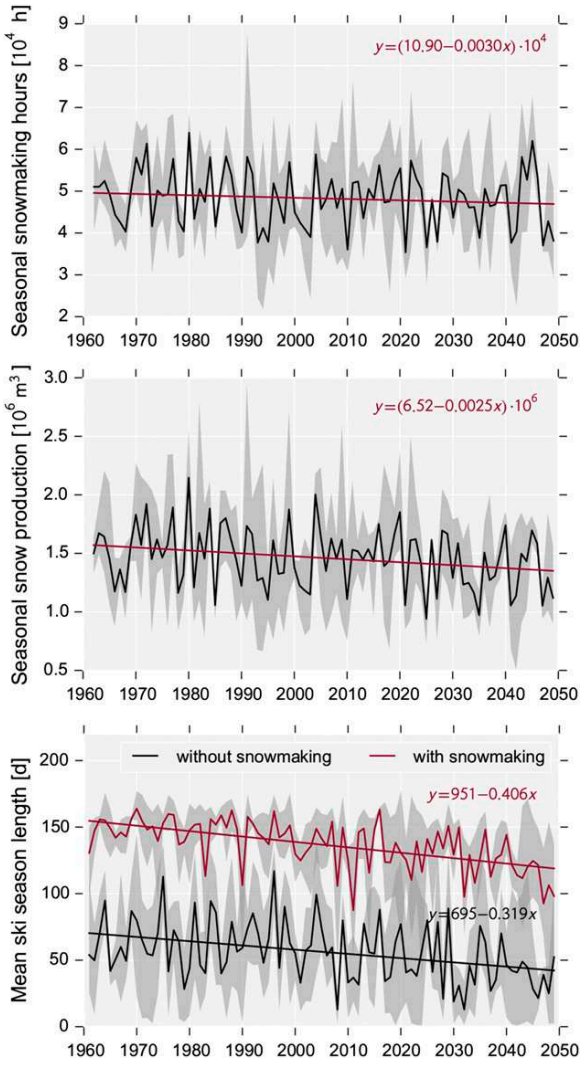

FIG. 13. (top) Temporal evolution of simulated snowmaking hours, (middle) seasonal snow production, and (bottom) ski season length for an exemplary ski area in the Schladming region. The colored lines represent the average of all model runs (including the ICTP, SMHI, and METNO runs), and gray areas represent the minimum and maximum within the realizations.

unchanged. Water extraction from rivers for snowmaking purposes is usually carried out during winter, when water levels are naturally low in the study region. Existing studies have shown that winter low flows in the region are likely to increase on the order of +20% up to the year 2050 because of the combined effect of increasing winter precipitation and rising winter temperatures (BMLFUW 2010). Still, it will depend on a variety of factors, such as the coordination between the main water users (here mainly the skiing and the energy production industry) and ecological aspects, such as minimum ecological flow regulations, as to whether future water extraction from local rivers will be possible to the same extent as today. Both potential conflicts in water utilization and regulatory frameworks are hard to predict and thus have not been considered in this study.

To overcome part of the deficiencies described above, a more sophisticated approach for snow production has recently been developed and is currently being validated. The latter accounts for the individual technical specifications and positions of the snow guns on ski slopes and therefore allows a detailed, snow-gun-based calculation of snow production as well as energy and water consumption. Furthermore, it provides the option to apply a variety of management strategies (e.g., the demand-driven transfer of snow guns to different parts of the skiing slopes, or an increased efficiency of the snow guns). Finally, it considers water losses during the snowmaking process owing to sublimation and evaporation as well as the specific properties of technically produced snow (e.g., the higher initial density, the higher densification rate and the more rapid albedo decline). First tests have revealed that this more sophisticated approach performs better, both on a daily and on a seasonal basis.

The results presented in this paper build a basis for a subsequent analysis of climate change impacts on the Austrian skiing business economy and winter tourism, as has been done in the follow-up project CC-Snow II. The coupled modeling approach applied in this study represents a part of an inter- and transdisciplinary integration design described in detail by Strasser et al. (2014). For the cost–benefit analysis carried out as part of the economic analyses, the water and energy consumption is determined by the actual snow production and the specifications of the technical instrumentation (water and energy consumed per produced volume snow). The respective scientific findings are currently published. In potential future applications, the developed coupled modeling scheme can be used for applying a variety of potential future climate developments, together with meaningful management options for the ski areas. It will be of high practical and scientific interest—for both the natural sciences and socioeconomics, as well as for practitioners, the community of stakeholders, the skiing industry, and policy makers—to jointly develop feasible, realistic, and coupled scenarios of future conditions for the skiing tourism sector in a highly participative process.

Acknowledgments. The work presented here could not have been realized without the support of all partners and colleagues participating in the CC-Snow projects. Special thanks go to Ulli Vilsmaier for organizing various stakeholder interviews. The authors also thank Robert Steiger for supporting the development of the snow production approach with his expert knowledge on

the snowmaking practice in the Austrian ski areas. Financial funding for the present study has kindly been provided by the Climate and Energy Fund of the Austria Climate Research Programme. Finally, the authors thank the Faculty of Geosciences and Atmospheric Sciences (University of Innsbruck, Austria) for the financial support for this publication.

REFERENCES

Abegg, B., M. Kolb, D. Sprengel, and V. H. Hoffmann, 2008: Klimawandel aus der Sicht der Schweizer Seilbahnunternehmer. *Jahrbuch der Schweizerischen Tourismuswirtschaft 2008,* IDT-HSG, 73–83.

Anderson, E. A., 1976: A point energy and mass balance model of a snow cover. NOAA Tech. Rep. NWS 19, 150 pp.

Aronica, G., P. D. Bates, and M. S. Horritt, 2002: Assessing the uncertainty in distributed model predictions using observed binary pattern information within GLUE. *Hydrol. Processes,* **16,** 2001–2016, doi:10.1002/hyp.398.

Blöschl, G., 1999: Scaling issues in snow hydrology. *Hydrol. Processes,* **13,** 2149–2175, doi:10.1002/(SICI)1099-1085(199910)13:14/15<2149::AID-HYP847>3.0.CO;2-8.

BMLFUW, 2010: Anpassungsstrategien an den Klimawandel für Österreichs Wasserwirtschaft. Public Rep., Bundesministerium für Land- und Forstwirtschaft, Umwelt und Wasserwirtschaft, Vienna, Austria, 486 pp.

Christensen, J. H., and O. B. Christensen, 2007: A summary of the prudence model projections of changes in European climate by the end of this century. *Climatic Change,* **81,** 7–30, doi:10.1007/s10584-006-9210-7.

Cline, D., K. Elder, and R. Bales, 1998: Scale effects in a distributed snow water equivalence and snowmelt model for mountain basins. *Hydrol. Processes,* **12,** 1527–1536, doi:10.1002/(SICI)1099-1085(199808/09)12:10/11<1527::AID-HYP678>3.0.CO;2-E.

Corripio, J. G., 2003: Vectorial algebra algorithms for calculating terrain parameters from DEMs and solar radiation modelling in mountainous terrain. *Int. J. Geogr. Inf. Sci.,* **17,** 1–23, doi:10.1080/713811744.

EEA, 2012: Climate change, impacts and vulnerability in Europe 2012: An indicator-based report. EEA Rep. 12/2012, 300 pp. [Available online at www.eea.europa.eu/publications/climate-impacts-and-vulnerability-2012.]

Elsasser, H., and P. Messerli, 2001: The vulnerability of the snow industry in the Swiss Alps. *Mt. Res. Dev.,* **21,** 335–339, doi:10.1659/0276-4741(2001)021[0335:TVOTSI]2.0.CO;2.

Fierz, C., P. Riber, E. E. Adams, A. C. Curran, P. M. B. Fohn, M. Lehning, and C. Plüss, 2003: Evaluation of snow-surface energy balance models in alpine terrain. *J. Hydrol.,* **282,** 76–94, doi:10.1016/S0022-1694(03)00255-5.

Formayer, H., M. Hofstätter, and P. Haas, 2009: Untersuchung der Schneesicherheit und der potenziellen Beschneiungszeiten in Schladming und Ramsau: Endbericht zum Projekt STRATEGE. BOKU-Met Rep. 11, 48 pp. [Available online at https://meteo.boku.ac.at/report/BOKU-Met_Report_11_online.pdf.]

Fowler, H. J., S. Blenkinsop, and C. Tebaldi, 2007: Linking climate change modelling to impacts studies: Recent advances in downscaling techniques for hydrological modelling. *Int. J. Climatol.,* **27,** 1547–1578, doi:10.1002/joc.1556.

Frei, C., and C. Schär, 1998: A precipitation climatology of the Alps from high-resolution rain-gauge observations. *Int. J. Climatol.,* **18,** 873–900, doi:10.1002/(SICI)1097-0088(19980630)18:8<873::AID-JOC255>3.0.CO;2-9.

Greuell, W., W. Knap, and P. Smeets, 1997: Elevational changes in meteorological variables along a midlatitude glacier during summer. *J. Geophys. Res.,* **102,** 25 941–25 954, doi:10.1029/97JD02083.

Gruber, S., 2007: A mass-conserving fast algorithm to parameterize gravitational transport and deposition using digital elevation models. *Water Resour. Res.,* **43,** W06412, doi:10.1029/2006WR004868.

Hall, D. K., G. A. Riggs, and V. V. Salomonson, 1995: Development of methods for mapping global snow cover using moderate resolution imaging spectroradiometer data. *Remote Sens. Environ.,* **54,** 127–140, doi:10.1016/0034-4257(95)00137-P.

Hanzer, F., T. Marke, and U. Strasser, 2014: Distributed, explicit modelling of technical snow production for a ski area in the Schladming region (Austrian Alps). *Cold Reg. Sci. Technol.,* doi:10.1016/j.coldregions.2014.08.003, in press.

Hewitt, C. D., and D. J. Griggs, 2004: Ensembles-based predictions of climate changes and their impacts. *Eos, Trans. Amer. Geophys. Union,* **85,** 566, doi:10.1029/2004EO520005.

Hinzman, L. D., D. L. Kane, C. S. Benson, and K. R. Everett, 1996: Energy balance and hydrological processes in an Arctic watershed. *Landscape Function: Implications for Ecosystem Response to Disturbance: A Case Study in Arctic Tundra,* J. F. Reynolds and J. D. Tenhunen, Eds., Ecologic Studies Series, Vol. 120, Springer, 131–154, doi:10.1007/978-3-662-01145-4_6.

Hock, R., 2003: Temperature index melt modelling in mountain areas. *J. Hydrol.,* **282,** 104–115, doi:10.1016/S0022-1694(03)00257-9.

Jordan, R., 1991: A one-dimensional temperature model for a snow cover: Technical documentation for SNTHERM.89. Tech. Rep., Cold Regions Research and Engineering Laboratory, Hanover, NH, 61 pp.

Kane, D., L. D. Hinzman, C. S. Benson, and G. E. Liston, 1991: Snow hydrology of a headwater Arctic basin: 1. Physical measurements and process studies. *Water Resour. Res.,* **27,** 1099–1109, doi:10.1029/91WR00262.

Kirnbauer, R., G. Blöschl, and D. Gutknecht, 1994: Entering the era of distributed snow models. *Nord. Hydrol.,* **25,** 1–24.

Klemes, V., 1990: The modelling of mountain hydrology: The ultimate challenge. *IAHS Publ.,* **190,** 29–43. [Available online at http://iahs.info/uploads/dms/iahs_190_0029.pdf.]

Liston, G. E., 2004: Representing subgrid snow cover heterogeneities in regional and global models. *J. Climate,* **17,** 1381–1397, doi:10.1175/1520-0442(2004)017<1381:RSSCHI>2.0.CO;2.

——, and K. Elder, 2006a: A distributed snow-evolution modeling system (SnowModel). *J. Hydrometeor.,* **7,** 1259–1276, doi:10.1175/JHM548.1.

——, and ——, 2006b: A meteorological distribution system for high-resolution terrestrial modeling (MicroMet). *J. Hydrometeor.,* **7,** 217–234, doi:10.1175/JHM486.1.

Loibl, W., A. Beck, M. Dorninger, H. Formayer, A. Gobiet, and W. Schöner, Eds., 2007: Kwiss-Programm reclip:more research for climate protection: Model run evaluation, Project Year 3 Rep. 2006, ARC-sys-0122, 73 pp. [Available online at http://foresight.ait.ac.at/SE/projects/reclip/reports/ARC-sys-reclip_more_PJ3rep.pdf.]

Luce, C. H., D. G. Tarboton, and K. R. Cooley, 1998: The influence of the spatial distribution of snow on basin-averaged snowmelt. *Hydrol. Processes,* **12,** 1671–1683,

doi:10.1002/(SICI)1099-1085(199808/09)12:10/11<1671::AID-HYP688>3.0.CO;2-N.

Marke, T., 2008: Development and application of a model interface to couple land surface models with regional climate models for climate change risk assessment in the upper Danube watershed. Ph.D. thesis, Ludwig Maximilians University, 188 pp.

——, W. Mauser, A. Pfeiffer, and G. Zängl, 2011a: A pragmatic approach for the downscaling and bias correction of regional climate simulations: Evaluation in hydrological modeling. *Geosci. Model Dev.,* **4,** 759–770, doi:10.5194/gmd-4-759-2011.

——, ——, ——, ——, and D. Jacob, 2011b: The effect of downscaling on river runoff modeling: A hydrological case study in the upper Danube watershed. *Hydrol. Earth Syst. Sci. Discuss.,* **8,** 6331–6384, doi:10.5194/hessd-8-6331-2011.

Marks, D., 1988: Climate, energy exchange, and snowmelt in Emerald Lake watershed, Sierra Nevada. Ph.D. thesis, University of California, Santa Barbara, 158 pp.

Marsh, P., 1999: Snowcover formation and melt: Recent advances and future prospects. *Hydrol. Processes,* **13,** 2117–2134, doi:10.1002/(SICI)1099-1085(199910)13:14/15<2117::AID-HYP869>3.0.CO;2-9.

Mauser, W., and R. Ludwig, 2002: GLOWA DANUBE: A research concept to develop integrative techniques, scenarios and strategies regarding the global change of the water cycle. *Climatic Change: Implications for the Hydrological Cycle and for Water Management,* M. Beniston, Ed., Advances in Global Change Research, Vol. 10, Springer, 171–188, doi:10.1007/0-306-47983-4_10.

Nakicenovic, N., and R. Swart, Eds., 2000: *Special Report on Emissions Scenarios.* Cambridge University Press, 570 pp.

Nešpor, V., and B. Sevruk, 1999: Estimation of wind-induced error of rainfall gauge measurements using a numerical simulation. *J. Atmos. Oceanic Technol.,* **16,** 450–464, doi:10.1175/1520-0426(1999)016<0450:EOWIEO>2.0.CO;2.

Olefs, M., A. Fischer, and J. Lang, 2010: Boundary conditions for artificial snow production in the Austrian Alps. *J. Appl. Meteor. Climatol.,* **49,** 1096–1113, doi:10.1175/2010JAMC2251.1.

Prein, A. F., A. Gobiet, and H. Truhetz, 2011: Analysis of uncertainty in large scale climate change projections over Europe. *Meteor. Z.,* **20,** 383–395, doi:10.1127/0941-2948/2011/0286.

Prettenthaler, F., 2009: Der Klimawandel als Herausforderung fr den steirischen Tourismus - Fokus Wintertourismus. InTeReg Research Rep. 04-2009, 18 pp. [Available online at www.linder-gruber.at/de/newsletter/druckversion/Joaneum_Klimawandel_Studie.pdf.]

Rohrer, M. B., 1992: *Die Schneedecke im Schweizer Alpenraum und ihre Modellierung.* Züricher Geographische Schriften, Vol. 49, Geographisches Institut, Eidgenössische Technische Hochschule Zürich, 178 pp.

Schmidt, P., R. Steiger, and A. Matzarakis, 2012: Artificial snowmaking possibilities and climate change based on regional climate modeling in the southern black forest. *Meteor. Z.,* **21,** 167–172, doi:10.1127/0941-2948/2012/0281.

Scott, D., G. McBoyle, and B. Mills, 2003: Climate change and the skiing industry in southern Ontario (Canada): Exploring the importance of snowmaking as a technical adaptation. *Climate Res.,* **23,** 171–181, doi:10.3354/cr023171.

——, ——, and A. Minogue, 2007: Climate change and Quebec's ski industry. *Global Environ. Change,* **17,** 181–190, doi:10.1016/j.gloenvcha.2006.05.004.

Steiger, R., 2010: The impact of climate change on ski season length and snowmaking requirements in Tyrol, Austria. *Climate Res.,* **43,** 251–262, doi:10.3354/cr00941.

Strasser, U., 2008: Modelling of the mountain snow cover in the Berchtesgaden National Park. Research Rep. 55, 184 pp.

——, and T. Marke, 2010: ESCIMO.spread—A spreadsheet-based point snow surface energy balance model to calculate hourly snow water equivalent and melt rates for historical and changing climate conditions. *Geosci. Model Dev.,* **3,** 643–652, doi:10.5194/gmd-3-643-2010.

——, J. G. Corripio, B. Brock, F. Pellicciotti, P. Burlando, and M. Funk, 2004: Spatial and temporal variability of meteorological variables at Haut Glacier d'Arolla (Switzerland) during the ablation season 2001: Measurements and simulations. *J. Geophys. Res.,* **109,** D03103, doi:10.1029/2003JD003973.

——, M. Bernhardt, M. Weber, G. E. Liston, and W. Mauser, 2008: Is snow sublimation important in the alpine water balance? *Cryosphere,* **2,** 53–66, doi:10.5194/tc-2-53-2008.

——, M. Warscher, and G. E. Liston, 2011: Modeling snow canopy processes on an idealized mountain. *J. Hydrometeor.,* **12,** 663–677, doi:10.1175/2011JHM1344.1.

——, and Coauthors, 2014: Coupled numerical modelling for inter- and transdisciplinary integration in climate change impact research: Dimensions of integration and examples of interface design. *Environ. Modell. Software,* **60,** 180–187, doi:10.1016/j.envsoft.2014.06.014.

Themeßl, M., A. Gobiet, and A. Leuprecht, 2011: Empirical-statistical downscaling and error correction of daily precipitation from regional climate models. *Int. J. Climatol.,* **31,** 1530–1544, doi:10.1002/joc.2168.

——, ——, and G. Heinrich, 2012: Empirical-statistical downscaling and error correction of regional climate models and its impact on the climate change signal. *Climatic Change,* **112,** 449–468, doi:10.1007/s10584-011-0224-4.

Uppala, S. M., and Coauthors, 2005: The ERA-40 reanalysis. *Quart. J. Roy. Meteor. Soc.,* **131,** 2961–3012, doi:10.1256/qj.04.176.

van der Linden, P., and J. F. B. Mitchell, 2009: ENSEMBLES: Climate change and its impacts: Summary of research and results from the ensembles project. Tech. Rep., 160 pp. [Available online at http://ensembles-eu.metoffice.com/docs/Ensembles_final_report_Nov09.pdf.]

Warscher, M., U. Strasser, G. Kraller, T. Marke, H. Franz, and H. Kunstmann, 2013: Performance of complex snow cover descriptions in a distributed hydrological model system: A case study for the high alpine terrain of the Berchtesgaden Alps. *Water Resour. Res.,* **49,** 2619–2637, doi:10.1002/wrcr.20219.

Wilby, R. L., and T. M. L. Wigley, 1997: Downscaling general circulation model output: A review of methods and limitations. *Prog. Phys. Geogr.,* **21,** 530–548, doi:10.1177/030913339702100403.

Wilcke, R. A. I., T. Mendlik, and A. Gobiet, 2013: Multi-variable downscaling and error-correction of regional climate models. *Climatic Change,* **120,** 871–887, doi:10.1007/s10584-013-0845-x.

WMO, 1986: Intercomparison of models of snowmelt runoff. Operational Hydrology Rep. 23/WMO Rep. 646, 442 pp.

Wolfsegger, C., S. Gössling, and D. Scott, 2008: Climate change risk appraisal in the Austrian ski industry. *Tourism Rev. Int.,* **12,** 13–23, doi:10.3727/154427208785899948.

Chapter 4

Distributed, explicit modeling of technical snow production for a ski area in the Schladming region (Austrian Alps)

Florian Hanzer, Thomas Marke, Ulrich Strasser

Published in *Cold Regions Science and Technology* (Volume 108, December 2014, Pages 113–124, doi: 10.1016/j.coldregions.2014.08.003).

My contribution to this article: developing the snowmaking module, setting it up for the study site, performing the model runs, producing the plots, analyzing the results, and writing the article.

Abstract

A module for simulating technical snow production in ski areas coupled to a spatially distributed physically based snow model (AMUNDSEN) is presented. The module explicitly considers individual snow guns and distributes the produced snow along the slopes. The amount of snow produced by each snow gun is a function of the snow gun type, wet-bulb temperature at the snow gun's location, ski area infrastructure (in terms of water supply and pumping capacity), and snow demand. Water losses during snowmaking due to evaporation and sublimation are considered, as well as the distinct properties of technical snow such as the higher density as compared to natural snow. An empirical rule for snow production derived from common snowmaking practices has been implemented, which splits the season into a period of maximum snowmaking and a period of selective on-demand snowmaking. The model is set up for a ski area in the Schladming region (Austrian Alps) using actual snowmaking infrastructure data as model parameters. Model validation is performed for the period 2003–2011 using recordings of snowmaking operations as well as a spatial comparison of remotely sensed and simulated snow-covered area. Simulated total seasonal snowmaking hours and water and energy consumption as well as the ski season length are in good agreement with observations, which indicates that the model is capable of accurately simulating real-world snowmaking operations. The explicit consideration of individual snow guns allows to easily play through different management strategies and changes in snowmaking infrastructure, such as replacing the snow guns with more efficient models, increasing the number of snow guns or concentrating them to certain slope segments, or increasing the capacity of reservoirs.

4.1 Introduction

Winter tourism, most importantly ski tourism, is highly dependent on snow conditions. Natural snow conditions, however, are subject to interannual variability as well as highly sensitive to climate change – rising temperatures lead to less snow precipitation and increased snowmelt, resulting in less reliable snow conditions and a shortening of the ski season. Snowmaking is the main adaptation strategy to these deteriorating natural snow conditions (Scott and McBoyle, 2007), helping to prolong the ski season as well as to guarantee a continuous snow cover during the season. In the Alpine countries, since the installation of the first large-scale snowmaking systems in the mid-1980s, snowmaking has become increasingly important due to the fact that the Alpine region has shown to be particularly affected by climate change – the warming signal since the early 1980s is approximately three-fold amplified as

compared to the global trend (Beniston, 2005). Today, almost half of the total skiable terrain in the Alpine countries is equipped with snowmaking systems (Hanzer, 2013), in elevations ranging from valleys as low as 500 m a.s.l. to glaciers (> 3000 m a.s.l.) (Mayer et al., 2007). Corresponding numbers from other countries range from 12 % in Australia (Pickering and Buckley, 2010) to (varying by region) 50–100 % in Canada (Scott et al., 2003) and 66–100 % in the United States (Scott and McBoyle, 2007). However, snowmaking operations – besides the need for considerable infrastructural investments in terms of piping, pumps, reservoirs, hydrants, snow guns, compressors, cooling towers, etc. – require large amounts of water and energy and are also dependent on meteorological conditions, as snowmaking is only possible in a certain temperature and humidity range and is increasingly efficient under colder and drier conditions. In Austria, during the extraordinarily warm winter 2006/07 – most likely the warmest European winter for more than 500 years (Luterbacher et al., 2007) – especially low-altitude ski areas could not guarantee continuous skiing operations despite being equipped with snowmaking systems (Steiger, 2011).

Studies investigating the impact of climate change on skiing conditions focusing on natural snow conditions alone project dramatic decreases in ski season length in the future (e. g., Breiling and Charamza, 1999; Elsasser and Bürki, 2002; Elsasser and Messerli, 2001; Fukushima et al., 2002; Koenig and Abegg, 1997; Moen and Fredman, 2007). Comparatively few studies so far have accounted for the effects of snowmaking when simulating future snow conditions using numerical snow models, which is however necessary in order to obtain more realistic estimates of the future situation. Scott et al. (2003) used a calibrated point-based snow model to calculate future ski season length in southern Ontario (Canada) under current and improved snowmaking conditions, using daily values of air temperature and precipitation in combination with a simple threshold-based snowmaking approach. Other studies applying a similar methodology were performed in Eastern North America (Dawson and Scott, 2013; Scott et al., 2006), Quebec (Scott et al., 2007), and Australia (Hennessy et al., 2003; Hennessy et al., 2008). Pröbstl and Prutsch (2008) applied a point-based snow model to calculate potential and actual snowmaking hours for selected elevations (valley, intermediate, summit) in an Austrian ski area for current and future climate conditions using daily temperature and precipitation values and a temperature threshold for snowmaking. Steiger and Mayer (2008) calculated potential and required monthly snowmaking days for Tyrolean (Austria) ski resorts in 100 m wide altitudinal bands for current and future temperature conditions using a degree day model and a threshold of −2 °C daily average temperature to define a potential snowmaking day. Steiger

(2010) and Schmidt et al. (2012) used an extended version of the original SkiSim model developed by Scott et al. (2003) to estimate future snowmaking potential in Tyrol (Austria) and the Southern Black Forest (Germany), respectively. They introduced a refined snowmaking module and applied the model in a semi-distributed manner in 100 m altitudinal bands. Using daily precipitation as well as minimum, maximum, and mean temperature, they calculated natural snow accumulation, snowmelt, as well as potential snowmaking hours (using a temperature threshold). In a predefined timeframe (the "snowmaking window"), as soon as temperatures are sufficient, snow is produced in all altitudinal bands up to a snow depth of 30 cm. Afterwards, snow is produced in the form of improvement snowmaking, i. e., only when the snow depth falls below a certain threshold value that should be maintained over the course of the season. Olefs et al. (2010) analyzed snowmaking conditions at 14 Austrian stations in various altitudes for the period 1948–2007. They used wet-bulb temperature as a combined measure of temperature and humidity to determine the snowmaking potential at given ambient conditions. Linear regressions between the snow production potential in meters cubed per hour and wet-bulb temperature were derived from technical specifications supplied by four Austrian snow gun manufacturers for both fan guns and lance guns for an average water temperature, water pressure and technical snow density. Hendrikx and Hreinsson (2012) calculated future snowmaking potential for ski areas in New Zealand using a point-based temperature index snow model. Their model incorporated snow gun manufacturer-specified water flow rates to estimate the snowmaking potential using hourly wet-bulb temperatures and produced the maximum possible amount of snow within a given snowmaking window.

All these studies have in common that they were either applied in a point-based or semi-distributed manner, consider snowmaking potential only, or use comparatively simple methods to calculate natural snow depths. To the knowledge of the authors no models currently exist that explicitly quantify technical snow production in a physically based, spatially distributed simulation of the mountain snow cover. In our study, we present a physically based sophisticated snowmaking module incorporated into a fully spatially distributed energy balance snow model (AMUNDSEN, Strasser (2008)). The snowmaking module is capable to distinguish different ski areas in the model domain and explicitly accounts for the technical specifications and locations of individual snow guns. This allows to calculate the amount of snow produced by each snow gun (influenced by the type of snow gun, the ambient conditions, and the water supply) and distribute the snow on the slopes, while keeping track of the individual water and power consumption and snowmaking time for each snow gun. We apply

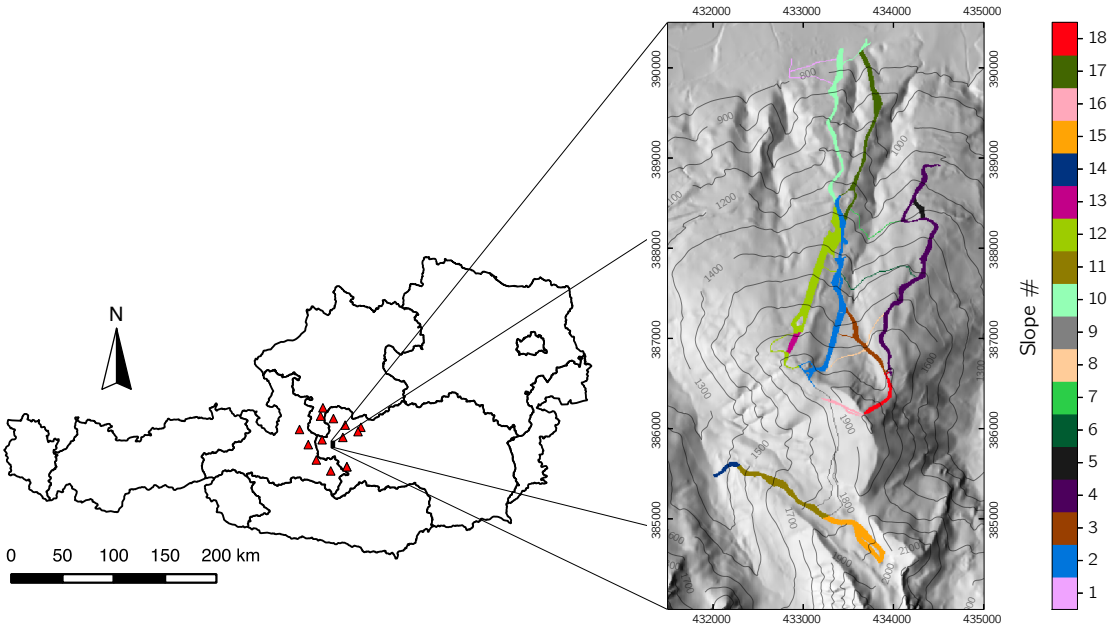

Figure 4.1: Location of the study region in Austria and the meteorological stations that were used, and map of the model domain showing the individual slopes of the ski area, color-coded with their internally used identifiers. Map coordinates are in meters (coordinate reference system: MGI / Austria Lambert).

the model in an Austrian ski area for historical conditions (2003–2011) in high temporal (hourly time steps) and spatial (10 m grid size) resolution and evaluate the results using snowmaking operation-based recordings provided by the ski area operators.

4.2 Study site and data

4.2.1 Study site

The study site for the present work is a ski area in the Schladming-Dachstein region, in the northwestern part of Styria (Austria). Schladming is located in the Enns valley, an east-west trending valley bordered by the Dachstein Mountains (2995 m a.s.l.) in the north and the Niedere Tauern (max. 2862 m a.s.l.) in the south. Figure 4.1 shows the location of the model domain within Austria as well as the individual slopes of the ski area and the meteorological stations surrounding the model domain.

From the ski area operators, comprehensive data sets regarding their infrastructure and operating practices were obtained, providing valuable information for modeling and validation purposes. These data sets include GIS data (ski lifts, slopes, hydrants, pipes, buildings, orthophotos, etc.), locations and types of snow guns, recordings of snowmaking days (snowmaking yes/no) for the seasons 2003/04–2010/11,

snow gun-based daily recordings of snowmaking hours as well as water and energy consumption for the seasons 2009/10 and 2010/11, and ski area operating days for the seasons 2003/04–2010/11.

For the present study, the ski area infrastructure of the season 2010/11 was taken as the basis for the simulations. The ski area operates 18 slopes with a total length of approximately 37 km and a total area of approximately 92 ha over an elevation range of 724–1999 m a.s.l. Locations and detailed information on the individual slopes are shown in fig. 4.1 and table 4.1. As of the season 2010/11, the ski area operates a total of 149 fan guns (no lance guns are in use) of two different manufacturers (in the following named Brand A and Brand B). The 23 Brand B guns (all mobile) are used on the slopes 1, 6, 7, 8, 9, 11, 14, and 15, and the 126 Brand A guns (61 mobile, 58 tower-mounted, 7 mounted on swing arms) on the remaining slopes. Six reservoirs in elevations between 1100 and 1720 m with a total capacity of 235 000 m^3 store the water required for snowmaking; additionally, a permanent external water supply from the Enns river with a flow rate of 145 $L\,s^{-1}$ is available. From a model perspective, accounting for this information allows to simulate technical snow[a] production in unprecedented detail.

4.2.2 The snow model AMUNDSEN

For our study, we applied the modular, physically based, distributed modeling system AMUNDSEN (Strasser, 2008) for the simulation of the natural snow cover and extended it with a new module for the simulation of technical snow production and slope management. AMUNDSEN has been designed to specifically address the requirements of snow modeling in mountain regions under climate change conditions and has been extensively validated in various Alpine sites in the past (Pellicciotti et al., 2005; Strasser, 2004; Strasser, 2008; Strasser et al., 2008, Marke et al., 2014 (submitted)). The functionality of the model includes, among others, several interpolation routines for scattered meteorological measurements (Marke, 2008; Strasser, 2008), rapid computation of topographic parameters from a digital elevation model (Strasser, 2008), simulation of shortwave and longwave radiation including topographic (e.g., shadows) and cloud effects (Corripio, 2003; Greuell et al., 1997), parameterization of snow albedo depending on snow age and temperature (Rohrer, 1992), parameterization of snow density (Anderson, 1976; Jordan, 1991), and simulation of snowmelt based on

[a] Within this paper, we use the term *technical snow* to refer to the snow produced by snow guns, while *artificial snow* refers to the actual snow on the ski slopes, i. e., a compressed and processed mixture of technical snow and natural snow.

Table 4.1: List of the slopes in the ski area including their length, area, and elevation range, as well as the number and type of snow guns used as parameters for the snowmaking module in this study.

Slope	Length [m]	Area [ha]	Min elevation [m]	Max elevation [m]	Number of snow guns	Snow gun type
1	1275	1.2	746	859	2	Brand B
2	4259	13.2	1263	1862	23	Brand A
3	1646	3.9	1551	1799	5	Brand A
4	4863	13.4	1121	1805	27	Brand A
5	524	1.2	1237	1325	3	Brand A
6	1234	0.6	1449	1527	0	–
7	943	0.5	1266	1303	0	–
8	1196	1.0	1647	1779	2	Brand B
9	1750	1.5	1725	1858	2	Brand B
10	3578	9.0	724	1268	23	Brand A
11	2028	7.0	1457	1767	8	Brand B
12	3899	15.8	1272	1841	23	Brand A
13	658	1.4	1687	1783	2	Brand A
14	879	1.5	1329	1461	3	Brand B
15	1275	7.9	1759	1942	6	Brand B
16	1161	1.6	1825	1999	2	Brand A
17	3885	9.1	736	1313	19	Brand A
18	1520	2.4	1794	1995	0	–

an energy balance approach (Strasser et al., 2008). As input data for the simulation of the natural snow cover the model requires a digital terrain model (DTM) of the model domain as well as either hourly, 2-hourly, or 3-hourly recordings of the meteorological variables air temperature, relative humidity, precipitation, global radiation, and wind speed. For the present study, the model was driven with hourly meteorological data and applied on a 10 m × 10 m grid.

For the conversion of simulated snow water equivalent (SWE) to snow depth, it is distinguished between two types of snow layers, herein called *new snow* and *old snow*. The density of freshly fallen snow is calculated as a function of air temperature (Anderson, 1976):

$$\rho_{\mathrm{ns}} = \begin{cases} 50 & T_a \leq -15\,^{\circ}\mathrm{C} \\ 50 + 1.7(T_a + 15)^{1.5} & T_a > -15\,^{\circ}\mathrm{C}. \end{cases} \tag{4.1}$$

Snow compaction is calculated for each layer following Anderson (1976) and Jordan (1991), with a phase of rapid compaction for newer snow with densities of less than 150 kg m^{-3}, followed by a phase of slower densification which is mainly influ-

enced by the snow load:

$$\frac{\mathrm{d}\rho_s}{\mathrm{d}t} = \rho_s \left(c_1 W^* \mathrm{e}^{-c_2(T^* - T_s)} \mathrm{e}^{-c_3 \rho_s} \right), \tag{4.2}$$

$$\frac{\mathrm{d}\rho_s}{\mathrm{d}t} = \rho_s \left(c_4 \mathrm{e}^{-c_5(T^* - T_s)} c_6 \right), \tag{4.3}$$

$$c_6 = \begin{cases} \mathrm{e}^{-c_7(\rho_s - \rho_d)} & \rho_s > \rho_d \\ 1 & \rho_s \leq \rho_d, \end{cases} \tag{4.4}$$

with ρ_s [kg m^{-3}] being the respective layer's (new snow or old snow) density, W^* [kg m^{-2}] the load of snow water equivalent (snow in the layer above and 50 % of the snow in the current layer), $c_1 = 0.01\,\mathrm{m}^{-1}\,\mathrm{h}$ (new snow), $c_1 = 0.001\,\mathrm{m}^{-1}\,\mathrm{h}$ (old snow), $c_2 = 0.08\,^{\circ}\mathrm{C}^{-1}$, $c_3 = 0.021\,\mathrm{m}^3\,\mathrm{kg}^{-1}$, $c_4 = 0.01\,\mathrm{m}^{-1}\,\mathrm{h}$, $c_5 = 0.04\,^{\circ}\mathrm{C}^{-1}$, $c_7 = 0.046\,\mathrm{m}^3\,\mathrm{kg}^{-1}$, $\rho_d = 150\,\mathrm{kg\,m}^{-3}$ and $T^* = 0\,^{\circ}\mathrm{C}$. New snow is converted to old snow when reaching a density of 200 kg m^{-3}. The compaction scheme has been calibrated (by slightly adapting the original parameters from Anderson (1976) due to the reduced number of layers in our model) and validated under Alpine conditions using snow depth and SWE measurements. For the present study, an additional *artificial snow* layer was introduced, which is described in more detail in section 4.3.6.

4.2.3 Meteorological data

For the present study, corrected station recordings from 13 automatic weather stations (with varying temporal coverage) operated by the Central Institute for Meteorology and Geodynamics (Zentralanstalt für Meteorologie und Geodynamik, ZAMG) surrounding the model domain were used (red triangles in fig. 4.1). The stations are located in elevations between 504 m and 1763 m a.s.l.

A meteorological preprocessor in AMUNDSEN is used to spatially interpolate the point information from the station locations to the model domain for every model time step. In case of temperature and precipitation, topographic corrections are carried out by applying monthly temperature lapse rates and elevation adjustment factors, as described by Marke (2008). Humidity is regionalized by first converting from relative humidity to dew point temperature and then applying dew point temperature lapse rates for altitudinal corrections, before a reconversion to relative humidity is carried out (Marke, 2008). The latter is necessary as relative humidity shows a non-linear temperature dependence, while dew point temperature decreases linearly with increasing terrain elevation (Liston and Elder, 2006b). Wind speed is corrected for terrain elevation using a linear regression function derived from the station data for a given model

time step (Strasser, 2008). Global radiation is spatially distributed by inverting a cloud factor from global radiation at the station locations which is later used to reduce simulated potential direct and diffuse solar radiation separately. For the calculation of global radiation, topographic slope and aspect as well as orographic shadowing and multiple reflection from clouds and surrounding snow covered slopes are taken into account (Strasser, 2008).

Since (especially) solid precipitation in higher altitudes is often considerably underestimated by measurements (e. g., Frei and Schär, 1998; Goodison et al., 1998; Nešpor and Sevruk, 1999), a polynomial elevation-based precipitation correction function was applied for this study. The function has been derived by comparing simulated snow depths and multi-year snow depth measurements at 55 snow gauges in Austria, resulting in an average correction term of approximately 12 % per 100 m for solid precipitation. Each pixel of the interpolated precipitation raster is thereby corrected using its elevation z by

$$P_{\text{corr}} = P\left(1 + 3 \times 10^{-7} z^2 - 2.36 \times 10^{-4} z + 6.107 \times 10^{-2}\right). \tag{4.5}$$

4.3 Methods

4.3.1 Overview and model parameters

An earlier version of the snowmaking module (described in Marke et al. (2014, submitted)) was implemented using a pragmatic bulk approach by requiring the total number of snow guns for the ski area as input data and distributing the snow guns evenly across the total slope area. This approach is due to its modest requirements in terms of input data comparatively easily transferable to other ski areas. For the work presented in this study, we implemented an improved version of the snowmaking module which allows for a more detailed simulation of snowmaking operations, however this version also requires comparatively detailed knowledge about the investigated ski area's snowmaking infrastructure. Most importantly, the new module explicitly considers actual snow guns, which are assigned to pixels along the slopes. This has several advantages over the bulk approach – first, for calculating the snow production potential, the ambient conditions (i. e., wet-bulb temperature) at the actual snow gun location (a single pixel) are considered, instead of calculating the snow production potential for the "fractional snow guns" at each slope pixel. This is a more realistic assumption and – in principle – allows to replicate the exact real-world snow gun locations in the model. In the current version, however, for each slope only the

Table 4.2: Required input data and parameters for the snowmaking module. The columns D (model domain), A (ski area), S (slope), T (snow gun type) indicate for which model element the respective parameter is required.

Name	Description	Unit / values	D	A	S	T
Ski areas grid	A grid where all pixels belonging to the same ski area are marked with a unique identifier.	1, 2, . . .	×			
Slopes grid	A grid where all pixels belonging to the same slope are marked with a unique identifier.	1, 2, . . .		×		
Maximum water flow	The maximum water flow for the entire ski area (depending on the ski area infrastructure such as pumps, pipes, etc.).	$m^3\,h^{-1}$		×		
Capacity of reservoirs	The combined capacity of all reservoirs in the ski area.	m^3		×		
External water supply	The flow rate of a possible external water supply to refill the reservoirs during the season.	$m^3\,h^{-1}$		×		
Number of snow guns	The total number of snow guns on the slope.	≥ 0			×	
Snow gun type	Type of the snow guns (used for calculating the snow production).	Brand A/B			×	
Elevation dependency	An optional factor for specifying a possible elevation dependency of the snow gun distribution (e. g., if more snow guns should be placed at lower elevations).	0 . . . 1			×	
Threshold wet-bulb temperature	Threshold wet-bulb temperature for which snowmaking is performed.	°C				×
Water flow	Water flow as a linear function of wet-bulb temperature.	$m^3\,h^{-1}$				×
Technical snow density	Initial density of the produced snow.	$kg\,m^{-3}$				×
Power consumption	Power consumption of the snow gun (assumed constant).	kW				×

total number of snow guns needs to be specified, and their respective locations are calculated automatically. Second, snow guns can be turned on or off on demand, and properties such as water flow, snowmaking hours, or energy consumption are tracked individually for each snow gun. The biggest advantage, however, is that different types and behaviors of snow guns can be considered, e. g., each snow gun may have an individual water flow rate, threshold temperature, or power consumption. This also allows to easily test different management strategies, such as replacing lance guns with fan guns, installing higher performance snow guns, or use of snow inducers.

In addition to explicitly considering individual snow guns, several features such as the consideration of limited water availability (reservoir storages) or the calculation of water losses during the snowmaking process have been introduced in the module, which are described in detail in the following sections. Table 4.2 shows the parameters required by the snowmaking module, while their respective values used in our study (derived from the actual ski area infrastructure) are listed in tables 4.1, 4.3 and 4.4.

Table 4.3: Ski area parameters used for the study.

Maximum water flow [$m^3\ h^{-1}$]	2481
Reservoir capacity [m^3]	195 000
External water supply rate [$m^3\ h^{-1}$]	522
External water supply capacity [m^3]	unlimited

4.3.2 Rules for snowmaking

The decision of when and where to produce snow in a ski area is difficult to describe in a numerical model, as it is influenced by many factors such as ambient conditions, snow demand, economic considerations, and past experiences. Common snowmaking practice is that the snowmaking season is divided into a base-layer snowmaking period before the start of the ski season in order to provide an appropriate ground layer of snow for subsequent natural snowfalls as well as to ensure an as early as possible ski season opening (especially before the highly profitable Christmas holidays), and a period of "improvement snowmaking" afterwards, where snowmaking is performed only selectively to maintain a minimum snow depth (Pröbstl, 2006, H. Landl, pers. comm., 2011). At ideal conditions, base-layer snowmaking (corresponding to a minimum snow depth of approximately 30 cm) can be finished in about 50 hours with high-end infrastructure (Steiger and Mayer, 2008).

For the present study, the following snowmaking rules were established in accordance with the ski area operators: From November 1 to December 15 the maximum possible amount of snow is produced (only influenced by the ambient conditions and the snowmaking infrastructure). From December 16 to February 28 it is then attempted to maintain a minimum snow base of 60 cm (as suggested by Scott et al. (2007)), i. e., snow is only produced when the snow depth is below this threshold.

4.3.3 Placement of the snow guns

As described earlier, the number and type of snow guns has to be specified for each slope. The slopes are subdivided into segments, with each snow gun producing snow exclusively for its respective slope segment. By default, the slopes are divided into segments of equal area, however, using an optional additional parameter snow gun density can be decreased with increasing elevation (i. e., to position more snow guns at lower elevations). Division of the slopes is done by sorting the slope pixels according to their elevation and then iteratively selecting ranges of pixels corresponding to the calculated segment sizes (i. e., we assume that the slopes only go downhill, as is

the case for our study area). The snow guns themselves are placed at the pixel corresponding to the median elevation of their respective slope segment.

4.3.4 Modeling of snow production

Generally, two basic methods of snowmaking exist – air-water (lance) guns and fan guns – however, both share the same principle: water is pumped into the snow gun, where it is forced through small nozzles and collides with pressurized air, thus being atomized into small water droplets. These droplets leave the snow gun at high speed and, due to the decompression of the air, freeze into ice crystals before hitting the ground. It is thus crucial to design the snowmaking system in a way that the droplets have ample time to freeze during their way through the atmosphere. The efficiency of snowmaking depends mainly on the ambient conditions, the water temperature, and the nucleation temperature of the water, the latter being able to be increased by use of snow inducers (additives). Ambient conditions affect the efficiency of heat transfer during the snowmaking process, which occurs by two mechanisms: convective heat transfer and evaporation of water. Radiative heat transfer is insignificant under these conditions (Chen and Kevorkian, 1971; Olefs et al., 2010). Hence, snowmaking efficiency is mainly influenced by air temperature and humidity, which should both be as low as possible. As a combined measure of both temperature and humidity, wet-bulb temperature is commonly used to assess the snowmaking efficiency under given ambient conditions.

Olefs et al. (2010) calculated linear regressions between the snow production potential pp (in cubic meters of snow per hour) and the wet-bulb temperature T_w (in °C) for then present-generation snow guns of four major Austrian snow gun manufacturers. The calculated regression functions are

$$\mathrm{pp_f} = -4.83 T_w + 3.94 \tag{4.6}$$

for fan guns, and

$$\mathrm{pp_{aw}} = -3.94 T_w - 4.23 \tag{4.7}$$

for air-water (lance) guns, and are assumed to be valid for water temperatures of less than 2 °C, a water pressure of 25 bar, wet-bulb temperatures in the range $-14\,^{\circ}\mathrm{C} \leq T_w \leq -2\,^{\circ}\mathrm{C}$, and a snow density of $400\,\mathrm{kg\,m^{-3}}$.

In our model we adopt this approach by assuming the water flow wf from a snow gun (in cubic meters per hour) to be linearly dependent on the wet-bulb temperature using the general equation

$$\mathrm{wf} = a T_w + b \tag{4.8}$$

valid for wet-bulb temperatures in the range $T_{w,\min} \leq T_w \leq T_{w,\max}$, while allowing to account for different types of snow guns by adapting the parameters a, b, $T_{w,\min}$, $T_{w,\max}$, as well as the snow density ρ_{ts}. Table 4.4 lists the parameters for the different types of snow guns (here referred as Brand A and Brand B) used in this study. For the Brand B guns, the parameters for the regression function (eq. (4.8)) were derived from the official product specifications (flow rate as a function of wet-bulb temperature, valid for a water temperature of 1 °C), while for the Brand A guns these specifications were not publicly available, hence we used the parameters for a "generic" fan gun (eq. (4.6)) derived by Olefs et al. (2010). Power consumption values are according to manufacturer specifications for both snow gun types.

Wet-bulb temperature is calculated in the model by numerically solving the psychrometric equation

$$\Delta e = e_l - (e_w - \gamma\,(T_a - T_w)) \tag{4.9}$$

for $\Delta e = 0$. Here,

$$e_l = \frac{\text{RH}}{100} e_s \tag{4.10}$$

is the water vapor partial pressure in hPa, RH the relative humidity in percent,

$$e_s = \begin{cases} 6.1078 \exp\left(\frac{17.08085 T_a}{234.175 + T_a}\right) & T_a \geq 0\,^\circ\text{C} \\ 6.1071 \exp\left(\frac{22.4429 T_a}{272.44 + T_a}\right) & T_a < 0\,^\circ\text{C} \end{cases} \tag{4.11}$$

the saturated vapor pressure at ambient temperature in hPa, and e_w the saturated vapor pressure for the wet-bulb temperature (calculated by evaluating eq. (4.11) with T_w instead of T_a).

$$\gamma = C_p \frac{p}{L_v} \tag{4.12}$$

is the psychrometric constant in $\text{hPa}\,\text{K}^{-1}$,

$$L_v = 2.5014 \times 10^6 - 2361 T_a \tag{4.13}$$

the latent heat of vaporization in $\text{J}\,\text{kg}^{-1}$, and

$$C_p = C_{p,\text{dry}}\,(1 + 0.84\,\text{SH}) \tag{4.14}$$

the specific heat capacity of moist air in $\text{J}\,\text{kg}^{-1}\,\text{K}^{-1}$, with $C_{p,\text{dry}} = 1004.67\,\text{J}\,\text{kg}^{-1}\,\text{K}^{-1}$ the specific heat capacity of dry air, and

$$\text{SH} = \frac{0.622 e_l}{p - 0.378 e_l} \tag{4.15}$$

Table 4.4: Model parameters for the snow guns used in this study.

Type	a [m³ h⁻¹ °C⁻¹]	b [m³ h⁻¹]	$T_{w,\min}$ [°C]	$T_{w,\max}$ [°C]	$æ_{ts}$ [kg m⁻³]	P [kW]
Brand A	−1.93	1.58	−14	−2	400	23.5
Brand B	−1.46	3.33	−14	−3	400	27.0

the specific humidity. Atmospheric pressure p (in hPa) is calculated by assuming a linear temperature gradient in the free atmosphere:

$$p = 1013.25 \left(1 - \frac{g_a h_e}{280}\right)^{\frac{M_a g}{R g_a}}, \tag{4.16}$$

where

$$g_a = \begin{cases} -0.0098\,\mathrm{K\,m^{-1}} & \text{(no rain)} \\ -0.0065\,\mathrm{K\,m^{-1}} & \text{(rain)} \end{cases} \tag{4.17}$$

is the atmospheric temperature gradient, h_e the elevation above sea level, $M_a = 28.97\,\mathrm{g\,mol^{-1}}$ the molecular mass of dry air, $g = 9.81\,\mathrm{m\,s^{-2}}$ the Earth-surface gravitational acceleration, and $R = 8.314\,\mathrm{J\,mol^{-1}\,K^{-1}}$ the universal gas constant.

Equation (4.8) describes the maximum water flow for a snow gun under given meteorological conditions. The actual water consumption for all snow guns in a given time step is calculated as follows:

- First, depending on the date and the meteorological and/or snow conditions (see section 4.3.2), it is decided which snow guns are activated (all, or only those which need to maintain a 60 cm snow base).
- Then, the possible water flow for all active snow guns is calculated using eq. (4.8) and added up to derive the possible total water flow for the entire ski area $\mathrm{wf_{tot}}$ (without yet considering infrastructural limitations). The corresponding possible total water consumption for the ski area $\mathrm{wc_{tot}}$ can then be expressed as

  $$\mathrm{wc_{tot}} = \mathrm{wf_{tot}} \cdot \Delta t, \tag{4.18}$$

  with Δt as the time step duration in hours.
- The actual total water consumption $\mathrm{wc_{act}}$ is limited by the maximum water flow $\mathrm{wf_{max}}$ and the amount of water stored in the reservoirs ws:

  $$\mathrm{wc_{act}} = \min\{\mathrm{wc_{tot}}, \mathrm{wf_{max}} \cdot \Delta t, \mathrm{ws}\}. \tag{4.19}$$

- The snowmaking time (i. e., the duration for which the snow guns are active in the current time step) in hours for each active snow gun is then

  $$\mathrm{st} = \frac{\mathrm{wc_{act}}}{\mathrm{wc_{tot}}} \cdot \Delta t, \tag{4.20}$$

and the water and energy consumption (in m^3 and kW h, respectively) accordingly

$$\mathrm{wc} = \mathrm{wf} \cdot \mathrm{st}, \tag{4.21}$$

$$\mathrm{ec} = P \cdot \mathrm{st}. \tag{4.22}$$

4.3.5 Water losses during snowmaking

Water losses during snowmaking (i. e., during the time the water droplets are airborne) due to evaporation and sublimation are calculated following the approach of Eisel et al. (1988), who derived an energy balance model for the snowmaking process. The water vapor loss m_v (in kg h^{-1}) at ambient temperature for each snow gun can be expressed as

$$m_v = 1000\,\mathrm{wf} \frac{e_s}{e_{s,0}} \frac{c_i + T_{\mathrm{water}} c_{\mathrm{sw}}}{c_i + L_{v,0}}, \tag{4.23}$$

with 1000 wf as the water flow in kg h^{-1}, T_{water} as the water temperature in °C, $c_{\mathrm{sw}} = 4.18 \times 10^3\,\mathrm{J\,kg^{-1}\,K^{-1}}$ as the specific heat of water, $c_i = 3.375 \times 10^5\,\mathrm{J\,kg^{-1}}$ as the melting heat of ice, $L_{v,0} = 2.5014 \times 10^6\,\mathrm{J\,kg^{-1}}$ as the latent heat of vaporization at 0 °C, and $e_{s,0} = 6.11$ hPa as the saturated vapor pressure at 0 °C.

For typical snowmaking conditions (air temperatures between −20 and 0 °C and water temperatures between 1 and 5 °C), the resulting water losses are in the range of 2–13 %, which is in agreement with the ranges given by Olefs et al. (2010), who estimated the losses to be around 5–15 % for fan guns and 15–40 % for lance guns (these values, however, also include losses due to wind drift, which we do not consider in our calculations). As the water temperature has a comparatively small effect on the resulting water losses, for our calculations a constant water temperature of 1 °C was assumed.

4.3.6 Snow on the slopes

When a snow gun is active, its water consumption is calculated according to eqs. (4.8) and (4.21). Aside from the water vapor losses during the snowmaking process due to evaporation and sublimation, which are calculated according to eq. (4.23), we assume that the entire water is converted to snow using the respective snow gun's snow density ρ_{ts}, i. e., there is no liquid water remaining. As we also do not consider wind drift losses, the entire snow produced by the snow gun is distributed evenly among its target pixels. To account for the distinct properties of the machine-made snow, a new *artificial snow* layer type has been introduced in AMUNDSEN, whose properties are as follows:

- The water equivalent of the produced technical snow is distributed equally among the snow gun's target pixels at the artificial snow layer.
- The artificial snow layer incorporates the new snow and old snow layers, i. e., as soon as technical snow is produced, possibly existing new snow and old snow layers along with their properties are merged into the new artificial snow layer at the respective pixels (the water equivalent of the new snow and old snow layers is added to the artificial snow layer's water equivalent, while for density and albedo a weighted mean of the three layers is calculated).
- The initial density of technical snow ρ_{ts} is assumed according to table 4.4. For the densification according to eqs. (4.2) to (4.4), artificial snow is assigned the same parameters as new snow; with the exception of the parameter c_1 of eq. (4.2), which is enlarged to a value of $0.5\,\mathrm{m}^{-1}\,\mathrm{h}$ each day at midnight in order to implicitly account for the increased snow compaction due to slope grooming.
- Following Keller et al. (2004), a more rapid albedo decline is assumed for artificial snow. Since no measurements of albedo on the ski slopes were available or could be found in the literature, we assume the albedo decline to be twice as fast as for natural snow.

In AMUNDSEN, snow accumulation is calculated as the sum of natural and technically produced snow, with snowmelt determined by the energy surplus at the snow surface.

4.3.7 Ski season length

Most studies define ski season length as the number of days with a snow depth of at least 30 cm in a certain period (e. g., Hendrikx and Hreinsson, 2012; Koenig and Abegg, 1997; Moen and Fredman, 2007; Rixen et al., 2011; Schmidt et al., 2012; Scott et al., 2003; Scott et al., 2007; Scott et al., 2006). We use a similar approach, however assume that skiing operations continue even if the snow depth falls below this threshold during the season, as long as a minimum snow base of 20 cm is maintained:

- Starting from November 1, as soon as the snowpack is at least 30 cm thick over five consecutive days, the *ski opening date* is set to the first of those five days.
- Starting from the ski opening date, as soon as the snowpack is less than 20 cm thick over ten consecutive days, the *ski closing date* is set to the first of those ten days. In accordance with common management practices for Austrian ski areas, we additionally limit the latest closing date to the Sunday after Easter or April 15 (to prevent too early closing), whichever is later.

- The *ski season length* is calculated as the number of days between the opening and the closing date, i. e., it is assumed that the ski area does not close during the season.

On the basis of these assumptions, a season length can be calculated for every pixel of the model domain. To estimate the season length on a ski area basis, first the season length for each *slope* is calculated as the number of days between the latest opening date and the earliest closing date of all slope pixels. The *ski area* season length is then selected as the maximum season length of all individual slopes.

4.4 Results

In the following, we describe the results of the model simulations for the period 2003–2011. The simulations were performed with the parameters for the snowmaking module as listed in tables 4.1, 4.3 and 4.4. Figure 4.2 shows the resulting locations of the snow guns as assigned by the model.

Again, it has to be noted that all simulations have been performed on the basis of the 2010/11 snowmaking infrastructure, since for earlier seasons the required detailed information regarding snow gun types and locations was unavailable. The snowmaking infrastructure in the ski area has been completely renewed and considerably extended during the period 2006–2010. This includes exchanging almost all existing snow guns with more efficient models and considerably increasing the total number of snow guns, installing new reservoirs (increasing the capacity from 125 000 to 195 000 m^3), increasing the external water supply rate (from 60 to 145 $L\,s^{-1}$) as well as renewing the piping and pumping system. Hence, only the model results of the season 2010/11 are directly comparable to observational data, while for earlier seasons the model is expected to overestimate technical snow production.

4.4.1 Snowmaking time

Figure 4.3 shows the total seasonal modeled and (where available) observed snowmaking time for the seasons 2003/04–2010/11. In the seasons with observational data, the total snowmaking hours for the Brand A snow guns are overestimated by 9 % in 2009/10 and by 16 % in 2010/11, while for the Brand B guns, they are overestimated by 34 % in 2008/09 and within 0.1 % of the observations in 2009/10.

Figure 4.4 shows the observed and modeled daily snowmaking time per snow gun (Brand A snow guns only) for the seasons 2009/10 and 2010/11. The observations re-

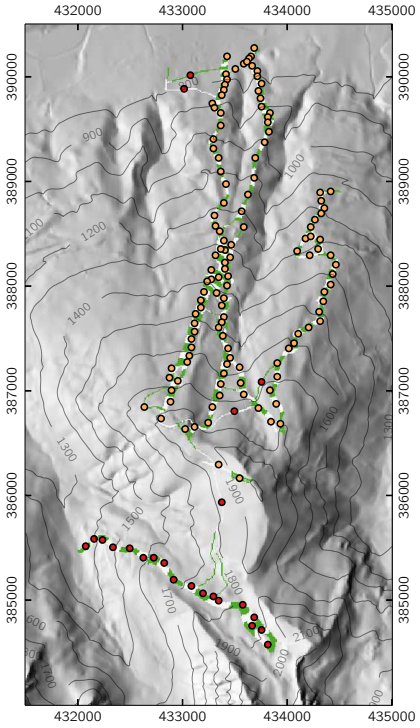

Figure 4.2: Locations of the snow guns (orange: Brand A, red: Brand B) and the associated slope segments as assigned by the model.

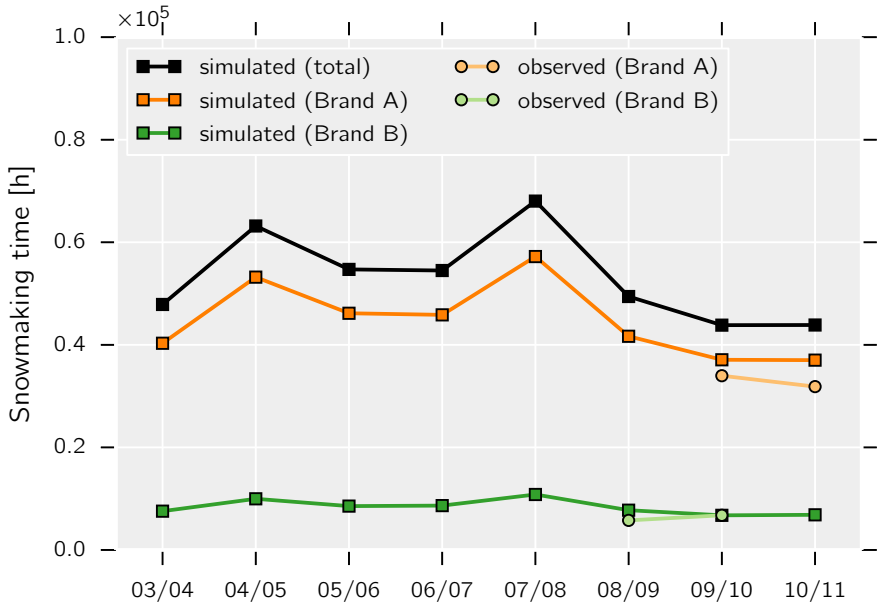

Figure 4.3: Simulated and (where available) observed total seasonal snowmaking time for the seasons 2003/04–2010/11.

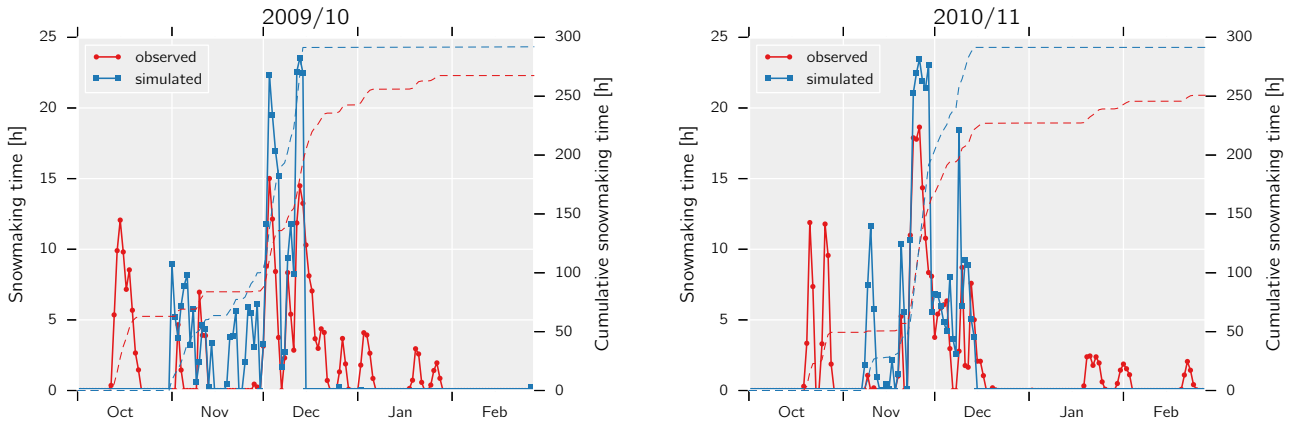

Figure 4.4: Observed and simulated daily snowmaking time (averaged over number of snow guns) for the seasons 2009/10 and 2010/11 (Brand A snow guns only; cumulative results displayed as dashed lines).

veal that, if the ambient conditions allow it, first snowmaking is already done in mid-October, while the model assumes snowmaking to start at the earliest on November 1. During the base-layer snowmaking period from November 1 to December 15, the observed snowmaking days (snowmaking yes/no) are very well reproduced for the season 2010/11, with only two short periods in mid-November and early December, where snow was produced in the model while not in reality. This is also the case for most of November in the season 2009/10, while for the first half of December the snowmaking days are again reproduced well. The actual amounts of snowmaking hours, however, tend to be largely overestimated, especially during the season 2009/10. This is on the one hand probably due to the larger number of snow guns in the model as compared to reality in this season, but also due to the fact that snowmaking in the model always starts at $T_w = -2\,°\mathrm{C}$ for Brand A guns (see table 4.4), while in reality the snowmakers might apply lower threshold temperatures, depending on the current snow demand and their experience. In both displayed seasons, snow depth on the slopes (almost) never falls below 60 cm until the end of February, hence only negligible amounts of snow are produced after the end of the base-layer snowmaking period. In reality however, considerable amounts of additional snow (10–15 % of the total seasonal snow production in these two seasons) are produced during periods with optimal snowmaking conditions in January and February.

Figure 4.5a shows for the season 2010/11 the spatially distributed total seasonal snowmaking time (i. e., for each slope pixel, the time for which its corresponding snow gun has been active). Since in this season snowmaking was mainly performed during

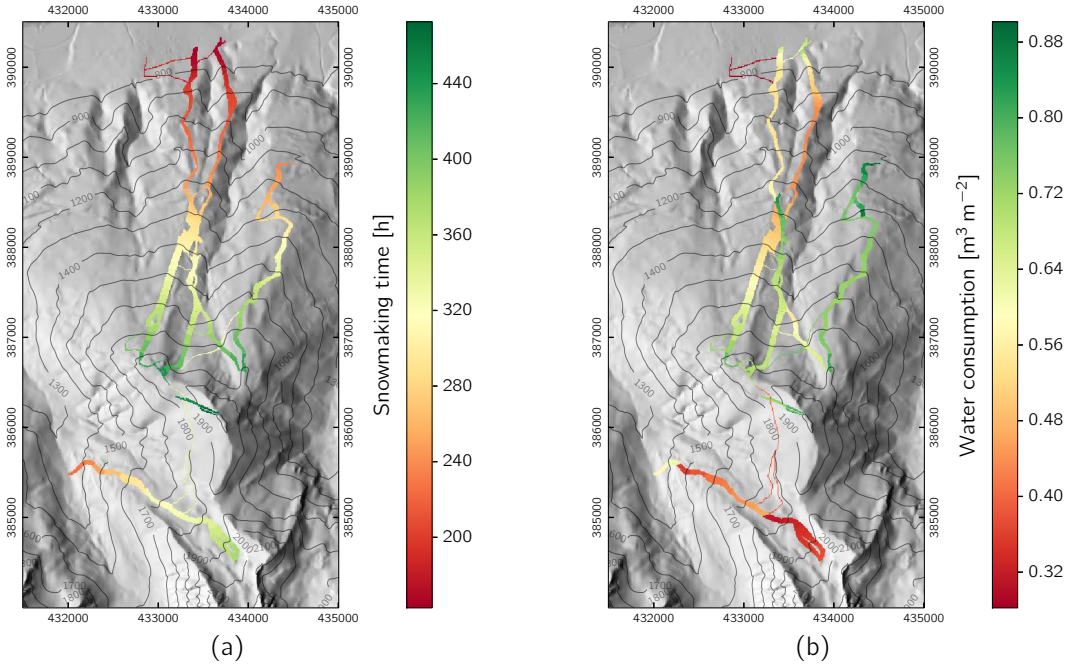

Figure 4.5: Spatially distributed seasonal snowmaking time (a), and water consumption (b) for the season 2010/11.

the maximum snowmaking period (see fig. 4.4), snowmaking time is mainly dependent on elevation (corresponding to wet-bulb temperature conditions) in this case.

For the seasons 2003/04–2008/09, only recordings of snowmaking days (snowmaking yes/no) are available. Figure 4.6 shows the observed and simulated monthly snowmaking days for the seasons 2003/04–2010/11. To account for the local snowmaking practice, for the model results only days with a total snowmaking time of at least 5 h were counted. Simulated snowmaking days are within ±15 d of the observations for all seasons except the exceptionally warm winter 2006/07 (with the mean winter temperature in the study region being approximately 3 °C above average), where the model simulates more than double the number of snowmaking days as compared to the observations. Further investigations reveal that for most parts of this season, snowmaking conditions are extremely unfavorable, however snowmaking is still possible (wet-bulb temperatures below the threshold). Hence, during the maximum snowmaking period (November to mid-December), snow is produced every day when the conditions allow it, although only for shorter durations and less efficiently (due to the decreased water throughput). Due to the higher temperatures (less natural snowfall and increased melt), snow depths on the slopes frequently fall below the 60 cm threshold, hence in this season also in the "improvement snowmaking" pe-

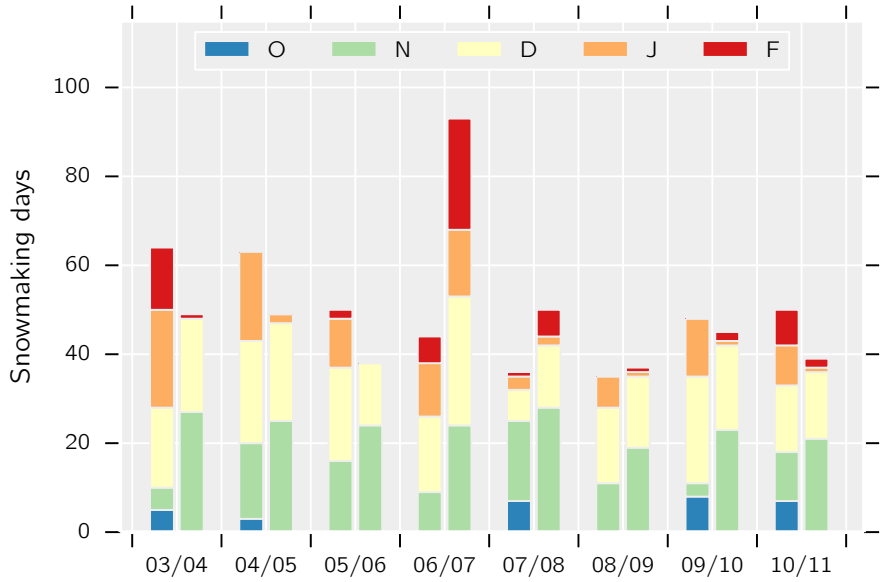

Figure 4.6: Monthly snowmaking days for the seasons 2003/04–2010/11. The two bars for each season depict the observed (first bar) and simulated (second bar) snowmaking days (for the model results, only days with a total snowmaking time of at least 5 h were counted).

riod from mid-December to February snow is produced almost every day when the conditions allow it. In reality, the base-layer snowmaking was performed in this season during a few days in early and mid-November with favorable snowmaking conditions, while afterwards maximum possible amounts of snow were produced during cold periods, which allowed snowmaking to be stopped during periods with unfavorable conditions.

4.4.2 Water consumption

Figure 4.7 shows the total seasonal modeled and (where available) observed water consumption for the seasons 2003/04–2010/11. For the seasons with observational data (Brand A guns), the simulated water consumption is underestimated by approximately 15 % in the season 2009/10, while it is within 0.5 % of the observations in the season 2010/11. This underestimation of water consumption in combination with the overestimation of snowmaking hours in both seasons suggests that a certain portion of technically produced snow can be attributed to times with unfavorable snowmaking conditions, resulting in inefficient snow production.

Figure 4.8 shows the observed and simulated daily water consumption per snow gun (Brand A snow guns only) for the seasons 2009/10 and 2010/11. The curves are similar to the daily snowmaking hours, although of course water consumption is ad-

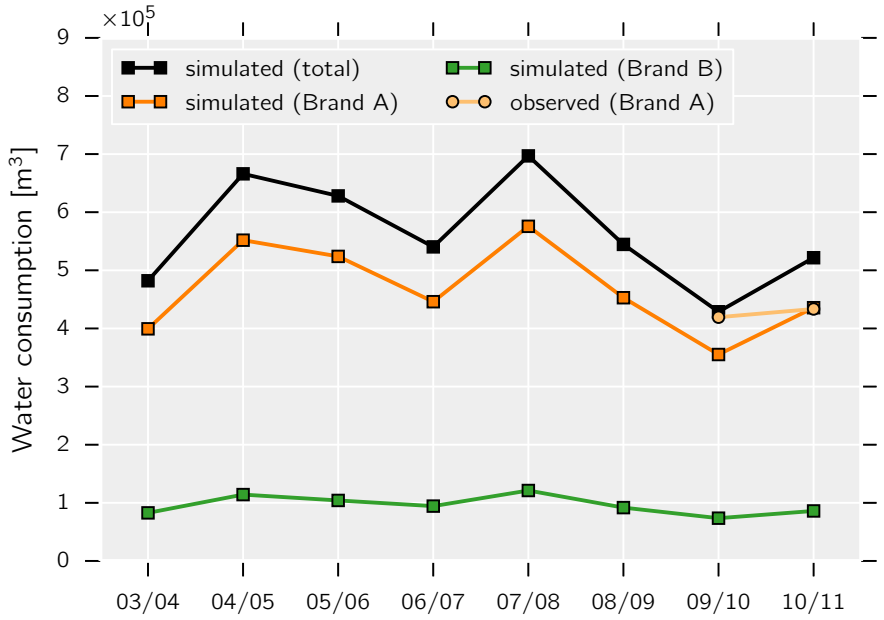

Figure 4.7: Simulated and (where available) observed total seasonal water consumption for the seasons 2003/04–2010/11.

ditionally influenced by the ambient conditions. In the season 2010/11, the influence of water availability on snowmaking can be seen: Starting from late November, the reservoirs are empty and (despite favorable snowmaking conditions) the water flow is limited to the external supply rate (see table 4.3). For two days (December 7–8), snowmaking conditions then deteriorate while the reservoirs continue to be refilled, resulting in a peak in water consumption on the next day as soon as snowmaking is continued, followed again by a period of limited water availability.

4.4.3 Energy consumption

Figure 4.9 shows the observed and simulated daily energy consumption per snow gun (Brand A snow guns only) for the seasons 2009/10 and 2010/11. As for the snow guns a constant power consumption is assumed (depending on the snow gun type, see table 4.4), the curves generally show the same course as the snowmaking hours.

4.4.4 Ski season length

Figure 4.10 shows the actual (observed) ski season length for the seasons 2003/04–2010/11 as well as the simulated season length (with and without snowmaking) according to the rules described in section 4.3.7. Deviations from the observed and sim-

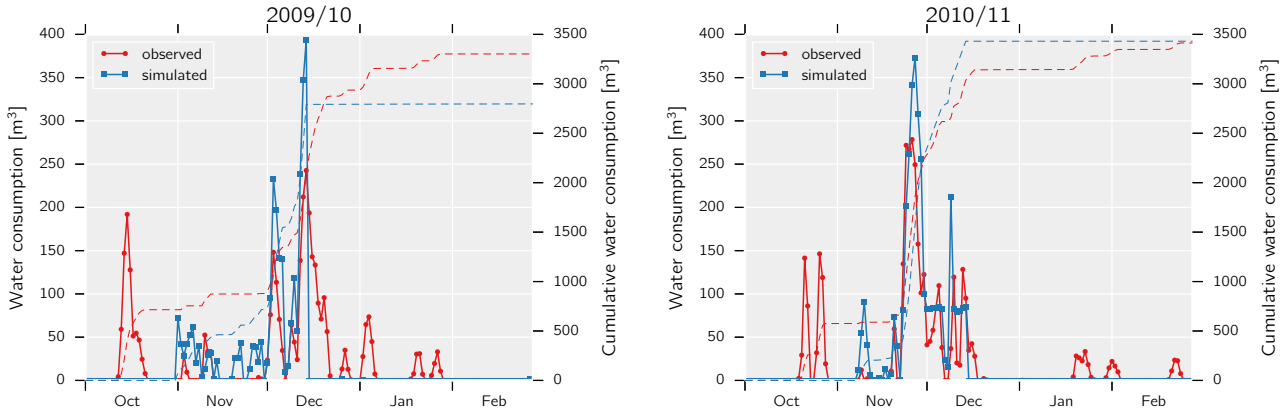

Figure 4.8: Observed and simulated daily water consumption (averaged over number of snow guns) for the seasons 2009/10 and 2010/11 (Brand A snow guns only; cumulative results displayed as dashed lines).

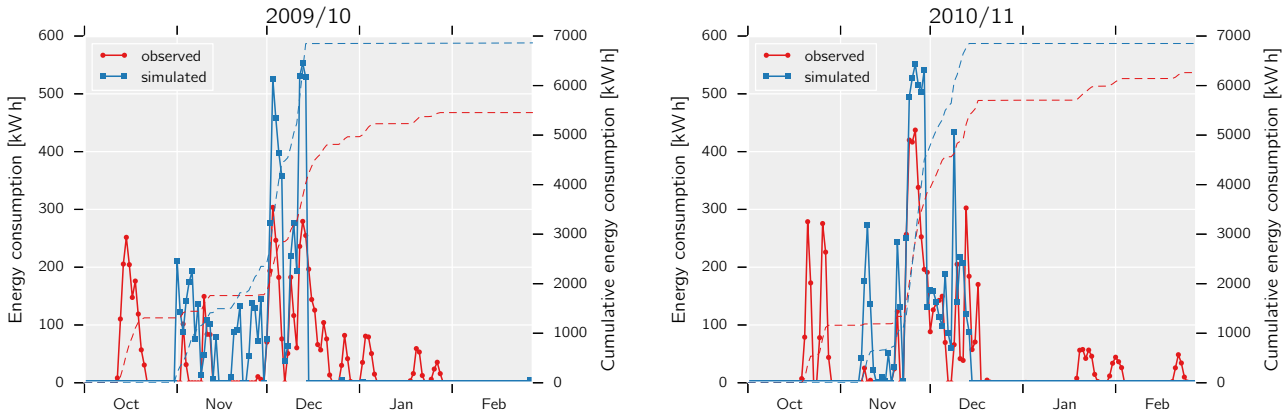

Figure 4.9: Observed and simulated daily energy consumption (averaged over number of snow guns) for the seasons 2009/10 and 2010/11 (Brand A snow guns only; cumulative results displayed as dashed lines).

ulated season length (with snowmaking) are less than one week for the four seasons 2007/08–2010/11, while the season length is overestimated by 3–4 weeks for the seasons further in the past. This is not surprising however, since the model runs were performed using the snowmaking infrastructure data for the season 2010/11 and not the actual data of the respective years. Starting with the season 2006/07, the snowmaking infrastructure in the ski area was considerably extended, which is a possible explanation for the increased season lengths (and better agreement with the model results) afterwards. The simulated season length for natural snow conditions only (dashed line in fig. 4.10) shows considerable interannual variations as well as is – for most seasons – significantly shorter than the season length with snowmaking consid-

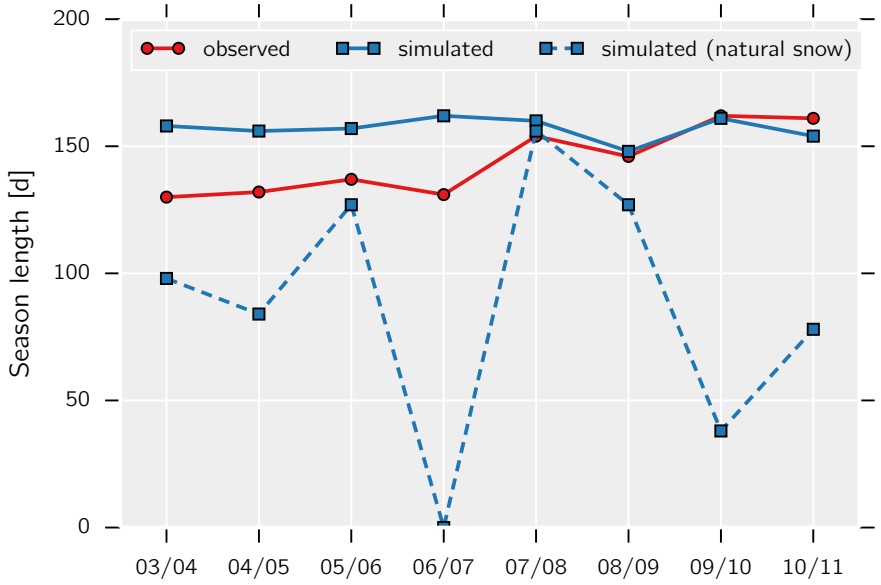

Figure 4.10: Observed and simulated (with (solid line) and without (dashed line) snowmaking) ski season length for the seasons 2003/04–2010/11.

ered. In the season 2006/07, according to the simulations skiing would not have been possible at all without snowmaking.

4.4.5 Spatial validation

For selected dates between mid-April and late May (i. e., around or after the end of the ski season) with available remote sensing observations (Landsat 7 ETM+ scenes), table 4.5 shows the fractional snow-covered area (SCA) of the slope pixels for the observations and the simulations, as well as the pixel-based agreement between observations and model results (i. e., the fraction of pixels correctly classified by the model). The Landsat images were classified by calculating the normalized difference snow index (NDSI) (Hall et al., 1995) and applying a threshold value of 0.4 (Dozier and Painter, 2004), while the model results were classified as snow-covered for SWE values $\geq$ 1 mm. Figure 4.11 shows the simulated SWE for April 9, 2011 and the corresponding Landsat image. The results indicate that in the model generally parts of the slopes become snow-free too early, as shown by the lower SCA values (with one exception), which seems unexpected, since the (extended) snowmaking infrastructure is applied also for seasons in the past, and the season length is being overestimated for those seasons (fig. 4.10). Possible explanations for this result could be that in the model too much snow is produced at higher elevations (hence the season length overesti-

Table 4.5: Observed and simulated fractional snow-covered area (SCA) of the slope pixels and agreement (i. e., fraction of pixels correctly classified by the model) for selected dates in April and May. Observed SCA is derived from Landsat 7 ETM+ scenes using an NDSI threshold of 0.4, and simulated SCA is derived using an SWE threshold of 1 mm.

Date	SCA observed	SCA simulated	Agreement
2005-04-15	0.864	0.978	0.872
2007-04-14	0.712	0.482	0.714
2007-04-21	0.507	0.258	0.668
2010-04-22	0.876	0.545	0.658
2010-04-29	0.736	0.271	0.526
2010-05-24	0.282	0.005	0.722
2011-04-09	0.764	0.767	0.794

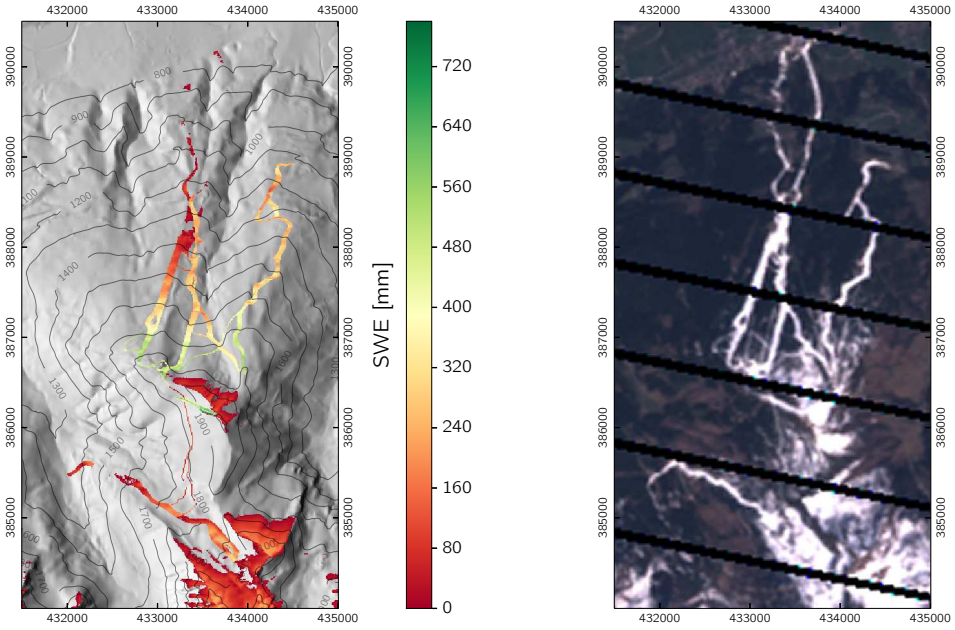

Figure 4.11: Simulated SWE for April 9, 2011 (snow-free pixels are transparent) and the corresponding Landsat 7 ETM+ scene (RGB image).

mation) and not enough at lower elevations (hence the lower SCA values) due to an overrepresentation of snow guns in higher elevations (which could be compensated by adapting the elevation dependency factor (see table 4.2) for the respective slopes), natural snow amounts are underestimated, or snowmelt is overestimated (possibly due to an underestimation of the artificial snow albedo).

4.5 Discussion and conclusions

In our study, a spatially distributed snowmaking module has been incorporated into a physically based energy balance snow model, and applied and evaluated for a ski area in Austria. The snowmaking module explicitly considers individual snow guns and the meteorological conditions at their locations, calculates water losses during the snowmaking process due due to evaporation and sublimation, and accounts for the available water supply and pumping capacity in the ski area, making it to our knowledge the most detailed approach for the modeling of snowmaking operation so far. However, the model requires comparatively high temporal (hourly to three-hourly) as well as spatial (depending on the ski area max. 10–50 m, since it is necessary that the area of the rasterized slopes matches the real slope area most closely in order to generate realistic snow depths) input data resolutions, leading to high computational costs. In addition, in order to accurately simulate snowmaking operations, detailed specifications about the ski area infrastructure (pumping capacity, water supply, number of snow guns) and snow guns (wet-bulb temperature-dependent water flow) as well as snowmaking operations (snowmaking window, threshold temperatures, minimum snow depth that should be maintained) should be available.

Our results show that for the few seasons for which observational data are available, the model performs well in terms of reproducing the total seasonal snowmaking time, water consumption, and energy consumption. For the comparisons on a daily basis, only for the peak snowmaking period (early to mid-December in 2009/10, and mid-November to mid-December in 2010/11) daily snowmaking amounts are reproduced well. This effect can be traced to the general assumptions made on the snowmaking periods, which might differ from the individual decisions made by the snowmaking experts in the ski area. In reality, in the two examined seasons considerable snow amounts in the form of depot snow are already produced during cold periods in October, while only little snow amounts are then produced during periods with more unfavorable snowmaking conditions in November. In the current model version, snowmaking starts at the earliest in November, where as soon as the temperatures are below the threshold snow is produced immediately and for up to 24 h a day, while in reality even with fully automated modern snowmaking systems snowmaking operations always depend on local practices and experiences from previous seasons. This becomes especially apparent in the "improvement snowmaking" period, where in the model snowmaking is performed continually as long as the snow depths are below 60 cm (and only until they are exactly 60 cm), while in reality only

during periods with favorable snowmaking conditions larger amounts of additional snow are produced. For a more accurate simulation of these processes, the snowmaking rules in the model could be refined in accordance with local practices, however, the currently implemented rule set should cover general practices applicable for most Austrian or Alpine ski areas.

The lack of a blowing snow module in the model setup may represent a limitation of this study. Snow transport by wind is a major factor in determining the heterogeneous snow distribution in complex terrain, generally resulting in erosion of snow in exposed areas (e. g., windward slopes or convex areas) and deposition of snow in sheltered areas (e. g., leeward slopes or small-scale depressions) – snow depths in sheltered areas can be several times as high than on adjacent exposed areas (Dadic et al., 2010; Föhn and Meister, 1983; Schirmer et al., 2011). With regard to our study area, we have estimated the significance of the following possible types of blowing snow events: i) Large-scale topography-induced redistribution events likely do not play a major role in our study region, due to the comparatively low elevation and gentle topography of the terrain. Significant redistribution events are expected to occur only near the exposed ridges at the highest elevated parts of the ski area. Additionally, most ski slopes are in forested areas, where wind speeds are lower than in open terrain. ii) Erosion of snow from the ski slopes is very limited due to the high degree of cohesive bonding between the snow crystals, resulting from the accelerated sintering of technical snow as compared to natural new snow as well as the additional hardening due to mechanical processing (Fauve et al., 2002). iii) Snow might be transported to the ski slopes from the surrounding forest canopy, however this effect depends on several factors such as the size of the openings and their orientation relative to the wind direction (Schmidt and Troendle, 1989; Varhola et al., 2010). Due to the lack of measurements for our study area or numerical models that are able to simulate this effect, we are unfortunately unable to estimate if it leads to any significant snow gains on the slopes. iv) Blowing snow during the production of technical snow is again likely insignificant due to the use of low-mounted fan guns and the low wind speeds in forested areas. However, simulating and quantifying all these effects would require substantial effort and was beyond the scope of the present work.

In this study we have focused on evaluating the model's ability to reproduce the historical conditions when driven with the current (as of the season 2010/11) infrastructural conditions as input data. However, the main advantage of this advanced snowmaking simulation approach as compared to simpler methods is the possibility to easily play through different management options and changes in snowmaking in-

frastructure. For example, one could examine the effects of upgrading the snowmaking infrastructure in terms of pumping capacity and reservoirs, increasing the number of snow guns, concentrating the snow guns to certain altitudes or slope segments, replacing lance guns with fan guns, installing higher performance snow guns (increased water flow and/or higher threshold temperatures), or use of snow inducers. Testing these management options including their analysis of economic effects is envisaged in future research projects.

Acknowledgements

We would like to thank the investigated ski area for providing extensive ski area and snowmaking operations related data, as well as the Austrian Central Institute for Meteorology and Geodynamics (ZAMG) for providing meteorological data. Special thanks go to Robert Steiger for supporting the development of the snow production approach with his expert knowledge on the snowmaking practice in Austrian ski areas. We also thank the two anonymous reviewers who helped to improve the paper considerably. This article has been supported by the research project "Effects of Future Snow Conditions on Tourism and Economy in Tyrol and Styria" (CC-Snow II, project number K10AC0K00049). CC-Snow II received financial support from the Climate and Energy Fund and was carried out within the framework of the "ACRP" Program.

Chapter 5

Multilevel spatiotemporal validation of snow/ice mass balance and runoff modeling in glacierized catchments

Florian Hanzer, Kay Helfricht, Thomas Marke, Ulrich Strasser

Published in *The Cryosphere* (Volume 10, August 2016, Pages 1859–1881, doi: 10.5194/tc-10-1859-2016).

My contribution to this article: setting up the model for the study site, implementing the precipitation correction, snow redistribution, cold content and liquid water content, and runoff concentration modules, performing the model runs, designing the validation approach, producing the plots, analyzing the results, and writing the article.

Abstract

In this study, the fully distributed, physically based hydroclimatological model AMUNDSEN is set up for catchments in the highly glacierized Ötztal Alps (Austria, 558 km^2 in total). The model is applied for the period 1997–2013, using a spatial resolution of 50 m and a temporal resolution of 1 h. A novel parameterization for lateral snow redistribution based on topographic openness is presented to account for the highly heterogeneous snow accumulation patterns in the complex topography of the study region. Multilevel spatiotemporal validation is introduced as a systematic, independent, complete and redundant validation procedure based on the observation scale of temporal and spatial support, spacing, and extent. This new approach is demonstrated using a comprehensive set of eight independent validation sources: (i) mean areal precipitation over the period 1997–2006 derived by conserving mass in the closure of the water balance, (ii) time series of snow depth recordings at the plot scale, (iii-iv) multitemporal snow extent maps derived from Landsat and MODIS satellite data products, (v) the snow accumulation distribution for the winter season 2010/11 derived from airborne laser scanning data, (vi) specific surface mass balances for three glaciers in the study area, (vii) spatially distributed glacier surface elevation changes for the entire area over the period 1997–2006, and (viii) runoff recordings for several subcatchments. The results indicate a high overall model skill and especially demonstrate the benefit of the new validation approach. The method can serve as guideline for systematically validating the coupled components in integrated snow-hydrological and glacio-hydrological models.

5.1 Introduction

Assessing the amount of water resources stored in mountain catchments as snow and ice as well as the timing of meltwater production and the resulting runoff is of high interest for glaciological and hydrological investigations and hydropower production. Climate change induced shifts in snow and ice melt will alter the hydrological regimes in glacierized catchments in terms of both timing and magnitude of streamflow discharge. Longer periods of negative glacier mass balances first result in increased runoff due to the enlarged contribution of glacier melt later on, followed by a decline of runoff amounts as a consequence of the reduced glacier area (e. g., Beniston, 2003; Bliss et al., 2014; Collins, 2008; Jansson et al., 2003). For some regions, this moment of "peak water" has already passed, while for others it is expected over the course of the current century (Bliss et al., 2014; Salzmann et al., 2014). Consequently, these catchments undergo a regime shift from icemelt-dominated towards snowmelt-dominated

runoff cycles, accompanied by a shift of the monthly maximum runoff amounts towards earlier periods of the year due to accelerated snowmelt (e. g., Horton et al., 2006).

When using hydroclimatological simulation models to investigate past, current or future water resources, it can generally be distinguished between conceptual and physically based models. Conceptual models often use simple transfer functions to translate input data (e. g., meteorological data) to the desired output variables (e. g., runoff). They tend to be comparatively parsimonious both in terms of input data and the number of parameters, however as the parameters often have no direct physical meaning their values usually have to be determined by calibration, i. e., by tuning them until the model produces the desired output. As conceptual models are usually calibrated to optimize results for a certain period of time, their performance under changing conditions (e. g., climate change) is uncertain. With physically based models on the contrary, it is aimed to explicitly simulate individual processes by following the laws of physics such as conservation of energy, mass, and momentum. In a fully physically based model, all parameters have a physical interpretation and can, in principle, be derived from field measurements. Determination of these parameters however is highly scale-dependent, both with respect to the investigated processes and the model itself (e. g., Blöschl and Sivapalan, 1995). In practice, often few direct measurements are available and a number of required input parameters has to be inter- and extrapolated in space and time.

When validating hydrological models, commonly only runoff records are applied as direct field measurements. It is however well established that validating hydrological models by only comparing observed and simulated runoff at the catchment outlet is not sufficient, as multiple parameter sets may yield the same results (the equifinality problem (Beven, 1993)) – for example, in glacierized catchments underestimations in simulated precipitation volumes may be compensated by increased ice melt contributions. This might be acceptable for short-term applications such as operational flood forecasting, where the main aim is to acquire accurate discharge simulations, however when applying such model parameterizations for long-term simulations (e. g., to determine future runoff changes due to climate change), the errors due to the misrepresentation of specific processes can accumulate and the model provides misleading results. Hence, whenever possible multiple independent data sets should be used for model calibration and validation (e. g., Finger et al., 2015; Grayson et al., 2002; Refsgaard, 1997; Schaefli et al., 2005).

For this purpose, for snow-hydrological applications frequently satellite-derived

snow extent observations are additionally used in the validation process (e. g., Finger et al., 2011; Parajka and Blöschl, 2008). As they are available operationally in high temporal resolution (up to daily, however always with the constraint of frequent cloud obstructions), they allow to spatially assess snow accumulation and melt processes in the model. Additionally, incorporating measured glacier mass balances has shown to lead to more realistic process representations in models (however not necessarily in terms of improved runoff results) (e. g., Finger et al., 2011; Konz and Seibert, 2010; Schaefli et al., 2005; Schaefli and Huss, 2011). Glacier mass balance is an integral measure of the accumulation and ablation processes over the glacier in a defined period, but observations are either available only for very few glaciers with direct measurements or are acquired using DEM differencing covering multi-year periods.

Since several studies have shown that especially accurately capturing the amount and distribution of snow accumulation during the winter is a prerequisite for reliable long-term runoff simulations (e. g., Huss et al., 2014; Magnusson et al., 2011), much work has been put in parameterizing models to better capture winter snow accumulation in terms of spatial distribution and volume. For this purpose, commonly point measurements of snow depth, snow water equivalent or precipitation are inter- and extrapolated, but information on the total water volume stored in entire mountain catchments is rare (e. g., Jonas et al., 2009). Measurements of solid precipitation are impaired with errors (e. g., Goodison et al., 1998; Sevruk, 1986), and the representativeness of point measurements for entire mountain catchments is uncertain (e. g., Grünewald and Lehning, 2011). A relatively recent technology is to use lidar-derived surface elevation differences to obtain snow depth maps in high spatial resolution (e. g., Deems et al., 2006; Grünewald et al., 2010; Grünewald et al., 2013; Grünewald and Lehning, 2011; Helfricht et al., 2014a; Helfricht et al., 2012; Helfricht et al., 2014b; Schöber et al., 2014). Schöber et al. (2014) demonstrated that using lidar-derived snow water equivalent (SWE) maps in the calibration of a spatially distributed snow hydrological model significantly improved the results for simulated snow accumulation, compared to the assimilation of optical remote sensing data of the snow-covered area only.

In our study, we set up the physically based hydroclimatological model AMUNDSEN (Strasser, 2008) for a study region in the highly glacierized Ötztal Alps (Austria). By introducing a concept for systematic model validation using the "observation scale" (Blöschl and Sivapalan, 1995) of temporal and spatial support, spacing, and extent, we validate the model results against (i) mean areal precipitation over the period 1997–2006, (ii) time series of point-based snow depth recordings at several locations,

(iii-iv) multitemporal snow extent maps acquired from Landsat and MODIS imagery, (v) the snow accumulation distribution for the winter season 2010/11 acquired using airborne laser scanning surveys, (vi) glacier-averaged annual surface mass balances for three glaciers in the study area, (vii) spatially distributed glacier surface elevation changes for the entire area over the period 1997–2006, and (viii) hourly runoff records for several subcatchments.

5.2 Study site and model input data

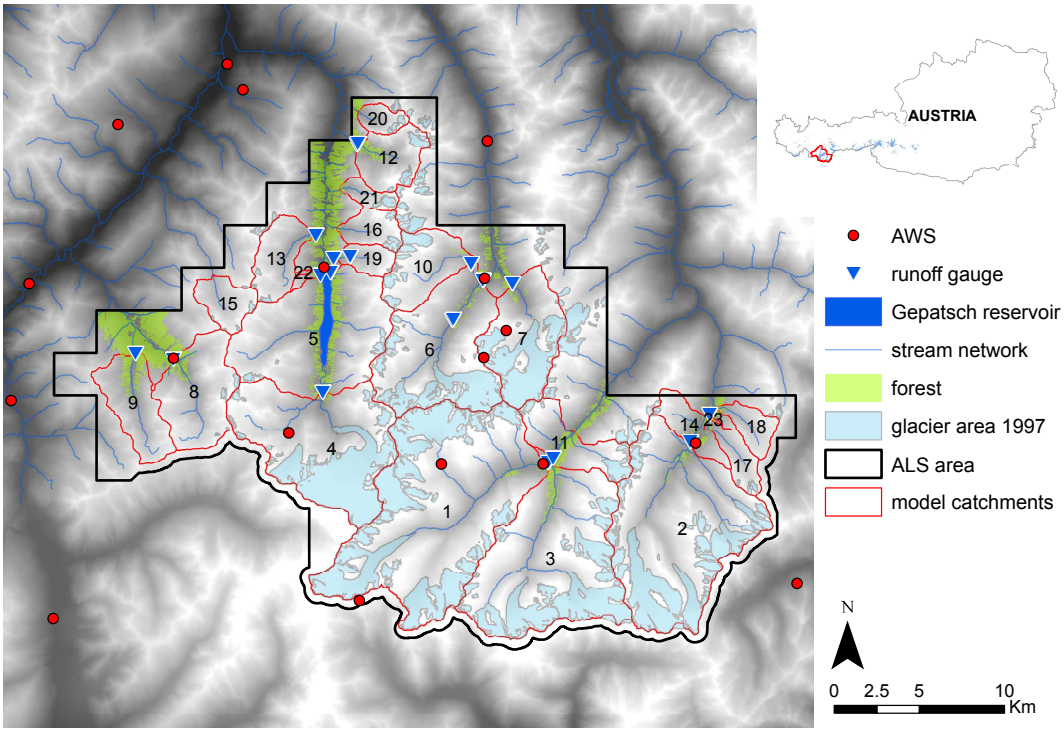

Figure 5.1: Location of the study site in the Ötztal Alps showing glacierized and forested areas, catchment boundaries, and the locations of the meteorological stations and runoff gauges. Numbers indicate catchment IDs (spatial statistics of the individual catchments are listed in table 5.1).

The study site is located in the mountain region of the Ötztal Alps (Tyrol, Austria, fig. 5.1) and comprises the headwater catchments of the valleys Ötztal, Pitztal, and Kaunertal, which contribute to the streamflow of the river Inn. The combined area of the investigated catchments is 558 km^2, of which 480 km^2 are gauged. Elevations range between 1760 m a.s.l. at the lowest elevated runoff gauge and 3770 m a.s.l. at the top of Wildspitze, the highest summit of Tyrol. The Ötztal Alps are the most glacierized mountain region of the Eastern Alps, accounting for almost one third of

the glacier area in Austria. According to the glacier outlines of the second Austrian Glacier Inventory (Fischer et al., 2015), in 1997 137 km^2 (24 %) of the investigated area were covered by glaciers. Only 11 km^2 (2 %) of the investigated area are covered by forests, and another 3 km^2 (0.5 %) by shrubs (source: Land Tirol – data.tirol.gv.at). Main surface types besides the ice-covered areas are alpine grass vegetation, debris cover, and rock walls. Due to the touristic development and the production of hydropower in the region, a large number of weather stations and discharge measurements ensure an extensive basis of meteorological and hydrological data. Approx. half of the study area (277 km^2) are catchments which supply water to the Gepatsch hydropower reservoir (see fig. 5.1). Table 5.1 lists the area, minimum/maximum/mean elevation, and glacierization (as of the year 1997) of the investigated catchments.

Table 5.1: Area, minimum/maximum/mean elevation, and glacierization (as of the year 1997) of the investigated catchments. The catchment IDs correspond to the labels in fig. 5.1.

ID	Catchment	Area [km^2]	z_{min} [m a.s.l.]	z_{max} [m a.s.l.]	z_{mean} [m a.s.l.]	Glacierization 1997 [%]
1	Rofenache	98.6	1891	3762	2890	38.3
2	Am Barst/Gurgler Ache	72.4	1883	3496	2780	31.8
3	Niedertalbach	66.7	1878	3585	2883	31.1
4	Gepatschalm	53.9	1893	3526	2821	39.7
5	Speicher Gepatsch	52.3	1744	3445	2480	1.7
6	Taschachbach	44.7	1789	3754	2737	26.1
7	Pitze	27.0	1812	3519	2830	48.2
8	Radurschlbach	24.0	1794	3349	2601	1.5
9	Tscheybach	16.4	1800	3055	2417	0.0
10	Rifflsee Ausfluss	15.9	2232	3386	2777	17.8
11	Venter Ache	15.0	1836	3498	2680	13.5
12	Verpeilbach	12.1	1807	3370	2562	9.3
13	Fissladbach	11.4	1797	3137	2576	2.1
14	Poschach/Gurgler Ache	8.1	1826	3217	2435	1.6
15	Platzertal	7.9	2298	3104	2667	2.8
16	Watzebach	6.7	1819	3525	2718	10.2
17	Ferwallbach	6.3	1851	3254	2608	4.5
18	Königsbach	5.9	1876	3077	2607	0.0
19	Rostizbach	4.8	1842	3389	2628	0.7
20	Gsallbach	3.9	1843	3250	2560	9.1
21	Madatschbach	3.8	1847	3339	2605	13.6
22	Bloabachl	0.2	1775	2638	2323	0.0
23	Poschach	0.2	1828	2328	2004	0.0
	Total	558.1	1744	3762	2740	24.6

An airborne laser scanning (ALS)-derived digital elevation model (DEM) from the year 2006 (source: Land Tirol – data.tirol.gv.at) resampled to 50 m resolution was used as input for the model and the calculation of derived terrain variables (e. g., slope,

aspect, sky-view factor, and catchment boundaries). Meteorological records (air temperature, precipitation, relative humidity, global radiation, and wind speed) in hourly resolution from 14 automatic weather stations in and surrounding the study region were used to drive the model. Initial ice thickness distribution of all glaciers in the Ötztal Alps was calculated using the approach by Huss and Farinotti (2012). The method is based on glacier mass turnover and ice flow mechanics and requires glacier outlines and a DEM. Mass balance gradients and constants recommended by M. Huss (pers. comm., 2011) were used to calculate volumetric balance fluxes of the individual glaciers. Required glacier surface elevations and glacier outlines of the year 1997 exist from the second Austrian Glacier Inventory (Fischer et al., 2015).

5.3 Methods

5.3.1 The hydroclimatological model AMUNDSEN

The modular, physically based, distributed modeling system AMUNDSEN (Strasser, 2008) was applied for the simulation of the snow and ice surface mass balance. AMUNDSEN has been designed to specifically address the requirements of snow modeling in mountain regions under climate change conditions and has already been extensively validated in various Alpine sites (Hanzer et al., 2014; Marke et al., 2015; Pellicciotti et al., 2005; Strasser, 2004; Strasser, 2008; Strasser et al., 2008).

As input data for the model, a digital elevation model of the model domain with a spatial resolution typically in the order of tens to hundreds of meters (the comparatively high resolution is necessary for adequately capturing the small-scale processes shaping the snow cover in complex terrain), as well as hourly to three-hourly recordings of the meteorological variables air temperature, relative humidity, precipitation, global radiation, and wind speed are required. Several derived topographic parameters (slope, aspect, sky-view factor, openness) can either be preprocessed or calculated during runtime. In order to enable specific submodules (canopy module, evapotranspiration, runoff), various other spatial input fields (land cover, soil, catchment boundaries) have to be prescribed. The calculations presented in this study have been performed on a 50 m grid and with hourly meteorological recordings.

Interpolated fields from the scattered point measurements are – in the case of temperature, precipitation, humidity, and wind speed – obtained using a combined lapse rate–inverse distance weighting scheme, either using automatically calculated lapse rates for each time step or using prescribed monthly lapse rates. The latter approach

has been chosen for this study – for temperature and humidity (dew point temperature), the lapse rates derived by Marke (2008) were used, while for precipitation monthly lapse rates were derived from time series recorded by accumulative precipitation gauges in the study area. In the case of radiation, first clear-sky global radiation is calculated following Corripio (2002) taking into account hillshading, transmission losses due to scattering (Rayleigh and aerosol scattering) and absorption (by water vapor, ozone, and other trace gases), transmission gains due to multiple reflections between the atmosphere and the ground, and reflections from surrounding terrain. Subsequently, actual global radiation is obtained by correcting the clear-sky radiation with interpolated cloud factor fields (obtained using radiation recordings at the meteorological stations). Incoming longwave radiation is also derived following Corripio (2002) using parameterizations for the radiation fractions coming from the clear sky, from clouds, and from surrounding slopes.

Precipitation phase is then determined using a wet-bulb temperature threshold of $T_w = 2\ ^\circ\mathrm{C}$. Wet-bulb temperature is calculated by iteratively solving the psychrometric equation. Four types of snow/ice layers are distinguished in the model, namely new snow, old snow, firn, and ice, with each layer having distinct properties in terms of water equivalent, density, and albedo. Fresh snowfall is always added to the new snow layer. New snow is converted to old snow when reaching a transition density of $200\ \mathrm{kg\,m^{-3}}$, old snow to firn always on September 30, and firn to ice when reaching a transition density of $900\ \mathrm{kg\,m^{-3}}$. Fresh snow density ρ_{ns} is calculated as a function of air temperature T_a [°C] following Anderson (1976) and Jordan (1991):

$$\rho_{\mathrm{ns}} = \begin{cases} 50 & T_a \leq -15\ ^\circ\mathrm{C} \\ 50 + 1.7(T_a + 15)^{1.5} & T_a > -15\ ^\circ\mathrm{C}. \end{cases} \tag{5.1}$$

Snow compaction for the new snow and old snow layer is calculated following Anderson (1976) and Jordan (1991), taking into account the effects of compaction and metamorphism:

$$\frac{\mathrm{d}\rho_s}{\mathrm{d}t} = \rho_s \left(c_1 W^* \mathrm{e}^{-c_2(T^* - T_s)} \mathrm{e}^{-c_3 \rho_s} \right), \tag{5.2}$$

$$\frac{\mathrm{d}\rho_s}{\mathrm{d}t} = \rho_s \left(c_4 \mathrm{e}^{-c_5(T^* - T_s)} c_6 \right), \tag{5.3}$$

$$c_6 = \begin{cases} \mathrm{e}^{-c_7(\rho_s - \rho_d)} & \rho_s > \rho_d \\ 1 & \rho_s \leq \rho_d, \end{cases} \tag{5.4}$$

with ρ_s [$\mathrm{kg\,m^{-3}}$] being the layer (new snow or old snow) density, W^* [$\mathrm{kg\,m^{-2}}$] the load of snow water equivalent (snow in the layer above and 50 % of the snow in the current

layer), $c_1 = 0.01\ \mathrm{m^{-1}\,h}$ (new snow), $c_1 = 0.001\ \mathrm{m^{-1}\,h}$ (old snow), $c_2 = 0.08\ ^\circ\mathrm{C}^{-1}$, $c_3 = 0.021\ \mathrm{m^3\,kg^{-1}}$, $c_4 = 0.01\ \mathrm{m^{-1}\,h}$, $c_5 = 0.04\ ^\circ\mathrm{C}^{-1}$, $c_7 = 0.046\ \mathrm{m^3\,kg^{-1}}$, $\rho_d = 150\ \mathrm{kg\,m^{-3}}$ and $T^* = 0\ ^\circ\mathrm{C}$. For the firn layer, a linear transition from firn to ice in 10 years is assumed, while ice density is kept constant at $900\ \mathrm{kg\,m^{-3}}$.

Snow surface albedo α is parameterized following Rohrer (1992) taking into account snow age and temperature:

$$\alpha = \alpha_{\min} + (\alpha_{t-1} - \alpha_{\min})\, \mathrm{e}^{-c_T/24}, \tag{5.5}$$

where $\alpha_{\min}$ is the (prescribed) minimum albedo, α_{t-1} the albedo in the previous time step, and c_T a temperature-dependent recession factor (implemented by prescribing two factors $c_{T\geq 0}$ and $c_{T<0}$ for positive and negative air temperatures, respectively). For the present study, fresh snow albedo was set to 0.85, while $\alpha_{\min}$, $c_{T\geq 0}$, and $c_{T<0}$ for new snow and old snow were set to 0.55, 0.12, and 0.05, respectively. Firn and ice albedo were held constant with $\alpha_{\mathrm{firn}} = 0.4$ and $\alpha_{\mathrm{ice}} = 0.2$.

In forested areas, a canopy submodule optionally modifies the meteorological variables for inside-canopy conditions (Strasser, 2008) and accounts for the forest snow processes of interception, sublimation, and melt unload following Liston and Elder (2006a). Evapotranspiration over vegetated areas is calculated using the FAO Penman-Monteith approach (Allen et al., 1998).

The snow and ice surface energy balance is calculated as

$$Q_N + Q_H + Q_E + Q_A + Q_B + Q_M = 0, \tag{5.6}$$

with Q_N being the shortwave and longwave radiation balance, Q_H the sensible heat flux, Q_E the latent heat flux, Q_A the advective energy supplied by solid or liquid precipitation, Q_B the soil heat flux, and Q_M the energy potentially available for melt. For a detailed description of the calculation of the individual energy fluxes see Strasser (2008).

For the application in this study, the original model setup of AMUNDSEN was adapted to the mountain region of the Ötztal Alps by adding modules which enable a more realistic simulation of the catchment precipitation, of the timing of snowmelt (by considering cold content and liquid water content of the snowpack), and of runoff concentration. These are described in the following sections.

5.3.2 Precipitation correction

With respect to the undercatch of solid precipitation by common rain gauges (e. g., Goodison et al., 1998; Sevruk, 1986), a number of previous studies showed that the

measured values of solid precipitation have to be corrected for systematic errors due to wetting loss, evaporation loss, and wind-induced undercatch (e. g., Farinotti et al., 2011; Rohrer and Braun, 1994; Schöber et al., 2014).

A common and straightforward method to apply a correction for snow undercatch is to introduce a fixed snow correction factor (SCF) which is applied to the fraction of precipitation identified as snow. However, it has been shown that errors due to wind-induced undercatch are especially large at lower temperatures, where snowfall mainly consists of smaller particles which are blown away more easily (e. g., Goodison et al., 1998; Sevruk, 1983). Using fixed SCF values thus tends to result either in underestimations of winter snowfall amounts or overestimations of snowfall events during spring and fall. A more robust method of snow correction is hence to introduce a variable correction factor derived from the meteorological variables (most importantly wind speed and temperature) measured at the gauge site.

For our study, we used the empirical correction for the Hellmann type precipitation gauge presented in Goodison et al. (1998). Catch ratio CR (i. e., the fraction of the actual precipitation amount that is captured by the gauge) in percent is thereby calculated as a function of air temperature T_a [°C] and wind speed WS [m s^{-1}]:

$$\mathrm{CR} = 96.63 + 0.41\mathrm{WS}^2 - 9.84\mathrm{WS} + 5.95T_a. \tag{5.7}$$

Adjusted precipitation values are then obtained by dividing the original values by CR.

This correction is applied to the station measurements at each model time step prior to the spatial interpolation of precipitation. However, since model results indicated that the simulated snowfall amounts were still underestimated, a post-interpolation adjustment of solid precipitation using a fixed snow correction factor (for details see section 5.5.1) was additionally implemented.

5.3.3 Snow redistribution

With the standard method for the spatial interpolation of point precipitation measurements implemented in AMUNDSEN, obtained interpolation values are influenced by the respective grid cell elevation and its distance to surrounding weather stations. However, it is well known that snow accumulation patterns in complex terrain are fundamentally influenced by topographic controls beyond elevation alone, most importantly being attributed to redistribution of snow by wind and gravitational forces (Bernhardt et al., 2010; Blöschl and Kirnbauer, 1992; Grünewald et al., 2014; McKay and Gray, 1981; Warscher et al., 2013). Considering these processes is a prerequisite

for reliable long-term mass balance simulations, hence the distribution of solid precipitation in AMUNDSEN has been updated using an empirical relation between SWE and topographic parameters.

Numerous studies have applied statistical models to explain snow cover variability using multiple regressions of topographic parameters such as elevation, slope, aspect, curvature, viewshed, and terrain roughness (e. g., Chang and Li, 2000; Elder et al., 1991; Grünewald et al., 2013; Lehning et al., 2011; Pomeroy et al., 2002; Winstral et al., 2002), However, Grünewald et al. (2013) showed that statistical relations between snow depth and topography are site-specific and performance decreases considerably when applying calibrated regression formulas to snow depth distributions in other catchments. Additionally, the topographic derivatives depend distinctly on the spatial scale used for calculation. Helfricht et al. (2014b) showed that the spatial variability of snow depth in a glacierized catchment is caused by a short-range variability based on small-scale terrain roughness, but also by a long-range variability with respect to the glacierized and wind-sheltered cirques and valleys in contrast to wind-exposed mountain ridges.

In this study we used topographic openness (Yokoyama et al., 2002) for the parameterization of the spatial snow distribution according to Helfricht (2014). Openness is a parameter originally developed to visualize topographic character and features in images, as it expresses the degree of dominance or enclosure of a location on an irregular surface. Topographic openness has two viewer perspectives in terms of positive and negative openness. Positive openness for a DEM grid point is obtained by averaging the zenith angles calculated for all eight compass directions from the grid point, while negative openness is obtained by averaging the respective nadir angles. The latter was used in this study to parameterize the spatial snow distribution, as it yields low values for convex forms and high values for concave forms. The openness values depend on the length scale L, which is the maximum distance considered for calculation: low L values result in a high spatial variability of openness, while high L values display large-scale topography of ridges and valley floors and hence highlight the overdeepening of, e. g., the surface elevations of glacier tongues compared to the surrounding ridges and peaks (Helfricht, 2014).

Negative openness Ψ_L was calculated for the entire Ötztal mountain range based on a 50 m DEM for $L = 50$ m and $L = 5000$ m, according to the definitions given in Yokoyama et al. (2002) (resulting values for a subset of the area are shown in fig. 5.2 (top)). A linear relation was applied between the minimum and the maximum threshold of negative openness to derive the snow redistribution factor SRF, shown in fig. 5.2

(bottom):

$$\tilde{\Psi}_{50} = 3 \cdot (\Psi_{50} - 1.2), \tag{5.8}$$

$$\tilde{\Psi}_{5000} = 3 \cdot (\Psi_{5000} - 1), \tag{5.9}$$

$$\mathrm{SRF} = \frac{1}{2}\left({}^{\top 1.6}_{\perp 0.1}\tilde{\Psi}_{50} + {}^{\top 1.6}_{\perp 0.1}\tilde{\Psi}_{5000}\right), \tag{5.10}$$

where ${}^{\top 1.6}_{\perp 0.1}\tilde{\Psi}$ denotes $\tilde{\Psi}$ clipped to values between 0.1 and 1.6. Hence, at least 10 % of the initial atmospheric solid precipitation can be stored even in almost vertical slopes and in very exposed areas for the time of the precipitation event, while wind-sheltered areas can hold a maximum of 1.6 times the initial amount. At each time step, solid precipitation of each raster cell is multiplied with the corresponding redistribution factor. The new total amount of solid precipitation over the entire area is related to the initial precipitation amount in order to keep the total precipitation volume constant (mass conservation). Consequently, simulated accumulation is reduced in areas of low negative openness (i. e., exposed ridges, sheer rock faces) and increased in sheltered areas (i. e., cirques and low elevated valley floors). The two length scales and the factors in eqs. (5.8)–(5.10) were determined by manual optimization for the best fit of the redistribution factor field with the ALS-derived surface elevation differences (interpreted as snow accumulation over the winter season).

To summarize, in total three steps of snow adjustments are applied: (i) the wind speed and temperature-dependent correction of measured precipitation at the meteorological stations (eq. (5.7); variable in time and space), (ii) the additional post-interpolation snowfall adjustment using a fixed snow correction factor (constant in time and space), and (iii) the adjustment using the snow redistribution factors acquired using eq. (5.10) (constant in time, variable in space). Whereas the first two steps are required to correct precipitation input towards a realistic precipitation volume, the latter does not change the total volume but rather redistributes the solid precipitation with respect to the terrain.

5.3.4 Cold content and liquid water content

To account for temperature changes inside the snow cover, a parameterization for cold content and liquid water content based on the work of Braun (1984) has been added to the model. Meltwater is thereby not immediately removed from the snowpack, but a certain amount of liquid water (originating from surface melt or rain) can be retained in the snowpack. In the case of negative surface energy balances, this liquid water can refreeze. Further heat loss is used to build up a cold content, which needs to be depleted again before actual melt can occur. The cold content corresponds to the

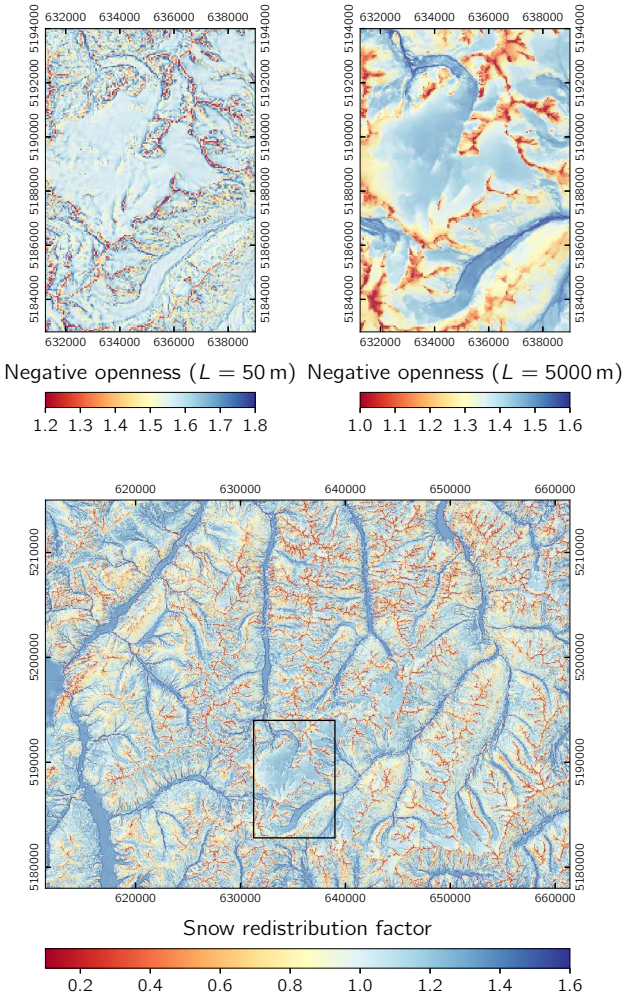

Figure 5.2: Negative openness of a subset of the study area for length scales $L = 50$ m and $L = 5000$ m (top), and the snow redistribution factor derived by a combination of both data sets (bottom; black frame shows the boundaries of the upper plots).

energy required to warm the entire (dry) snowpack to 0 °C. By relating this energy with the latent heat of fusion of ice (333.7 kJ kg^{-1}), cold content can alternatively also be expressed in units of water equivalent (corresponding to the equivalent amount of liquid water needed to release the required amount of energy by freezing), which is the formulation we use within this study. The module for cold content and liquid water content is described in more detail in the article supplement.

Following Blöschl and Kirnbauer (1991), for the new snow and old snow layers the liquid water retention capacity of the snowpack was set to 10 % of the total snowpack weight, and the maximum possible cold content to 3 % of the total snowpack weight

for this study. The refreezing factor (the amount of heat loss that is used to build up the cold content) was set to 0.65. This value, slightly higher than the literature value of 0.5, was determined by comparison of observed and simulated snow depth recordings.

5.3.5 Runoff concentration

For runoff concentration, a linear reservoir cascade approach (Nash, 1960) following Asztalos et al. (2007) was implemented in the model. Runoff originating from rainfall and from meltwater released from glaciers and the snowpack is thereby cumulated in each time step and catchment and routed through four parallel linear reservoir cascades for unglacierized areas, bare ice areas, firn-covered areas on glaciers, and snow-covered areas on glaciers (the latter consisting of the AMUNDSEN "new snow" and "old snow" layers, which are not treated separately in terms of runoff concentration). A constant fraction $f_{\text{glacierized}}$ of the inflow into the snow, firn, and ice reservoirs, as well as a fraction $f_{\text{unglacierized}}$ of the inflow into the unglacierized reservoir is diverted into an additional soil reservoir. The parameters of the linear reservoir model (for each cascade the number of parallel reservoirs n and the storage constant k, as well as $f_{\text{glacierized}}$ and $f_{\text{unglacierized}}$) are determined by calibration separately for each catchment. Calibration is performed using an automatic optimization routine with the aim to maximize the objective function

$$\text{NSE}_V = \text{NSE} - 0.1|V_E|, \tag{5.11}$$

i. e., maximizing the Nash-Sutcliffe efficiency NSE and minimizing the relative volume error V_E (following Lindström (1997)). Table 5.2 shows the allowed ranges for the parameters during the automatic calibration.

5.4 Validation approach and data

In this study, the individual model components are validated against (i) mean areal precipitation values for the period 1997–2006 for the gauged catchments, (ii) daily to hourly snow depth recordings at five locations in the study area, (iii-iv) snow-covered area maps acquired by Landsat and MODIS imagery, respectively, (v) the snow accumulation distribution for the winter season 2010/11 acquired using airborne laser scanning surveys, (vi) glacier-averaged annual surface mass balances for three glaciers in the study area, (vii) spatially distributed glacier surface elevation changes for the entire area over the period 1997–2006, and (viii) hourly runoff records for 8 of the

Table 5.2: Parameter ranges for the runoff module calibration.

Parameter	Lower limit	Upper limit
k_{snow} [h]	5	20
k_{firn} [h]	5	20
k_{ice} [h]	1	5
$k_{unglacierized}$ [h]	5	20
k_{soil} [h]	10	100
n_{snow} [–]	1	20
n_{firn} [–]	2	6
n_{ice} [–]	1	4
$n_{unglacierized}$ [–]	1	7
n_{soil} [–]	2	10
$f_{glacierized}$ [–]	0.05	0.50
$f_{unglacierized}$ [–]	0.05	0.80

investigated catchments. Besides the satellite-derived snow extent maps which only give binary information (snow yes/no), all other data sets also include volumetric information about the water resources in the study area (in varying spatial and temporal scales).

According to Blöschl and Sivapalan (1995), any finite set of observations is accompanied by an "observation scale" in space and time, that can be defined by a "scale triplet" of support, spacing, and extent. Support is the integration volume or time of a single sample, spacing is the distance or time between individual samples, and extent is the total coverage in space or time of the entire data set. These concepts are illustrated in fig. 5.3. Table 5.3 lists the spatial and temporal support, spacing, and extent of the used validation data sets, as well as the associated information type (binary vs. continuous information).

However, as the tabular representation of the scales makes it rather difficult to interpret and compare them, a visual method to display the observation scale of a data set is proposed: The seven dimensions (support, spacing, and extent in both space and time, as well as information type) are arranged as axes on a radar chart, where the left and right halves of the chart represent the spatial and temporal dimensions, respectively. The ranges of the individual axes and their ordering (from low to high or from high to low values) are designed such that a "perfect" validation data set (i. e., having the lowest possible support and spacing, the highest possible extent, and continuous information) is represented by a regular heptagon with the maximum possible diameter (i. e., extending to the maximum axis extent in each dimension). This implies that the ordering of the axis values is not consistent (extent ranges from low

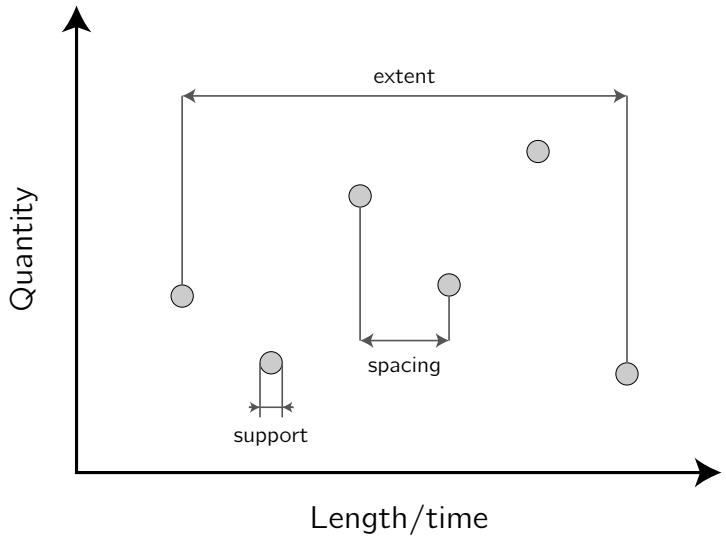

Figure 5.3: Illustration of the observation scale of a set of measurements (based on Blöschl and Sivapalan (1995)). Support is the integration volume or time of a single sample, spacing is the distance or time between individual samples, and extent is the total coverage in space or time of the entire data set.

Table 5.3: Information type (binary or continuous) as well as spatial and temporal support, spacing, and extent of the validation data sets used in this study.

		Space			Time		
Data set	Information type	Support	Spacing	Extent	Support	Spacing	Extent
Snow depth	continuous	point	varying	point	instant	1 d	17 yr
Runoff	continuous	catchment	varying	catchment	1 h	1 h	17 yr
MODIS snow-covered area	binary	500 m	500 m	catchment	instant	1 d	14 yr
Landsat snow-covered area	binary	50 m	50 m	catchment	instant	16 d	17 yr
Glacier mass balance	continuous	glacier	varying	glacier	1 yr	1 yr	17 yr
Long-term glacier mass balance	continuous	50 m	50 m	glacier	10 yr	once	10 yr
ALS-based snow accumulation	continuous	50 m	50 m	catchment	6 mo	once	6 mo
Areal precipitation	continuous	catchment	varying	catchment	10 yr	once	10 yr

to high values, while support and spacing range from high to low values), however it allows for an easier visual interpretation (bigger is always better). Fig. 5.4 shows the resulting axes including the possible values for our particular case study, while fig. 5.5 shows the resulting charts for the eight validation data sets used in this study. As the charts are supposed mainly for a qualitative interpretation and comparison between the different data sets, they are shown without axis and tick labels in the latter.

The various data sets and the respective validation strategies are outlined in the

following sections.

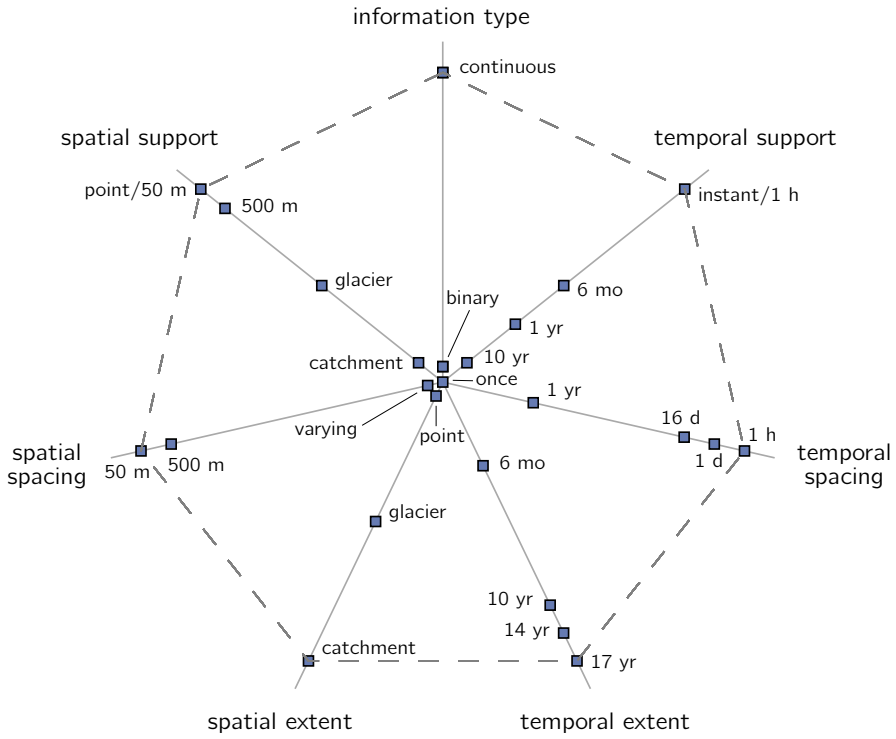

Figure 5.4: Radar chart axes for the visualization of the observation scale of the used validation data sets.

5.4.1 Areal precipitation

As a method to estimate long-term mean annual catchment precipitation for all gauged catchments to use as a validation data set for the respective AMUNDSEN simulation results, the OEZ approach (Kuhn, 2000; Kuhn and Batlogg, 1998) was used. This method calculates catchment-scale precipitation P from measured runoff Q, evaporation E and glacier mass changes ΔS as the remainder from the water balance equation

$$P = Q + E + \Delta S, \tag{5.12}$$

and has proven to be very robust for the simulation of decadal mean values (Kuhn, 2000). Evaporation E, typically comparatively small in glacierized catchments, is approximated using constant values depending on the surface type (ranging between 15 mm/month for snow and ice surfaces and 60 mm/month for forested areas). Liquid water storage within the snowpack and the ground is accounted for by the residuals of measured runoff vs. calculated monthly runoff originating from snow melt, ice

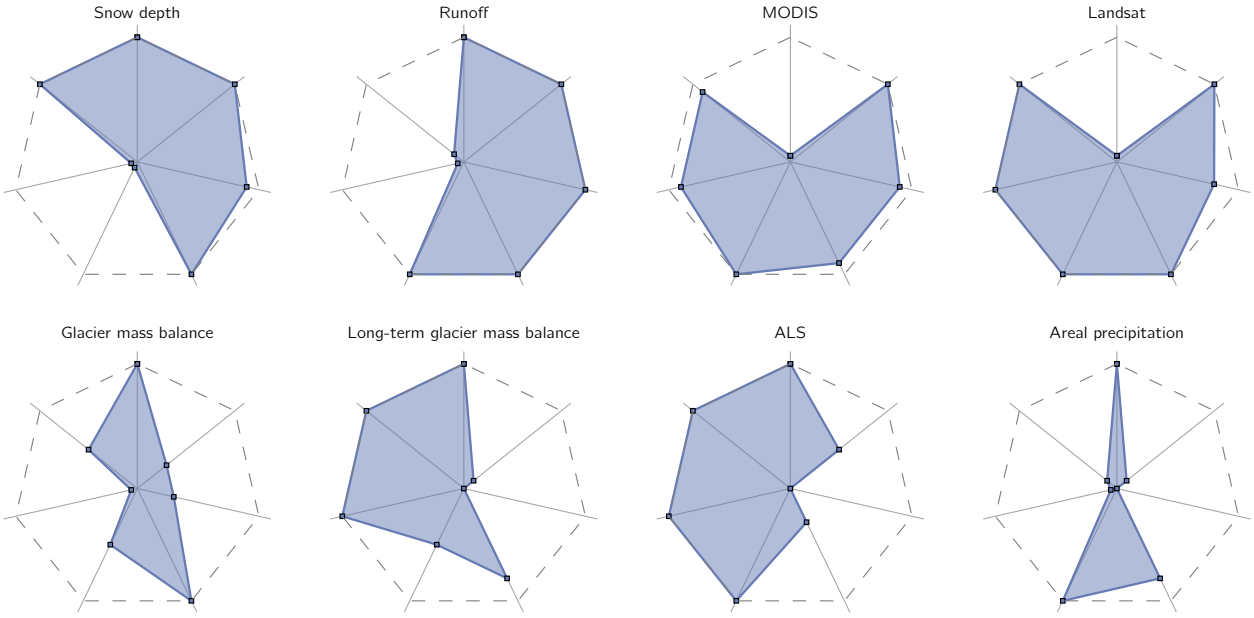

Figure 5.5: Radar charts (using the axis scales from fig. 5.4) showing the observation scale of the validation data sets used in this study. The dashed gray heptagons represent an "optimal" validation data set.

melt, and precipitation minus evaporation (Kuhn et al., 2016). Interannual changes in ground water storage are neglected, as the method aims at mean annual values over longer periods.

To calculate areal precipitation values for our study catchments, for runoff Q the respective measurements at the catchment outlets were used, while glacier volume changes ΔS were derived from the surface elevation changes between 1997 and 2006 according to the glacier inventories performed in these years (Abermann et al., 2009).

5.4.2 Snow depth

Comparisons with snow depth measurements at the locations of meteorological stations allow to evaluate model performance in terms of realistic representation of accumulation (adequate correction for gauge undercatch, snow/rain separation) and ablation (surface albedo evolution, cold content and liquid water content, surface energy balance) at the point scale, as well the conversion of snow water equivalent to snow depth. The latter has however already been evaluated in previous studies (e. g., Marke et al. (2015)) and has proven to be robust. Snow depth is evaluated at five locations covering an elevation range of almost 2000 m: Prutz (871 m a.s.l.), Nauders (1330 m a.s.l.), Obergurgl (1942 m a.s.l.), Weisssee (2480 m a.s.l.), and Pitztaler

Gletscher (2864 m a.s.l.).

5.4.3 Snow distribution

5.4.3.1 Satellite-derived snow distribution

Satellite-derived snow cover images allow to spatially validate simulation results in comparatively high spatial and temporal resolutions. For this study, we used a comprehensive set of Landsat (5/7) and MODIS scenes to derive snow extent maps for the study area. Landsat products are available in 30 m spatial resolution and a 16-day revisit time, while MODIS snow products are available daily from two satellites (Aqua and Terra), however with a coarser spatial resolution of 500 m. However, both Landsat and MODIS images are subject to frequent cloud obstructions, hence only a limited subset of the available scenes was usable for this study.

With regard to Landsat data, a set of 26 suitable scenes covering the period 1998–2012 was manually selected (a list of the scenes can be found in the article supplement). Besides the requirement of no or minimum cloud coverage over the study area, images acquired in the early morning hours especially during winter were not taken into account, as illumination effects from low sun elevation angles often pose problems in terms of sensor saturation on sun-facing slopes and topographic shadowing, making it difficult to retrieve snow cover.

To derive snow maps from the raw Landsat bands, first the digital numbers (DNs) of the individual bands were converted to top-of-atmosphere reflectances using the `i.landsat.toar` module from GRASS GIS (GRASS Development Team, 2012). Subsequently, the reflectances were topographically corrected using `i.topo.corr`. Then, the normalized difference snow index (NDSI) (Hall et al., 1995) was calculated using the band ratio

$$\mathrm{NDSI} = \frac{\mathrm{green} - \mathrm{SWIR}}{\mathrm{green} + \mathrm{SWIR}}, \tag{5.13}$$

where green and SWIR (shortwave infrared) correspond to TM bands 2 and 5, respectively, for both Landsat 5 and 7. Several NDSI thresholds for the binary snow/no snow classification were subsequently evaluated, however the commonly chosen value of 0.4 (Hall et al., 1995) provided adequate results and was thus used for all 26 scenes. Following Hall et al. (1998), additional to the NDSI threshold a threshold of the near-infrared (NIR) channel (TM band 4) was used to avoid misclassifying water bodies as snow – pixels with NIR < 11 % are thereby never classified as snow.

The applied NDSI threshold generally also classifies ice surfaces as snow. To discriminate snow from glacier ice, for all glacier pixels (according to the used glacier

mask) broadband albedo α was calculated from Landsat TM bands 2 and 4 (green and NIR) following the relation by Knap et al. (2010):

$$\alpha = 0.726\alpha_2 - 0.322\alpha_2^2 - 0.051\alpha_4 + 0.581\alpha_4^2, \tag{5.14}$$

where α_2 = TM 2 and α_4 = TM 4. Then, for each scene an α threshold for discriminating snow from ice was manually derived using a histogram analysis of the α values over the glaciers. For 22 of the 26 scenes a threshold of $\alpha = 0.3$ was found to be applicable, while for the remaining scenes values of 0.25, 0.35, and 0.4 were used.

In contrast to Landsat, precomputed MODIS snow cover products are readily available for download (Hall et al., 2002). For our study we used the binary snow cover products MYD10A1 and MOD10A1 (for the Aqua and Terra satellites, respectively), which are available in 500 m resolution on a daily basis. To reduce the influence of clouds and misclassifications, Aqua and Terra scenes for each day were merged into a composite image: if a pixel in one scene was classified as cloud-covered in one scene and cloud-free in the other, the respective value of the cloud-free scene was taken, while if one pixel was considered snow-covered in one scene and snow-free in the other, the pixel was classified as snow. This approach is similar to methods applied in other studies (e. g., Gafurov and Bárdossy (2009) and Xie et al. (2009)).

MODIS snow products are calculated using a NDSI thresholding approach and hence also do not discriminate between snow and ice surfaces. Some studies have used the 250 m visible and near-infrared MODIS bands to classify snow and ice surfaces (e. g., Shea et al. (2013)), however we found this method not applicable for our study, since the coarse resolution of the MODIS scenes makes it challenging to differentiate between snow and ice facies for the majority of (small) glaciers in the study area. As a pragmatic solution we excluded all MODIS scenes taken in the months July–September from the analyses, since it can be assumed that outside of this period the glaciers are snow-covered and MODIS "snow" pixels are actually snow rather than ice.

To compare simulation results with the satellite products, the daily AMUNDSEN SWE maps were converted into binary snow cover images using an SWE threshold of 1 mm (this amount of snowfall is required to turn a summer landscape into "white winter" landscape). For the Landsat validation, the Landsat 30 m pixels were resampled to the 50 m model resolution, while for the MODIS validation the AMUNDSEN snow maps were resampled to the MODIS resolution using mode resampling, i. e., a 500 m pixel was classified as snow if at least 50 % of the 50 m pixels it comprises were snow-covered.

For the comparison and evaluation of observed and simulated snow cover patterns, we use the contingency table-based efficiency criteria ACC, BIAS, and CSI (Zappa, 2008):

$$\mathrm{ACC} = \frac{n_{11} + n_{00}}{n_{xx}}, \tag{5.15}$$

$$\mathrm{BIAS} = \frac{n_{1x}}{n_{x1}}, \tag{5.16}$$

$$\mathrm{CSI} = \frac{n_{11}}{n_{xx} - n_{00}}. \tag{5.17}$$

For the definitions of n_{00} to n_{xx} see table 5.4. Accuracy ACC is the number of correct predictions divided by the total number of samples (values between 0 and 1, with a perfect score being 1). This score, however, tends to be comparatively optimistic, as it usually yields high values both during winter (where most of the pixels are snow-covered) and summer (where most of the pixels are snow-free). A more sensitive score is the critical success index CSI, which is the number of correctly predicted snow events divided by the number of times where snow is predicted in the model and/or observed. Finally, BIAS corresponds to the frequency of correct snow predictions, i. e., the number of times where snow is present in the simulations divided by the number of times where it is observed. Again, a value of 1 is a perfect match, while here values below 1 indicate that snow cover is underrepresented in the model, and values above 1 indicate that the model overestimates the snow cover.

Table 5.4: 2 × 2 contingency table for the comparison of binary snow cover observations and simulations (after Zappa (2008)). *O* and *S* denote observations and simulations, while the subscripts 0 and 1 correspond to snow-free and snow-covered situations, respectively.

	S_1	S_0	Σ
O_1	n_{11}	n_{01}	n_{x1}
O_0	n_{10}	n_{00}	n_{x0}
Σ	n_{1x}	n_{0x}	n_{xx}

5.4.3.2 ALS-derived snow distribution

While satellite-derived snow cover maps can be used to analyze binary snow coverage (snow yes/no) in high temporal resolution, lidar-derived surface elevation fields allow to obtain snow depth maps in very high spatial resolution. For this purpose, two lidar surveys are required: one for mapping the snow-free terrain, and one for recording the snow-covered terrain. The difference between both surface elevations can be interpreted as snow depth (in case of glacier surfaces, the vertical component

of the ice flow has to be evaluated and considered for error analysis (e. g., Helfricht et al., 2014a; Sold et al., 2013)).

Airborne laser scanning (ALS) surveys of a 746 km^2 large area encompassing all investigated catchments were performed for the winter 2010/2011 to determine the spatial snow distribution and depth at the end of the accumulation season. The two ALS surveys were performed from October 7–12, 2010, and April 20–23, 2011, respectively. An Optech ALTM Gemini device was used for both surveys, with a mean flight speed of 65 $m\,s^{-1}$ and a mean flight altitude above ground of 1000 m. Mean point densities of 3.6 and 3.8 points per square meter, respectively, were achieved. Digital elevation models with 1 m resolution were processed and surface elevation changes were calculated in the original 1 m resolution. The DEM differences were then resampled to the grid size of 50 m according to the model resolution. On the basis of the determined distribution of snow depth, SWE was calculated using an empirical relation between snow depth SD_{ALS} [m] and snow density ρ_{ALS} [$kg\,m^{-3}$] derived by Schöber et al. (2014):

$$\rho_{ALS} = SD_{ALS} \cdot 14.8 + 347. \tag{5.18}$$

This relation has already been applied for the investigation area in previous studies and has proven to be robust, with average errors in the order of 10 % (Schöber, 2014).

5.4.4 Glacier mass balance

For three glaciers in the study region (Hintereisferner, Kesselwandferner, and Vernagtferner), long-term annual mass balance series are available. For these glaciers, the simulated specific annual mass balance is compared with the observations, as well as the cumulative values over the entire simulation period 1997–2013. In addition, using two DEMs of the study region acquired in 1997 and 2006 spatially distributed glacier surface elevation changes during this period were calculated, which allows assessing the performance of the multiannual simulated mass balance for all glaciers in the study region over this period. The respective snow/ice volume changes as simulated by AMUNDSEN are thereby converted to surface elevation changes using the respective layer densities as calculated by the model (see section 5.3.1).

5.4.5 Runoff

Hydrological data from eight runoff gauges with adequate hourly records are used. Runoff is modeled in an hourly resolution for the time period 1997–2013. The period 1998–2006 is used for model calibration, while the period 2007–2013 is used for the

validation of simulated runoff. Model performance is evaluated using the efficiency criteria percent bias PBIAS and Nash-Sutcliffe efficiency NSE, as well as the benchmark efficiency BE (Schaefli and Gupta, 2007):

$$\mathrm{PBIAS} = 100 \cdot \frac{\sum_t \left(Q_{\mathrm{sim},t} - Q_{\mathrm{obs},t}\right)}{\sum_t Q_{\mathrm{obs},t}}, \tag{5.19}$$

$$\mathrm{NSE} = 1 - \frac{\sum_t \left(Q_{\mathrm{obs},t} - Q_{\mathrm{sim},t}\right)^2}{\sum_t \left(Q_{\mathrm{obs},t} - \overline{Q}_{\mathrm{obs}}\right)^2}, \tag{5.20}$$

$$\mathrm{BE} = 1 - \frac{\sum_t \left(Q_{\mathrm{obs},t} - Q_{\mathrm{sim},t}\right)^2}{\sum_t \left(Q_{\mathrm{obs},t} - Q_{\mathrm{bench},t}\right)^2}. \tag{5.21}$$

For BE, the benchmark model runoff Q_{bench} is calculated as the multiannual mean observed runoff per calendar day and hour.

5.5 Results and discussion

5.5.1 Precipitation

Mean areal precipitation for the gauged catchments in the region for the period 1997–2006 as derived by closing the water balance using the OEZ method (see section 5.4.1) was compared to the respective AMUNDSEN simulation results.

As the applied correction of the precipitation recordings using wind speed and temperature (eq. (5.7)) still resulted in an underestimation of precipitation amounts (as indicated by comparisons with (i) the catchment precipitation simulated by closing the water balance (table 5.5), (ii) the temporal progress of snow depth (fig. 5.6), (iii) the spatial distribution of accumulation at the end of the winter season (fig. 5.10), and (iv) the long-term glacier mass changes in the Ötztal Alps (fig. 5.15)), an additional post-interpolation snow correction factor (i. e., a constant factor with which the interpolated snowfall field is multiplied in each time step) was applied. By comparing precipitation amounts derived by closing the water balance with the respective AMUNDSEN results over all gauged catchments, this factor was set to a value of 1.15 (i. e., 15 % increase of snowfall amounts). Using this additional adjustment, AMUNDSEN mean areal precipitation for all gauged catchments deviates less than 1 % from the respective values as acquired by closing the water balance, as compared to a difference of −31 % when using uncorrected values (table 5.5). Especially considering that precipitation amounts for the largest catchments are reproduced very well, these results can be considered satisfactory. The largest differences occur in the medium-

sized catchments, with the maximum deviation being approx. 25 %, while the smaller catchments generally show the smallest deviations.

Table 5.5: Mean annual areal precipitation for the gauged catchments in the study area as calculated by closing the water balance (OEZ method) and AMUNDSEN (using uncorrected and corrected precipitation, respectively) for the period 1997–2006.

ID	Catchment	Area [km^2]	Precipitation OEZ [mm]	Precipitation AMUNDSEN uncorrected [mm]	Difference uncorrected [%]	Precipitation AMUNDSEN corrected [mm]	Difference corrected [%]
1	Rofenache	98.6	1507	1056	−30.0	1627	8.0
2	Am Barst/Gurgler Ache	72.4	1745	1137	−34.8	1617	−7.3
3	Niedertalbach	66.7	1410	1111	−21.2	1593	13.0
4	Gepatschalm	53.9	1799	1079	−40.0	1606	−10.7
6	Taschachbach	44.7	1632	1034	−36.6	1523	−6.7
7	Pitze	27.0	1552	1056	−32.0	1706	9.9
8	Radurschlbach	24.0	1402	882	−37.1	1113	−20.6
9	Tscheybach	16.4	1309	905	−30.9	1130	−13.6
11	Venter Ache	15.0	1253	1030	−17.8	1473	17.5
12	Verpeilbach	12.1	1093	1135	3.8	1360	24.4
13	Fissladbach	11.4	1481	1147	−22.5	1473	−0.6
14	Poschach/Gurgler Ache	8.1	1584	1019	−35.6	1441	−9.0
15	Platzertal	7.9	1395	1073	−23.1	1399	0.3
17	Ferwallbach	6.3	1537	1094	−28.8	1489	−3.1
18	Königsbach	5.9	1554	1089	−30.0	1490	−4.1
19	Rostizbach	4.8	1413	1135	−19.6	1465	3.7
	Total	475.2	1545	1067	−30.9	1543	−0.2

In several of the following sections, results obtained using uncorrected and corrected precipitation are compared and evaluated. “Uncorrected” in this terminology corresponds to the elevation-dependent remapping of unaltered precipitation recordings alone, while “corrected” refers to the combination of the adjustment of snowfall amounts (eq. (5.7) and the additional increase by 15 %) and the topographic snow redistribution (eq. (5.10)).

5.5.2 Snow depth

Table 5.6 lists the performance measures R^2, Nash-Sutcliffe efficiency NSE, and percent bias PBIAS for the comparison of daily snow depth observations at the point scale to the respective simulation results for five stations located in elevations between 871 and 2864 m a.s.l. for the model runs using uncorrected and corrected precipitation, respectively.

At the stations Obergurgl, Weisssee, and Pitztaler Gletscher, using corrected precipitation leads to significantly improved results in terms of all three performance measures. At the low-elevated stations Prutz and Nauders, the applied precipitation

Table 5.6: R^2, Nash-Sutcliffe efficiency NSE, and percent bias PBIAS for observed vs. simulated snow depth obtained using uncorrected and corrected precipitation, respectively.

			Uncorrected			Corrected		
Station	Elevation [m a.s.l.]	Period	R^2	NSE	PBIAS [%]	R^2	NSE	PBIAS [%]
Prutz	871	2005–2013	0.62	0.60	10.3	0.66	−2.21	222.5
Nauders	1330	2004–2013	0.84	0.74	−29.2	0.74	−0.35	119.5
Obergurgl	1942	1999–2013	0.65	0.60	−28.8	0.85	0.85	−6.0
Weisssee	2480	2006–2013	0.39	−0.13	−69.6	0.76	0.52	28.7
Pitztaler Gletscher	2864	1997–2013	0.57	−0.52	−76.8	0.71	0.68	7.1

correction leads to a severe overestimation of snow depth of 223 and 120 %, respectively, on average. However, while these stations are within the simulation area (i. e., the rectangle surrounding the study catchments shown in fig. 5.1), they are located outside of the investigated catchments and are significantly lower elevated (minimum elevation of the study catchments is 1760 m).

Fig. 5.6 shows observed and simulated (using both uncorrected and corrected precipitation, respectively) snow depth for the stations Obergurgl and Pitztaler Gletscher and the period 2003–2013. While some uncertainty also can be attributed to the applied snow densification parameterization for the conversion from water equivalent to snow depth, these results show that the applied precipitation corrections (correction for undercatch as well as topography-based correction) considerably improve results especially at high elevations, as can be seen for the station Pitztaler Gletscher. Nevertheless, at this station snow depth is still underestimated in most seasons despite using corrected precipitation. For the medium-elevated station Obergurgl, while the differences between uncorrected and corrected precipitation are less distinct, the applied corrections result in a very satisfying representation of snow depth over the course of the seasons.

5.5.3 Snow distribution

5.5.3.1 Comparison with satellite data

For the comparison of simulated snow distributions, 26 cloud-free Landsat scenes as well as daily MODIS scenes (starting in the year 2000) were obtained. With regard to the latter, as outlined in section 5.4.3.1 images acquired in the months July–September were discarded due to difficulties in discriminating snow and ice surfaces. Additionally, only scenes with less than 5 % total cloud coverage over the study area were

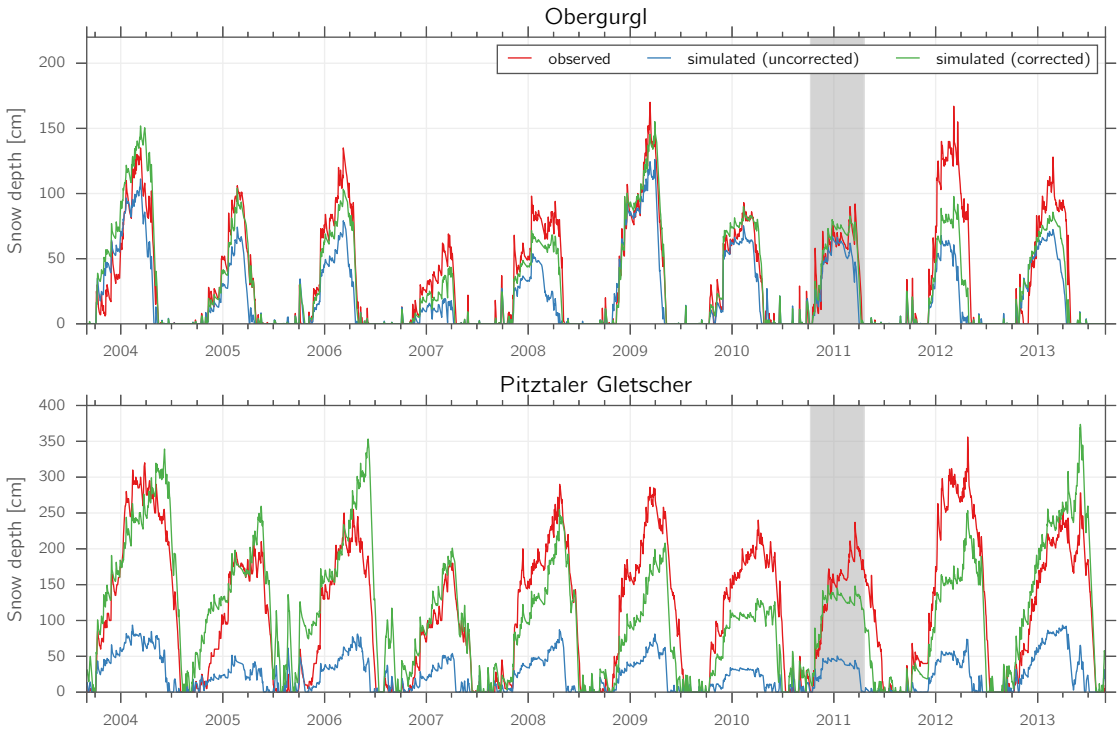

Figure 5.6: Observed and simulated (using uncorrected and corrected precipitation, respectively) snow depth for stations Obergurgl (1942 m a.s.l.) and Pitztaler Gletscher (2864 m a.s.l.). The gray shaded area corresponds to the period in between the two ALS surveys.

considered. This left 733 usable MODIS scenes, corresponding to approx. one image every 5 days (in the period October–June) on average.

Fig. 5.7 exemplarily shows the observed and simulated snow cover distributions for the Landsat and MODIS scenes from June 1, 2002. With regard to the observations, the effect of the reduced resolution of the MODIS product is clearly visible – while the Landsat image also highlights small-scale variations in snow cover (e. g., snow-free ridges, small snow patches), a large amount of detail is smoothed out in the MODIS image. This is also illustrated in the total snow-covered area – in the Landsat image, 45 % of the total area are classified as snow-covered, as compared to 37 % for the MODIS image. Simulation results agree well with the observations for this date, both with regard to the visual comparison as well as to the performance measures, being for Landsat (MODIS): ACC = 0.85 (0.87), CSI = 0.72 (0.73), BIAS = 0.98 (1.18).

Fig. 5.8 shows the obtained values for ACC, CSI, and BIAS for all selected Landsat and MODIS scenes sorted by calendar date, as well as the 30-day running means for the MODIS values (blue lines). Generally, the average performance measures (displayed in the bottom left of each figure) show better results for MODIS, however it

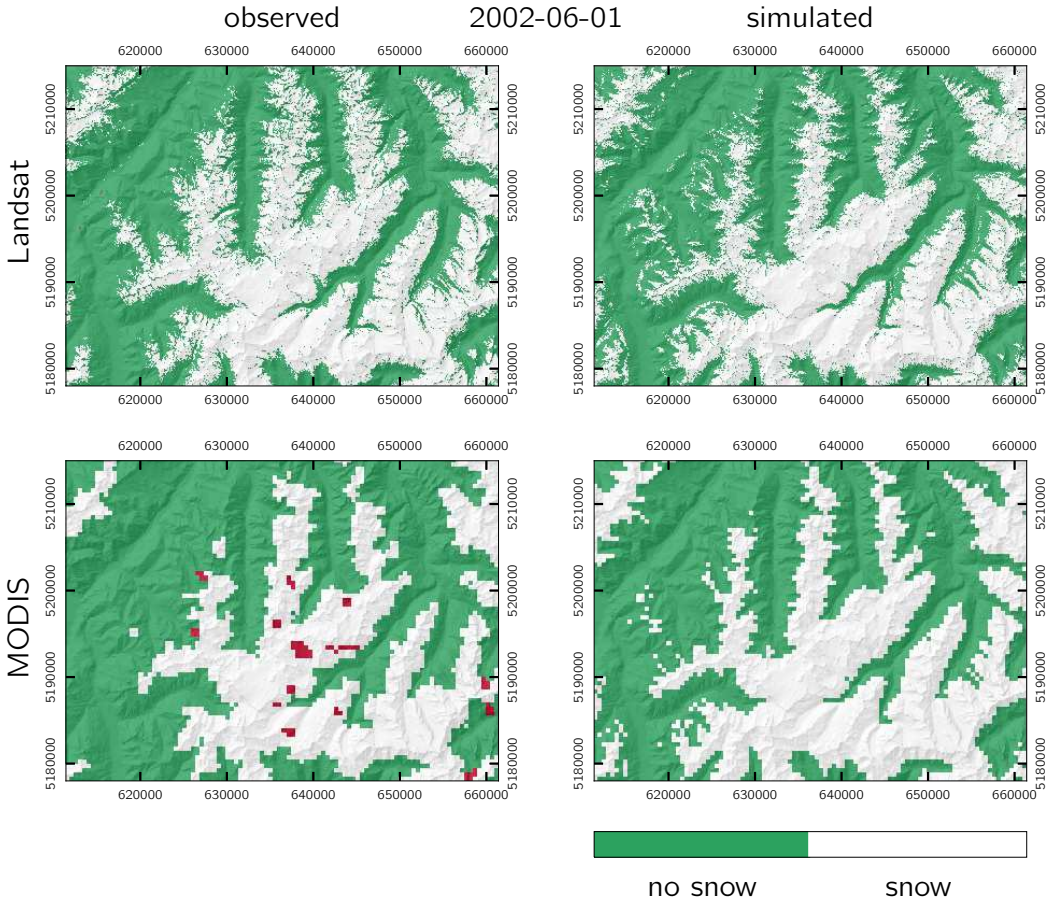

Figure 5.7: Observed and simulated snow cover distribution for June 1, 2002, using Landsat (top, 50 m resolution) and MODIS (bottom, 500 m resolution) scenes.

has to be noted that the average values are not directly comparable, since in the case of Landsat they are calculated from significantly fewer samples and additionally – in contrast to MODIS – also include scenes acquired during the summer months. As expected, for all three measures performances are very good during the winter months (particularly January to March), where most of the area is snow-covered. However, they deteriorate during spring and fall. ACC shows the highest performance values, with on average approx. 90 % of all pixels being correctly classified for MODIS data, and 83 % for Landsat data. Values decrease during spring and fall, however are rarely (in 9 % of the MODIS scenes and 8 % of the Landsat scenes) below 0.7. The range of CSI values in contrast is much larger, with – when looking at the MODIS 30-day running mean – an approximately linear in-/decrease during fall and spring from values around 0.4 in late spring to approx. 0.95 during winter. Lowest values (between 0.25

and 0.4) are obtained for the 8 Landsat scenes during the summer months. With regard to BIAS, values are very close to the optimal value of 1 during winter. Outside of this period, larger deviations occur. It is notable, that – with very few exceptions – BIAS values are always above 1, meaning that the model tends to overestimate the snow cover. The particularly high values during fall might indicate that rainfall events are frequently misinterpreted as snowfall events in the model, as well as early-season snowfall events that rapidly melt again in reality, while in the model the snow lasts on the ground. However, if only little snow is present in the observation, even comparatively moderate overestimations in the model can lead to high BIAS values, which is also an explanation for the particularly high values of this parameter for some of the Landsat scenes during summer.

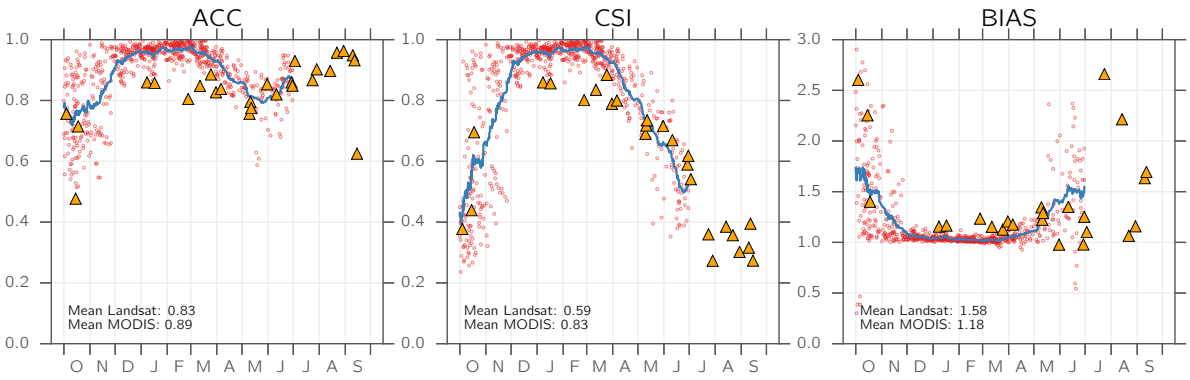

Figure 5.8: ACC, CSI, and BIAS for all selected Landsat (triangles) and MODIS (red circles; blue line is the 30-day running mean) scenes, sorted by calendar date.

The performance measures can be calculated not only space-integrated (i. e., for each scene), but also time-integrated, i. e., calculating them on a pixel-by-pixel basis over all scenes. The results are shown in fig. 5.9 for Landsat at the top and MODIS at the bottom. For all three performance measures, best results are obtained on the glaciers and high-elevated regions (where a snow cover is present most of the time). Largest deviations occur in forested areas, which becomes particularly visible for the CSI and BIAS scores. Satellite-based snow cover mapping in forests is notoriously difficult and associated with larger errors than in the open due to the obstruction of snow on the ground by the trees. While in the MODIS snow mapping algorithm in forested areas the NDSI threshold is lowered in order to increase the classification accuracy (Klein et al., 1998), no such distinction was made for the Landsat snow classification performed for this study, which might be one reason for the lower model skill for Landsat as compared to MODIS in these areas. For most non-forested pixels, ACC

and CSI values are above 0.7 for both Landsat and MODIS, underlining the satisfying model performance. BIAS is in the range of 20 % over- or underestimation for most MODIS pixels, while in the Landsat comparison larger areas fall into the class of BIAS values up to 2. Once again it has to be noted however that most of the Landsat scenes were acquired during spring or summer, where a correct representation of snow/rain distinction is especially crucial, hence the lower performance scores for Landsat are not unexpected.

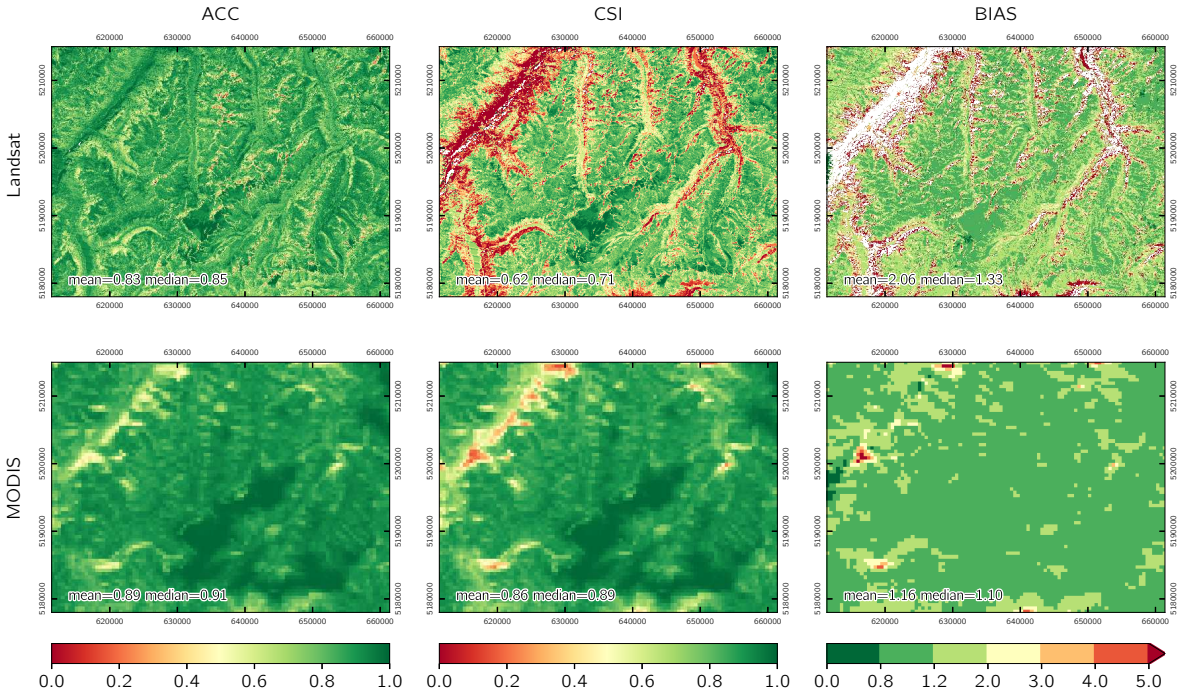

Figure 5.9: Pixel-based statistics of ACC, CSI, and BIAS over all selected Landsat and MODIS scenes.

To summarize, these results show that the total snow-covered area is frequently overestimated, on average by 20 % (60 %) for MODIS (Landsat). Whereas in only 1 % (0 %) of all investigated scenes snow cover is underestimated by more than 5 %, it is overestimated by more than 5 % in 51 % (92 %) of all scenes. The largest mismatches between the observations and the simulations occur during the summer months (where accurately reproducing the snow cover is the most challenging), followed by fall and spring. Elevation-wise the largest errors occur below the lowest-elevated runoff gauge (further analyses are shown in the supplementary material). A likely explanation for this effect (which is also observed in the snow depth comparisons) is that snow correction and snow redistribution factors are overestimated in these low elevations.

5.5.3.2 Comparison with ALS data

Fig. 5.10 shows the observed and simulated snow distributions (i. e., observed surface elevation differences between the ALS acquisition dates converted to SWE using eq. (5.18), and simulated SWE differences for the same period) for the winter 2010/11. A 746 km^2 large area was covered by the ALS acquisitions, resulting in a sample size of 298468 pixels (with 50 m resolution) available for model validation. As seen in fig. 5.10, despite the applied precipitation corrections the total snow volume is still underrepresented in the model by approx. 15 % in this particular period, however the applied snow redistribution parameterization leads to a significantly improved representation of the accumulation patterns (snow-free ridges, increased accumulation on glacierized areas) as compared to model results using elevation-dependent precipitation fields only. Fig. 5.11 shows the high correlation of simulated with observed snow water equivalent values with an R^2 value of 0.57. This is a considerable improvement in model performance considering the results using uncorrected precipitation (elevation-dependent remapping only) ($R^2 = 0.07$) and using undercatch-corrected precipitation without topographic redistribution ($R^2 = 0.23$) (plots are shown in the supplementary material). Fig. 5.12 shows the SWE differences by elevation (50 m bands) for the ALS data, the simulation results without any precipitation adjustment (elevation-dependent remapping only), the simulation results derived using corrected precipitation but no topographic redistribution (eq. (5.7) + constant snow correction factor (15 %)), and the simulation results derived using corrected precipitation and topographic redistribution (eq. (5.10)). From this figure it is evident that the snowfall adjustments strongly increase model performance in the lower and medium elevations (where snow accumulation is dramatically underestimated in the simulation run without precipitation correction), however only the simulation run including topographic redistribution is able to reproduce the observed decline in SWE following the peak at approx. 3000 m a.s.l.

The obtained correlations are in the range of the results by Schöber et al. (2014), who obtained $R^2 = 0.52$ in a 166 km^2 large subcatchment of our study region, also using a cell size of 50 m. Grünewald et al. (2013) obtained R^2 values between 0.30 and 0.91 for different investigation areas between 1.5 and 28 km^2, however using a coarser cell size of 400 m, and Schirmer et al. (2011) obtained $R^2 = 0.42$ for a site in Switzerland using 10 m resolution (however, both of these studies used statistical models based on topographic parameters alone to model snow depth distribution and did not employ snow cover models). Hence, considering the size of the investigated area and the high

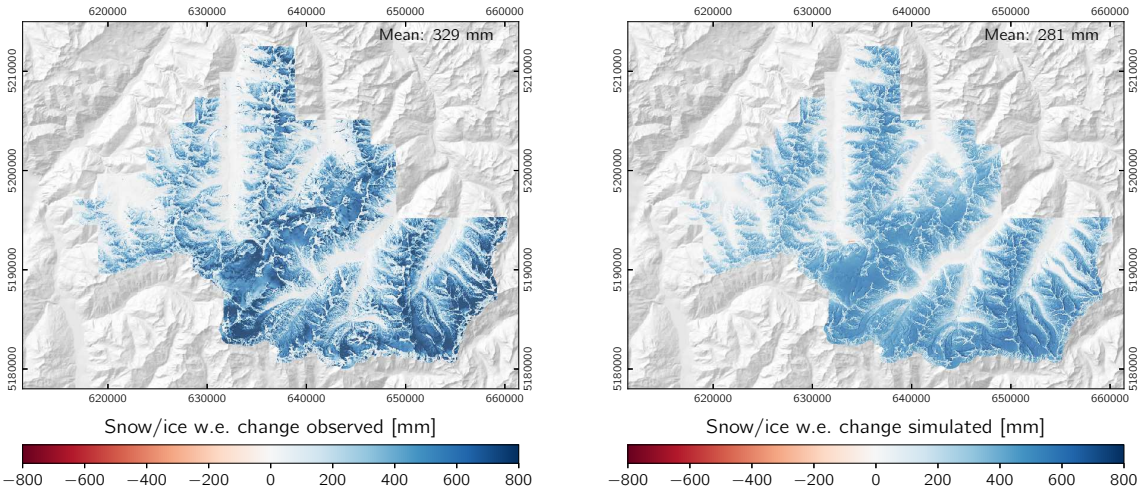

Figure 5.10: Observed (i. e., surface elevation differences converted to SWE using eq. (5.18)) and simulated end-of-season snow distribution for the winter 2010/11 (October 8 to April 22).

spatial resolution, our results can be considered very satisfactory. However, again it has to be emphasized that – as also shown in other studies (e. g., Grünewald et al. (2013)) – the relations between snow depth and topography are site-specific and hence have to be calibrated for different study regions individually. In the case of the openness-based correction applied in this study, this concerns the choice of the scale parameters L for negative openness, the value range of negative openness for the different scale parameters (eqs. (5.8) and (5.9)), and the final relation to precipitation correction (eq. (5.10)).

5.5.4 Glacier mass balance

Figs. 5.13 and 5.14 show the annual and cumulative mass balances for Hintereisferner (HEF), Kesselwandferner (KWF), and Vernagtferner (VF). The individual annual mass balances of the three glaciers are reproduced reasonably well by the model, with $R^2 = 0.46$ for HEF, $R^2 = 0.64$ for KWF, and $R^2 = 0.81$ for VF. The cumulative mass balance over the period 1997–2013 is captured very well for VF and HEF, with differences of only 39 mm (0.3 %) for VF and -377 mm (2.1 %) for HEF, while KWF shows the lowest performance with a deviation of -2633 mm (32 %). For all three glaciers, results improve with increasing simulation time, possibly due to the improved representation of the interpolated meteorological fields due to increased station density (cf. Schöber, 2014, p. 40f.). A meteorological station is located in direct vicinity to VF, which is a possible explanation for the distinctively good performance of the model with regard

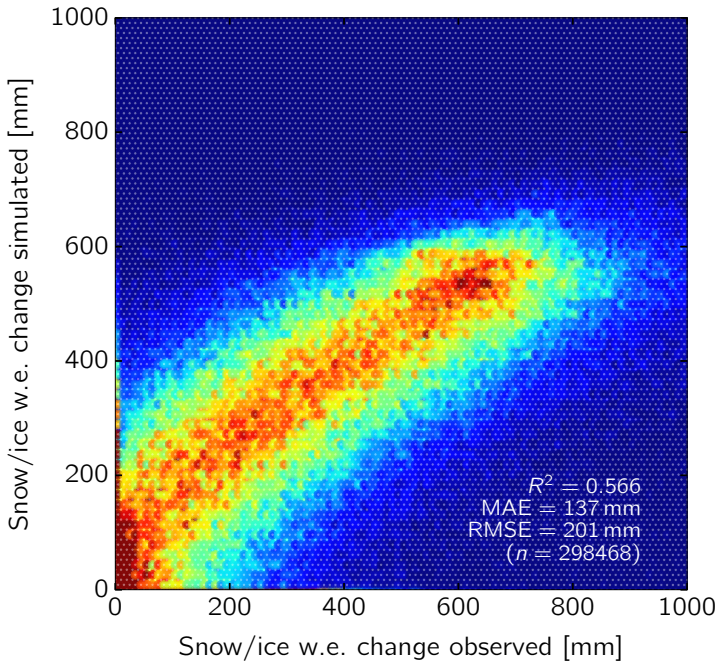

Figure 5.11: Binned scatter plot (colors represent point density) of observed vs. simulated water equivalent differences for the winter 2010/11 (October 8 to April 22).

to this glacier. The largest errors in mass balance simulations for all three glaciers occur in the year 2003. Further investigation reveals that this can at least partly be traced back to the meteorological forcing data, specifically two precipitation events in October and November 2002 which have not been captured by the precipitation recordings at the station Vernagtbach. Excluding the precipitation recordings from this station in the period October–November 2002 distinctly improves the simulated mass balances for the glaciological year 2003 (a more detailed analysis and further results are shown in the article supplement).

The generally satisfying model performance for the three glaciers indicates that the model setup is suitable for glacier mass balance simulations at the regional scale, as no glacier-specific model calibration has been performed. This is further underlined when looking at the long-term glacier surface elevation changes in the period 1997–2006. The respective observations are derived from the glacier inventories of the respective years and allow to spatially assess the model performance in simulating the surface mass balance for all glaciers in the study region over this period. The mean surface elevation change derived from the glacier inventory was -5.81 m between 1997 and 2006, while surface elevation changes simulated with AMUNDSEN amount to -5.50 m for the same period (fig. 5.15, $R^2 = 0.44$). Hence, the mean

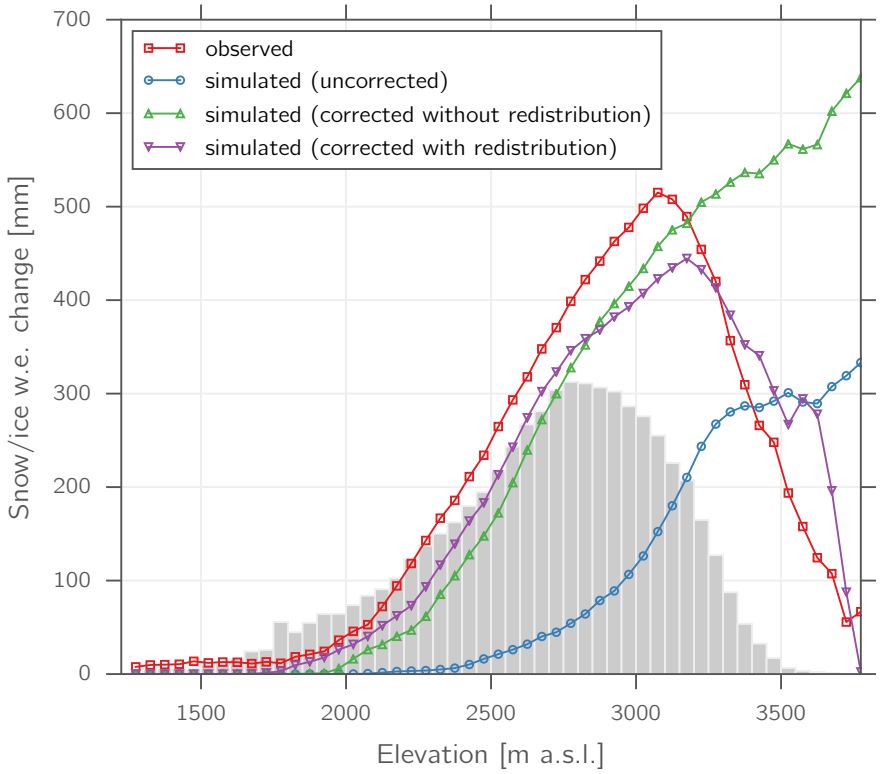

Figure 5.12: Observed vs. simulated water equivalent differences for the winter 2010/11 (October 8 to April 22) by elevation (50 m bands). Simulation results are displayed for using uncorrected precipitation (elevation-dependent remapping only), corrected precipitation without topographic redistribution (eq. (5.7) + constant snow correction factor (15 %)), and corrected precipitation with topographic redistribution (eq. (5.10)). The gray bars represent the relative area distribution of the elevation bands.

value of simulated multi-annual snow and ice water resources loss is approx. 0.3 m (5 %) more positive compared to the observed value. This relatively low value is in the same order of magnitude as the uncertainties arising from glacier volume change measurements. Hence, the model can be considered capable of realistically simulating the runoff contribution by glacier melt. Possible explanations for the deviation – beside the measurement uncertainty – are processes such as basal melt or collapsing glacier tongues, which are not represented in the model. Additionally, the albedo of the dirty glacier tongues covered with mineral dust and cryoconite might be overestimated by the model. Since no ice flow is considered in AMUNDSEN up to now, the spatial distribution of glacier thickness changes is biased at the low elevated glacier tongues and in high elevated accumulation areas. Although glacier ice flow velocities slowed down in the past decades and the contribution of vertical ice flow is low at most of the glaciers in the study region (e. g., Helfricht et al., 2014a), surface elevation

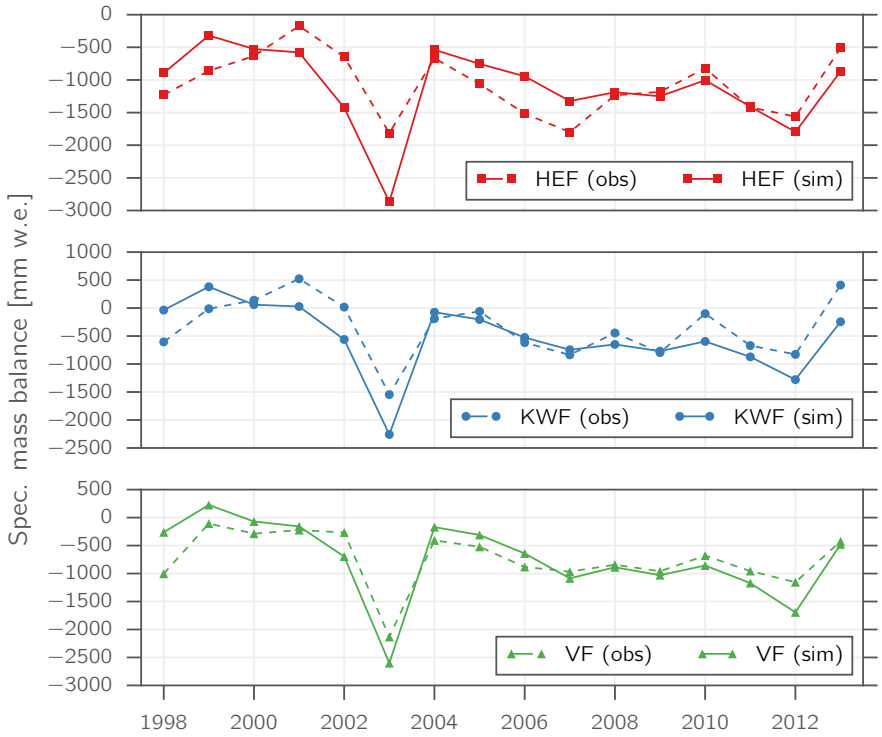

Figure 5.13: Observed (dashed) and simulated (solid) specific mass balance for Hintereisferner (HEF, top), Kesselwandferner (KWF, center), and Vernagtferner (VF, bottom) in the period 1997/98–2012/13.

changes caused by ice flow accumulate to considerable values in multi-annual time periods. Hence, in order to prevent systematic model biases in long-term applications it is crucial to integrate a dynamic tracking of the glacier surface, which is proposed to be implemented in a future version of AMUNDSEN.

5.5.5 Runoff

For the runoff simulations, calibration and validation periods were generally 1998–2006 and 2007–2013, respectively, however for some catchments only shorter time series of runoff measurements were available. Table 5.7 shows the results (Nash-Sutcliffe efficiency NSE, benchmark efficiency BE, and percent bias PBIAS) of the simulations for the catchments in which respective hourly runoff observations were available, while fig. 5.16 shows the fractions of the individual runoff components as simulated by AMUNDSEN using uncorrected and corrected precipitation, respectively, for the calibration period (1998–2006). Fig. 5.17 exemplarily shows the observed and simulated runoff as well as the individual runoff components for the gauge Gepatschalm (1893–3526 m a.s.l.) and the year 2012.

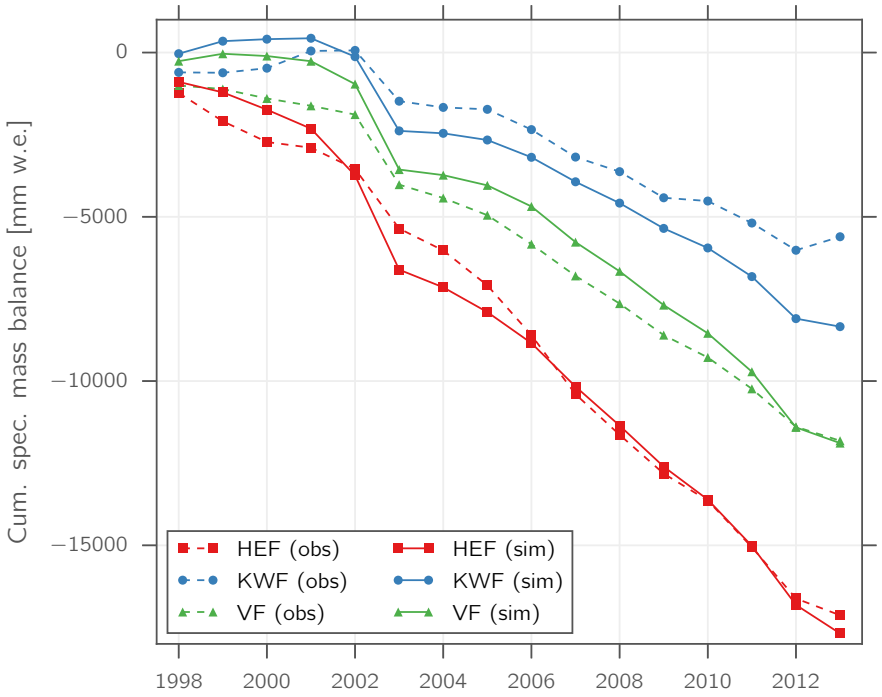

Figure 5.14: Observed (dashed) and simulated (solid) cumulative specific mass balance for Hintereisferner (HEF), Kesselwandferner (KWF), and Vernagtferner (VF) in the period 1997/98–2012/13.

By means of the applied precipitation correction, NSE values for almost all catchments slightly improve as compared to the model run using uncorrected precipitation, with values of around or above 0.8, with the exception of two small catchments with very low glacierization (as the runoff module is specifically designed for glacierized catchments it is expected to perform worse in catchments with no or low glacierization). However, for most catchments even the use of uncorrected precipitation leads to comparatively high NSE values. This is typical for catchments with a strong runoff seasonality: the fact that NSE uses the mean observed runoff as reference makes it a rather inefficient skill score in these cases – high NSE values can be obtained as soon as the seasonality is represented in the model, regardless if smaller scale fluctuations are misrepresented (Schaefli and Gupta, 2007). Looking at benchmark efficiency BE, variations between catchments as well as the effects of the applied precipitation correction are much more pronounced. Using corrected precipitation significantly increases BE in almost all catchments in both the calibration and validation period. Despite using corrected precipitation, in the two smallest and least glacierized gauged catchments BE values are below zero, indicating that the multiannual mean per calendar day and hour as predictor would be better than the model. When looking not only

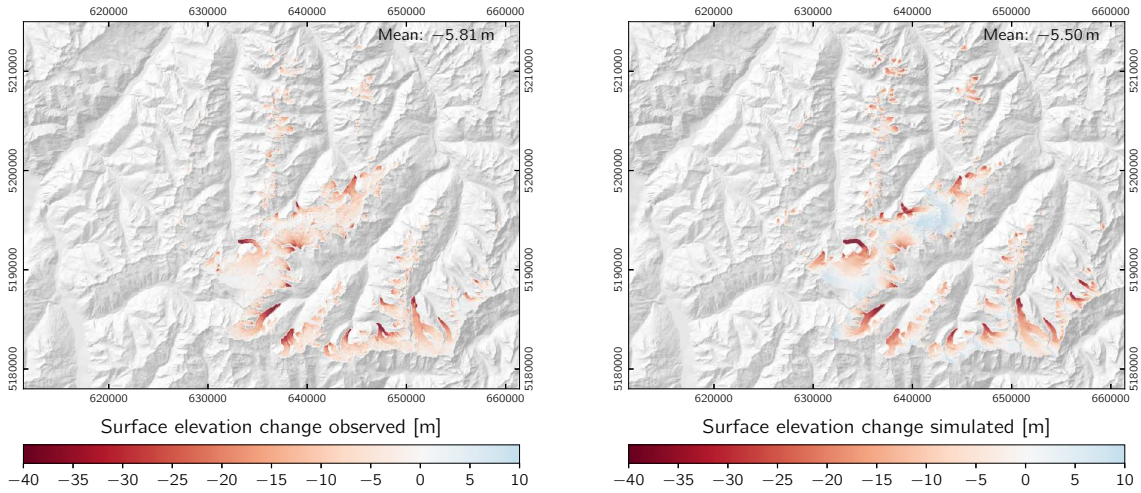

Figure 5.15: Observed and simulated glacier surface elevation change for the period 1997–2006.

Table 5.7: NSE, BE, and PBIAS of simulated vs. observed runoff obtained using uncorrected and corrected precipitation. Calibration and validation periods are – if not otherwise stated – 1998–2006 and 2007–2013, respectively. The subscripts *c* and *v* denote calibration and validation periods, respectively.

		Uncorrected						Corrected					
ID	Catchment	NSE_c	NSE_v	BE_c	BE_v	$PBIAS_c$ [%]	$PBIAS_v$ [%]	NSE_c	NSE_v	BE_c	BE_v	$PBIAS_c$ [%]	$PBIAS_v$ [%]
1	Rofenache Am	0.81	0.75	0.11	0.30	6.1	0.1	0.81	0.78	0.56	0.35	12.1	20.0
2	Barst/Gurgler Ache[a]	0.81	0.77	0.25	0.28	−3.0	0.3	0.82	0.80	0.46	0.26	5.6	20.8
3	Niedertalbach[b]	0.79	–	0.07	–	7.6	–	0.79	–	0.47	–	14.1	–
4	Gepatschalm	0.86	0.84	0.11	0.23	3.6	−3.5	0.88	0.87	0.57	0.50	4.9	7.3
6	Taschachbach[c]	0.85	0.82	0.28	0.18	−14.2	−18.7	0.90	0.88	0.49	0.45	3.4	2.2
7	Pitze[c]	0.85	0.84	−0.60	−0.24	10.3	2.9	0.88	0.87	0.61	0.53	6.3	4.4
8	Radurschlbach[d]	0.46	0.56	−1.09	−0.80	−31.9	−10.9	0.66	0.67	−0.26	−0.43	−8.4	22.7
13	Fissladbach[d]	0.60	0.68	−0.46	−0.10	−17.4	−3.0	0.67	0.63	−0.16	−0.23	12.8	31.9
	Mean	0.75	0.75	−0.17	−0.02	−4.86	−4.69	0.80	0.79	0.34	0.20	6.4	15.6

[a] No runoff observations for 2013
[b] No runoff observations for 2003–2013
[c] No runoff observations for 2009–2013
[d] No runoff observations for 2011–2013

at the respective single best-performing parameter set (with regard to eq. (5.11)) for each catchment but at a range of similarly performing parameter sets, it shows that similarly performing parameter sets result in a remarkably large spread of BE (results shown in the supplementary material). However, the best-performing parameter sets in terms of eq. (5.11) are also among the best-performing sets in terms of BE.

The total runoff volume bias PBIAS is (absolutely) smaller for the model runs with

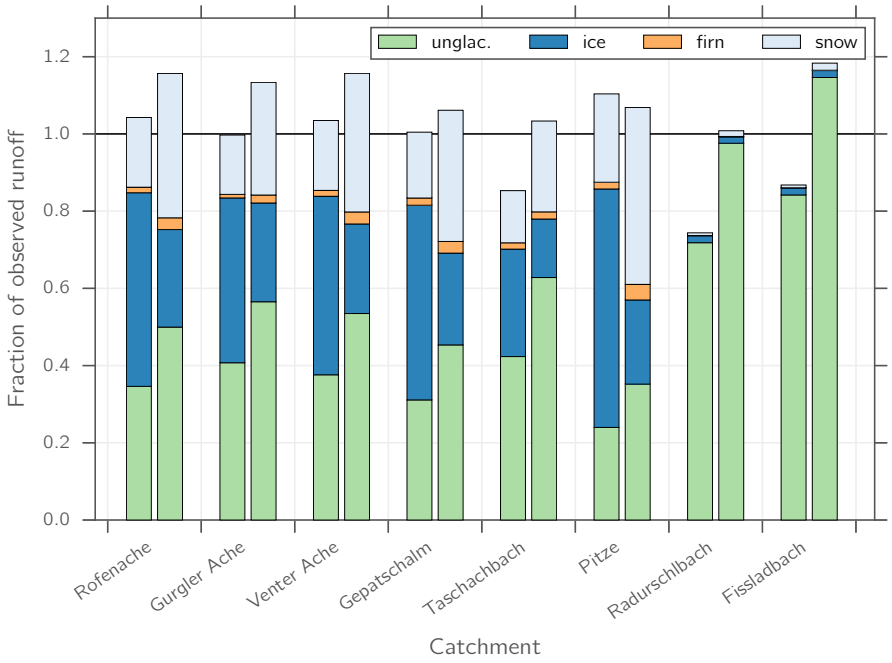

Figure 5.16: Runoff components (prior to the diversion into the soil reservoir) as simulated by AMUNDSEN for the calibration period 1998–2006 shown as fractions of the mean observed runoff in the same period. The two bars for each catchment show the results for the model runs using uncorrected (left) and corrected (right) precipitation, respectively.

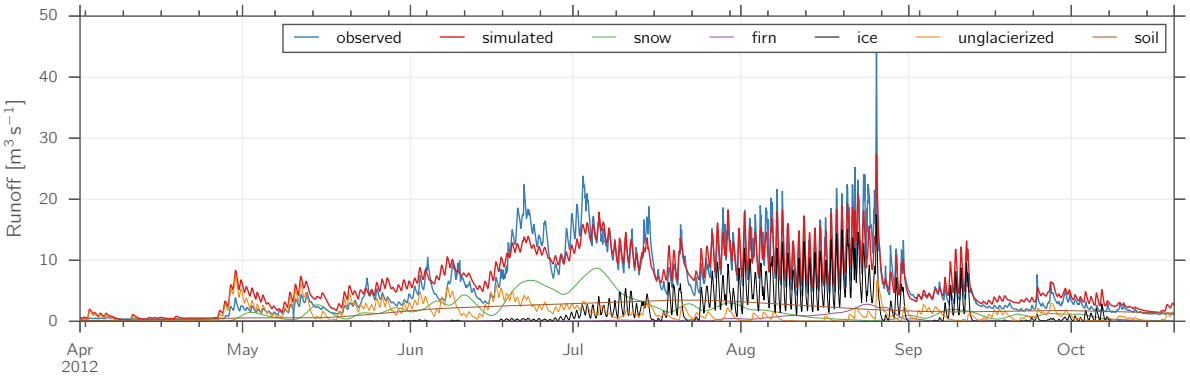

Figure 5.17: Observed vs. simulated runoff (including individual runoff components) for gauge Gepatschalm (1893–3526 m a.s.l.) in the period April–October 2012.

uncorrected precipitation (with runoff on average underestimated by approx. 5 % in both the calibration and the validation period) than when corrected precipitation is used, where runoff is on average overestimated by 6.4 % and 15.6 %, respectively, with even higher values for the two largest catchments. This can also be seen in fig. 5.16, which also illustrates that underestimated precipitation amounts are compensated by

increased ice melt amounts in the model runs using uncorrected precipitation. The calibration criterion NSE_V (eq. (5.11), values not shown in table 5.7) shows little variation in all catchments, with mean values between 0.74 and 0.79 for both runs (uncorrected vs. corrected) and in both the calibration and validation period.

5.6 Conclusions

The physically based hydroclimatological model AMUNDSEN was set up and applied for a partly glacierized, 558 km^2 large region in the Ötztal Alps (Austria) on a 50 m grid. Model validation was performed by comparing mean areal precipitation, point-based snow depth recordings, remotely sensed snow extent maps from MODIS and Landsat satellites, lidar-derived surface elevation changes for the accumulation season 2010/11, glacier-averaged annual surface mass balances for three glaciers, spatially distributed glacier surface elevation changes for the entire area over the period 1997–2006, and hourly runoff observations for 8 catchments. A correction function for solid precipitation has been added to the model in order to compensate for the severe undercatch of precipitation measurements in high elevated and wind-exposed areas. This pre-interpolation correction of the recorded precipitation depths using temperature and wind speed has proven to significantly improve model results, however an additional snow correction factor of 15 % had to be applied to the resulting snowfall fields. A parameterization for cold content and liquid water content of the snowpack has been implemented to account for the delayed start of melting of the snowpack following cold periods and nights with clear-sky conditions. Finally, a parameterization for snow redistribution using topographic openness has been added to the model, helping to significantly better represent the complex snow accumulation patterns in the study site as compared to assuming an elevation dependency alone.

The results of the study especially emphasize the importance of a systematic model validation based on multiple data sources. When looking solely at runoff, also using entirely implausible precipitation inputs for the model leads to acceptable results as the respective missing snow melt inputs are compensated by enlarged ice melt contributions, even though the spatial patterns of snow accumulation and snow depth amounts are misrepresented in the model. Hence, in order to produce realistic contributions of the individual runoff components, it is necessary to assess and validate the individual model components and processes separately: Areal catchment precipitation derived from the hydrological balance can be used to derive realistic total precipitation volumes. Point-based snow depth observations are necessary for the eval-

uation of the simulated temporal evolution of the snowpack in terms of the correct timing and magnitude of accumulation and melt. Binary snow extent maps allow a multitemporal evaluation of the simulated snow distribution, while lidar-derived surface elevation differences add detailed information about the amount of snow resources stored in the area during the winter. Finally, annual glacier mass balances from field surveys as well as long-term mass balances derived from DEM differencing allow the evaluation of model performance in reproducing the long-term surface mass balance over the glaciers, which is essential prior to applying the model for scenario studies. Currently, an ice flow parameterization is being implemented in the model, which will allow to apply the model setup for climate change scenarios in order to estimate future runoff conditions and glacier retreat in the study site.

While the value of using multiple data sets for model validation has already been investigated in previous studies, our concept of multilevel spatiotemporal validation represents a new approach for assessing glacio-hydrological simulation accuracy on a fully comprehensive level. Usually, exemplary comparisons of single simulated model variables are utilized for validation, either (i) with time series of local recordings of the respective variable, (ii) with discrete (in time) shots of the spatial distribution of the variable, or (iii) runoff is compared to gauge recordings. The latter is a measure that summarizes all relevant processes (of accumulation, redistribution and ablation of snow and ice in our case), but does not allow for separating these processes. Multilevel spatiotemporal validation is a systematic, independent, complete and – here – even fully redundant validation procedure for the simulated key variables in the model. The spatial distribution of the simulation result is validated in all six dimensions of the observation scale – temporal as well as spatial support, spacing, and extent – by means of two independent satellite data products. Likewise, the water volume (i. e., the mass balance) of the simulation results is validated by at least two independent validation data sources for each dimension, e. g., spatial spacing (in high model resolution) by long-term glacier mass balances and ALS. Redundancy of the validation data sources will only seldom be available in most applications and in practice. It may serve here as additional proof of robustness and reliance for both the simulation results and the validation concept. This concept may serve as a next piece for a new generation of integrated environmental system models with coupled components, separately validated, and defined interface design in between them (Strasser et al., 2014).

Acknowledgements

This work was carried out within the framework of the projects "H03 MUSICALS A – Multiscale Snow/Ice Melt Discharge Simulation for Alpine Reservoirs", carried out in the research programme of alpS – Centre for Climate Change Adaptation in Innsbruck, and "hiSNOW – High resolution monitoring and modelling under climate change conditions – Combining ALS and TLS data acquisition with energy and mass balance modelling at Hochjochferner/Val Senales, Italy", financed by the Autonomous Province of Bozen/Bolzano. The authors want to thank the COMET research programme of the Austrian Research Promotion Agency (FFG), the TIWAG – Tiroler Wasserkraft AG, and the Autonomous Province of Bozen/Bolzano. Meteorological and hydrological data were provided by the Central Institution for Meteorology and Geodynamics (ZAMG), the Hydrographic Service of Tyrol, the TIWAG – Tiroler Wasserkraft AG, the Commission for Glaciology of the Bavarian Academy of Sciences and Humanities, and the Autonomous Province of Bozen/Bolzano. We also thank Johannes Schöber for valuable discussions during the preparation of the manuscript. Finally, we gratefully acknowledge the valuable and constructive comments by Bettina Schaefli and one anonymous referee which helped to improve this manuscript.

Chapter 6

Projected cryospheric and hydrological impacts of 21st century climate change in the Ötztal Alps (Austria) simulated using a physically based approach

Florian Hanzer, Kristian Förster, Johanna Nemec, Ulrich Strasser

Submitted to *Hydrology and Earth System Sciences* (Discussion paper published as doi: 10.5194/hess-2017-309).

My contribution to this article: co-developing the spatial and temporal downscaling approaches, acquiring and processing the historical station data and the RCM data, implementing the glacier retreat parameterization, performing the model runs, producing the plots, analyzing the results, and writing the article.

Abstract

A physically based hydroclimatological model (AMUNDSEN) is used to assess future climate change impacts on the cryosphere and hydrology of the Ötztal Alps (Austria) until 2100. The model is run in 100 m spatial and 3 h temporal resolution using in total 31 downscaled, bias-corrected, and temporally disaggregated EURO-CORDEX climate projections for the RCP2.6, RCP4.5, and RCP8.5 scenarios as forcing data. Changes in snow coverage, glacierization, and hydrological regimes are discussed both for a larger area encompassing the Ötztal Alps (1850 km^2, 862–3770 m a.s.l.) as well as for seven catchments in the area with varying size (11–165 km^2) and glacierization (24–77 %).

Results show generally declining snow amounts with moderate decreases (0–20 % depending on the emission scenario) of mean annual snow water equivalent in high elevations ($>$ 2500 m a.s.l.) until the end of the century, however decreases of 25–80 % in elevations below 1500 m a.s.l. Glaciers in the region will continue to retreat strongly, leaving only 4–20 % of the initial (as of 2006) ice volume left by 2100. Total and summer (JJA) runoff will change little during the early 21st century (2011–2040) with simulated decreases (compared to 1997–2006) of up to 11 % (total) and 13 % (summer) depending on catchment and scenario, whereas runoff volumes decrease by up to 39 % (total) and 47 % (summer) towards the end of the century (2071–2100), accompanied by a shift in peak flows from July towards June.

6.1 Introduction

Current and future climate change is expected to significantly alter the mountain cryosphere of the European Alps. Rising temperatures are expected to result in more precipitation falling as rain rather than snow, a delayed onset of the snow-covered period, and an earlier onset of snowmelt, regardless of the considered emission scenarios (e. g., Frei et al., 2017; Gobiet et al., 2014; Marty et al., 2017). Possibly increasing winter precipitation amounts are expected to partly compensate for these temperature-induced effects of reduced average snowpack depths only in very high-elevated regions (e. g., Schmucki et al., 2015b).

The European mountain glaciers have already lost substantial parts of their volume and area during the past decades. Due to their delayed response to changed climatic conditions, they are still out of balance with the current climate and would continue to recede throughout the century even without any further climatic changes (e. g., Jouvet et al., 2011; Marzeion et al., 2014; Zekollari et al., 2014). Further rising temperatures will only amplify this process, resulting in a total glacier volume reduc-

tion in the European Alps of 65–100 % by 2100 according to several global-scale studies (Bliss et al., 2014; Huss and Hock, 2015; Marzeion et al., 2012; Radić et al., 2013).

Consequently, the runoff regimes of snow- and ice melt-dominated Alpine catchments will also undergo significant changes. Meltwater contribution of the seasonal snow cover will be reduced, resulting in increased winter low flows, declining summer runoff, and shifts of the peak flows towards earlier periods of the year (Barnett et al., 2005; Horton et al., 2006; Stewart, 2009). These general projected patterns of change are of high confidence, as they are mainly triggered by increasing temperatures (shift from snowfall to rainfall, earlier onset of snowmelt), whereas in lower-elevated catchments changes in precipitation exhibit a larger impact on changes in runoff (Horton et al., 2006). Besides a projected future increase in winter precipitation on which most current climate projections agree on, future changes in precipitation over the Alpine region are however highly uncertain (Gobiet et al., 2014; Smiatek et al., 2016). Consequently, future trends in total annual streamflow volume for purely snowmelt-dominated catchments are also uncertain, as changes in precipitation might (over)compensate increased evaporation rates due to higher temperatures. While in glacierized catchments on the other hand runoff volumes will eventually decrease due to the retreating glaciers and subsequently reduced ice melt runoff volumes, prolonged periods of glacier mass loss can lead to increased glacier runoff volumes in the short- to midterm, depending on if increased melt rates are able to overcompensate the loss in glacier area (e. g., Beniston, 2003; Bliss et al., 2014; Collins, 2008; Jansson et al., 2003). Detecting the occurrence of this moment of peak water is of high interest, e. g., for hydropower production and planning (Schaefli, 2015).

While there are numerous studies on climate change impacts on the future of glaciers and hydrology for various parts of the European Alps, particularly Switzerland (e. g., Addor et al., 2014; Bosshard et al., 2013; Farinotti et al., 2011; Fatichi et al., 2015; Finger et al., 2012; Horton et al., 2006; Huss et al., 2008; Huss et al., 2014; Kobierska et al., 2013; Milano et al., 2015), few such studies exist for Austria. Kuhn and Batlogg (1998) used hypothetical temperature change scenarios to simulate future runoff for nine Austrian catchments with varying glacierization using a simple conceptual water balance model while assuming constant glacier areas. The same model was applied by Kuhn and Olefs (2007) for three catchments in the Ötztal Alps while accounting for changed glacier areas using an approach taking into account observed mean annual ice thickness changes with an additional constant surface lowering per degree of temperature increase. Tecklenburg et al. (2012) investigated climate change impacts on the Ötztaler Ache catchment using the conceptual semidistributed

model HBV-D REG and one realization of the A1B climate scenario, however without accounting for glacier geometry changes but rather investigating only the two extremes of either constant glacier areas or entirely ice-free areas through the entire simulation period, respectively. Weber et al. (2010) used the fully distributed physically based model PROMET with the subgrid-scale extension SURGES for simulating glacier processes (Prasch et al., 2011) to calculate future hydrological changes in the Upper Danube basin using a single RCM realization based on the A1B scenario, and Wijngaard et al. (2016) applied the two conceptual hydrological models HBV and HQsim for the simulation of future hydrology in two catchments of the Ötztal Alps while updating glacier extents in 10-year intervals using precalculated ice thickness distributions.

Most of the cited studies rely on air temperature and precipitation as meteorological forcing data, applying simple temperature index methods for calculating snow and ice melt. However, the degree-day factors are calibrated for past conditions and their transferability in space and time is uncertain. Several studies hence have pointed out that more physical methods should be favored over classical temperature index melt calculations in climate change impact studies (e. g., Farinotti et al., 2011; Huss et al., 2009; Radić et al., 2013; Viviroli et al., 2011). Some studies have for example applied enhanced temperature index methods that also take solar radiation into account for melt calculation (e. g., Addor et al., 2014; Bosshard et al., 2013; Fatichi et al., 2015; Finger et al., 2012), addressing the fact that glacier melt rates are especially sensitive to variations in solar radiation (e. g., Huss et al., 2009; Ohmura et al., 2007). Only very few studies (e. g., Kobierska et al., 2013; Weber et al., 2010) however have applied full energy balance melt models for climate change impact assessment. While their superiority to more empirical methods is undisputed under the premise of in situ recordings of the required meteorological variables at the point scale, it remains challenging to provide adequate meteorological forcing data for their application in distributed mode. Nevertheless, due to their physical basis energy balance models are in principle better suited to account for changed climatic conditions than conceptual models (e. g., Klemeš, 1990; Pomeroy et al., 2007; Walter et al., 2005).

In this study we apply the fully distributed energy and mass balance model AMUNDSEN (Strasser, 2008) to assess future climate change impacts on the cryosphere and hydrology of the Ötztal Alps (Austria). Downscaled, bias-corrected and temporally disaggregated EURO-CORDEX scenario simulations for the RCP2.6, RCP4.5 and RCP8.5 scenarios are used as climatic forcing data. We analyze the simulation results with regard to changes in snow cover, glacier extent and volume, and hydrology, and discuss

the associated uncertainties.

6.2 Study site and data

The study site (fig. 6.1) is situated in the Ötztal Alps (Austria), a heavily glacierized Central-Alpine mountain range stretching east-west at the main ridge, with Austria in the north and Italy in the south. The Ötztal Alps are characterized by a warm and dry climate, with average annual precipitation sums being as low as 660 mm at station Vent (1890 m a.s.l.). In the study, we focus on the headwaters of the three north-south trending valleys Kaunertal, Pitztal, and Ötztal (located from west to east in fig. 6.1), which are tributaries to the Inn river in the north. Elevations in the study site range from 862 to 3770 m a.s.l., with a mean elevation of approx. 2400 m a.s.l. For the analysis of the cryospheric impacts in terms of changes in snow and glacierization, we take the entire area shown in fig. 6.1 into account (1850 km^2), while the hydrological investigations are carried out for the seven gauged catchments highlighted in the figure and listed in table 6.1, with a total area of 379 km^2. The runoff regimes are characterized by a strong seasonality due to being fed mostly by snow and ice melt (glacial to nival regime types). Several of the catchments contribute to the Gepatsch hydropower reservoir situated in the south of the Kaunertal valley, whose natural catchment area of 106 km^2 is extended by a further 171 km^2 by diversion from the adjacent Pitztal and Radurschltal valleys. In the year 1997, 206 glaciers with a combined area of 150.7 km^2 were located in the area as determined from the second Austrian glacier inventory (Kuhn et al., 2015).

For the model simulations, a digital elevation model (DEM) resampled to 100 m resolution was used. Initial ice thickness distributions for all glaciers in the region were calculated based on the glacier outlines and surface elevations of the year 1997 using the methodology by Huss and Farinotti (2012). The resulting ice thicknesses as shown in fig. 6.1 were validated against ground-penetrating radar measurements for eleven glaciers in the region, with deviations ranging between −12 and 26 % and an average deviation of −3.2 % (Seiser et al., 2012).

Meteorological stations with long-term data records availability in the region were used to drive the model in 3-hourly temporal resolution for the historical simulations. For the scenario simulations until 2100, we used the EURO-CORDEX climate change projections (Jacob et al., 2013) as climatic forcing. The entire range of (as of July 2016) publicly available EURO-CORDEX simulations for the the high-resolution ($0.11° \approx 12.5$ km) EUR-11 domain that contained all required meteorological vari-

ables (minimum, maximum and mean 2 m air temperature, precipitation, relative or specific humidity, global radiation, and wind speed) in daily temporal resolution was selected, amounting to a total of 14 GCM-RCM combinations (table 6.2). All of these 14 model combinations include simulations for both the RCP4.5 and RCP8.5 scenarios. In contrast to many other impact studies, we also included the intervention scenario RCP2.6, for which however only three realizations among the EURO-CORDEX pool were available. Hence, in total 31 different sets of climate projections were available for the glaciohydrological simulations. The scenario period of the models is 2006–2100, with the exception of the three HadGEM-driven models which terminate in November 2099.

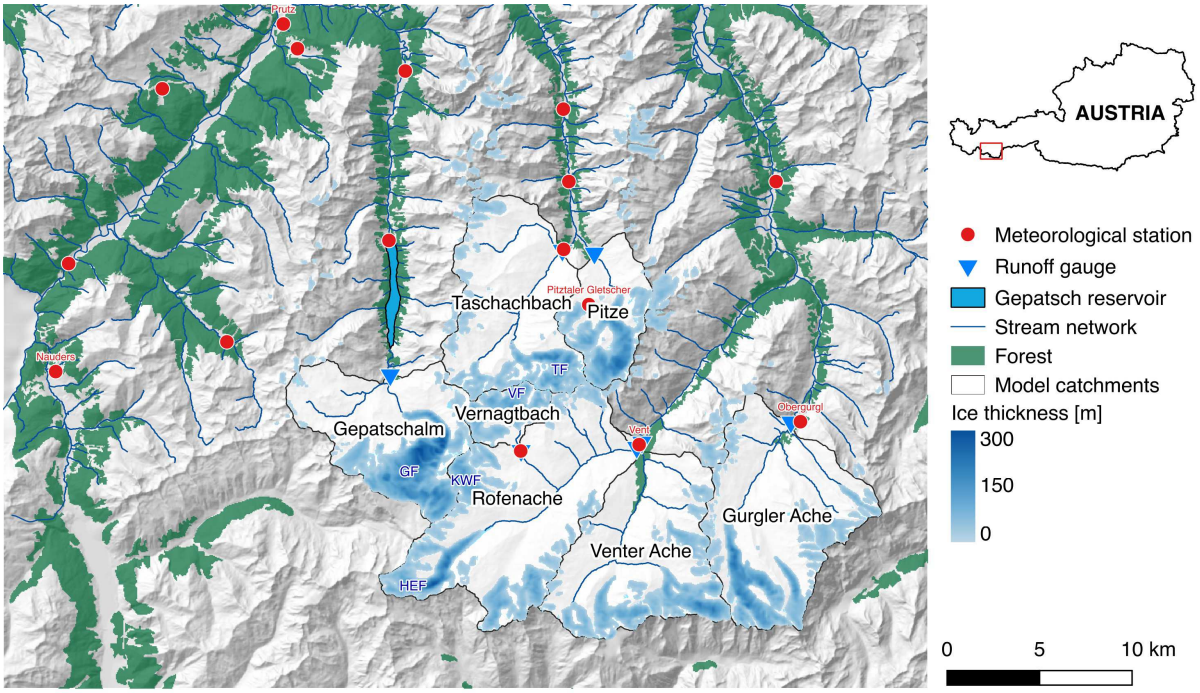

Figure 6.1: Location and topography of the study site including forested areas, catchment boundaries, the locations of the meteorological stations and runoff gauges, and the calculated initial ice thickness distribution for the year 1997. Selected meteorological stations and glaciers explicitly mentioned in the article are labeled in red and blue, respectively. Glacier abbreviations refer to Hintereisferner (HEF), Kesselwandferner (KWF), Vernagtferner (VF), Taschachferner (TF), and Gepatschferner (GF).

Table 6.1: Area, elevation, and glacierization (as of 1997) of the investigated catchments. The catchment IDs correspond to the labels in fig. 6.1. Indentations indicate subcatchments.

ID	Catchment	Area [km²]	z_{min} [m a.s.l.]	z_{max} [m a.s.l.]	z_{mean} [m a.s.l.]	Glacierization 1997 [%]
1	Venter Ache	165.3	1880	3762	2887	35.4
2	— Rofenache	98.6	1893	3762	2889	38.3
3	—— Vernagtbach	11.5	2638	3622	3120	77.0
4	Gurgler Ache	72.4	1885	3533	2785	31.8
5	Gepatschalm	53.9	1898	3524	2824	39.7
6	Taschachbach	60.5	1791	3761	2753	24.0
7	Pitze	27.0	1812	3548	2835	48.2
	Total	379.1	1791	3762	2833	34.4

Table 6.2: EURO-CORDEX scenario simulations used in this study.

ID	RCM	GCM	RCPs
1	CCLM4-8-17	CNRM-CM5	4.5, 8.5
2	CCLM4-8-17	EC-EARTH	4.5, 8.5
3	CCLM4-8-17	HadGEM2-ES	4.5, 8.5
4	CCLM4-8-17	MPI-ESM-LR	4.5, 8.5
5	HIRHAM5	EC-EARTH	2.6, 4.5, 8.5
6	RACMO22E	EC-EARTH	4.5, 8.5
7	RACMO22E	HadGEM2-ES	4.5, 8.5
8	RCA4	CNRM-CM5	4.5, 8.5
9	RCA4	EC-EARTH	2.6, 4.5, 8.5
10	RCA4	CM5A-MR	4.5, 8.5
11	RCA4	HadGEM2-ES	4.5, 8.5
12	RCA4	MPI-ESM-LR	4.5, 8.5
13	REMO2009	MPI-ESM-LR	2.6, 4.5, 8.5
14	WRF331F	CM5A-MR	4.5, 8.5

6.3 Methods

6.3.1 Model

For the glaciohydrological simulations in this study, we used the fully distributed hydroclimatological model AMUNDSEN (Strasser, 2008). AMUNDSEN has specifically been designed as a scenario-capable model for the application in high-mountain regions, and has been set up and extensively validated for historical conditions in the study site in a recent study (Hanzer et al., 2016). In the following, the most important model components are briefly discussed – for a more detailed model description, we refer to, e. g., Hanzer et al. (2016) and Hanzer et al. (2014), Marke et al. (2015), Pellicciotti et al. (2005), Strasser (2004) and Strasser (2008), and Strasser et al. (2008).

The model is capable of operating in temporal resolutions of 1–3 h, while the spa-

tial resolution is generally arbitrary but typically chosen in the order of 10–100 m for the application in high-mountain regions in order to accurately capture the complex topography and the underlying processes in these regions. As meteorological variables, AMUNDSEN requires point measurements or gridded inputs of air temperature, precipitation, relative humidity, global radiation, and wind speed. For the application using point data, the model includes a meteorological preprocessor for the spatial interpolation of scattered point measurements using a combination of lapse rates and inverse distance weighting. Lapse rates are either calculated from the point measurements in each time step or are presupplied as average monthly values. A radiation model based on the method by Corripio (2002) is used to calculate potential clear-sky solar radiation while taking into account hill shading, transmission losses and gains due to scattering, absorption, and reflections, and uses measured point values of global radiation to derive cloud factor fields and subsequently actual global radiation fields. Similarly, incoming longwave radiation is calculated using parameterizations for radiation received from the clear sky, clouds, and surrounding terrain. The precipitation phase (rain or snow) is determined as a function of the wet-bulb temperature. For solid precipitation, different correction methods are implemented in order to account for the undercatch of precipitation gauges when measuring snow accumulation. Hanzer et al. (2016) showed that a combination of a station-based snow correction factor (SCF) taking into account wind speed and air temperature with a subsequent constant post-interpolation SCF of 1.15 yielded plausible long-term precipitation amounts for the study area, while an additional redistribution of the interpolated snowfall fields using an approach based on topographic openness (Yokoyama et al., 2002) distinctly improved the spatial snow accumulation patterns. Accumulated snow on the surface is subdivided into three layers called new snow, old snow, and firn. Transitions between new snow and old snow occur depending on snow density (which is calculated based on approaches by Anderson (1976) and Jordan (1991)), while remaining snow amounts at the end of the ablation season (September 30) are transferred to the firn layer. In glacierized catchments, an additional layer is used to track the evolution of ice amounts. A linear densification of the firn layer is employed, while firn is converted to ice once reaching a threshold density of 900 $\mathrm{kg\,m^{-3}}$. Snow albedo is parameterized using an aging curve approach with exponential decay down to a specified minimum value, while firn and ice albedo is kept constant for this application (with values of 0.4 and 0.2, respectively). In forested areas the interpolated meteorological fields are modified in order to capture sub-canopy conditions, while additionally the effects of the forest snow processes of interception, sublimation, and

melt unload are accounted for (Strasser et al., 2011a). Snow and ice melt is calculated using an energy balance approach taking into account short- and longwave radiation fluxes, latent and sensible heat fluxes, advective energy, as well as the ground heat flux. The delay of the onset of snowmelt in cold snowpacks is accounted for by a parameterization of the cold content of the snowpack, whereas melting snow may persist in the snowpack in the form of liquid water up to a certain amount (and possibly refreeze again) before actual outflow occurs (Hanzer et al., 2016). Evapotranspiration in snow-free areas is calculated following Allen et al. (1998). Finally, runoff at predefined catchment outlets is calculated using a linear reservoir approach for snow on glaciers, firn, bare ice, snow outside of glaciers, and soil (Hanzer et al., 2016). Apart from the parameters of this linear reservoir model which have to be calibrated individually for each catchment, most parameters in the model have a physical meaning, and in general no site-specific calibration is performed.

The setup and extensive validation of the model for the study region under historical conditions has been described in Hanzer et al. (2016). Essentially the same model setup was used for this study, aside from (i) the newly implemented glacier retreat parameterization as described in the following section, (ii) reducing the spatial and temporal model resolution from 50 m and 1 h to 100 m and 3 h due to performance reasons, and (iii) the fact that only a subset of the meteorological stations that were utilized in the simulations presented in the aforementioned study was available for this study due to the constraints of a sufficiently long measurement period required for the bias correction of the RCM data (see section 6.3.3).

6.3.2 Glacier geometry change

The model setup as described in Hanzer et al. (2016) already incorporated spatially distributed glacier thicknesses, however only accounted for the climatic forcing on the glaciers without any adjustment of glacier geometry. Due to the generally small vertical ice flow contribution for the majority of the glaciers in the study region (Helfricht et al., 2014a) this is a reasonable approach for shorter simulation periods, however when performing simulations on multidecadal scales, the effect of ice flow dynamics must be considered in glaciohydrological models. Otherwise, systematic errors in the simulated ice distributions (and subsequently in glacier runoff) are introduced as the glaciers thicken in their accumulation areas and retreat too quickly in the tongue parts.

For this study, we implemented the Δh method (Huss et al., 2010) to periodically update the simulated glacier geometries. This approach is particularly suited for spatially distributed models operating on the regional scale, as it does not necessarily

require glacier-specific parameterizations but rather uses simple assumptions to translate the climatic forcing (i. e., the surface mass balance as computed by the mass balance model) into a geometric response in terms of the glacier thickness distribution.

Essentially, the Δh parameterization scales the spatial distribution of the annual glacier surface mass balance such that the changes in glacier surface elevation match patterns observed in the past. This is accomplished by applying a prescribed function to each glacier in regular time intervals, which adjusts the simulated surface elevation change as a function of the normalized glacier elevation (assumed to be a proxy for the central flowline). To derive the Δh function, two glacier surface DEMs are required, preferably covering multidecadal periods to reduce possible errors due to DEM uncertainty.

In principle, a separate Δh function could be derived for each glacier, however Huss et al. (2010) showed that glaciers with similar characteristics show similar geometric responses, and derived three Δh functions for glaciers of different size classes: large valley glaciers ($A \geq 20\,\mathrm{km}^2$), medium valley glaciers ($5\,\mathrm{km}^2 \leq A < 20\,\mathrm{km}^2$), and small glaciers ($A < 5\,\mathrm{km}^2$):

$$\Delta h = \begin{cases} (h_r - 0.02)^6 + 0.12(h_r - 0.02) & A \geq 20\,\mathrm{km}^2 \\ (h_r - 0.05)^4 + 0.19(h_r - 0.05) + 0.01 & 5\,\mathrm{km}^2 \leq A < 20\,\mathrm{km}^2 \\ (h_r - 0.30)^2 + 0.60(h_r - 0.30) + 0.09 & A < 5\,\mathrm{km}^2, \end{cases} \tag{6.1}$$

where h_r corresponds to the normalized surface elevation between 0 and 1.

While these parameterizations have been derived for the Swiss Alps, they are assumed to be applicable for all mountain glaciers (Huss et al., 2010), and have already been applied in other regions of the world (e. g., Huss and Hock, 2015; Ragettli et al., 2013). While for our study region DEMs and glacier outlines exist for the years 1997 and 2006, we chose to adopt these generalized parameterizations, as (i) they have been derived over much longer time periods, hence likely being more robust, and (ii) match the average observed Δh patterns for our study area in the period 1997–2006 well (fig. 6.2).

In AMUNDSEN, the glacier geometry update is performed at the end of each glaciological year (September 30): for each glacier, the total volume change in terms of the surface mass balance is used to scale the thickness change prescribed by the Δh function (determined by eq. (6.1)) which is applied to each glacier pixel and the respective normalized elevations. Following Huss et al. (2010), the maximum surface lowering is limited to the surface mass balance lowering at the glacier terminus, and

the glacier borders (pixels with ice thicknesses < 10 m) are not modified by the geometry update but rather change their thickness only due to the respective surface mass balance change.

Figure 6.3 demonstrates the effect of the glacier geometry update as implemented in AMUNDSEN exemplarily for the Hintereisferner and Taschachferner glaciers. While the average change in surface elevation between 1997 and 2006 is reproduced reasonably well for both glaciers in the run without updating the glacier geometries, the increase in surface elevation at the uppermost glacier parts is severely overestimated for both glaciers, whereas mass losses in the middle to lower parts of the glaciers are too high. Adding the glacier retreat module to the model distinctly improves the spatial distribution of mass gain or loss for both glaciers.

One limitation of the Δh approach is that it allows only for geometric changes in terms of glacier retreat, essentially limiting its applicability for periods with largely negative mass balances. Huss and Hock (2015) present an extension of the method that enables to also account for advancing glaciers, however using a semidistributed model operating in elevation bands. A possible, comparatively simple extension of the method when applied in a fully distributed way could be to allow the glaciers to grow within their historical extents, similar to the approach applied by Stahl et al. (2008). In this study, however, we apply the original retreat-only version of the Δh parameterization, which is seen a feasible approach given that future climate scenarios indicate climatic conditions causing intensive melt and, hence, glacier shrinkage.

6.3.3 Spatial downscaling of RCM data

While state-of-the-art RCM simulations already feature comparatively high spatial resolutions, usually the performance of the raw RCM data is still inadequate for directly using it in hydrological impact studies, both due to still-present mismatches in space as well as due to systematic model errors (biases) introduced by the RCMs. A common approach for impact studies is hence to use ensembles of GCM-RCM chains in combination with statistial bias correction methods (Teutschbein and Seibert, 2012).

In this study, we use quantile mapping (QM) (e. g., Déqué, 2007; Themeßl et al., 2011), an empirical bias correction method that corrects the distribution functions of the RCM variables to fit the distribution functions of the observations. QM has regularly shown to outperform other statistical bias correction methods (e. g., Teutschbein and Seibert, 2013; Teutschbein and Seibert, 2012), is applicable in mountain regions (e. g., Finger et al., 2012; Themeßl et al., 2012; Themeßl et al., 2011), and allows for correcting climate variables other than temperature and precipitation (e. g., Finger et al.,

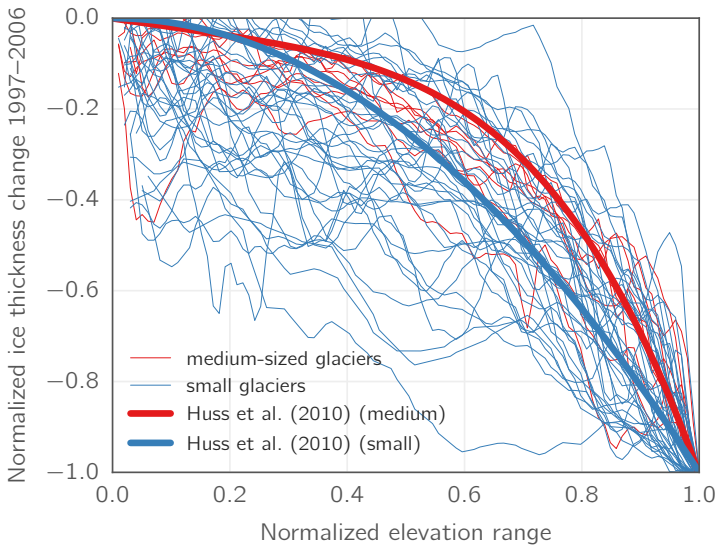

Figure 6.2: Normalized observed ice thickness change for 42 small ($A < 5\,\mathrm{km}^2$, thin blue lines) and 8 medium-sized ($5\,\mathrm{km}^2 \leq A < 20\,\mathrm{km}^2$, thin red lines) glaciers in the Ötztal Alps during the period 1997–2006, and the corresponding parameterizations from Huss et al. (2010) (thick lines).

2012; Wilcke et al., 2013). Like most statistical bias correction methods, QM does not explicitly account for spatial, temporal, or intervariable correlations, however it has shown to perform well under changed climatic conditions (Teutschbein and Seibert, 2013) and to retain intervariable relations (Wilcke et al., 2013).

In the study, we used the QM methodology by Gudmundsson et al. (2012) as implemented in the R package *qmap*. Due to strong season-dependent biases in the RCM data, we performed the bias correction separately for DJF, MAM, JJA, and SON. Only stations and variables with a minimum amount of 20 years of data within the period 1971–2005 were considered for the bias correction procedure, with the exception of global radiation where two stations with only approx. 10 years of data were also included due to an otherwise insufficient number of stations. Given these constraints, in total 16 precipitation time series were available, as well as 13 for air temperature, 6 for wind speed, 5 for relative humidity, and 3 for global radiation.

In order to avoid the possibility of unrealistic temperature values in terms of corrected $T_{\mathrm{min}} > T_{\mathrm{max}}$, following Thrasher et al. (2012) we did not correct T_{min} and T_{max} independently, but rather corrected T_{max} and the diurnal temperature range (DTR) ($T_{\mathrm{max}} - T_{\mathrm{min}}$) with a subsequent calculation of corrected T_{min}.

For the EURO-CORDEX realizations for which only specific rather than relative humidity was available (IDs 1–4 and 13 in table 6.2), mean daily specific humidity q

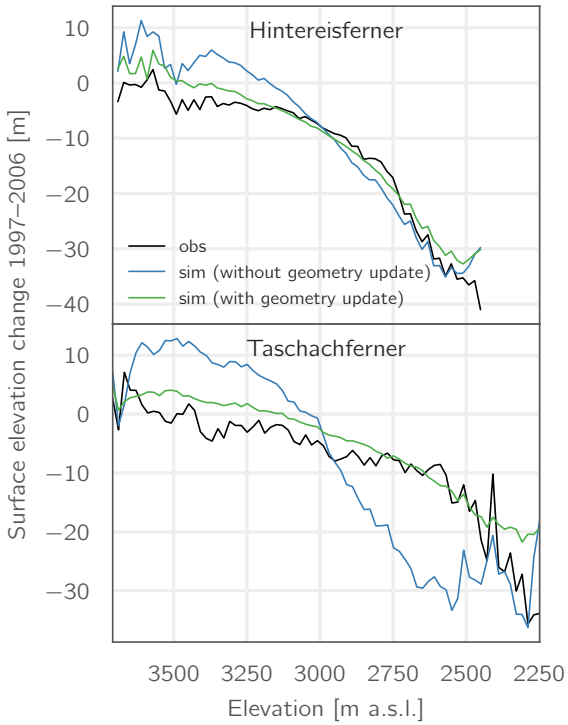

Figure 6.3: Observed and simulated glacier surface elevation change during the period 1997–2006 as a function of elevation for the glaciers Hintereisferner and Taschachferner (see fig. 6.1 for their geographical setting). "Without geometry update" refers to the simulated surface mass balances without accounting for ice flow, while "with geometry update" refers to the simulation results obtained after implementing the Δh parameterization.

[kg kg^{-1}] was first converted to relative humidity RH [%] as

$$\mathrm{RH} = 100\frac{e}{e_s}, \tag{6.2}$$

with the vapor pressure e [hPa] calculated as

$$e = \frac{qp}{0.622 + 0.378q}, \tag{6.3}$$

with p being air pressure [hPa]. Saturated vapor pressure e_s [hPa] was calculated following Sonntag (1990) as

$$e_s = \begin{cases} 6.112\exp\left(\frac{17.62T}{243.12+T}\right) & T \geq 0\,^\circ\mathrm{C} \\ 6.112\exp\left(\frac{22.46T}{272.62+T}\right) & T < 0\,^\circ\mathrm{C} \end{cases} \tag{6.4}$$

with $T = T_{\mathrm{mean}}$ [°C].

With regard to the selection of RCM grid points for the downscaling to the point scale, we followed the approach by Hofer et al. (2017) (who however used linear

regressions rather than QM) to find the *optimum scale* (OS) for each station and target variable: For each station and variable, spatial averages of the closest $1 \times 1, 2 \times 2, \ldots, 10 \times 10$ RCM grid points were calculated and subsequently used for bias correction. The OS for a given station and variable was then defined as the spatial window which minimizes the deviations between the cumulative distribution functions of the corrected and observed data in terms of the mean absolute error (MAE). Histograms of the resulting OS values for the different variables are shown in fig. 6.4. While for all variables an OS of 1 (corresponding to using only the closest RCM grid point without spatial averaging) is the most common value, for all variables except global radiation all OS values from 1 to 10 are found – for precipitation, the maximum possible OS of 10 is even the second most common value.

RCM outputs from models using fixed 360- or 365-day calendars were linearly rescaled to Gregorian calendar dates (e. g., for a 360-day calendar each day from 1–360 was mapped to a respective day from 1–365 (or 366) in the Gregorian calendar). Resulting days with missing values were filled by duplicating the values from the preceding day.

Figure 6.5 shows the mean deviation (MD) and the standard deviation ratio (SDR) of the bias-corrected RCM data vs. the daily observations for the stations in the study area in the historical period 1971–2005. The model IDs (x-axis) correspond to the IDs in table 6.2. While some models tend to perform slightly better than others on average, both measures are in general close to their optimum values (0 and 1, respectively) for all realizations, indicating that the corrected RCM outputs adequately represent the observed climate in terms of mean and variability. The higher deviations in the variability of relative humidity for some models are not a result of the bias correction per se, but rather of the required conversion of specific to relative humidity for these models.

6.3.4 Temporal downscaling of RCM data

As the EURO-CORDEX simulations were only available in daily temporal resolution, an additional processing step was necessary to derive the required sub-daily (1–3-hourly) data. This step was performed with the open-source temporal disaggregation tool MELODIST (Förster et al., 2016a). MELODIST provides simple, empirical disaggregation routines for the sub-daily disaggregation of daily point-scale data for the variables air temperature, precipitation, relative humidity, solar radiation, and wind speed. For the application in this study several new disaggregation methods were added to MELODIST:

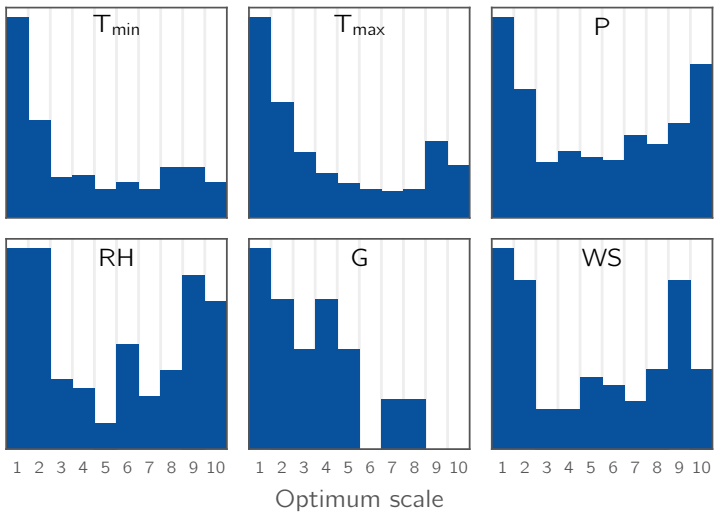

Figure 6.4: Histograms of the optimum scales for bias correction found using the approach by Hofer et al. (2017) for the variables minimum temperature (T_{min}), maximum temperature (T_{max}), precipitation (P), relative humidity (RH), global radiation (G), and wind speed (WS). Histograms are calculated using the derived optimum scales for all available stations for a given variable and all 14 GCM-RCM combinations (table 6.2).

1) For air temperature, a disaggregation method conserving the daily mean temperature and the DTR ($T_{\text{max}} - T_{\text{min}}$) while applying a sinusoidal temperature course in the same way as the default method (which preserves T_{min} and T_{max} but not T_{mean}) was implemented. However, most stations showed no clear sinusoidal temperature course, hence the application of this method still resulted in a (positive) temperature bias for most stations. Therefore, a new method based on mean values depending on the calendar month and hour of the day derived from hourly recordings was implemented. In a preprocessing step, for each month and station an average temperature course (normalized to a $[0, 1]$ range) is calculated. Then, daily values are disaggregated on the basis of these temperature courses again by either preserving T_{min} and T_{max}, or T_{mean} and the DTR ($T_{\text{max}} - T_{\text{min}}$).
2) With regard to solar radiation, a similar method was implemented, which uses monthly varying average diurnal radiation courses derived from observations to scale the daily mean radiation. In addition, the methods for deriving daily radiation values from sunshine duration or the diurnal temperature range have been updated to allow monthly or seasonally varying conversion factors.
3) For relative humidity, an additional disaggregation method using [month, hour, dry/wet day] categorical mean values was implemented following Waichler and

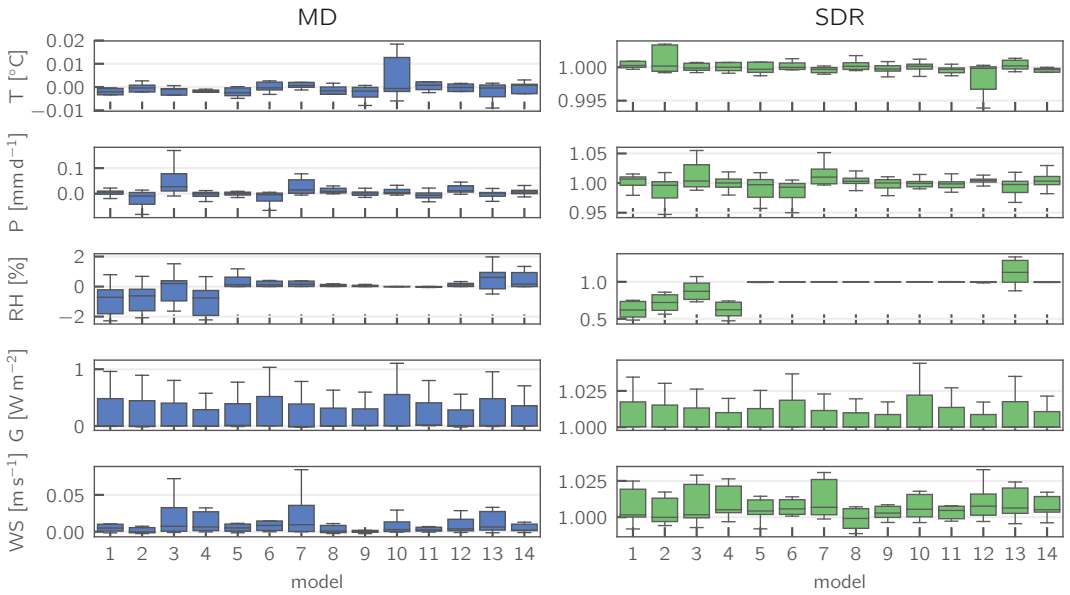

Figure 6.5: Mean deviation (MD) and standard deviation ratio (SDR) of simulated (i. e., downscaled and bias-corrected RCM data) vs. observed meteorological data for the historical period 1971–2005. The individual boxes represent the downscaled station meteorology for a given GCM/RCM combination (model IDs correspond to the ones in table 6.2). Units given for the different variables apply only to MD (SDR is unitless).

Wigmosta (2003). If daily humidity values are available, they can be used to scale the thereby derived values to preserve the daily mean.

Figure 6.6 shows the density functions for the observed hourly values (black lines) as well as for the various disaggregation methods exemplarily for station Obergurgl (1938 m a.s.l.) and the variables air temperature, relative humidity, global radiation, and wind speed. Based on these comparisons and the results of the multilevel validation of the glaciohydrological simulation results when driven with the disaggregated values using multiple configurations, we decided for the following disaggregation methods: for all stations, air temperature was disaggregated using the "mean course" method while preserving daily minimum and maximum temperatures, daily precipitation amounts were distributed uniformly across the day, relative humidity was disaggregated using [month, hour, dry/wet day] categorical mean values while preserving daily mean radiation, solar radiation was disaggregated using the "mean course" method while preserving daily mean radiation, and wind speed was distributed uniformly over the day.

Not all of these disaggregation methods performed best with regard to the reproduction of hourly values at the station scale, however this method combination

yielded the best overall glaciohydrological model performance according to the multi-level validation procedure described in Hanzer et al. (2016). This is partly explainable from the fact that the disaggregation is performed independently for each station and variable.

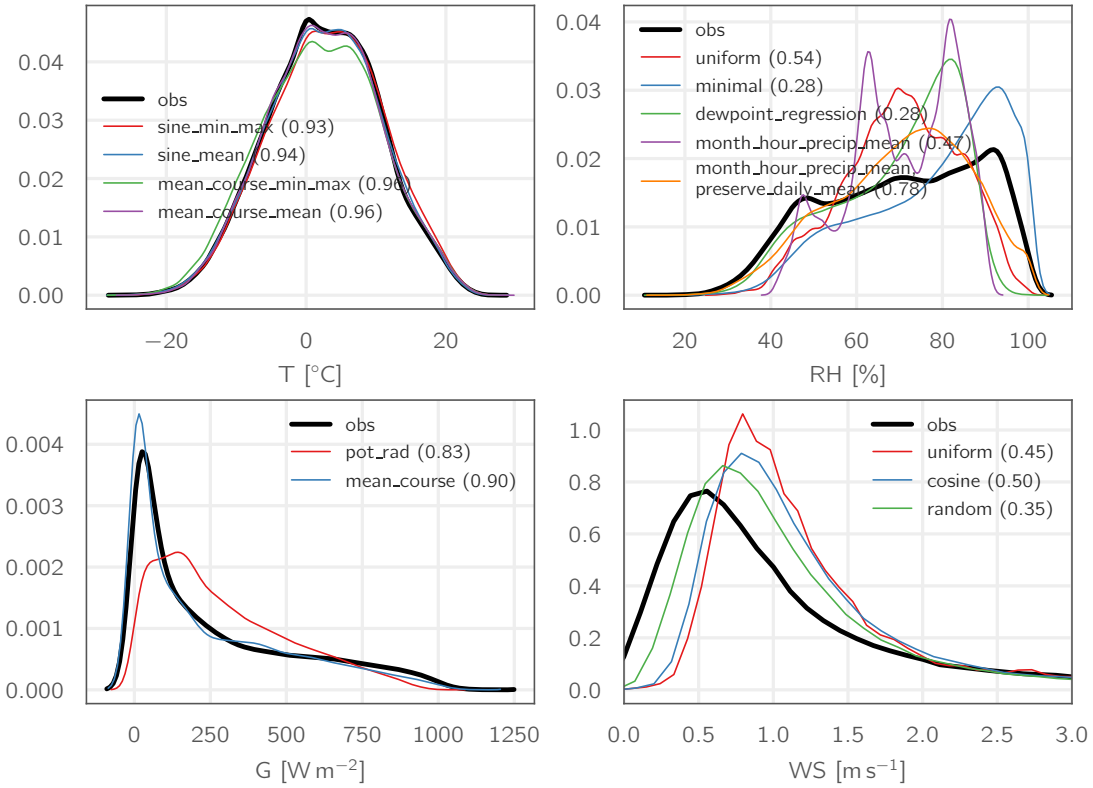

Figure 6.6: Density functions of the observed hourly values (black lines) for station Obergurgl (period 1999–2013) and the respective aggregated-and-disaggregated values using different disaggregation methods for the variables temperature, relative humidity, global radiation, and wind speed. Numbers in parentheses indicate the R^2 of the regression against the observations.

6.4 Results and discussion

In the following sections, first we discuss the future climatic changes in the study area as projected by the EURO-CORDEX scenarios. Then, we analyze the subsequent changes in snow, glaciers, and hydrology according to the AMUNDSEN simulations for the scenario period. These simulations were carried out by initializing the model in 1997 (using the glacier inventory and ice thickness data) and running it until September 2006 using the observed meteorological data. Afterwards, we switched to the EURO-CORDEX scenario period and carried out the scenario simulations until 2100

(with the exception of the three HadGEM-driven models for which the simulations could only be carried out until the year 2098).

We did not perform the entire range of glaciohydrological simulations for a longer historical period due to restrictions of the current model setup: (i) the initial ice thickness distributions were calculated for the year 1997 and are hence not applicable for earlier periods, and (ii) the generally negative mass balances of the glaciers in the Ötztal Alps during the last decades were interrupted by a short period of glacier advance between the mid-1970s and the early 1980s (Abermann et al., 2009), which cannot adequately be accounted for using the currently implemented Δh parameterization for the glacier geometry update. However, for discussing solely the changes in snow conditions, we also carried out model runs for the period 1971–2005 (hence obtaining transient runs from 1971 to 2100) using the historical RCM simulations as forcing, while neglecting the effect of glaciers in this case.

6.4.1 Future climate

Figure 6.7 shows the range of the projected seasonal and overall changes (spatial averages, relative to the baseline period 1971–2000) of the five meteorological variables for the study area as provided by the climate simulations. These changes are calculated based on areal means of the respective variables as calculated by the meteorological preprocessor in AMUNDSEN (i. e., after bias correction). While in the figure the changes are plotted for three time slices throughout the 21st century, for the following short discussion of the changes we focus on the period 2071–2100. If not otherwise stated, values refer to multi-model means in the following.

Temperature is projected to increase by all models and for all seasons, with average values of 1.1 (RCP2.6) to 3.8 °C (RCP8.5) in the annual mean, and a maximum spread of 2.2 °C between individual models for a given scenario. The highest warming is projected for the winter season, with up to 4.5 °C in the RCP8.5 scenario, while the smallest increases are projected for spring.

For precipitation, no clear general trend can be discerned with regard to annual sums. Both decreases (up to −14 %) and increases (up to 24 %) are projected by individual models, while the multi-model averages are close to zero for all three scenarios. However, with the exception of some outliers, there is a general consensus between the model towards a precipitation shift from summer towards winter. Projected multi-model average increases in winter precipitation are between 8 % (RCP2.6) and 21 % (RCP8.5), with individual models projecting increases of up to 57 %.

Changes in relative humidity largely follow the trend of precipitation changes, with decreases in summer (up to −1.5 %) and smaller increases in winter (up to 0.7 %). At least for the RCP8.5 scenario slight decreases in the annual mean are projected.

For global radiation, the disagreement between the individual models is considerable. The multi-model means indicate a decrease in overall global radiation for all RCPs, with values between $-1.2\,\mathrm{W\,m^{-2}}$ for RCP4.5 and $-2.4\,\mathrm{W\,m^{-2}}$ for RCP2.6, however with individual model results ranging between $-20\,\mathrm{W\,m^{-2}}$ and $4\,\mathrm{W\,m^{-2}}$. The spread between the models is even larger when looking at seasonal changes. While all models agree on a decrease of global radiation in winter and (with one exception) spring, projections for summer are uncertain. Here, most models tend towards an increase in radiation for the RCP4.5 and RCP8.5 scenarios, however individual results range between $-29\,\mathrm{W\,m^{-2}}$ and $26\,\mathrm{W\,m^{-2}}$.

Finally, wind speed projections also show quite a large spread between individual models. Multi-model means indicate a very small overall decrease in wind speed, with seasonal increases of up to $0.12\,\mathrm{m\,s^{-1}}$ during winter and decreases of up to $-0.12\,\mathrm{m\,s^{-1}}$ during summer.

Comparing to other studies, the projected changes over the Ötztal Alps and their seasonal patterns are similar to the average changes projected for the entire Alpine region (Gobiet et al., 2014; Jacob et al., 2013; Smiatek et al., 2016). Notable differences are found for temperature, where the multi-model median change for 2071–2100 compared to 1971–2000 is 0.3 °C lower than in Jacob et al. (2013) for RCP4.5, and 1.0 °C lower for RCP8.5. Seasonal temperature changes for the RCP4.5 scenario are between 0.1 °C and 0.4 °C lower than in Smiatek et al. (2016).

6.4.2 Changes in snow

Changes in the amount and duration of the simulated seasonal snow cover in the study area were analyzed both temporally and spatially. As a reference for computing the changes, we performed AMUNDSEN simulation runs using the historical periods of the EURO-CORDEX simulations for the period 1970–2005. Through combination with the scenario runs we hence obtained transient simulations for the period 1970–2100.

Figure 6.8 shows the evolution of the simulated mean annual snow water equivalent (SWE) for three meteorological stations covering an approx. 2000 m elevation range: Prutz (870 m a.s.l.), Obergurgl (1938 m a.s.l.), and Pitztaler Gletscher (2864 m a.s.l.). At the highest-elevated station, Pitztaler Gletscher, the mean snow amounts remain relatively unchanged for all three RCPs until the middle of the century, whereas only

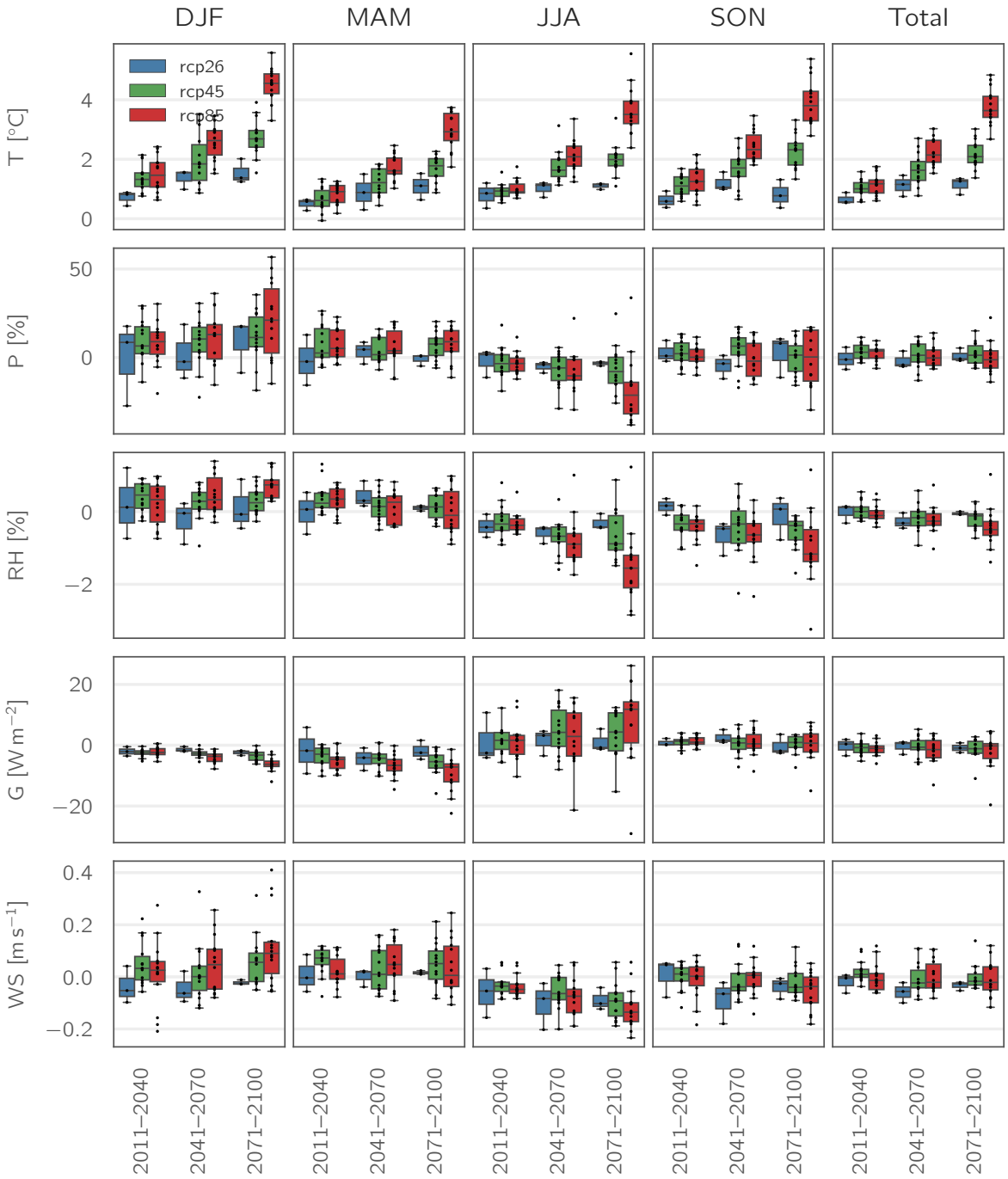

Figure 6.7: Projected seasonal changes for temperature (T), precipitation (P), relative humidity (RH), global radiation (G), and wind speed (WS) according to the selected EURO-CORDEX scenario simulations (spatial averages over the study area; changes calculated relative to 1971–2000). Small dots represent the individual GCM-RCM realizations.

afterwards stronger decreases can be seen for the RCP4.5 and RCP8.5 scenarios. For RCP2.6, snow amounts are slowly increasing during the last third of the century, reaching an average level of 517 mm (multi-model mean), almost as high as the 530 mm in the historical period 1971–2000. However, also for the RCP4.5 and RCP8.5 scenarios, only comparatively small decreases in average SWE are simulated, amounting to 427 mm (−18 %) and 357 mm (−31 %), respectively. For station Obergurgl, similarly no strong changes in average snow amounts are simulated within the first half of the century, whereas afterwards the curves of the three scenarios begin to diverge more strongly than for Pitztaler Gletscher. For RCP2.6 again a general trend of increasing SWE after 2050 is projected, while snow amounts in the RCP4.5 scenario decrease to 94 mm (−31 %) in the period 2071–2100, and 59 mm (−57 %) for the RCP8.5 scenario. The largest relative changes are found for the lowest-elevated station, Prutz, where the curves for the three scenarios begin to divert by around 2020. RCP2.6 snow amounts then stay relatively constant during the remainder of the century at 6 mm (−31 %), while RCP4.5 and RCP8.5 snow amounts continue to decrease strongly, amounting to −63 % and −80 %, respectively, at the end of the century.

Similar results of stronger declining snow amounts for lower elevations can be seen in fig. 6.9, where the multi-model mean change in SWE relative to the baseline period 1971–2000 is plotted against elevation. For RCP2.6, with the exception of the very lowest-elevated parts of the study area, the strongest decreases in snow amounts generally are projected for the period 2041–2070, whereas the largest average snow amounts are found at the end of the century. Generally, however, the projected decreases are comparatively small, with maximum values of approx. 12 % for elevations above 2500 m a.s.l., up to 25 % for elevations between 1500 and 2500 m a.s.l., and slightly stronger below. For both RCP4.5 and RCP8.5, average snow amounts stay virtually constant (even slightly increasing for RCP4.5) during the period 2011–2040 in elevations above 2500 m a.s.l., whereas for the lower-elevated parts decreases during this period amount to up to 37 %. However, for both scenarios strong decreases are projected for the remainder of the century, with the largest changes in the lowest-elevated areas, amounting to up to −64 % and −83 % for RCP4.5 and RCP8.5, respectively.

The analysis of seasonal changes (fig. 6.10) reveals that the strongest relative changes are projected for the summer months, while simulated changes for winter are comparatively small, amounting to maximum decreases of approx. 30 % for RCP8.5. For all three scenarios, a gradual shift in the timing of peak SWE amounts from April towards March is simulated.

These projected changes in snow coverage generally show similar patterns to studies for other Alpine sites (e. g., Beniston et al., 2003; Marty et al., 2017; Schmucki et al., 2015a; Steger et al., 2012), however with a tendency to lower relative decreases in average snow amounts. This is likely due to the comparatively strong increases in winter precipitation especially for the warmest (RCP8.5) scenario (fig. 6.7). A comprehensive study recently done for Switzerland (Marty et al., 2017) for example projected more dramatic changes in snow amounts especially in high elevations (> 3000 m a.s.l.) until the end of the century for the A2 scenario (similar warming as in the RCP8.5 scenario), however projecting only very minor winter precipitation increases. Especially in high elevations however, increases in precipitation amounts are more likely to compensate for temperature increases, as temperatures in these elevations are usually still below melting conditions for most parts of the year.

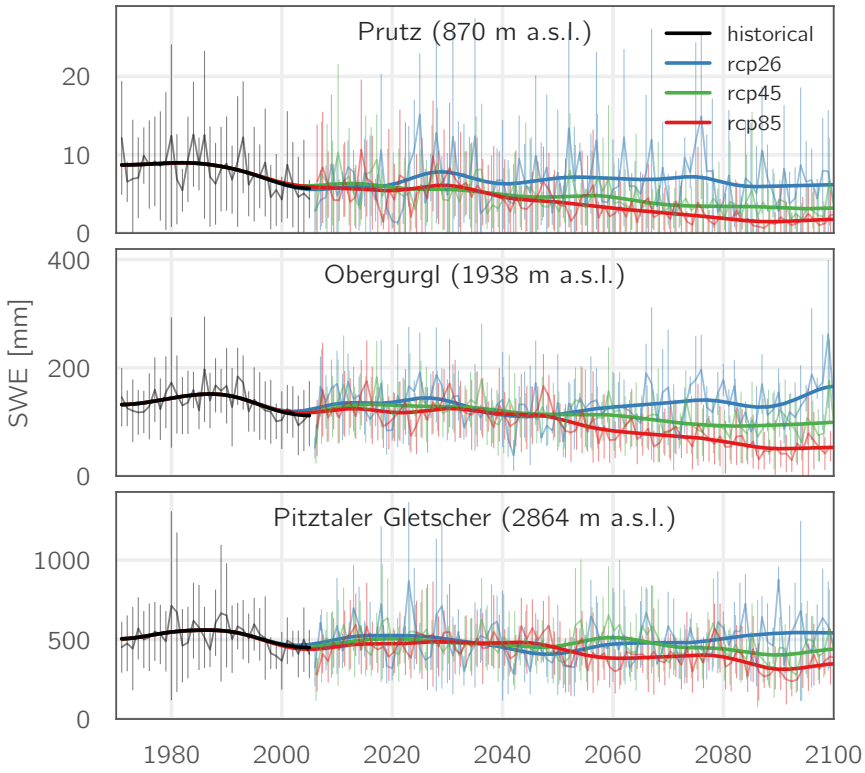

Figure 6.8: Evolution of mean annual SWE for the stations Prutz, Obergurgl, and Pitztaler Gletscher as simulated using the EURO-CORDEX scenarios for the RCPs 2.6, 4.5, and 8.5. Thin lines and error bars indicate the multi-model mean and standard deviation, respectively, while the thick lines show the 5-year Gaussian low-pass filtered multi-model mean.

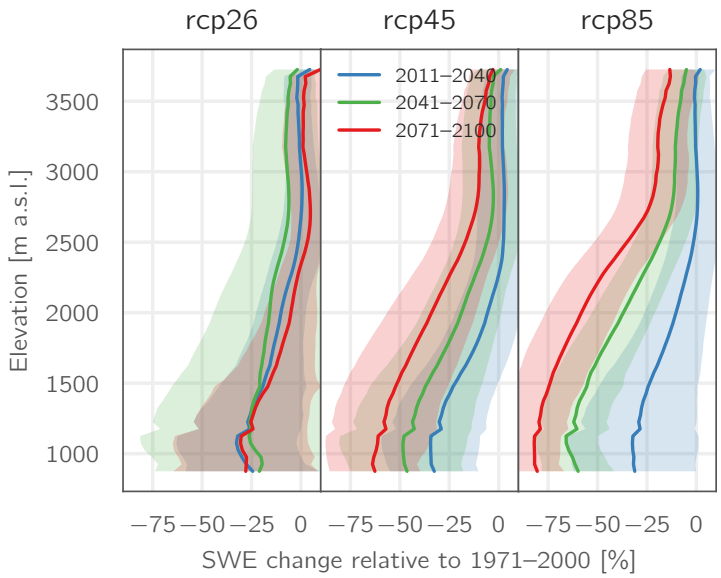

Figure 6.9: Elevation-dependent projected change in SWE (multi-model means, shadings indicate ± one standard deviation) relative to the period 1971–2000 for the RCPs 2.6, 4.5, and 8.5.

6.4.3 Changes in glaciers

According to the simulation results, all glaciers in the study region will continue to retreat significantly throughout the 21st century. This is illustrated in fig. 6.11, where the evolution of glacier volume and area (relative to the respective values of 2006) are plotted for all 31 model combinations as well as the respective multi-model means. In general, the evolution of glacier area and volume is very similar, with only a slightly stronger decline of glacier volume compared to the area. Looking at the multi-model mean values for the three emission scenarios, the largest changes in glacierization occur already within the first half of the century, where – relatively independent of the emission scenario – the glaciers lose between approx. 60 % (RCP2.6) and 65 % (RCP8.5) of their volume from the beginning of the century. After 2050, the slope of the curves decreases and differences between the three scenarios become more prominent. In the RCP2.6 scenario, glacier volume decreases to approx. 25 % until 2080, whereas the glaciers stabilize afterwards and only slightly further retreat until 2100. In the RCP8.5 scenario, glaciers decrease more rapidly than in the RCP4.5 case between between 2050 and 2080, whereas afterwards the two curves again follow a similar course. For both scenarios, the glaciers have mostly vanished by the end of the century, with only small remains of approx. 10 % (RCP4.5) and 4 % (RCP8.5) still left in terms of their initial volume. Results for the evolution of glacier area are similar.

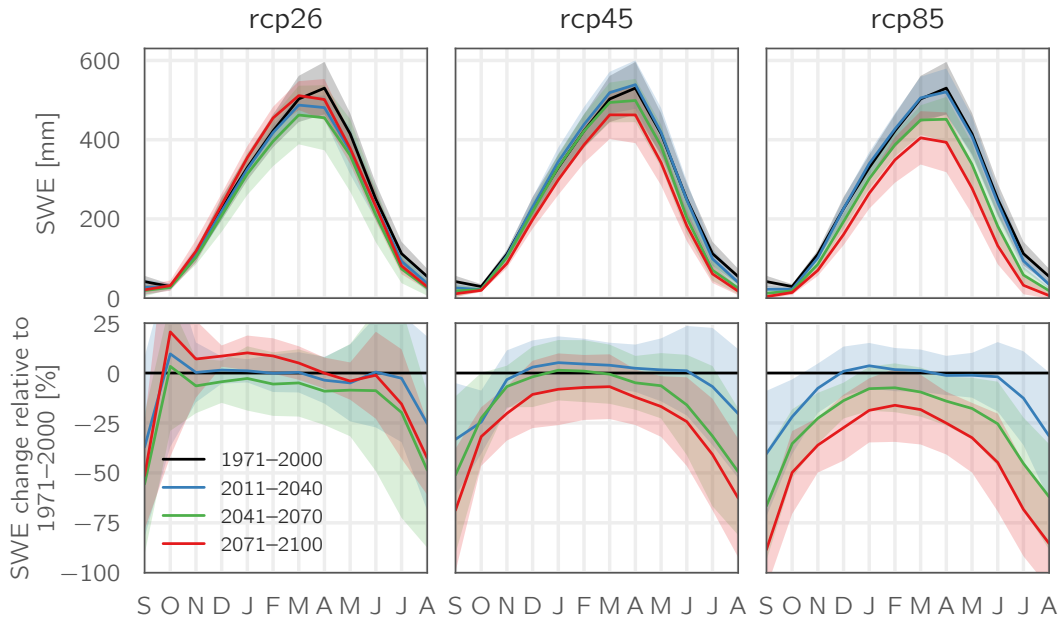

Figure 6.10: Mean monthly SWE (multi-model means, shadings indicate ± one standard deviation) over the entire study area (fig. 6.1) for the three RCPs (top) and relative changes compared to 1971–2000 (bottom).

Looking beyond the multi-model mean, it becomes clear that there is a remarkable spread between the individual model runs, most strikingly for the RCP2.6 scenario, where the glacier volume decrease is between 58 % and 97 % until 2100 for the three model runs. Also for the RCP4.5 and RCP8.5 scenarios the range between the individual model realizations is considerable, with individual realizations resulting in practically ice-free conditions as early as 2070, while in other realizations up to 33 % of glacier volume are preserved until 2100.

The comparatively small influence of the different emission scenarios on the other side is visualized in fig. 6.12, where the ice thickness evolution of a single glacier (Hintereisferner) along its centerline is plotted in 10-year intervals for a single GCM-RCM combination (REMO2009 driven by MPI-ESM-LR) and the RCPs 2.6, 4.5, and 8.5. Here again a strong loss of glacier volume can be seen in the first decades of the century. Regardless of the emission scenario, by 2040 the glacier retreats by approx. 1.4 km in length and loses approx. half of its volume (49–54 %). Only after 2060, the RCP8.5 scenario generates a markedly stronger loss in ice volume compared to the other two scenarios, resulting in an almost complete disappearance of the glacier by 2100. The results for RCP2.6 and RCP4.5 largely follow the same evolution until 2090. Only in the last decade of the century, the RCP4.5 scenario produces an accelerated retreat of

the glacier, whereas the RCP2.6 glacier surface stays approximately constant. However, also for these two less extreme scenarios, only 25 % (RCP2.6) and 13 % (RCP4.5) of the original ice volume is left by the end of the century.

Figure 6.13 shows the evolution of the absolute and relative glacierization as well as the absolute glacier volume and mean ice thickness for each catchment in the RCP4.5 scenario, illustrating that different catchments partly show different responses to the climatic forcing. For some of them (most notably Taschachbach) the average ice thickness stays approximately the same during the entire simulation period due to the similar rates of volume reduction and area reduction. For the Gepatschalm catchment, which includes the largest and thickest glacier in the study area (Gepatschferner), this is also the case for the first third of the century, whereas afterwards the rate of volume decline increases. In other catchments such as Vernagtbach and Gurgler Ache the reverse effect is observed during the last part of the century: glacier area retreats more quickly than the volume decreases (visible by the increase in mean ice thickness in this period).

The spatial evolution of glacier coverage within the study area is shown in fig. 6.14, where the simulated multi-model mean glacier coverage is displayed in 10-year intervals for the three emission scenarios. The rate of glacier retreat is mainly dependent on elevation and glacier thickness. In all three scenarios, most of today's small glaciers have disappeared by 2050 according to the model. However, for the largest glaciers considerable differences resulting from the different emission scenarios appear. Gepatschferner, for example, loses comparatively moderate 54 % of its 1997 area (17.1 km^2) by 2100 in the RCP2.6 scenario, while in the RCP4.5 and RCP8.5 scenarios 71 % and 95 %, respectively, of the glacier area disappears.

6.4.4 Changes in hydrology

Figure 6.15 exemplarily shows the simulated seasonal runoff cycle for present-day conditions as well as the projected values for the future periods for four of the study catchments. While the reaction of the catchments are slightly different depending on their characteristics, the general pattern of change is the same for all catchments and emission scenarios: summer runoff strongly decreases with simultaneously increasing spring runoff, indicating a shift from glacial/glacio-nival to nivo-glacial runoff regimes. While in the RCP2.6 scenario the month of peak runoff remains unchanged, in the RCP4.5 and RCP8.5 scenarios the peak gradually shifts from July towards June for all catchments, with the exception of Vernagtbach in the RCP4.5 scenario. For the Rofenache, Gepatschalm, and Pitze catchments, this shift already occurs in the period

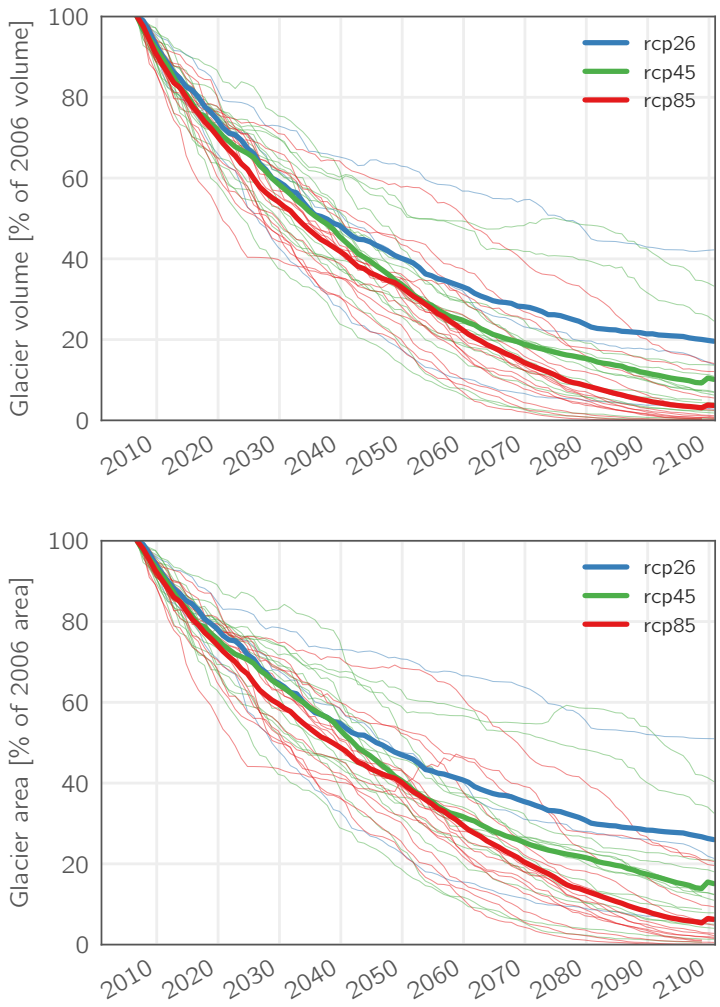

Figure 6.11: Simulated total glacier volume (top) and area (bottom, both shown as changes relative to the year 2006) for all glaciers in the study area and all 31 available climate scenarios. Thin lines indicate individual model results, thick lines show the multi-model mean. The small spikes in the multi-model means for RCP4.5 and RCP8.5 at the very end of the century are due to the fact that three models could only be run until 2098.

.

2041–2070 in both scenarios. Only for Vernagtbach, the most glacierized catchment, in the RCP8.5 scenario the shift occurs only towards the end of the century. Monthly peak runoff slightly increases for the Pitze catchment in the period 2011–2040, however total annual runoff volumes stay approximately constant due to lower August runoff volumes. In the other three catchments, both monthly peak runoff and total annual runoff volumes do not exceed the levels simulated for the historical period in all scenarios. With regard to ice runoff (dashed lines), Gepatschalm is the only catchment where ice runoff does not decrease monotonically over time, but rather increases

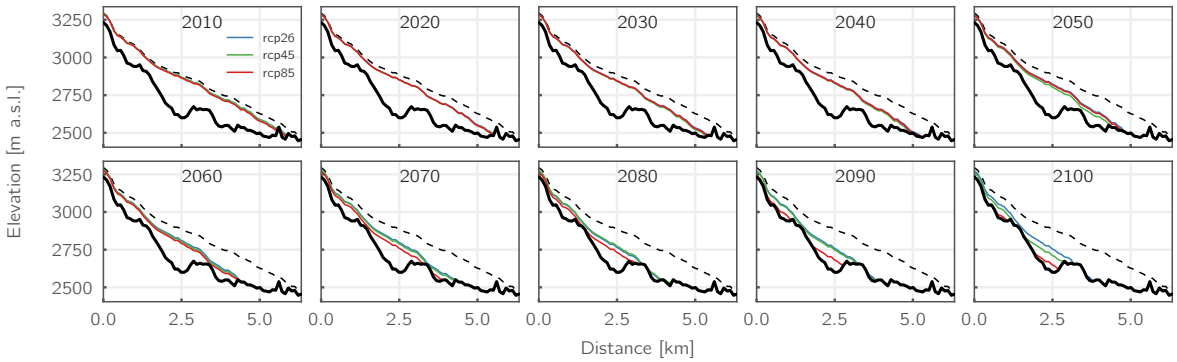

Figure 6.12: Bedrock topography (thick black lines) and simulated glacier thickness (thin colored lines) along the centerline of Hintereisferner as simulated for a single GCM-RCM combination (REMO2009 driven by MPI-ESM-LR) and the three RCPs, shown in 10-year intervals. Dashed black lines indicate the initial ice thickness as of the year 1997.

in the period 2041–2070 compared to 2011–2040 before it strongly decreases towards the end of the century.

A more detailed analysis of the changes in monthly runoff is shown in fig. 6.16, where the average monthly changes in runoff relative to the historical period 1998–2013 for the catchments in the study region throughout the 21st century are displayed. With respect to the different emission scenarios, again the differences between them are very small within the first considered period (2011–2040). In this period, also no clear trend of changes in the seasonality of the runoff regimes can be discerned, apart for slight increases during the winter months and slight decreases during summer. In the following period, 2041–2071, a clearer pattern begins to emerge. While May to June runoff stays approximately unchanged, runoff strongly decreases during August and September in all three scenarios, amounting to up to –55 %. From October to November, a transition period between decreasing and increasing runoff occurs, while during winter and spring increases of up to 50–125 % (depending on emission scenario) are projected (although still amounting to very small absolute values in comparison to summer as can be seen in fig. 6.15). During the last part of the century (2071–2100), summer runoff continues to decrease, although not as strongly as between the first two periods. Winter runoff also increases, most notably for the RCP8.5 scenario, where November to March runoff is at least approximately doubled for all catchments compared to the reference period. In this period, also different catchment characteristics can be more clearly distinguished. The largest changes are simulated for Vernagtbach, the smallest, highest-elevated, and (initially) most glacierized catchment. Here, increases between 43 % and 225 % for November to May runoff

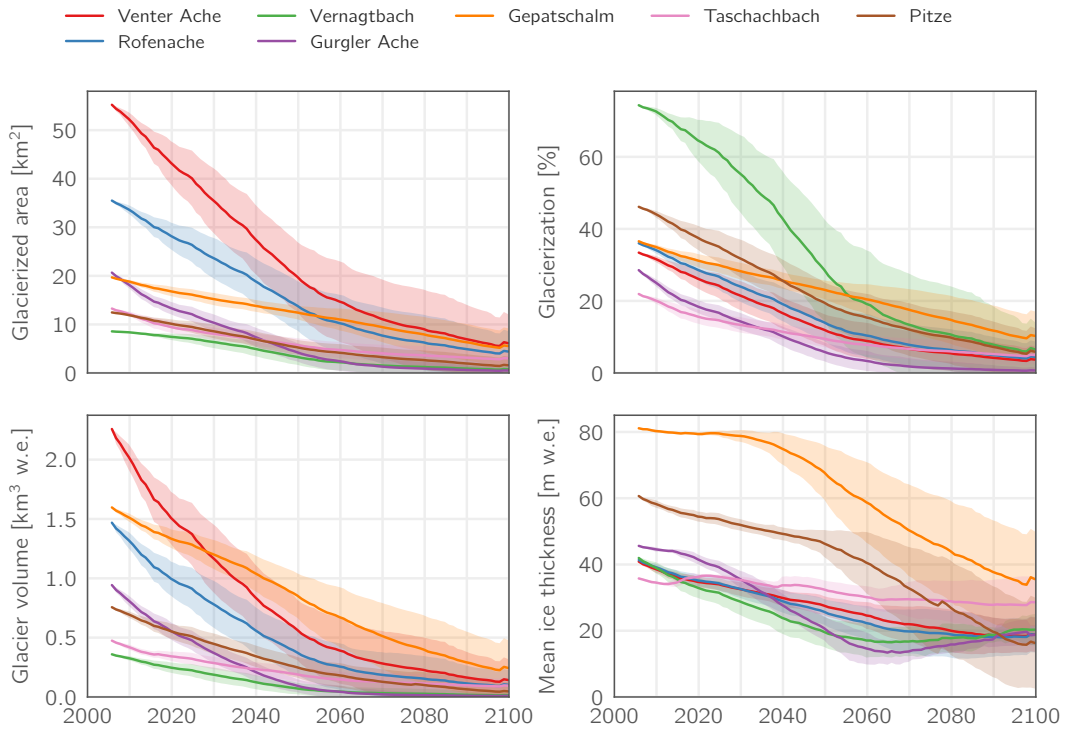

Figure 6.13: Evolution of the absolute (top left) and relative (top right) glacierized area for each catchment in the RCP4.5 scenario, as well as the absolute glacier volume (bottom left) and the mean ice thickness (bottom right). Note that the latter is calculated only over the glacierized fraction of the catchment and not the entire catchment area (i. e., it is the result of dividing the bottom left plot by the top left plot). Lines and shadings represent multi-model means ± one standard deviation.

are simulated for the RCP8.5 scenario, while the corresponding runoff decreases by 70–75 % during August and September due to the by then almost completely melted glacier (Vernagtferner). However, while in the figure the relative (positive) changes during winter appear similar or larger than the (negative) changes during summer for all catchments, it has to be emphasized that this still corresponds to a strong relative decrease in total annual runoff considering the respective absolute values (for example as seen in fig. 6.15, the absolute JJA runoff volumes are approx. 2 orders of magnitude larger than the respective DJF values).

The simulated future streamflow composition of the components ice melt, snowmelt and rainfall at the end of the scenario period (2071–2100) is shown in fig. 6.17. While the ice melt fractions at the end of the century are negligible for all but the most glacierized catchments, snowmelt is still the major contributor to total runoff for all seasons. Rainfall runoff contributions are comparatively low in general, which is however partly due to the model structure – as rain falling on snow contributes to the

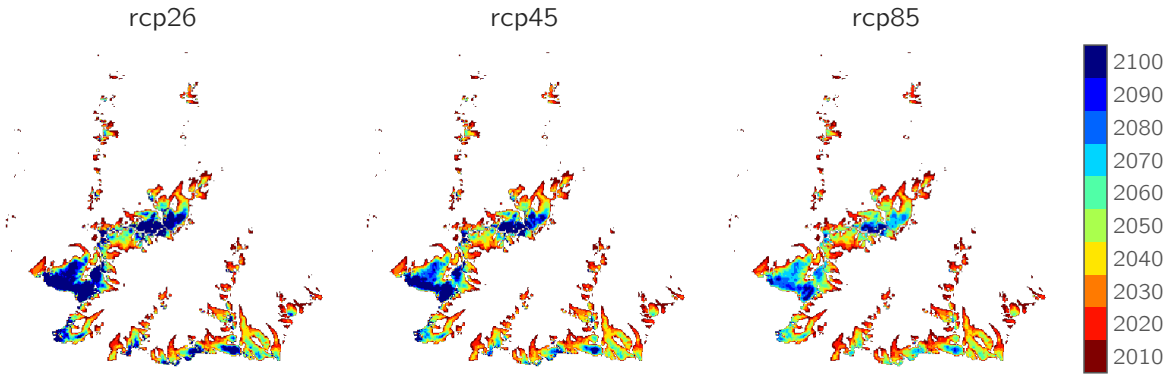

Figure 6.14: Spatially distributed simulated glacier coverage (multi-model mean) shown in 10-year intervals for the three RCPs.

liquid water storage of the snowpack up to a certain amount, these rainfall amounts are part of the snowmelt contribution in the runoff concentration scheme. Only rain falling on bare ground, ice, firn or already saturated snow is part of the rainfall runoff contribution in this case.

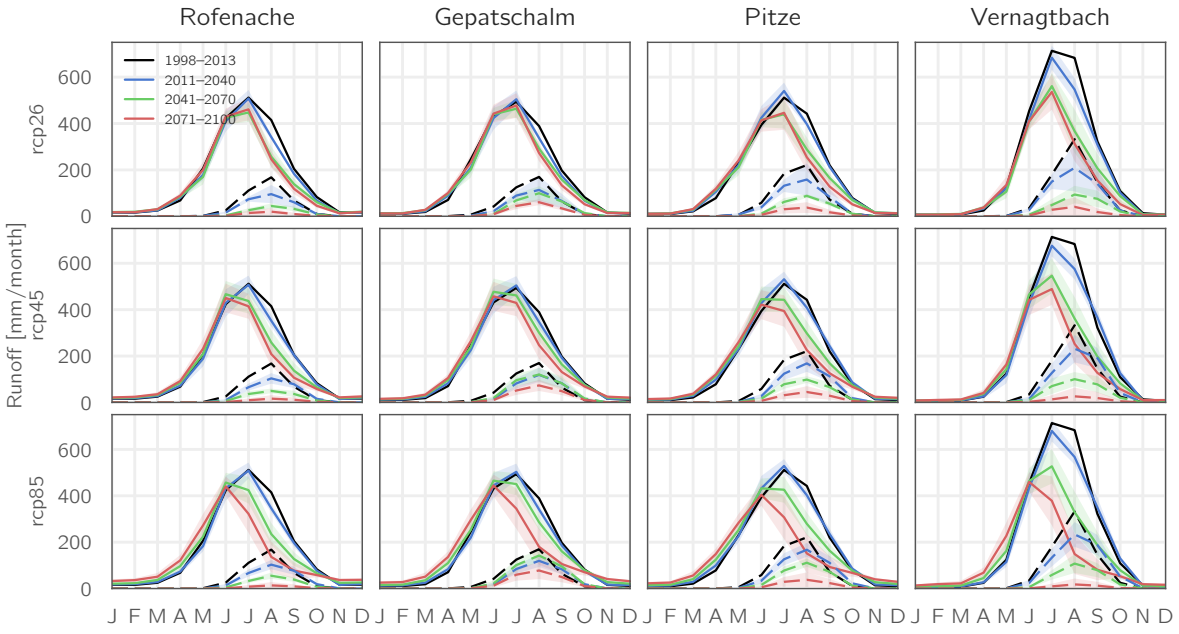

Figure 6.15: Average monthly runoff (multi-model mean $\pm$ one standard deviation indicated as shaded bands) as simulated for the early, middle, and late 21st century for four catchments and the three emission scenarios. Dashed lines indicate bare ice melt runoff.

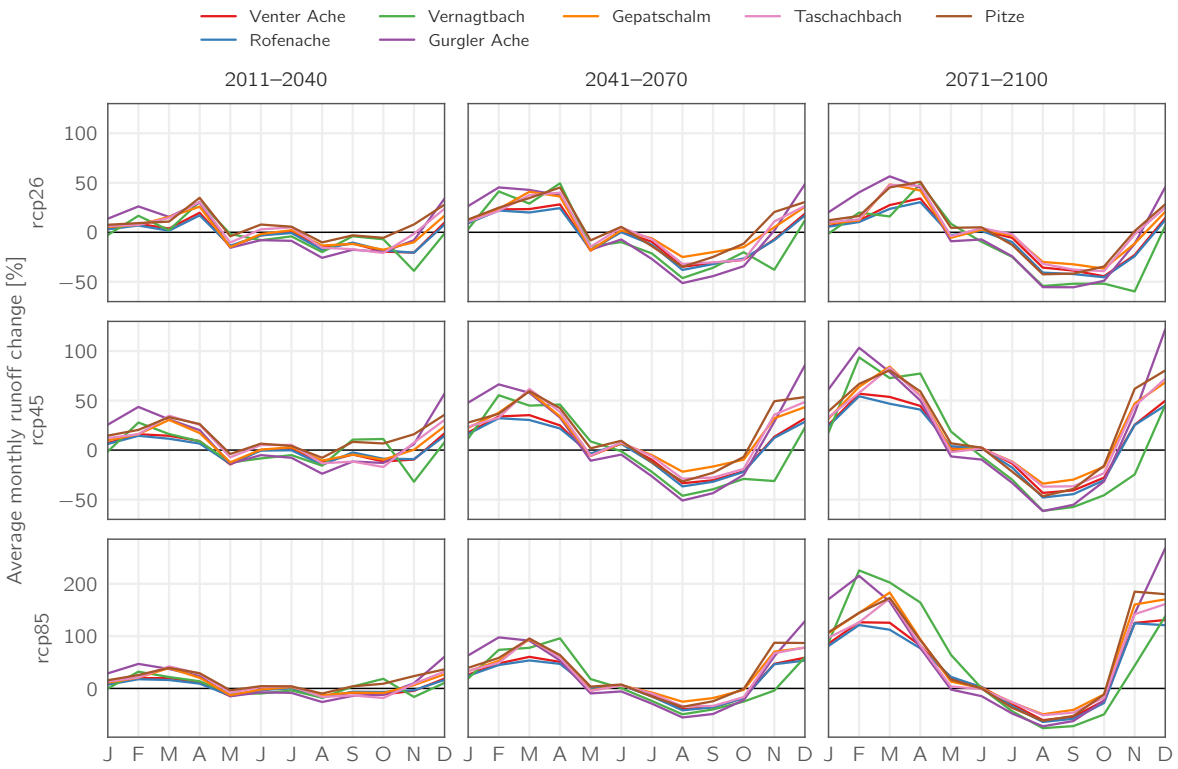

Figure 6.16: Average changes in monthly runoff relative to the historical period 1998–2013 over the course of the 21st century for the study catchments as simulated for the three emission scenarios (lines are multi-model means; note the differently scaled y-axes for RCP8.5).

6.4.5 Uncertainty

Huss et al. (2014) assessed the influence of various model assumptions in projections of glacier evolution and runoff in high-mountain catchments. Their results indicate that major uncertainty sources are especially (i) the winter snow accumulation in terms of both volume and spatial distribution, (ii) the approach to account for glacier geometry changes, (iii) the initial glacier ice volume distribution, and (iv) the individual climate projections.

While the model has shown to capture (i) the amount and distribution of winter snow accumulation well for the study area in a recent study (Hanzer et al., 2016), the model setup was slightly altered for the present study. The most substantial changes result from the requirement of a sufficiently long historical measurement period of the meteorological stations. As a consequence of this, only a subset of the stations utilized in the aforementioned study could be used, and from these stations only daily instead of hourly recordings were available, requiring an additional processing step in terms

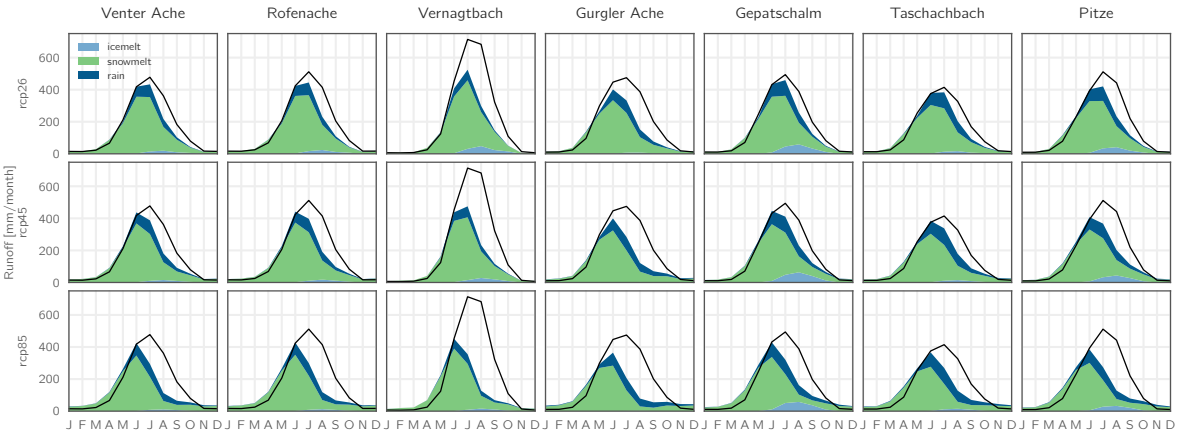

Figure 6.17: Average monthly runoff and composition (multi-model mean) for the period 2071–2100. The black lines show the average runoff in the historical period 1997–2013.

of temporal disaggregation. In addition, at several of these stations the daily and (sub-)hourly measurements are performed with different instruments, resulting in considerable differences in the recorded meteorological variables as illustrated in fig. 6.18 for three stations. Especially the latter impacted model performance, resulting in a tendency to slightly overestimate winter snow accumulation and spring runoff volumes. Reducing the spatial and temporal model resolution from 50 m and 1 h to 100 m and 3 h on the other hand only resulted in minor impacts on model performance. Figure 6.19 shows the average observed monthly runoff for the seven study catchments and the period 1998–2006, as well as the corresponding simulation results for the 50 m/1 h run using original hourly meteorological recordings and the 100 m/3 h run using disaggregated daily data, highlighting the tendency to overestimate runoff particularly during spring for the latter run. Table 6.3 shows the corresponding skill scores derived from these two simulation runs: NSE, the benchmark efficiency (BE) (Schaefli and Gupta, 2007), and the percent bias (PBIAS). However, as for the scenario simulations mainly changes rather than absolute values are analyzed, these partial model biases likely do not affect the main conclusions of our study.

Overestimations of winter snow accumulation and, subsequently, glacier mass balances might partly also have consequences for (ii) the approach to account for glacier geometry changes. The Δh parameterization as implemented is able to account only for conditions of glacier retreat, while in case of positive mass balances no update of the glacier extents is performed. As fig. 6.20 shows, 14–24 % of all simulated specific mass balances are positive in our simulations. However, as in previous studies the Δh parameterization performed significantly better than alternative approaches such as

accumulation area ratio-based methods and similarly well as complex ice flow models (Huss et al., 2010), we believe that this approach is an adequate tradeoff for the application on the regional scale where the application of of process-based ice flow models is not feasible.

We also assessed the influence of (iii) the initial glacier volume distribution by scaling the original initial ice thickness distribution by factors of 0.7 and 1.3, respectively (i. e., 30 % decrease/increase) and re-running the entire set of RCP4.5 simulations. However, as fig. 6.21 (b–c) exemplarily shows for selected catchments, this does not significantly change the model results with regard to the evolution of glaciers and runoff volume. Similar results are obtained also for all other catchments.

With regard to (iv), many studies (e. g., Addor et al., 2014; Bosshard et al., 2013; Horton et al., 2006; Huss et al., 2014) have shown that the largest uncertainty in hydrological impact studies usually is due to the chosen climate models, and that the spread between individual climate model simulations is often larger than the spread between different emission scenarios within a single climate model. In the case of GCM-RCM chains, GCMs tend to have a larger impact on the hydrological model results than the RCMs. We addressed these uncertainties by utilizing the entire range of available EURO-CORDEX simulations, resulting in a total of 14 GCM-RCM chains with five different GCMs (each driving 2–4 RCMs) and six different RCMs for the RCP4.5 and RCP8.5 scenarios. The results for the RCP2.6 scenario have to be interpreted with care, as for this scenario only three GCM-RCM combinations (using two different GCMs) were available. Hence, especially when looking at multi-model averages, the RCP2.6 results are not directly comparable to the other two scenarios.

Besides the climate models themselves, also the spatial and temporal downscaling approaches from the coarse daily-resolution grids to the 3-hourly resolution point-scale time series add an uncertainty component to the results, as they are statistically derived from past conditions for which it is uncertain if they will persist in the future.

The influence of the climate models on the hydrological results is illustrated in fig. 6.21 (a). Here, average monthly runoff for the period 2071–2100 as simulated by all 31 individual GCM-RCM realizations is shown exemplarily for the Pitze catchment. While the influence of the emission scenarios is visible to a part, there is significant overlap between the realizations of the different emission scenarios. For example, the realizations resulting in both the lowest and the highest August streamflow volumes are both driven by the RCP8.5 scenario. Similar results were already shown for the simulated glacier volume and area in fig. 6.11.

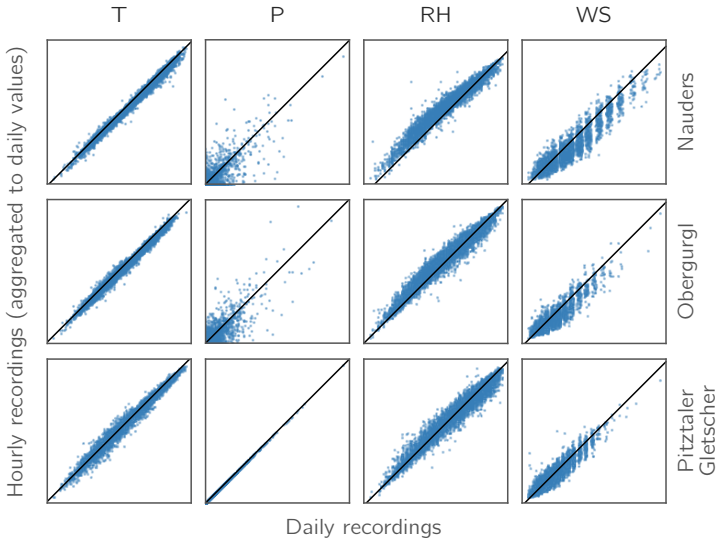

Figure 6.18: Scatter plots of daily vs. aggregated hourly recordings of air temperature (T), precipitation (P), relative humidity (RH), and wind speed (WS) for three stations in the study area.

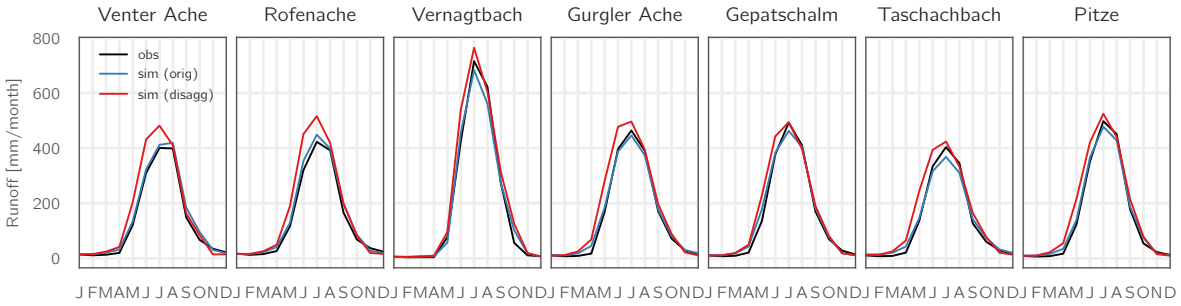

Figure 6.19: Seasonal cycle of observed (black lines) and simulated monthly runoff for the study catchments and the period 1998–2006. Blue lines correspond to the simulation results for the "reference run" (50 m spatial resolution, 1 h temporal resolution, original hourly meteorological data as forcing), while the red lines correspond to the simulation run using 100 m spatial and 3 h temporal resolution as well as disaggregated daily data as forcing.

6.5 Conclusions

In this study, we have forced a fully distributed physically based hydroclimatological model with the most state-of-the-art climate projections available. This is the most detailed study on cryospheric-hydrological climate change impacts in the Ötztal Alps to date, and to our knowledge also in high-elevation glacierized catchments in Austria in general.

While some uncertainty in the results is due to the model configuration, the largest

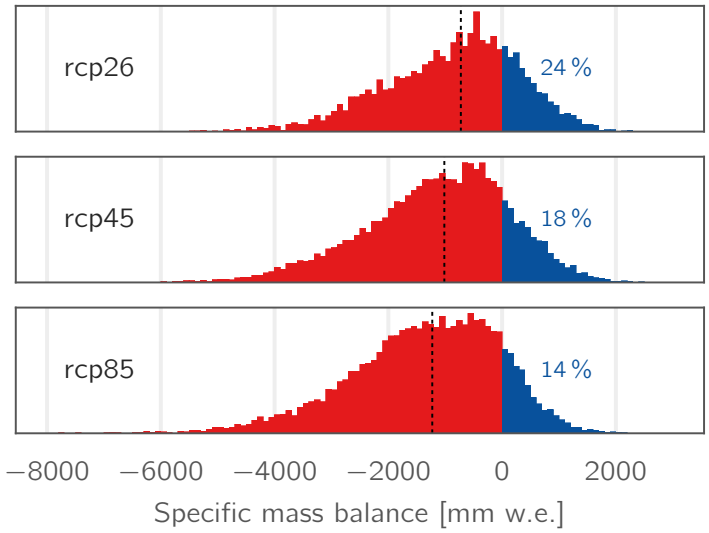

Figure 6.20: Histograms of the specific mass balance values as simulated for all (initially) 206 study area glaciers, all simulation years (2006–2100), and all GCM-RCM combinations. Dashed vertical lines refer to the median mass balance, and percentages indicate the total fractions of positive mass balances.

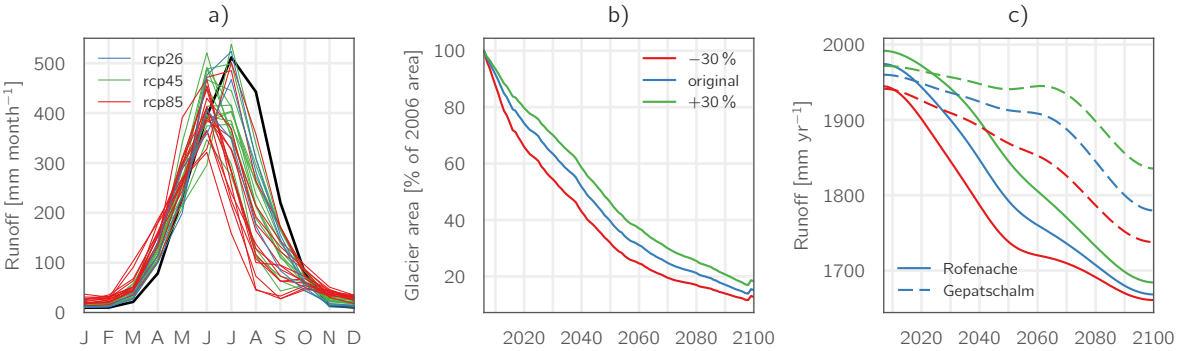

Figure 6.21: a) Average monthly runoff (period 2071–2100) for the Pitze catchment as simulated for all 31 individual GCM-RCM realizations, b) evolution of the total glacierized area for the entire Ötztal Alps study site as simulated by altering the initial ice thickness distribution by $\pm 30\,\%$ (multi-model mean values for the RCP4.5 scenario), and c) corresponding runoff evolution (10-year Gaussian low-pass filtered) for the Rofenache and Gepatschalm catchments.

uncertainty can be traced back to the climate projections. This leads to a considerable range in the projected snow coverage, glacier extents and hydrological regimes. However, some common results can be found for all model runs. Snow cover is projected to decrease, however not as dramatic as presented in some other studies for Alpine regions due to the high elevation of the study site and strongly increasing winter precipitation, which partly compensates for the increased warming. Glaciers

Table 6.3: NSE, BE, and PBIAS of observed vs. simulated runoff in the period 1998–2006 for the model runs using original hourly meteorological data and disaggregated daily data, respectively.

		Original			Disaggregated		
ID	Catchment	NSE	BE	PBIAS [%]	NSE	BE	PBIAS [%]
1	Venter Ache	0.92	0.60	8.71	0.79	−0.09	21.44
2	Rofenache	0.93	0.70	8.27	0.78	0.12	23.54
3	Vernagtbach	0.92	0.70	−1.12	0.88	0.57	13.19
4	Gurgler Ache	0.91	0.59	1.96	0.83	0.22	18.87
5	Gepatschalm	0.94	0.68	3.09	0.88	0.41	11.95
6	Taschachbach	0.92	0.54	0.01	0.84	0.08	19.19
7	Pitze	0.94	0.72	2.30	0.88	0.45	16.46

will continue to recede strongly throughout the century, and by 2100 most glaciers in the Ötztal Alps might have disappeared (depending on the considered emission scenario). Resulting total glacierized area and glacier volume will likely amount to less than a quarter of today's state even for the RCP2.6 scenario. Consequently, glacier runoff will diminish proportionally and summer runoff will strongly decrease in all investigated catchments, resulting in a shift of the annual runoff peak from July towards June. Winter runoff volumes will increase, however to still low absolute values. While the total annual runoff volumes stay approximately constant during the early 21st century compared to present-day levels, they gradually decrease throughout the rest of the century. Only for some catchments and scenarios runoff volumes slightly exceed present-day levels, indicating that the peak water period of maximum runoff is currently under way or has already passed.

Acknowledgements

This work was carried out within the framework of the projects "W01 MUSICALS II – Multiscale Snow/Ice Melt Discharge Simulation into Alpine Reservoirs", carried out in the research programme of alpS – Centre for Climate Change Adaptation in Innsbruck, and "HydroGeM3", financed by the Austrian Academy of Sciences. The computational results presented have been achieved in part using the Vienna Scientific Cluster (VSC). The authors want to thank the COMET research programme of the Austrian Research Promotion Agency (FFG), the TIWAG – Tiroler Wasserkraft AG, and the Austrian Academy of Sciences. Meteorological and hydrological data were provided by the Zentralanstalt für Meteorologie und Geodynamik (ZAMG), the Hydrographic Service of Tyrol, the TIWAG – Tiroler Wasserkraft AG, the Commission for Glaciology of the Bavarian Academy of Sciences and Humanities, and the Autonomous Province of Bozen/Bolzano. We also would like to thank Matthias Huttenlau for managing the MUSICALS II project and many helpful discussions, and Johannes Schöber for valuable comments during the preparation of the manuscript.

Chapter 7

Conclusions and outlook

7.1 Conclusions

In this thesis, an integrative assessment of current and future snow and ice water resources stored in the mountain cryosphere of two regions in the Austrian Alps was performed by applying the hydroclimatological model AMUNDSEN for the simulation of the mass and energy fluxes, while the coupled component modeling framework with the interface tools variables, indicators, and thresholds as presented in chapter 2 enabled the linkages of the quantitative model calculations to the socioeconomic systems winter tourism and hydropower generation.

Especially the winter tourism case studies in chapters 3 and 4 made heavy use of these interface tools. In chapter 3, AMUNDSEN was applied to simulate future snow conditions in the Schladming region until 2050. While these simulations were performed for both natural snow conditions only and the additional consideration of snowmaking, the latter was accounted for using a pragmatic bulk approach without considering limited water availability and detailed infrastructure data. The results show a general shortening of the (natural) snow cover period in the region of up to approx. one month until 2050, however – in contrast to recent studies by, e. g., Klein et al. (2016) and Marty et al. (2017), which show a significantly larger shift of the end of the season compared to the start – no clear signal could be detected on whether the shortening tends to occur at the beginning or the end of the winter season. The ski

season length is projected to decrease on average by approx. 20 days (with the largest decreases in medium elevations) regardless if snowmaking is performed or not, however snowmaking increases the natural ski season length by approx. 80 days. Based on these results, in a follow-up study (Damm et al., 2014) a cost-revenue analysis of snowmaking until 2050 was performed, showing that the future profitability of skiing operations in the area to a large extent depends on future electricity costs, which are however challenging to predict.

In the light of the tradeoffs inherent in the pragmatic snowmaking approach, in chapter 4 an entirely new snowmaking module was developed, allowing for a much more comprehensive treatment of snowmaking operations. The explicit consideration of individual snow guns and the ski area infrastructure allows for an in-depth simulation of snowmaking operations by tailoring the model parameters for a specific ski area. The results demonstrate that the coupled system is able to accurately reproduce real-world ski area management and snowmaking operations under the premise that the detailed technical infrastructure and a comparatively simple set of management rules is provided to the system. In addition, the analysis of the simulated "ski season length" indicator shows that, despite its simplicity, this indicator very well replicates the actual season length at least for the considered ski area.

In chapters 5 and 6, the model system was applied for the simulation of hydropower potential in the glacierized catchments of the Ötztal Alps. In chapter 5, the multilevel validation concept was introduced and applied to the study site. This concept builds on using multiple data sets for model validation to formalize and visualize the scales of the observations with respect to the model simulations. The method represents a generic concept that might be applicable for environmental modeling in general, allowing an independent, complete, and fully redundant validation procedure for the simulated key variables in a model. The results of the validation procedure using a multitude of available validation data sets demonstrate the high overall model performance in the historical simulations. Subsequently, in the last study, chapter 6, the results of a comprehensive analysis of climate change impacts on the snow and ice water resources and hydrology of the study region until 2100 were presented. The results indicate considerable decreases of snow amounts until the end of the century in elevations below 2500 m a.s.l. especially for the RCP4.5 and RCP8.5 scenarios, whereas only in the highest elevated parts of the study region snow amounts are projected to stay approximately stable. Accompanied by further receding glaciers (leaving only 4–20 % of total ice volume left by 2100), this development will lead to strongly decreasing summer runoff in the investigated catchments and shifts of the annual runoff peak.

For the hydropower related investigations, no explicit human interactions (e. g., in terms of reservoir management) were considered, partly because no such management practices were publicly available, which is a common challenge in transdisciplinary research (as discussed in section 2.2 with regard to the communicative, social, and cognitive dimensions of integration). However, the simulated future runoff evolution and seasonality as an indicator for hydropower potential is a valuable basis for future hydropower management and planning in the area.

7.2 Outlook

In this final section, first a selection of potential improvements of the existing methodology as applied in the thesis is presented, mainly concerning disciplinary process representations within the AMUNDSEN model. Subsequently, a a broader discussion with respect to the conceptual framework of coupled component modeling is given, suggesting the definition of a new interface tool and highlighting promising future research paths with regard to both spatial and temporal modeling scales inherent in environmental models.

7.2.1 Potential disciplinary advancements

Downscaling

In hydrological climate change impact studies, usually the raw GCM or RCM data cannot be utilized directly, but rather some sort of bias correction needs to be applied (see also section 6.3.3). For the impact studies presented in this thesis (chapters 3 and 6), RCM data was statistically downscaled to station locations and bias corrected using a quantile mapping approach. While quantile mapping and other statistical bias correction methods are widely applied in impact studies due to their simplicity and low computational demands compared to dynamical downscaling methods, a major drawback of these methods is that they usually rely on the assumption of stationarity of the biases. Several studies have shown that this assumption can lead to significant alterations of the raw climate change signal (e. g., Christensen et al., 2008; Maraun, 2012; Maurer and Pierce, 2014). In addition, when applied for downscaling from the grid box scale to the local scale, quantile mapping can to lead to effects such as overestimated areal precipitation means due to misrepresented spatial variability (Maraun, 2013). Recent developments of statistical bias correction methods that attempt to address these issues (e. g., Cannon et al., 2015; Haerter et al., 2015; Sunyer et al., 2015; Volosciuk et al., 2017) might further increase the reliability and robustness of future

impact studies. Going beyond statistical downscaling, novel quasi-dynamical downscaling methods such as the Intermediate Complexity Atmospheric Research (ICAR) model (Gutmann et al., 2016) show high potential. ICAR has shown to produce similar results as traditional numerical weather prediction models such as WRF (Skamarock and Klemp, 2008) in some applications, while reducing the required computational resources by more than two orders of magnitude (Gutmann et al., 2016). Hence, in the future the application of such approaches including many climate model runs might also be feasible for impact studies. Generally, it is increasingly recognized that attention should be given on fostering collaboration between the providers and users (e. g., impact modelers) of regional climate change scenarios in order to gain a common understanding of the potential, but also the uncertainties and limitations inherent in these data (e. g., Maraun et al., 2015).

Detailed snow production simulations

In chapter 4, the detailed snowmaking simulation module was developed. Although it accurately reproduced real-world snowmaking operations for a single ski area, an application besides this case study is yet missing. While an application of the model setup as-is for a climate change impact study might not generate vastly different results than those obtained with the simple bulk approach (chapter 3), the real potential of the detailed approach could unfold when assessing the effects of different management options under climate change conditions. For example, one could analyze the effects of upgrading the snowmaking infrastructure in terms of pumping capacity, reservoir volume, or snow gun quantity, or of altered snowmaking potential due to technological advancements or legislative changes (e. g., allowing the use of snow inducers). While this is envisaged to be part of a future research project, another application of the module will also occur as part of the upcoming Horizon 2020 PROSNOW project, where short- to long-range meteorological forecasts with lead times from a few days to several months will be utilized to forecast snow conditions (natural and technical) for several pilot ski areas in the European Alps.

Snowpack layering and energy transfer

As outlined in section 1.2, in the wide range of existing snow models, one method to classify them is according to their complexity. One important distinction is if they use simplified approaches for calculating snowmelt such as temperature index or enhanced temperature index approaches, or if they – such as AMUNDSEN – solve the full energy balance of the snow surface. Another distinction can be made based on

the representation of the internal snowpack structure, i. e., if – such as AMUNDSEN in its original form – the snowpack is treated as a single bulk layer, or a vertical subdivision of the snowpack is performed. While AMUNDSEN now allows to account for four layers (new snow, old snow, firn, and ice), these are mainly used to keep track of snow accumulation, calculation of densification, and to calculate catchment runoff using the implemented linear reservoir approach, however no exchange of energy takes place between the layers and solving the energy balance is still performed in a bulk approach. One underlying assumption of this approach is that the near-surface air temperature is never negative in the case of surface melt. The robustness of this empirical assumption has been confirmed by several measurement campaigns (Weber, 2005) – exceptions only occur in rare cases such as for highly positive radiation balances, which are however largely negligible for water balance simulations due to the low melt rates generated by such events. However, one next step in improving the representation of snow processes in AMUNDSEN which would allow a consistent tracking of state variables between snow layers could be implementing a layered snowpack scheme allowing for temperature variations within the snowpack and mass and energy fluxes between layers. Models of this type have shown to perform better than simple bulk models and comparable to more complex multilayer models (Koivusalo et al., 2001). As a first step in this direction, a loose coupling of AMUNDSEN and the Factorial Snowpack Model (FSM, Essery (2015)) has recently been established (Günther et al., 2017). Future work will focus on extending this towards a fully bidirectionally coupled system allowing a consistent tracking of state variables.

Wind-induced snow transport

The snow redistribution parameterization based on topographic openness (section 5.3.3) as applied in chapters 5 and 6 has shown high skill in reproducing snow distribution patterns for the Ötztal Alps study area. However, similar as for other terrain-based snow redistribution parameterizations (e. g., Farinotti et al., 2010; Schöber et al., 2014; Warscher et al., 2013; Winstral et al., 2002), the applied parameters (eqs. 5.8–5.10) are site-specific and not generally transferable to other regions. Besides, similar as for other terrain-based redistribution parameterizations (e. g., Grünewald et al., 2013), redistribution based on topographic openness alone might not be sufficient for the application in larger regions with high altitudinal variations, as it has shown to lead to overestimated snow accumulation in low-elevated valley regions. For such applications, additional factors such as elevation or vegetation might have to be taken

into account for deriving the snow redistribution fields. In addition, future work on the openness-based redistribution should focus on a systematic analysis of the optimal spatial scales (the L values) that should be used for deriving the openness fields as well as evaluating the transferability of the derived parameterizations for regions lacking sufficient validation data sets such as ALS measurements. While for water balance simulations the application of simple terrain-based parameterizations such as the one used here is still justified, an explicit simulation of snow transport processes (such as, e. g., in Bernhardt et al., 2010; Liston et al., 2007; Sauter et al., 2013; Schneiderbauer and Prokop, 2011; Vionnet et al., 2013) should ideally be preferred over only implicitly considering these processes. This however requires the provision of local wind fields, which are highly scale dependent (see also the discussion on scales in the following section 7.2.2.2).

Hydrological process representation

AMUNDSEN as originally developed focused on the distributed simulation of snow-hydrological processes in high mountain regions: interpolation of meteorological point measurements under consideration of the complex topography, simulation of snow accumulation as well as lateral processes that shape the snow cover in mountainous regions, and generation of snowmelt. While in recent versions a module for the simulation of catchment runoff has been added to the model (section 5.3.5), it has to be emphasized that the application of this approach as originally developed by Asztalos et al. (2007) is limited to smaller, glacierized catchments, where for example soil and groundwater related processes can be approximated using rather simple parameterizations. In regions where hydrological processes that are not adequately captured by the model are dominant, it should be coupled with an appropriate streamflow generation and propagation model.

7.2.2 Advancements in coupled component modeling

7.2.2.1 *System state update* as a new interface tool

In chapter 2, the interface tools of the here developed methodological concept of coupled component modeling were defined: variables, indicators, and thresholds. They are used to enable the combination of model components, as well as to transmit information of various kinds across them and and to transform quantitative information into qualities and vice versa. These three interface tools were sufficient to describe the coupled component models for the winter tourism case studies in chapters 3 and 4.

During the work on the glaciohydrological impact studies in chapters 5 and especially 6, it however was recognized that one interface tool was missing for these types of coupled systems. This new interface tool, which could be called *system state update*, is utilized whenever internal system states of a coupled component model are replaced by the output of another model component. Hence, similar to variables, system state updates comprise quantitative information passed from one model component to another, however in this case the information flow is not continuous, i. e., the temporal resolution in the two model components is different.

The specific example of system state update applied in the hydropower-related studies is the glacier geometry update as described in section 6.3.2. In this implementation, during each glaciological year the surface elevation of the model glaciers is changed solely depending on their surface mass balance: the glaciers thicken in the parts where snowfall accumulates, and experience thinning in the parts where melt is occurring. As the process of ice flow is not explicitly considered in the model, the Δh parameterization is applied at the end of each glaciological year to empirically account for this effect. Only the total mass change for the entire glacier is passed to the geometry update function, which then applies the Δh function to the distributed glacier surface elevation from the end of the previous mass balance year – hence, the spatial distribution of surface elevation change as simulated during a given mass balance year is entirely neglected. Consequently, since glacier flow is not continuously updated, ice melt might be underestimated to a small degree as exposed glacier tongues might melt away "too early" and already ice-free zones might again be ice covered after the geometry update. This is however partly mitigated by the fact that the Δh parameterization is only applied to glacier surfaces above a certain thickness threshold whereas the glacier borders only change their thickness due to the surface mass balance change.

Other examples of system state updates commonly applied in hydrological modeling are land use changes in climate change impact studies, where prescribed land use maps are used to periodically update the land use information in the model (e. g., Dwarakish and Ganasri, 2015), or the "direct insertion" data assimilation method, where for example remotely sensed snow cover or albedo maps are used to modify the model system states (e. g., Rodell and Houser, 2004). These procedures usually introduce inconsistencies between state variables, which are however challenging to overcome (e. g., NASEM, 2016) and hence are frequently simply neglected in, e. g., operational forecasting systems.

A further generalization of this concept can be performed with respect to the tem-

poral discretization in which the system states are updated. A possible categorization of the discretization could be the trichotomy *periodic*, *episodic*, and *sporadic*. If the updates occur in regular intervals such as the annual glacier geometry updates, they can be considered periodic. Episodic updates on the other hand do not occur in regular intervals, however still frequently (e. g., data retrieved from satellite products which are however commonly cloud-covered), whereas sporadic updates refer to aperiodic updates which occur infrequently (e. g., in-situ measurements of albedo or snow depth in remote field locations). Of course, the distinction between frequently and infrequently is subjective and will vary between different applications.

To summarize, while system state updates are implicitly applied in chapter 6, the formal definition of this newly identified interface tool and its embedding in the interface design framework presented in chapter 2 is yet missing. This is however foreseen to be part of future work.

7.2.2.2 Linkages across scales

Environmental modeling is intimately linked with the concept of scales in both space and time. Blöschl and Sivapalan (1995) define three types of scales: (i) the process scale, i. e., the spatial or temporal scale on which an investigated process occurs, (ii) the observation scale, i. e., the scale on which a process is observed, and (iii) the modeling scale, i. e., the scale on which the respective process is simulated in a model. It is evident that ideally both the modeling and the observation scale should be equal or at least very close to the process scale. Not only because the temporal and spatial scales of important environmental processes range over many orders of magnitude (e. g., Blöschl and Sivapalan, 1995; Blöschl, 1999) this is obviously not feasible, however the question can be raised if the common "one size fits all" philosophy of many models, i. e., that all (or at least most) processes are simulated in the same resolution, must be taken for granted.

In many distributed models both the spatial and temporal model resolution are to some extent freely selectable, however fixed within a single model run. In the case of fully distributed models that are spatially discretized in a rectangular grid, this means that all processes that are explicitly resolved are calculated for the same predefined model elements (pixels), while some models additionally employ subgrid parameterizations to implicitly represent smaller-scale processes. In AMUNDSEN specifically, the spatial resolution is (from a technical point of view) not subject to any constraints, while the temporal resolution can be set to 1, 2, or 3 h. With even coarser temporal resolutions, the diurnal cycle of the meteorological variables could not be adequately

represented any more (Strasser, 2008). While some submodules such as the gravitational snow slides (called once a day) or the glacier geometry update (called once a year) are run with a different resolution than the 1–3-hourly model resolution, the spatial resolution is the same for all submodules.

Table 7.1: Spatial and temporal model resolutions applied in the AMUNDSEN simulations presented in this thesis.

Chapter	Spatial resolution	Temporal resolution
3	50 m	3 h
4	10 m	1 h
5	50 m	1 h
6	100 m	3 h

The choice of model resolution for a given simulation experiment usually depends on several factors such as the scales of the processes that have to be considered, but also on technical and practical considerations such as numerical stability, calculation time, memory usage, or storage requirements of the model outputs. Table 7.1 lists the spatial and temporal resolutions used in the AMUNDSEN simulations presented in the thesis. In most of these cases, an approximate limit of "maximum coarseness" in terms of model resolution can be identified at least qualitatively from the individual research questions. For example, the detailed snowmaking simulation approach presented in chapter 4 relies on an accurate representation of the ski slopes with respect to the model grid. As no subgrid parameterizations are used, a model pixel can either be part of a slope or not. A too coarse model resolution would hence introduce sampling artifacts and lead to misrepresentations of the total slope area in the model, which is however crucial for accurately distributing the produced technical snow. Likewise, for an accurate assessment of snowmaking conditions (i. e., wet-bulb temperature) a temporal resolution of 3 h could be too coarse, as otherwise shorter time windows with adequate snowmaking conditions could be missed. Similar considerations can be made for the glaciohydrological investigations in chapters 5 and 6. For one, it is well known that the choice of spatial resolution is crucial for an adequate representation of catchment areas and flow paths in hydrological models (e. g., Strasser, 1998; Zhang and Montgomery, 1994). In addition, an adequate representation of glaciers and glacier areas imposes an upper limit on spatial model resolution similar to the ski slopes in chapter 4. As many small glaciers are located in the Ötztal Alps study area, a too coarse spatial resolution would impact for example the investigations of the evolution of glacierized area in chapter 6.

However, such scale constraints often concern only individual processes within a

given application, whereas many other processes could very well be modeled in other resolutions. Much potential could hence lie in providing structured generic frameworks which allow specific model components to simulate each process in its individual scale. For example, snow transport processes or radiation modeling could be performed at very high spatial resolutions, while for other processes such as temperature interpolation or evapotranspiration coarser resolutions could be sufficient. Similarly, some processes such as radiation modeling or the parameterization of turbulent fluxes might require high (e. g., sub-hourly) temporal resolutions to better capture phenomena such as clouds or wind gusts, whereas others such as land use changes or glacier geometry updates could be modeled in (multi-)annual scales. This would require on the one hand interconnecting the individual process modules with appropriate up- and downscaling (i. e., aggregation or disaggregation) schemes, and on the other hand defining criteria to decide which scale is appropriate for a given process. While existing frameworks such as DANUBIA (Barth et al., 2004) or CRHM (Pomeroy et al., 2007) partly already allow such flexible process interconnections, these criteria have not yet been systematically investigated. In the following, an exemplary application based on the Ötztal Alps AMUNDSEN model setup is presented attempting to define such criteria based on available validation data sets.

While by means of the validation concept developed in chapter 5 the observation scales of the utilized validation data sets in terms of spatial and temporal support, spacing, and extent were investigated and related to the modeling scale on which they were simulated (i. e., the 50 m spatial and 1 h temporal resolution), no further discussion with regard to the modeling scale occurred. As the considerable calculation times for the scenario simulations until 2100 in chapter 6 required to adapt the spatial and temporal model resolution from 50 m and 1 h in chapter 5 to 100 m and 3 h in chapter 6 (resulting in a twelvefold speedup of simulation time), the question is raised how model performance is impacted by these changes.

In the light of these changes in model resolution as well as the fact that in chapter 6 not observed hourly meteorological data but rather disaggregated daily data was used, in the following the associated changes in model skill are investigated in detail. For this purpose, the same validation data sets as used in chapter 5 are utilized: (i) mean areal precipitation over the period 1997–2006, (ii) time series of point-based snow depth recordings at several locations, (iii-iv) multitemporal snow extent maps acquired from Landsat and MODIS imagery, (v) the snow accumulation distribution for the winter season 2010/11 acquired using airborne laser scanning surveys, (vi) glacier-averaged annual surface mass balances for three glaciers in the study area,

(vii) spatially distributed glacier surface elevation changes for the entire area over the period 1997–2006, and (viii) hourly runoff records for several subcatchments.

The results of this comparison are summarized in fig. 7.1. Each of the eight axes of this parallel coordinates plot represents a single skill measure for one AMUNDSEN model run:

1) the mean absolute percentage error (MAPE) between the simulated AMUNDSEN areal precipitation and the respective values derived by closure of the water balance for the 16 subcatchments shown in table 5.5,
2) the mean Nash-Sutcliffe efficiency (NSE) of observed vs. simulated snow depth for the stations Obergurgl (1938 m a.s.l.) and Pitztaler Gletscher (2864 m a.s.l.) in the period 1999–2013,
3) the mean value of the runoff skill score $\mathrm{NSE}_V = \mathrm{NSE} - 0.1|V_E|$ (Lindström, 1997), a combined value of NSE (calculated on daily values in this case) and the relative volume error V_E, for the seven subcatchments and the period 1998–2013,
4) the mean value of the spatially averaged accuracy (ACC), i. e., the fraction of correctly predicted snow-covered or snow-free pixels, obtained from comparing 733 MODIS snow cover images over the period 1997–2013 with the respective simulation results,
5) the same but derived from the validation against a total of 26 Landsat scenes in the same period,
6) the average mean absolute error (MAE) between annual observed and simulated mass balances of three glaciers (Hintereisferner, Kesselwandferner, and Vernagtferner) in the same period,
7) the MAE between observed and simulated spatially distributed glacier surface elevation changes over the period 1997–2006,
8) and the MAE between the ALS-derived observed and the respective simulated end-of-season snow distribution for the winter season 2010/11.

The ranges of the axes are scaled such that model skill decreases from top to bottom. While the choice of the skill functions is to some extent arbitrary, this plot type allows for a quick overview of the validation performance between individual model runs. In fig. 7.1, six individual model runs can be compared: (i) the model run using all available meteorological stations with 50 m spatial and 1 h temporal resolution (i. e., essentially the same results as presented in chapter 5 aside from the newly implemented glacier retreat parameterization), (ii) the same as (i) but with 3 h temporal resolution, (iii) the same as (i) but with 100 m spatial resolution, (iv) the same as (ii) but with 100 m spatial resolution, (v) a model run using the same stations, however whose

hourly recordings were first aggregated to daily data and subsequently disaggregated again to 3-hourly values (in the following termed *aggregated-and-disaggregated*) with MELODIST (Förster et al., 2016a) using the methodology described in section 6.3.4, also with 100 m spatial resolution, and (vi) a run where only the daily recordings of the stations with long-term coverage (cf. section 6.3.3) were disaggregated to hourly values, also with 100 m spatial and 3 h temporal resolution. In the following, the model results with respect to the eight efficiency criteria are discussed.

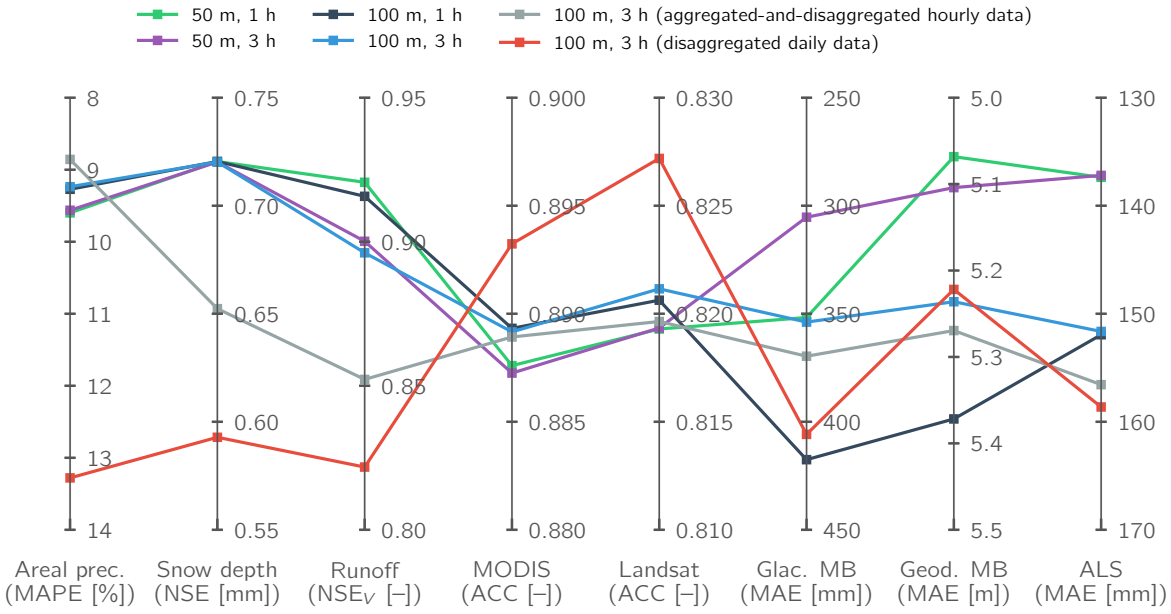

Figure 7.1: Comparison of the model skill for historical conditions when running the model using different combinations of temporal (1 and 3 h) and spatial (50 and 100 m) resolutions. The first four lines represent the runs where hourly meteorological recordings were used as forcing data, whereas the gray line corresponds to a run using aggregated-and-disaggregated hourly data (i. e., hourly → daily → 3-hourly), and the red line to a run using disaggregated daily data (i. e., daily → 3-hourly) for a reduced number of stations with partly different instrumentation.

1) With regard to the results for areal precipitation, all runs except for the one using disaggregated daily data show similar scores of MAPEs between 8.9 % and 9.6 %. The run with disaggregated daily data yields markedly higher deviations of 13.2 % on average due to overestimated precipitation amounts for several catchments.
2) For the point-based snow depth comparison, spatial resolution by design has no effect on the model results. However, also changing the temporal resolution from 1 h to 3 h does not change the model skill in this case, yielding an average NSE value of 0.72 for these runs (using the same meteorological input). Only

the different meteorological input data sets influence model skill in reproducing observed snow depths: aggregating-and-disaggregating the original input data results in average NSEs of 0.65, while using disaggregated daily data yields even lower values of 0.59.

3) With regard to the validation against runoff, temporal resolution in this case trumps spatial resolution: the 1-hourly runs both result in average NSE_V scores of 0.92, with only a very slight advantage of the 50 m run over the 100 m run, whereas the 3-hourly runs score slightly lower (0.90). Again, aggregating and disaggregating the meteorological data lowers model performance, resulting in a skill score of 0.85, while the run using disaggregated daily ranks last with a score of 0.82 due to the additional effects of the reduced number of stations and the differences in instrumentation at some stations, as discussed in section 6.4.5 (see also fig. 6.19 and table 6.3).

4–5) The validation against snow-covered area appears to be largely insensitive to changes in model configuration in this case, yielding a very small spread between the individual runs for both the MODIS and Landsat satellite products regardless of temporal and spatial resolution or forcing data. Similar results are also obtained when using skill scores other than ACC, for example the critical success index or the bias (cf. section 5.4.3.1), or when only considering the spring season for the analysis. Interestingly though, both for the MODIS and Landsat validation the run using disaggregated data here results in the highest scores, however only by margins of 0.004 and 0.007, respectively, hence conclusions from this result should be drawn with care given the possible range of this skill score (0–1).

6) With regard to the comparison of simulation results with annual glaciological mass balances for three glaciers in the study area, the results are not straightforward to interpret. The 50 m run with 3 h temporal resolution shows the highest skill in this case with an average MAE of 305 mm, while the 50 m/1 h and 100 m/3 h runs both result in scores of approx. 350 mm. Surprisingly, the 100 m/1 h run results in the lowest model skill here, while the runs using aggregated-and-disaggregated and disaggregated data are in between.

7) The 100 m/1 h run also ranks lowest in the validation against the long-term geodetic mass balance, however in this case the 50 m runs perform best, with MAEs of 5.07–5.10 m. Although not pictured in the validation comparison plot, the implementation of the glacier retreat parameterization (section 6.3.2) does not increase the model skill with regard to the simulation of glacier mass bal-

ances in this comparatively short time period – or, more specifically, the chosen skill score (MAE) is not increased. The spatial distribution of mass balances is in fact distinctly improved at least for the large glaciers in the study area, as exemplarily shown in fig. 6.3.

8) Finally, the validation against the ALS-derived snow distribution for the winter season 2010/11 results in a "natural" ranking of the individual runs: spatial resolution beats temporal resolution (both 50 m runs result in MAEs of 137 mm), while the runs using aggregated-and-disaggregated and disaggregated data rank lowest with MAE values of up to 159 mm.

To summarize, these results on the one hand again show the benefit of using multiple validation data sets for evaluating model performance. From this analysis, no clear "best resolution" can be discerned – in some cases (especially runoff), temporal resolution seems to be more important than spatial resolution, while it is the other way around in other cases, and for other cases as in the validation against glaciological mass balances, no correlation at all between model skill and spatial or temporal resolution can be discerned (at least when looking solely at these aggregated skill scores – in fact, model performance is obviously both spatially and temporally variable, which should also be taken in consideration). However, the results also show that disaggregation of daily meteorological time series still results in an acceptable glaciohydrological model skill. The run using disaggregated daily data performs worst in most cases, however this is not an effect of the disaggregation alone but a combination of disaggregation, a reduced number of available stations, and partial differences in the instrumentation of the stations. For the climate change impact analyses in chapter 6, the main conclusion that can be derived is that the reduced model resolution compared to the original model setup for historical conditions as in chapter 5 does not significantly impact model performance, but the largest differences are rather due to the changes in meteorological data.

While of course this analysis only has exemplary character and is far from a complete and systematic evaluation of modeling scales even when considering only the traditional single-resolution modeling paradigm, the results confirm that using different modeling scales for different processes could be beneficial and that promising scientific potential may lie in developing such modeling frameworks. As a first step in this direction, on a conceptual level the framework of coupled component modeling could be extended such that the interfaces between the coupled components should allow converting between spatial and temporal scales, both at the disciplinary and the cross-disciplinary interfaces. Temporal scale conversions here include the

above discussion on the "system state update" interface tool and the related temporal discretizations (section 7.2.2.1). The practical implementation of coupled component models following these guidelines will require the development of modular frameworks that include appropriate up- and downscaling routines which can be applied to convert between modeling scales during runtime. Finally and perhaps most importantly, criteria need to be defined in order to decide which modeling scale is most appropriate for a given process. Basing them on model skill measures such as in the above analyses is one possible option, however the choice of criteria likely will also depend on the individual research questions. Systematically validating the models and their coupled components using approaches such as the concept developed in section 5.4 might facilitate this process.

Bibliography

Abegg, B., Agrawala, S., Crick, F., and Montfalcon, A. de (2007). "Climate change impacts and adaptation in winter tourism". In: *Climate Change in the European Alps. Adapting Winter Tourism and Natural Hazards Management*. Ed. by S. Agrawala. Paris: OECD, pp. 25–60.

Abermann, J., Lambrecht, A., Fischer, A., and Kuhn, M. (2009). "Quantifying changes and trends in glacier area and volume in the Austrian Ötztal Alps (1969-1997-2006)". In: *The Cryosphere* 3.2, pp. 205–215. DOI: 10.5194/tc-3-205-2009.

Addor, N., Rössler, O., Köplin, N., Huss, M., Weingartner, R., and Seibert, J. (2014). "Robust changes and sources of uncertainty in the projected hydrological regimes of Swiss catchments". In: *Water Resources Research* 50.10, pp. 7541–7562. DOI: 10.1002/2014WR015549.

Allen, R. G., Pereira, L. S., Raes, D., and Smith, M. (1998). *Crop evapotranspiration - Guidelines for computing crop water requirements*. Tech. rep.

Anderson, E. A. (1976). *A point energy and mass balance model of a snow cover*. Tech. rep. NWS 19. NOAA.

Asztalos, J., Kirnbauer, R., Escher-Vetter, H., and Braun, L. (2007). "A distributed energy balance snowmelt model as a component of a flood forecasting system for the Inn river". In: *Alpine*Snow*Workshop*. Munich, pp. 9–17.

Bammer, G. (2013). *Disciplining Interdisciplinarity: Integration and Implementation Sciences for Researching Complex Real-world Problems*. ANU Press.

Barnett, T. P., Adam, J. C., and Lettenmaier, D. P. (2005). "Potential impacts of a warming climate on water availability in snow-dominated regions". In: *Nature* 438.7066, pp. 303–309. DOI: 10.1038/nature04141.

Barth, M., Hennicker, R., Kraus, A., and Ludwig, M. (2004). "DANUBIA: an integrative simulation system for global change research in the Upper Danube Basin". In: *Cybernetics and Systems* 35.7-8, pp. 639–666. DOI: 10.1080/01969720490499425.

Barthel, R. (2011). "An indicator approach to assessing and predicting the quantitative state of groundwater bodies on the regional scale with a special focus on the impacts of climate change". In: *Hydrogeology Journal* 19.3, pp. 525–546. DOI: 10.1007/s10040-010-0693-y.

Beniston, M. (2005). "Mountain climates and climatic change: an overview of processes focusing on the European Alps". In: *Pure and Applied Geophysics* 162.8, pp. 1587–1606.

Beniston, M., Keller, F., Koffi, B., and Goyette, S. (2003). "Estimates of snow accumulation and volume in the Swiss Alps under changing climatic conditions". In: *Theoretical and Applied Climatology* 76.3-4, pp. 125–140. DOI: 10.1007/s00704-003-0016-5.

Beniston, M. (2003). "Climatic Change in Mountain Regions: A Review of Possible Impacts". In: *Climatic Change* 59.1/2, pp. 5–31. DOI: 10.1023/A:1024458411589.

Bergmann, M., Jahn, T., Knobloch, T., Krohn, W., Pohl, C., and Schramm, E. (2012). *Methods for inter- and transdisciplinary research. A primer for practice*. Frankfurt New York Campus.

Bernhardt, M., Liston, G. E., Strasser, U., Zängl, G., and Schulz, K. (2010). "High resolution modelling of snow transport in complex terrain using downscaled MM5 wind fields". In: *The Cryosphere* 4.1, pp. 99–113. DOI: 10.5194/tc-4-99-2010.

Best, M. J. et al. (2011). "The Joint UK Land Environment Simulator (JULES), model description – Part 1: Energy and water fluxes". In: *Geoscientific Model Development* 4.3, pp. 677–699. DOI: 10.5194/gmd-4-677-2011.

Beven, K. (1989). "Changing ideas in hydrology — The case of physically-based models". In: *Journal of Hydrology* 105.1-2, pp. 157–172. DOI: 10.1016/0022-1694(89)90101-7.

— (1993). "Prophecy, reality and uncertainty in distributed hydrological modelling". In: *Advances in Water Resources* 16.1, pp. 41–51. DOI: 10.1016/0309-1708(93)90028-E.

Bliss, A., Hock, R., and Radić, V. (2014). "Global response of glacier runoff to twenty-first century climate change". In: *Journal of Geophysical Research: Earth Surface* 119.4, pp. 717–730. DOI: 10.1002/(ISSN)2169-9011.

Blöschl, G., Carr, G., Bucher, C., Farnleitner, A. H., Rechberger, H., Wagner, W. K., and Zessner, M. (2012). "Promoting interdisciplinary education – the Vienna Doctoral Programme on Water Resource Systems". In: *Hydrology and Earth System Sciences* 16.2, pp. 457–472. DOI: 10.5194/hess-16-457-2012.

Blöschl, G. and Kirnbauer, R. (1991). "Point snowmelt models with different degrees of complexity—internal processes". In: *Journal of Hydrology* 129.1, pp. 127–147.

Blöschl, G. and Sivapalan, M. (1995). "Scale issues in hydrological modelling: A review". In: *Hydrological Processes* 9.3-4, pp. 251–290. DOI: 10.1002/hyp.3360090305.

Blöschl, G. (1999). "Scaling issues in snow hydrology". In: *Hydrological Processes* 13.14-15, pp. 2149–2175.

Blöschl, G. and Kirnbauer, R. (1992). "An analysis of snow cover patterns in a small alpine catchment". In: *Hydrological Processes* 6.1, pp. 99–109. DOI: 10.1002/hyp.3360060109.

Bock, A. R., Hay, L. E., McCabe, G. J., Markstrom, S. L., and Atkinson, R. D. (2016). "Parameter regionalization of a monthly water balance model for the conterminous United States". In: *Hydrology and Earth System Sciences* 20.7, pp. 2861–2876. DOI: 10.5194/hess-20-2861-2016.

Booch, G., Rumbaugh, J., and Jacobson, I. (1999). *The Unified Modeling Language User Guide*. Addison Wesley.

Bosshard, T., Carambia, M., Goergen, K., Kotlarski, S., Krahe, P., Zappa, M., and Schär, C. (2013). "Quantifying uncertainty sources in an ensemble of hydrological climate-impact projections". In: *Water Resources Research* 49.3, pp. 1523–1536. DOI: 10.1029/2011WR011533.

Braun, L. N. (1984). "Simulation of snowmelt-runoff in lowland and lower alpine regions of Switzerland". PhD thesis. ETH Zurich. DOI: 10.3929/ethz-a-000334295.

Breiling, M. and Charamza, P. (1999). "The impact of global warming on winter tourism and skiing: a regionalised model for Austrian snow conditions". In: *Regional Environmental*

Change 1.1, pp. 4–14. DOI: 10.1007/s101130050003.

Bulatewicz, T., Allen, A., Peterson, J. M., Staggenborg, S., Welch, S. M., and Steward, D. R. (2013). "The simple script wrapper for OpenMI: enabling interdisciplinary modeling studies". In: *Environmental Modelling & Software* 39, pp. 283–294.

Cannon, A. J., Sobie, S. R., Murdock, T. Q., Cannon, A. J., Sobie, S. R., and Murdock, T. Q. (2015). "Bias Correction of GCM Precipitation by Quantile Mapping: How Well Do Methods Preserve Changes in Quantiles and Extremes?" In: *dx.doi.org* 28.17, pp. 6938–6959. DOI: 10.1175/JCLI-D-14-00754.1.

Chang, K.-T. and Li, Z. (2000). "Modelling snow accumulation with a geographic information system". In: *International Journal of Geographical Information Science* 14.7, pp. 693–707. DOI: 10.1080/136588100424981.

Chen, J. and Kevorkian, V. (1971). "Heat and mass transfer in making artificial snow". In: *Industrial & Engineering Chemistry Process Design and Development* 10.1, pp. 75–78.

Christensen, J. H., Boberg, F., Christensen, O. B., and Lucas Picher, P. (2008). "On the need for bias correction of regional climate change projections of temperature and precipitation". In: *Geophysical Research Letters* 35.20, p. 7. DOI: 10.1029/2008GL035694.

Clarvis, M. H. et al. (2014). "Governing and managing water resources under changing hydroclimatic contexts: The case of the upper Rhone basin". In: *Environmental Science & Policy* 43, pp. 56–67. DOI: 10.1016/j.envsci.2013.11.005.

Collins, D. N. (2008). "Climatic warming, glacier recession and runoff from Alpine basins after the Little Ice Age maximum". In: *Annals of Glaciology* 48.1, pp. 119–124.

Corripio, J. (2002). "Modelling the energy balance of high altitude glacierised basins in the Central Andes". PhD thesis. University of Edinburgh.

— (2003). "Vectorial algebra algorithms for calculating terrain parameters from DEMs and solar radiation modelling in mountainous terrain". In: *International Journal of Geographical Information Science* 17.1, pp. 1–23. DOI: 10.1080/13658810210157796.

Dadic, R., Mott, R., Lehning, M., and Burlando, P. (2010). "Parameterization for wind-induced preferential deposition of snow". In: *Hydrological Processes* 24.14, pp. 1994–2006. DOI: 10.1002/hyp.7776.

Damm, A., Köberl, J., and Prettenthaler, F. (2014). "Does artificial snow production pay under future climate conditions? – A case study for a vulnerable ski area in Austria". In: *Tourism Management* 43, pp. 8–21. DOI: 10.1016/j.tourman.2014.01.009.

Dawson, J. and Scott, D. (2013). "Managing for climate change in the alpine ski sector". In: *Tourism Management* 35, pp. 244–254.

Deems, J. S., Fassnacht, S. R., and Elder, K. J. (2006). "Fractal Distribution of Snow Depth from Lidar Data". In: *Journal of Hydrometeorology* 7.2, pp. 285–297.

Defila, R., Di Guiolio, A., and Scheuermann, M. (2006). *Forschungsverbundmanagement. Handbuch für die Gestaltung inter- und transdisziplinärer Projekte*. Zurich: vdf.

Déqué, M. (2007). "Frequency of precipitation and temperature extremes over France in an anthropogenic scenario: Model results and statistical correction according to observed values". In: *Global and Planetary Change* 57.1-2, pp. 16–26. DOI: 10.1016/j.gloplacha.2006.11.

030.

Dozier, J. and Painter, T. H. (2004). "Multispectral and Hyperspectral Remote Sensing of Alpine Snow Properties". In: *Annual Review of Earth and Planetary Sciences* 32.1, pp. 465–494. DOI: 10.1146/annurev.earth.32.101802.120404.

Dwarakish, G. S. and Ganasri, B. P. (2015). "Impact of land use change on hydrological systems: A review of current modeling approaches". In: *Cogent Geoscience* 1.1, p. 2391. DOI: 10.1080/23312041.2015.1115691.

Eisel, L., Mills, K., and Leaf, C. (1988). "Estimated Consumptive Loss From Man-Made Snow". In: *JAWRA Journal of the American Water Resources Association* 24.4, pp. 815–820.

Elder, K., Dozier, J., and Michaelsen, J. (1991). "Snow accumulation and distribution in an alpine watershed". In: *Water Resources Research* 27.7, pp. 1541–1552.

Elsasser, H. and Bürki, R. (2002). "Climate change as a threat to tourism in the Alps". In: *Climate Research* 20.3, pp. 253–257.

Elsasser, H. and Messerli, P. (2001). "The vulnerability of the snow industry in the Swiss Alps". In: *Mountain Research and Development* 21.4, pp. 335–339.

Essery, R. (2015). "A factorial snowpack model (FSM 1.0)". In: *Geoscientific Model Development* 8.12, pp. 3867–3876. DOI: 10.5194/gmd-8-3867-2015.

Farinotti, D., Magnusson, J., Huss, M., and Bauder, A. (2010). "Snow accumulation distribution inferred from time-lapse photography and simple modelling". In: *Hydrological Processes*. DOI: 10.1002/hyp.7629.

Farinotti, D., Usselmann, S., Huss, M., Bauder, A., and Funk, M. (2011). "Runoff evolution in the Swiss Alps: projections for selected high-alpine catchments based on ENSEMBLES scenarios". In: *Hydrological Processes* 26.13, pp. 1909–1924. DOI: 10.1002/hyp.8276.

Fatichi, S., Rimkus, S., Burlando, P., Bordoy, R., and Molnar, P. (2015). "High-resolution distributed analysis of climate and anthropogenic changes on the hydrology of an Alpine catchment". In: *Journal of Hydrology* 525, pp. 362–382. DOI: 10.1016/j.jhydrol.2015.03.036.

Fauve, M., Rhyner, H., and Schneebeli, M. (2002). *Preparation and maintenance of pistes: Handbook for practitioners*. Swiss Federal Institute for Snow and Avalanche Research SLF. ISBN: 9783905621037.

Ferguson, R. I. (1999). "Snowmelt runoff models". In: *Progress in physical geography* 23.2, pp. 205–227. DOI: 10.1177/030913339902300203.

Finger, D., Heinrich, G., Gobiet, A., and Bauder, A. (2012). "Projections of future water resources and their uncertainty in a glacierized catchment in the Swiss Alps and the subsequent effects on hydropower production during the 21st century". In: *Water Resources Research* 48.2. DOI: 10.1029/2011WR010733.

Finger, D., Pellicciotti, F., Konz, M., Rimkus, S., and Burlando, P. (2011). "The value of glacier mass balance, satellite snow cover images, and hourly discharge for improving the performance of a physically based distributed hydrological model". In: *Water Resources Research* 47.7, W07519. DOI: 10.1029/2010WR009824.

Finger, D., Vis, M., Huss, M., and Seibert, J. (2015). "The value of multiple data set calibration versus model complexity for improving the performance of hydrological models in

mountain catchments". In: *Water Resources Research* 51.4, pp. 1939–1958. DOI: 10.1002/2014WR015712.

Fischer, A., Seiser, B., Stocker Waldhuber, M., Mitterer, C., and Abermann, J. (2015). "Tracing glacier changes in Austria from the Little Ice Age to the present using a lidar-based high-resolution glacier inventory in Austria". In: *The Cryosphere* 9.2, pp. 753–766. DOI: 10.5194/tc-9-753-2015.

Föhn, P. and Meister, R. (1983). "Distribution of snow drifts on ridge slopes: measurements and theoretical approximations". In: *Annals of Glaciology* 4, pp. 52–57.

Förster, K., Hanzer, F., Winter, B., Marke, T., and Strasser, U. (2016a). "An open-source MEteoroLOgical observation time series DISaggregation Tool (MELODIST v0.1.1)". In: *Geoscientific Model Development* 9.7, pp. 2315–2333. DOI: 10.5194/gmd-9-2315-2016.

Förster, K., Oesterle, F., Hanzer, F., Schöber, J., Huttenlau, M., and Strasser, U. (2016b). "A snow and ice melt seasonal prediction modelling system for Alpine reservoirs". In: *Proceedings of the International Association of Hydrological Sciences* 374, pp. 143–150. DOI: 10.5194/piahs-374-143-2016.

Frei, C. and Schär, C. (1998). "A precipitation climatology of the Alps from high-resolution rain-gauge observations". In: *International Journal of Climatology* 18.8, pp. 873–900.

Frei, P., Kotlarski, S., Liniger, M. A., and Schär, C. (2017). "Snowfall in the Alps: Evaluation and projections based on the EURO-CORDEX regional climate models". In: *The Cryosphere*, pp. 1–38. DOI: 10.5194/tc-2017-7.

Frodemann, R. (2010). *The Oxford Handbook of Interdisciplinarity*. New York: Oxford University Press.

Fukushima, T., Kureha, M., Ozaki, N., Fujimori, Y., and Harasawa, H. (2002). "Influences of air temperature change on leisure industries – case study on ski activities". In: *Mitigation and Adaptation Strategies for Global Change* 7.2, pp. 173–189.

Gafurov, A. and Bárdossy, A. (2009). "Cloud removal methodology from MODIS snow cover product". In: *Hydrology and Earth System Sciences* 13.7, pp. 1361–1373. DOI: 10.5194/hess-13-1361-2009.

Giupponi, C., Borsuk, M. E., Vries, B. J. M. de, and Hasselmann, K. (2013). "Innovative approaches to integrated global change modelling". In: *Environmental Modelling & Software* 44, pp. 1–9. DOI: 10.1016/j.envsoft.2013.01.013.

Gobiet, A., Kotlarski, S., Beniston, M., and Heinrich, G. (2014). "21st century climate change in the European Alps—A review". In: *Science of the Total Environment* 493, pp. 1138–1151. DOI: 10.1016/j.scitotenv.2013.07.050.

Goodison, B. E., Louie, P., and Yang, D. (1998). *WMO solid precipitation measurement intercomparison*. Tech. rep. WMO/TD 872. Geneva.

GRASS Development Team (2012). *Geographic Resources Analysis Support System (GRASS GIS) Software*. Open Source Geospatial Foundation.

Grayson, R. B., Blöschl, G., Western, A. W., and McMahon, T. A. (2002). "Advances in the use of observed spatial patterns of catchment hydrological response". In: *Advances in Water Resources* 25.8-12, pp. 1313–1334. DOI: 10.1016/S0309-1708(02)00060-X.

Greuell, W., Knap, W. H., and Smeets, P. C. (1997). "Elevational changes in meteorological variables along a midlatitude glacier during summer". In: *Journal of Geophysical Research* 102.D22, pp. 25941–25954. DOI: 10.1029/97JD02083.

Grünewald, T., Bühler, Y., and Lehning, M. (2014). "Elevation dependency of mountain snow depth". In: *The Cryosphere* 8.6, pp. 2381–2394. DOI: 10.5194/tc-8-2381-2014.

Grünewald, T., Schirmer, M., Mott, R., and Lehning, M. (2010). "Spatial and temporal variability of snow depth and ablation rates in a small mountain catchment". In: *The Cryosphere* 4.2, pp. 215–225. DOI: 10.5194/tc-4-215-2010.

Grünewald, T., Stötter, J., Pomeroy, J. W., Dadic, R., Moreno Baños, I., Marturià, J., Spross, M., Hopkinson, C., Burlando, P., and Lehning, M. (2013). "Statistical modelling of the snow depth distribution in open alpine terrain". In: *Hydrology and Earth System Sciences* 17.8, pp. 3005–3021. DOI: 10.5194/hess-17-3005-2013.

Grünewald, T. and Lehning, M. (2011). "Altitudinal dependency of snow amounts in two small alpine catchments: can catchment-wide snow amounts be estimated via single snow or precipitation stations?" In: *Annals of Glaciology* 52.58, pp. 153–158.

Gudmundsson, L., Bremnes, J. B., Haugen, J. E., and Engen-Skaugen, T. (2012). "Technical Note: Downscaling RCM precipitation to the station scale using statistical transformations – a comparison of methods". In: *Hydrology and Earth System Sciences* 16.9, pp. 3383–3390. DOI: 10.5194/hess-16-3383-2012.

Günther, D., Hanzer, F., Hanzer, Marke, T., Essery, R., and Strasser, U. (2017). "Evaluating the performance of a distributed snow model with varying degrees of complexity and spatio-temporal resolution". In: *Geophysical Research Abstracts*. Vienna.

Gutmann, E., Barstad, I., Clark, M., Arnold, J., and Rasmussen, R. (2016). "The Intermediate Complexity Atmospheric Research Model (ICAR)". in: *Journal of Hydrometeorology* 17.3, pp. 957–973. DOI: 10.1175/JHM-D-15-0155.1.

Haerter, J. O., Eggert, B., Moseley, C., Piani, C., and Berg, P. (2015). "Statistical precipitation bias correction of gridded model data using point measurements". In: *Geophysical Research Letters* 42.6, pp. 1919–1929. DOI: 10.1002/2015GL063188.

Hall, D. K., Foster, J. L., Verbyla, D. L., Klein, A. G., and Benson, C. S. (1998). "Assessment of snow-cover mapping accuracy in a variety of vegetation-cover densities in central Alaska". In: *Remote sensing of Environment* 66.2, pp. 129–137. DOI: 10.1016/S0034-4257(98)00051-0.

Hall, D. K., Riggs, G. A., and Salomonson, V. V. (1995). "Development of methods for mapping global snow cover using moderate resolution imaging spectroradiometer data". In: *Remote sensing of Environment* 54.2, pp. 127–140.

Hall, D. K., Riggs, G. A., Salomonson, V. V., DiGirolamo, N. E., and Bayr, K. J. (2002). "MODIS snow-cover products". In: *Remote sensing of Environment* 83.1-2, pp. 181–194. DOI: 10.1016/S0034-4257(02)00095-0.

Hanzer, F. (2013). "Explicit modeling of technical snow production". MA thesis. Graz: University of Graz.

Hanzer, F., Helfricht, K., Marke, T., and Strasser, U. (2016). "Multilevel spatiotemporal vali-

dation of snow/ice mass balance and runoff modeling in glacierized catchments". In: *The Cryosphere* 10.4, pp. 1859–1881. DOI: 10.5194/tc-10-1859-2016.

Hanzer, F., Marke, T., and Strasser, U. (2014). "Distributed, explicit modeling of technical snow production for a ski area in the Schladming region (Austrian Alps)". In: *Cold Regions Science and Technology* 108, pp. 113–124. DOI: 10.1016/j.coldregions.2014.08.003.

Helfricht, K. (2014). "Analysis of the spatial and temporal variation of seasonal snow accumulation in Alpine catchments using airborne laser scanning". PhD thesis. Innsbruck.

Helfricht, K., Kuhn, M., Keuschnig, M., and Heilig, A. (2014a). "Lidar snow cover studies on glaciers in the Ötztal Alps (Austria): comparison with snow depths calculated from GPR measurements". In: *The Cryosphere* 8.1, pp. 41–57. DOI: 10.5194/tc-8-41-2014.

Helfricht, K., Schöber, J., Seiser, B., Fischer, A., Stötter, J., and Kuhn, M. (2012). "Snow accumulation of a high alpine catchment derived from LiDAR measurements". In: *Advances in Geosciences* 32, pp. 31–39.

Helfricht, K., Schöber, J., Schneider, K., Sailer, R., and Kuhn, M. (2014b). "Interannual persistence of the seasonal snow cover in a glacierized catchment". In: *Journal of Glaciology* 60.223, pp. 889–904. DOI: 10.3189/2014JoG13J197.

Hendrikx, J. and Hreinsson, E. Ö. (2012). "The potential impact of climate change on seasonal snow in New Zealand: part II—industry vulnerability and future snowmaking potential". In: *Theoretical and Applied Climatology* 110.4, pp. 619–630.

Hennessy, K. J., Whetton, P. H., Smith, I. N., Bathols, J. M., Hutchinson, M., and Sharples, J. (2003). *The impact of climate change on snow conditions in mainland Australia*. Tech. rep. CSIRO Atmospheric Research Aspendale, Australia.

Hennessy, K. J., Whetton, P. H., Walsh, K., Smith, I. N., Bathols, J. M., Hutchinson, M., and Sharples, J. (2008). "Climate change effects on snow conditions in mainland Australia and adaptation at ski resorts through snowmaking". In: *Climate Research* 35.3, pp. 255–270. DOI: 10.3354/cr00706.

Hirsch Hadorn, G. (2008). *Handbook of Transdisciplinary Research*. Ed. by G. Hirsch Hadorn, H. Hoffmann-Riem, S. Biber-Klemm, W. Grossenbacher-Mansuy, D. Joye, C. Pohl, U. Wiesmann, and E. Zemp. Berlin: Springer.

Hirsch Hadorn, G., Pohl, C., and Bammer, G. (2010). "Solving problems through transdisciplinary research". In: *The Oxford Handbook of Interdisciplinarity*. New York: Oxford University Press, pp. 431–452.

Hock, R. (2003). "Temperature index melt modelling in mountain areas". In: *Journal of Hydrology* 282.1, pp. 104–115.

Hofer, M., Nemec, J., Cullen, N. J., and Weber, M. (2017). "Evaluating predictor strategies for regression-based downscaling with a focus on glacierized mountain environments". In: *Journal of Applied Meteorology and Climatology*, JAMC–D–16–0215.1. DOI: 10.1175/JAMC-D-16-0215.1.

Horton, P., Schaefli, B., Mezghani, A., Hingray, B., and Musy, A. (2006). "Assessment of climate-change impacts on alpine discharge regimes with climate model uncertainty". In: *Hydrological Processes* 20.10, pp. 2091–2109.

Huss, M. and Farinotti, D. (2012). "Distributed ice thickness and volume of all glaciers around the globe". In: *Journal of Geophysical Research: Earth Surface (2003–2012)* 117.F4, F04010. DOI: 10.1029/2012JF002523.

Huss, M., Farinotti, D., Bauder, A., and Funk, M. (2008). "Modelling runoff from highly glacierized alpine drainage basins in a changing climate". In: *Hydrological Processes* 22.19, pp. 3888–3902.

Huss, M., Funk, M., and Ohmura, A. (2009). "Strong Alpine glacier melt in the 1940s due to enhanced solar radiation". In: *Geophysical Research Letters* 36.23, p. 17. DOI: 10.1029/2009GL040789.

Huss, M. and Hock, R. (2015). "A new model for global glacier change and sea-level rise". In: *Frontiers in Earth Science* 3.54, p. 22. DOI: 10.3389/feart.2015.00054.

Huss, M., Jouvet, G., Farinotti, D., and Bauder, A. (2010). "Future high-mountain hydrology: a new parameterization of glacier retreat". In: *Hydrology and Earth System Sciences* 14.5, pp. 815–829. DOI: 10.5194/hess-14-815-2010.

Huss, M., Zemp, M., Joerg, P. C., and Salzmann, N. (2014). "High uncertainty in 21st century runoff projections from glacierized basins". In: *Journal of Hydrology* 510, pp. 35–48.

Jacob, D. et al. (2013). "EURO-CORDEX: new high-resolution climate change projections for European impact research". In: *Regional Environmental Change* 14.2, pp. 563–578. DOI: 10.1007/s10113-013-0499-2.

Jahn, T., Bergmann, M., and Keil, F. (2012). "Transdisciplinarity: Between mainstreaming and marginalization". In: *Ecological Economics* 79, pp. 1–10. DOI: 10.1016/j.ecolecon.2012.04.017.

Jakeman, A. and Letcher, R. (2003). "Integrated assessment and modelling: features, principles and examples for catchment management". In: *Environmental Modelling & Software* 18.6, pp. 491–501. DOI: 10.1016/S1364-8152(03)00024-0.

Jansson, P., Hock, R., and Schneider, T. (2003). "The concept of glacier storage: a review". In: *Journal of Hydrology* 282.1-4, pp. 116–129. DOI: 10.1016/S0022-1694(03)00258-0.

Jasanoff, S. (2004). *States of Knowledge: Co-production of Science and the Social Order*. London/New York: Routledge.

Jonas, T., Marty, C., and Magnusson, J. (2009). "Estimating the snow water equivalent from snow depth measurements in the Swiss Alps". In: *Journal of Hydrology* 378.1, pp. 161–167.

Jong, C. de (2011). "Artificial Production of Snow". In: *Encyclopedia of Snow, Ice and Glaciers*. Springer. ISBN: 9789048126422.

Jordan, R. (1991). *A one-dimensional temperature model for a snow cover: Technical documentation for SNTHERM. 89.* Tech. rep. Hanover, NH.

Jouvet, G., Huss, M., Funk, M., and Blatter, H. (2011). "Modelling the retreat of Grosser Aletschgletscher, Switzerland, in a changing climate". In: *Journal of Glaciology* 57.206, pp. 1033–1045. DOI: 10.3189/002214311798843359.

Kalaugher, E., Bornman, J. F., Clark, A., and Beukes, P. (2013). "An integrated biophysical and socio-economic framework for analysis of climate change adaptation strategies: The case of a New Zealand dairy farming system". In: *Environmental Modelling & Software* 39,

pp. 176–187. DOI: 10.1016/j.envsoft.2012.03.018.

Kaser, G., Großhauser, M., and Marzeion, B. (2010). "Contribution potential of glaciers to water availability in different climate regimes". In: *Proceedings of the National Academy of Sciences* 107.47, pp. 20223–20227. DOI: 10.1073/pnas.1008162107.

Keller, T., Pielmeier, C., Rixen, C., Gadient, F., Gustafsson, D., and Stahli, M. (2004). "Impact of artificial snow and ski-slope grooming on snowpack properties and soil thermal regime in a sub-alpine ski area". In: *Annals of Glaciology* 38.1, pp. 314–318.

Kelly Letcher, R. A. et al. (2013). "Selecting among five common modelling approaches for integrated environmental assessment and management". In: *Environmental Modelling & Software* 47, pp. 159–181. DOI: 10.1016/j.envsoft.2013.05.005.

Kirchner, J. W. (2006). "Getting the right answers for the right reasons: Linking measurements, analyses, and models to advance the science of hydrology". In: *Water Resources Research* 42.3, p. 2465. DOI: 10.1029/2005WR004362.

Klein, A. G., Hall, D. K., and Riggs, G. A. (1998). "Improving snow cover mapping in forests through the use of a canopy reflectance model". In: *Hydrological Processes* 12.10-11, pp. 1723–1744. DOI: 10.1002/(SICI)1099-1085(199808/09)12:10/11<1723::AID-HYP691>3.0.CO;2-2.

Klein, G., Vitasse, Y., Rixen, C., Marty, C., and Rebetez, M. (2016). "Shorter snow cover duration since 1970 in the Swiss Alps due to earlier snowmelt more than to later snow onset". In: *Climatic Change* 139.3-4, pp. 637–649. DOI: 10.1007/s10584-016-1806-y.

Klein, J. T. (2000). "A conceptual vocabulary of interdisciplinary science". In: *Practicing Interdisciplinarity*. Ed. by P. Weingart and N. Stehr. Toronto/Buffalo/London, pp. 3–24.

Klemeš, V. (1982). "Empirical and causal models in hydrology". In: *Scientific Basis of Water Resource Management*. Washington, D.C., pp. 95–104.

— (1990). "The modelling of mountain hydrology: the ultimate challenge". In: *IAHS Publ*.

Knap, W. H., Reijmer, C. H., and Oerlemans, J. (2010). "Narrowband to broadband conversion of Landsat TM glacier albedos". In: *International Journal of Remote Sensing* 20.10, pp. 2091–2110. DOI: 10.1080/014311699212362.

Kobierska, F., Jonas, T., Zappa, M., Bavay, M., Magnusson, J., and Bernasconi, S. M. (2013). "Future runoff from a partly glacierized watershed in Central Switzerland: A two-model approach". In: *Advances in Water Resources* 55, pp. 204–214. DOI: 10.1016/j.advwatres.2012.07.024.

Koenig, U. and Abegg, B. (1997). "Impacts of Climate Change on Winter Tourism in the Swiss Alps". In: *Journal of Sustainable Tourism* 5.1, pp. 46–58.

Koivusalo, H., Heikinheimo, M., and Karvonen, T. (2001). "Test of a simple two-layer parameterisation to simulate the energy balance and temperature of a snow pack". In: *Theoretical and Applied Climatology* 70.1-4, pp. 65–79.

Konz, M. and Seibert, J. (2010). "On the value of glacier mass balances for hydrological model calibration". In: *Journal of Hydrology* 385.1-4, pp. 238–246. DOI: 10.1016/j.jhydrol.2010.02.025.

Kragt, M. E., Robson, B. J., and Macleod, C. J. A. (2013). "Modellers' roles in structuring integrative research projects". In: *Environmental Modelling & Software* 39, pp. 322–330. DOI:

10.1016/j.envsoft.2012.06.015.

Krohn, W. (2010). "Interdisciplinary cases and disciplinary knowledge". In: *The Oxford Handbook of Interdisciplinarity*. New York: Oxford University Press.

Kuhn, M. (2000). "Verification of a hydrometeorological model of glacierized basins". In: *Annals of Glaciology* 31.1, pp. 15–18. DOI: 10.3189/172756400781820228.

Kuhn, M. and Batlogg, N. (1998). "Glacier Runoff In Alpine Headwaters In A Changing Climate". In: *IAHS PUBLICATION no. 248*, p. 79.

Kuhn, M., Helfricht, K., Ortner, M., Landmann, J., and Gurgiser, W. (2016). "Liquid water storage in snow and ice in 86 Eastern Alpine basins and its changes from 1970–97 to 1998–2006". In: *Annals of Glaciology*, pp. 1–8. DOI: 10.1017/aog.2016.24.

Kuhn, M., Lambrecht, A., and Abermann, J. (2015). *The Austrian glacier inventory GI 2, 1998, in ArcGIS (shapefile) format*. PANGAEA. DOI: 10.1594/PANGAEA.844984.

Kuhn, M. and Olefs, M. (2007). *Auswirkung von Klimaänderungen auf das Abflussverhalten von vergletscherten Einzugsgebieten im Hinblick auf Speicherkraftwerke*. Tech. rep.

Lang, D. J., Wiek, A., Bergmann, M., Stauffacher, M., Martens, P., Moll, P., Swilling, M., and Thomas, C. J. (2012). "Transdisciplinary research in sustainability science: practice, principles, and challenges". In: *Sustainability Science* 7.1, pp. 25–43. DOI: 10.1007/s11625-011-0149-x.

Lehner, B., Czisch, G., and Vassolo, S. (2005). "The impact of global change on the hydropower potential of Europe: a model-based analysis". In: *Energy Policy* 33.7, pp. 839–855. DOI: 10.1016/j.enpol.2003.10.018.

Lehning, M., Bartelt, P., Brown, B., and Fierz, C. (2002). "A physical SNOWPACK model for the Swiss avalanche warning". In: *Cold Regions Science and Technology* 35.3, pp. 169–184. DOI: 10.1016/S0165-232X(02)00072-1.

Lehning, M., Grünewald, T., and Schirmer, M. (2011). "Mountain snow distribution governed by an altitudinal gradient and terrain roughness". In: *Geophysical Research Letters* 38.19, p. L19504. DOI: 10.1029/2011GL048927.

Lindström, G. (1997). "A Simple Automatic Calibration Routine for the HBV Model". In: *Nordic Hydrology* 28, pp. 153–168.

Liston, G. E. and Elder, K. (2006a). "A distributed snow-evolution modeling system (SnowModel)". In: *Journal of Hydrometeorology* 7.6, pp. 1259–1276.

— (2006b). "A Meteorological Distribution System for High-Resolution Terrestrial Modeling (MicroMet)". In: *Journal of Hydrometeorology* 7.2, pp. 217–234. DOI: 10.1175/JHM486.1.

Liston, G. E., Haehnel, R. B., Sturm, M., Hiemstra, C. A., Berezovskaya, S., and Tabler, R. D. (2007). "Simulating complex snow distributions in windy environments using SnowTran-3D". in: *Journal of Glaciology* 53.181, pp. 241–256.

Luterbacher, J., Liniger, M. A., Menzel, A., Estrella, N., Della-Marta, P. M., Pfister, C., and Xoplaki, E. (2007). "Exceptional European warmth of autumn 2006 and winter 2007: Historical context, the underlying dynamics, and its phenological impacts". In: *Geophysical Research Letters* 34.12, p. L12704.

Magnusson, J., Farinotti, D., Jonas, T., and Bavay, M. (2011). "Quantitative evaluation of different hydrological modelling approaches in a partly glacierized Swiss watershed". In:

Hydrological Processes 25.13, pp. 2071–2084. DOI: 10.1002/hyp.7958.

Maraun, D. (2012). "Nonstationarities of regional climate model biases in European seasonal mean temperature and precipitation sums". In: *Geophysical Research Letters* 39.6. DOI: 10.1029/2012GL051210.

Maraun, D. (2013). "Bias Correction, Quantile Mapping, and Downscaling: Revisiting the Inflation Issue". In: *Journal of Climate* 26.6, pp. 2137–2143. DOI: 10.1175/JCLI-D-12-00821.1.

Maraun, D., Widmann, M., Gutiérrez, J. M., Kotlarski, S., Chandler, R. E., Hertig, E., Wibig, J., Huth, R., and Wilcke, R. A. I. (2015). "VALUE: A framework to validate downscaling approaches for climate change studies". In: *Earth's Future* 3.1, pp. 1–14. DOI: 10.1002/2014EF000259.

Marke, T. (2008). "Development and Application of a Model Interface to couple Land Surface Models with Regional Climate Models for Climate Change Risk Assessment in the Upper Danube Watershed". PhD thesis. Ludwig-Maximilians-Universität München.

Marke, T., Strasser, U., Hanzer, F., Stötter, J., Wilcke, R. A. I., and Gobiet, A. (2015). "Scenarios of Future Snow Conditions in Styria (Austrian Alps)". In: *Journal of Hydrometeorology* 16, pp. 261–277. DOI: 10.1175/JHM-D-14-0035.1.

Marty, C., Schlögl, S., Bavay, M., and Lehning, M. (2017). "How much can we save? Impact of different emission scenarios on future snow cover in the Alps". In: *The Cryosphere* 11.1, pp. 517–529. DOI: 10.5194/tc-11-517-2017.

Marzeion, B., Jarosch, A. H., and Gregory, J. M. (2014). "Feedbacks and mechanisms affecting the global sensitivity of glaciers to climate change". In: *The Cryosphere* 8.1, pp. 59–71. DOI: 10.5194/tc-8-59-2014.

Marzeion, B., Jarosch, A. H., and Hofer, M. (2012). "Past and future sea-level change from the surface mass balance of glaciers". In: *The Cryosphere* 6.6, pp. 1295–1322. DOI: 10.5194/tc-6-1295-2012.

Maurer, E. P. and Pierce, D. W. (2014). "Bias correction can modify climate model simulated precipitation changes without adverse effect on the ensemble mean". In: *Hydrology and Earth System Sciences* 18.3, pp. 915–925. DOI: 10.5194/hess-18-915-2014.

Mayer, M., Steiger, R., and Trawöger, L. (2007). "Technischer Schnee rieselt vom touristischen Machbarkeitshimmel". In: *Mitteilungen der Österreichischen Geographischen Gesellschaft* 149, pp. 157–180.

McKay, G. A. and Gray, D. M. (1981). "The distribution of snowcover". In: *Handbook of Snow*. Ed. by D. M. Gray and D. H. Male. Toronto: Pergamon Press, pp. 153–190.

Meybeck, M., Green, P., and Vörösmarty, C. (2009). "A New Typology for Mountains and Other Relief Classes". In: *dx.doi.org* 21.1, pp. 34–45. DOI: 10.1659/0276-4741(2001)021[0034:ANTFMA]2.0.CO;2.

Milano, M., Reynard, E., Bosshard, N., and Weingartner, R. (2015). "Simulating future trends in hydrological regimes in Western Switzerland". In: *Journal of Hydrology: Regional Studies* 4, pp. 748–761. DOI: 10.1016/j.ejrh.2015.10.010.

Moen, J. and Fredman, P. (2007). "Effects of climate change on alpine skiing in Sweden". In:

Journal of Sustainable Tourism 15.4, pp. 418–437.

Montanari, A. et al. (2013). ""Panta Rhei—Everything Flows": Change in hydrology and society—The IAHS Scientific Decade 2013–2022". In: *Hydrological Sciences Journal* 58.6, pp. 1256–1275. DOI: 10.1080/02626667.2013.809088.

Moore, R. V. and Tindall, C. I. (2005). "An overview of the open modelling interface and environment (the OpenMI)". in: *Environmental Science & Policy* 8.3, pp. 279–286. DOI: 10.1016/j.envsci.2005.03.009.

Morgan, M. and Morrison, M. (1999). *Models as mediators: Perspectives on natural and social sciences*. Cambridge University Press.

Muhar, A., Vilsmaier, U., Glanzer, M., and Freyer, B. (2006). "Initiating transdisciplinarity in academic case study teaching". In: *International Journal of Sustainability in Higher Education* 7.3, pp. 293–308. DOI: 10.1108/14676370610677856.

NASEM (2016). *Next Generation Earth System Prediction: Strategies for Subseasonal to Seasonal Forecasts*. Strategies for Subseasonal to Seasonal Forecasts. Washington, D.C.: National Academies Press. ISBN: 978-0-309-38880-1. DOI: 10.17226/21873.

Nash, J. E. (1960). "A unit hydrograph study, with particular reference to British catchments". In: *Proc. Inst. Civ. Eng.* 17.3, pp. 249–282. DOI: 10.1680/iicep.1960.11649.

Nešpor, V. and Sevruk, B. (1999). "Estimation of wind-induced error of rainfall gauge measurements using a numerical simulation". In: *Journal of Atmospheric and Oceanic Technology* 16.4, pp. 450–464.

Ohmura, A., Bauder, A., Müller, H., and Kappenberger, G. (2007). "Long-term change of mass balance and the role of radiation". In: *Annals of Glaciology* 46.1, pp. 367–374. DOI: 10.3189/172756407782871297.

Ohmura, A. (2001). "Physical Basis for the Temperature-Based Melt-Index Method". In: *Journal of Applied Meteorology* 40.4, pp. 753–761. DOI: 10.1175/1520-0450(2001)040<0753:PBFTTB>2.0.CO;2.

Olefs, M., Fischer, A., and Lang, J. (2010). "Boundary Conditions for Artificial Snow Production in the Austrian Alps". In: *Journal of Applied Meteorology and Climatology* 49.6, pp. 1096–1113. DOI: 10.1175/2010JAMC2251.1.

Ostrom, E. (2008). "Frameworks and theories of environmental change". In: *Global Environmental Change* 18.2, pp. 249–252. DOI: 10.1016/j.gloenvcha.2008.01.001.

Parajka, J. and Blöschl, G. (2008). "The value of MODIS snow cover data in validating and calibrating conceptual hydrologic models". In: *Journal of Hydrology* 358.3-4, pp. 240–258. DOI: 10.1016/j.jhydrol.2008.06.006.

Pellicciotti, F., Brock, B., Strasser, U., Burlando, P., Funk, M., and Corripio, J. (2005). "An enhanced temperature-index glacier melt model including the shortwave radiation balance: Development and testing for Haut Glacier d'Arolla, Switzerland". In: *Journal of Glaciology* 51.175, pp. 573–587.

Pickering, C. M. and Buckley, R. C. (2010). "Climate response by the ski industry: the shortcomings of snowmaking for Australian resorts". In: *AMBIO: A Journal of the Human Environment* 39.5, pp. 430–438.

Pohl, C. et al. (2010). "Researchers' roles in knowledge co-production: experience from sustainability research in Kenya, Switzerland, Bolivia and Nepal". In: *Science and Public Policy* 37.4, pp. 267–281. DOI: 10.3152/030234210X496628.

Pomeroy, J. W., Gray, D. M., Brown, T., Hedstrom, N. R., Quinton, W. L., Granger, R. J., and Carey, S. K. (2007). "The cold regions hydrological model: a platform for basing process representation and model structure on physical evidence". In: *Hydrological Processes* 21.19, pp. 2650–2667. DOI: 10.1002/hyp.6787.

Pomeroy, J. W., Gray, D. M., Hedstrom, N. R., and Janowicz, J. R. (2002). "Prediction of seasonal snow accumulation in cold climate forests". In: *Hydrological Processes* 16.18, pp. 3543–3558. DOI: 10.1002/hyp.1228.

Pomeroy, J. W., Gray, D. M., Shook, K. R., Toth, B., Essery, R. L. H., Pietroniro, A., and Hedstrom, N. (1998). "An evaluation of snow accumulation and ablation processes for land surface modelling". In: *Hydrological Processes* 12.15, pp. 2339–2367. DOI: 10.1002/(SICI)1099-1085(199812)12:15<2339::AID-HYP800>3.0.CO;2-L.

Prasch, M., Marke, T., Strasser, U., and Mauser, W. (2011). "Large scale integrated hydrological modelling of the impact of climate change on the water balance with DANUBIA". in: *Advances in Science and Research* 7.1, pp. 61–70. DOI: 10.5194/asr-7-61-2011.

Pröbstl, U. (2006). *Kunstschnee und Umwelt*. Entwicklung und Auswirkungen der technischen Beschneiung. Bern, Switzerland: Haupt. ISBN: 9783258069364.

Pröbstl, U. and Prutsch, A. (2008). *Endbericht STRATEGE*. tech. rep.

Radić, V., Bliss, A., Beedlow, A. C., Hock, R., Miles, E., and Cogley, J. G. (2013). "Regional and global projections of twenty-first century glacier mass changes in response to climate scenarios from global climate models". In: *Climate Dynamics* 42.1-2, pp. 37–58. DOI: 10.1007/s00382-013-1719-7.

Ragettli, S., Pellicciotti, F., Bordoy, R., and Immerzeel, W. W. (2013). "Sources of uncertainty in modeling the glaciohydrological response of a Karakoram watershed to climate change". In: *Water Resources Research* 49.9, pp. 6048–6066. DOI: 10.1002/wrcr.20450.

Ragg, H., Egger, C., Hanzer, F., and Strasser, U. (2011). "Application of the snow cover models AMUNDSEN and SNOWREG for the simulation of past and future snow conditions in Tyrol and Styria (Austria)". In: *12. Österreichischer Klimatag*.

Rango, A. and Martinec, J. (1995). "Revisiting the Degree-day Method for Snowmelt Computations". In: *JAWRA Journal of the American Water Resources Association* 31.4, pp. 657–669. DOI: 10.1111/j.1752-1688.1995.tb03392.x.

Refsgaard, J. C. (1997). "Parameterisation, calibration and validation of distributed hydrological models". In: *Journal of Hydrology* 198.1-4, pp. 69–97. DOI: 10.1016/S0022-1694(96)03329-X.

Rixen, C., Teich, M., Lardelli, C., Gallati, D., Pohl, M., Puetz, M., and Bebi, P. (2011). "Winter Tourism and Climate Change in the Alps: An Assessment of Resource Consumption, Snow Reliability, and Future Snowmaking Potential". In: *Mountain Research and Development* 31.3, pp. 229–236. DOI: 10.1659/MRD-JOURNAL-D-10-00112.1.

Rodell, M. and Houser, P. R. (2004). "Updating a Land Surface Model with MODIS-Derived

Snow Cover". In: *Journal of Hydrometeorology* 5.6, pp. 1064–1075. DOI: 10.1175/JHM-395.1.

Rohrer, M. B. (1992). "Die Schneedecke im schweizerischen Alpenraum und ihre Modellierung". In: *Zürcher Geographische Schriften* 49, 178pp. DOI: 10.3929/ethz-a-000601662.

Rohrer, M. B. and Braun, L. N. (1994). "Long-Term Records of Snow Cover Water Equivalent in the Swiss Alps". In: *EGS XVII General Assembly*. Edinburgh, pp. 65–78.

Roy, E. D., Morzillo, A. T., Seijo, F., Reddy, S. M. W., Rhemtulla, J. M., Milder, J. C., Kuemmerle, T., and Martin, S. L. (2013). "The Elusive Pursuit of Interdisciplinarity at the Human—Environment Interface". In: *BioScience* 63.9, pp. 745–753. DOI: 10.1525/bio.2013.63.9.10.

Salzmann, N., Huggel, C., Rohrer, M., and Stoffel, M. (2014). "Data and knowledge gaps in glacier, snow and related runoff research – A climate change adaptation perspective". In: *Journal of Hydrology* 518, pp. 225–234. DOI: 10.1016/j.jhydrol.2014.05.058.

Sauter, T., Möller, M., Finkelnburg, R., Grabiec, M., Scherer, D., and Schneider, C. (2013). "Snowdrift modelling for the Vestfonna ice cap, north-eastern Svalbard". In: *The Cryosphere* 7.4, pp. 1287–1301. DOI: 10.5194/tc-7-1287-2013.

SBS (2016). *Fakten & Zahlen zur Schweizer Seilbahnbranche – Ausgabe 2016*. Tech. rep. Bern.

Schaefli, B., Hingray, B., and Musy, A. (2007). "Climate change and hydropower production in the Swiss Alps: quantification of potential impacts and related modelling uncertainties". In: *Hydrology and Earth System Sciences* 11.3, pp. 1191–1205. DOI: 10.5194/hess-11-1191-2007.

Schaefli, B., Hingray, B., Niggli, M., and Musy, A. (2005). "A conceptual glacio-hydrological model for high mountainous catchments". In: *Hydrology and Earth System Sciences* 9, pp. 95–109. DOI: 10.5194/hess-9-95-2005.

Schaefli, B. and Huss, M. (2011). "Integrating point glacier mass balance observations into hydrologic model identification". In: *Hydrology and Earth System Sciences* 15.4, pp. 1227–1241. DOI: 10.5194/hess-15-1227-2011.

Schaefli, B. (2015). "Projecting hydropower production under future climates: a guide for decision-makers and modelers to interpret and design climate change impact assessments". In: *Wiley Interdisciplinary Reviews: Water* 2.4, pp. 271–289. DOI: 10.1002/wat2.1083.

Schaefli, B. and Gupta, H. V. (2007). "Do Nash values have value?" In: *Hydrological Processes* 21.15, pp. 2075–2080.

Schirmer, M., Wirz, V., Clifton, A., and Lehning, M. (2011). "Persistence in intra-annual snow depth distribution: 1. Measurements and topographic control". In: *Water Resources Research* 47.9. DOI: 10.1029/2010WR009426.

Schmidt, P., Steiger, R., and Matzarakis, A. (2012). "Artificial snowmaking possibilities and climate change based on regional climate modeling in the Southern Black Forest". In: *Meteorologische Zeitschrift* 21.2, pp. 167–172. DOI: 10.1127/0941-2948/2012/0281.

Schmidt, R. A. and Troendle, C. A. (1989). "Snowfall into a forest and clearing". In: *Journal of Hydrology* 110.3-4, pp. 335–348. DOI: 10.1016/0022-1694(89)90196-0.

Schmucki, E., Marty, C., Fierz, C., and Lehning, M. (2015a). "Simulations of 21st century snow response to climate change in Switzerland from a set of RCMs". In: *International Journal of*

Climatology 35.11, pp. 3262–3273. DOI: 10.1002/joc.4205.

Schmucki, E., Marty, C., Fierz, C., Weingartner, R., and Lehning, M. (2015b). "Impact of climate change in Switzerland on socioeconomic snow indices". In: *Theoretical and Applied Climatology* 127.3-4, pp. 875–889. DOI: 10.1007/s00704-015-1676-7.

Schneiderbauer, S. and Prokop, A. (2011). "The atmospheric snow-transport model: SnowDrift3D". in: *Journal of Glaciology* 57.203, pp. 526–542.

Schöber, J. (2014). "Improved snow and runoff modelling of glacierized catchments for flood forecasting". PhD thesis. Innsbruck.

Schöber, J., Schneider, K., Helfricht, K., Schattan, P., Achleitner, S., Schöberl, F., and Kirnbauer, R. (2014). "Snow cover characteristics in a glacierized catchment in the Tyrolean Alps - Improved spatially distributed modelling by usage of Lidar data". In: *Journal of Hydrology* 519, pp. 3492–3510. DOI: 10.1016/j.jhydrol.2013.12.054.

Scholz, R. W. (2011). *Environmental Literacy in Science and Society*. New York: Cambridge University Press.

Scott, D. and McBoyle, G. (2007). "Climate change adaptation in the ski industry". In: *Mitigation and Adaptation Strategies for Global Change* 12.8, pp. 1411–1431.

Scott, D., McBoyle, G., and Mills, B. (2003). "Climate change and the skiing industry in southern Ontario (Canada): exploring the importance of snowmaking as a technical adaptation". In: *Climate Research* 23.2, pp. 171–181.

Scott, D., McBoyle, G., and Minogue, A. (2007). "Climate change and Quebec's ski industry". In: *Global Environmental Change* 17.2, pp. 181–190.

Scott, D., McBoyle, G., Minogue, A., and Mills, B. (2006). "Climate change and the sustainability of ski-based tourism in eastern North America: A reassessment". In: *Journal of Sustainable Tourism* 14.4, pp. 376–398.

Seiser, B., Helfricht, K., Huss, M., Fischer, A., Veulliet, E., Schönlaub, H., Kuhn, M., and Strasser, U. (2012). "MUSICALS - (MUltiscale Snow/ICemelt Discharge Simulation into ALpine ReservoirS): Validation of a method to estimate ice volume and ice thickness distribution in the Ötztal Alps, Tyrol, Austria". In: *Geophysical Research Abstracts*.

Sevruk, B. (1983). "Correction of Measured Precipitation in the Alps Using the Water Equivalent of New Snow". In: *Nordic Hydrology* 14.2, pp. 49–58.

— (1986). "Correction of precipitation measurements: Swiss experience". In: *Precipitation Measurement*. Ed. by B. Sevruk. Zurich: Swiss Federal Institute of Technology, pp. 187–196.

Shea, J. M., Menounos, B., Moore, R. D., and Tennant, C. (2013). "An approach to derive regional snow lines and glacier mass change from MODIS imagery, western North America". In: *The Cryosphere* 7.2, pp. 667–680. DOI: 10.5194/tc-7-667-2013.

Shrestha, M., Wang, L., Koike, T., Xue, Y., and Hirabayashi, Y. (2010). "Improving the snow physics of WEB-DHM and its point evaluation at the SnowMIP sites". In: *Hydrology and Earth System Sciences* 14.12, pp. 2577–2594. DOI: 10.5194/hess-14-2577-2010.

Sivapalan, M., Savenije, H. H. G., and Blöschl, G. (2012). "Socio-hydrology: A new science of people and water". In: *Hydrological Processes* 26.8, pp. 1270–1276. DOI: 10.1002/hyp.8426.

Skamarock, W. C. and Klemp, J. B. (2008). "A time-split nonhydrostatic atmospheric model for weather research and forecasting applications". In: *Journal of Computational Physics* 227.7, pp. 3465–3485. DOI: 10.1016/j.jcp.2007.01.037.

Smiatek, G., Kunstmann, H., and Senatore, A. (2016). "EURO-CORDEX regional climate model analysis for the Greater Alpine Region: Performance and expected future change". In: *Journal of Geophysical Research: Atmospheres* 121.13, pp. 7710–7728. DOI: 10.1002/2015JD024727.

Smit, B. and Wandel, J. (2006). "Adaptation, adaptive capacity and vulnerability". In: *Global Environmental Change* 16.3, pp. 282–292. DOI: 10.1016/j.gloenvcha.2006.03.008.

Sold, L., Huss, M., Hoelzle, M., Andereggen, H., Joerg, P. C., and Zemp, M. (2013). "Methodological approaches to infer end-of-winter snow distribution on alpine glaciers". In: *Journal of Glaciology* 59.218, pp. 1047–1059. DOI: 10.3189/2013JoG13J015.

Sonntag, D. (1990). "Important new values of the physical constants of 1986, vapour pressure formulations based on the ITS-90, and psychrometer formulae". In: *Zeitschrift für Meteorologie* 70, pp. 340–344.

Stahl, K., Moore, R. D., Shea, J. M., Hutchinson, D., and Cannon, A. J. (2008). "Coupled modelling of glacier and streamflow response to future climate scenarios". In: *Water Resources Research* 44.2. DOI: 10.1029/2007WR005956.

Steger, C., Kotlarski, S., Jonas, T., and Schär, C. (2012). "Alpine snow cover in a changing climate: a regional climate model perspective". In: *Climate Dynamics* 41.3-4, pp. 735–754. DOI: 10.1007/s00382-012-1545-3.

Steiger, R. (2010). "The impact of climate change on ski season length and snowmaking requirements in Tyrol, Austria". In: *Climate Research* 43.3, pp. 251–262. DOI: 10.3354/cr00941.

— (2011). "The impact of snow scarcity on ski tourism: an analysis of the record warm season 2006/2007 in Tyrol (Austria)". In: *Tourism Review* 66.3, pp. 4–13. DOI: 10.1108/16605371111175285.

Steiger, R. and Mayer, M. (2008). "Snowmaking and Climate Change". In: *Mountain Research and Development* 28.3, pp. 292–298.

Steiger, R. et al. (2012). "CC-Snow: ein multidiziplinäres Projekt zu den Einflüssen des Klimawandels auf Wintertourismus in Tirol und der Steiermark". In: *Tourismus 2020+ interdisziplinär*. Ed. by A. Zehrer and A. Grabmüller. Berlin: ESV Verlag, pp. 243–256.

Stewart, I. T. (2009). "Changes in snowpack and snowmelt runoff for key mountain regions". In: *Hydrological Processes* 23.1, pp. 78–94. DOI: 10.1002/hyp.7128.

Stokols, D., Hall, K. L., and Vogel, A. L. (2013). "Transdisciplinary Public Health: Definitions, Core Characteristics, and Strategies for Success". In: *Transdisciplinary Public Health: Research, Methods, and Practice*, pp. 3–30.

Strasser, U. (1998). *Regionalisierung des Wasserhaushalts mit einem SVAT-Modell am Beispiel des Weser-Einzugsgebietes*. Münchner Geographische Abhandlungen.

— (2004). "Spatial and temporal variability of meteorological variables at Haut Glacier d'Arolla (Switzerland) during the ablation season 2001: Measurements and simulations". In: *Journal of Geophysical Research* 109.D3, p. D03103. DOI: 10.1029/2003JD003973.

— (2008). *Modelling of the mountain snow cover in the Berchtesgaden National Park*. Tech. rep. 55.

Berchtesgaden.

Strasser, U., Bernhardt, M., Weber, M., Liston, G. E., and Mauser, W. (2008). "Is snow sublimation important in the alpine water balance?" In: *The Cryosphere* 2, pp. 53–66. DOI: 10.5194/tc-2-53-2008.

Strasser, U., Vilsmaier, U., Prettenthaler, F., Marke, T., Steiger, R., Damm, A., Hanzer, F., Wilcke, R. A. I., and Stötter, J. (2014). "Coupled component modelling for inter- and transdisciplinary climate change impact research: Dimensions of integration and examples of interface design". In: *Environmental Modelling & Software* 60, pp. 180–187. DOI: 10.1016/j.envsoft.2014.06.014.

Strasser, U., Warscher, M., and Liston, G. E. (2011a). "Modeling Snow-Canopy Processes on an Idealized Mountain". In: *Journal of Hydrometeorology* 12.4, pp. 663–677.

Strasser, U. et al. (2011b). "Effects of climate change on future snow conditions, winter tourism and economy in Tyrol and Styria (Austria): CC-Snow, an interdisciplinary project". In: *Managing Alpine Future II*. ed. by A. Borsdorf, J. Stötter, and E. Veulliet.

Sunyer, M. A. et al. (2015). "Inter-comparison of statistical downscaling methods for projection of extreme precipitation in Europe". In: *Hydrology and Earth System Sciences* 19.4, pp. 1827–1847. DOI: 10.5194/hess-19-1827-2015.

Tecklenburg, C., Francke, T., Kormann, C., and Bronstert, A. (2012). "Modeling of water balance response to an extreme future scenario in the Ötztal catchment, Austria". In: *Advances in Geosciences* 32, pp. 63–68. DOI: 10.5194/adgeo-32-63-2012.

Teich, M., Lardelli, C., Bebi, P., Gallati, D., Kytzia, S., Pohl, M., Pütz, M., and Rixen, C. (2007). *Klimawandel und Wintertourismus: Ökonomische und ökologische Auswirkungen von technischer Beschneiung*. Eidg. Forschungsanstalt für Wald, Schnee und Landschaft WSL. Birmensdorf.

Teutschbein, C. and Seibert, J. (2013). "Is bias correction of regional climate model (RCM) simulations possible for non-stationary conditions?" In: *Hydrology and Earth System ...*

Teutschbein, C. and Seibert, J. (2012). "Bias correction of regional climate model simulations for hydrological climate-change impact studies: Review and evaluation of different methods". In: *Journal of Hydrology* 456-457, pp. 12–29. DOI: 10.1016/j.jhydrol.2012.05.052.

Themeßl, M. J., Gobiet, A., and Heinrich, G. (2012). "Empirical-statistical downscaling and error correction of regional climate models and its impact on the climate change signal". In: *Climatic Change* 112.2, pp. 449–468. DOI: 10.1007/s10584-011-0224-4.

Themeßl, M. J., Gobiet, A., and Leuprecht, A. (2011). "Empirical-statistical downscaling and error correction of daily precipitation from regional climate models". In: *International Journal of Climatology* 31.10, pp. 1530–1544. DOI: 10.1002/joc.2168.

Thrasher, B., Maurer, E. P., McKellar, C., and Duffy, P. B. (2012). "Technical Note: Bias correcting climate model simulated daily temperature extremes with quantile mapping". In: *Hydrology and Earth System Sciences* 16.9, pp. 3309–3314. DOI: 10.5194/hess-16-3309-2012.

Varhola, A., Coops, N. C., Weiler, M., and Moore, R. D. (2010). "Forest canopy effects on snow accumulation and ablation: An integrative review of empirical results". In: *Journal of Hydrology* 392.3-4, pp. 219–233. DOI: 10.1016/j.jhydrol.2010.08.009.

Vasbinder, J. W. et al. (2010a). "Transdisciplinary EU science institute needs funds urgently". In: *Nature* 463.7283, pp. 876–876. DOI: 10.1038/463876a.

— (2010b). "Transdisciplinary EU science institute needs funds urgently". In: *Nature* 463.7283, pp. 876–876. DOI: 10.1038/463876a.

Vionnet, V., Brun, E., Morin, S., Boone, A., Faroux, S., Moigne, P. L., Martin, E., and Willemet, J. M. (2012). "The detailed snowpack scheme Crocus and its implementation in SURFEX v7.2". In: *Geoscientific Model Development* 5.3, pp. 773–791. DOI: 10.5194/gmd-5-773-2012.

Vionnet, V., Martin, E., Masson, V., Guyomarc'h, G., Naaim-Bouvet, F., Prokop, A., Durand, Y., and Lac, C. (2013). "Simulation of wind-induced snow transport in alpine terrain using a fully coupled snowpack/atmosphere model". In: *The Cryosphere* 7.3, pp. 2191–2245.

Viviroli, D., Dürr, H. H., Messerli, B., Meybeck, M., and Weingartner, R. (2007). "Mountains of the world, water towers for humanity: Typology, mapping, and global significance". In: *Water Resources Research* 43.7, pp. 14, 827. DOI: 10.1029/2006WR005653.

Viviroli, D., Weingartner, R., and Messerli, B. (2003). "Assessing the Hydrological Significance of the World's Mountains". In: *Mountain Research and Development* 23.1, pp. 32–40. DOI: 10.1659/0276-4741(2003)023[0032:ATHSOT]2.0.CO;2.

Viviroli, D. et al. (2011). "Climate change and mountain water resources: overview and recommendations for research, management and policy". In: *Hydrology and Earth System Sciences* 15.2, pp. 471–504. DOI: 10.5194/hess-15-471-2011.

Volosciuk, C., Maraun, D., Vrac, M., and Widmann, M. (2017). "A combined statistical bias correction and stochastic downscaling method for precipitation". In: *Hydrology and Earth System Sciences* 21.3, pp. 1693–1719. DOI: 10.5194/hess-21-1693-2017.

Vos, M. G. de, Janssen, P. H. M., Kok, M. T. J., Frantzi, S., Dellas, E., Pattberg, P., Petersen, A. C., and Biermann, F. (2013). "Formalizing knowledge on international environmental regimes: A first step towards integrating political science in integrated assessments of global environmental change". In: *Environmental Modelling & Software* 44, pp. 101–112. DOI: 10.1016/j.envsoft.2012.08.004.

Waichler, S. R. and Wigmosta, M. S. (2003). "Development of Hourly Meteorological Values From Daily Data and Significance to Hydrological Modeling at H. J. Andrews Experimental Forest". In: *Journal of Hydrometeorology* 4.2, pp. 251–263. DOI: 10.1175/1525-7541(2003)4<251:DOHMVF>2.0.CO;2.

Walter, M. T., Brooks, E. S., McCool, D. K., King, L. G., Molnau, M., and Boll, J. (2005). "Process-based snowmelt modeling: does it require more input data than temperature-index modeling?" In: *Journal of Hydrology* 300.1-4, pp. 65–75. DOI: 10.1016/j.jhydrol.2004.05.002.

Warscher, M., Strasser, U., Kraller, G., Marke, T., Franz, H., and Kunstmann, H. (2013). "Performance of complex snow cover descriptions in a distributed hydrological model system: A case study for the high Alpine terrain of the Berchtesgaden Alps". In: *Water Resources Research* 49, pp. 2619–2637. DOI: 10.1002/wrcr.20219.

Weber, M. (2005). "Mikrometeorologische Prozesse bei der Ablation eines Alpengletschers". PhD thesis.

Weber, M., Braun, L., Mauser, W., and Prasch, M. (2010). "Contribution of rain, snow-and

icemelt in the Upper Danube discharge today and in the future". In: *Geogr Fis Dinam Quat*.

Wehren, B., Schädler, B., and Weingartner, R. (2010a). "Human Interventions". In: *Alpine Waters*. Ed. by U. Bundi. Berlin/Heidelberg: Springer, pp. 71–92. ISBN: 978-3-540-88274-9.

Wehren, B., Weingartner, R., Schädler, B., and Viviroli, D. (2010b). "General Characteristics of Alpine Waters". In: *Alpine Waters*. Ed. by U. Bundi. Berlin/Heidelberg: Springer. ISBN: 978-3-540-88274-9.

Wijngaard, R. R., Helfricht, K., Schneeberger, K., Huttenlau, M., Schneider, K., and Bierkens, M. F. P. (2016). "Hydrological response of the Ötztal glacierized catchments to climate change". In: *Nordic Hydrology* 47.5, pp. 979–995. DOI: 10.2166/nh.2015.093.

Wilcke, R. A. I., Mendlik, T., and Gobiet, A. (2013). "Multi-variable error correction of regional climate models". In: *Climatic Change* 120.4, pp. 871–887. DOI: 10.1007/s10584-013-0845-x.

Winstral, A., Elder, K., and Davis, R. E. (2002). "Spatial Snow Modeling of Wind-Redistributed Snow Using Terrain-Based Parameters". In: *Journal of Hydrometeorology* 3.5, pp. 524–538. DOI: 10.1175/1525-7541(2002)003<0524:SSMOWR>2.0.CO;2.

WKO (2016). "FACTSHEET – Technische Beschneiung in Österreich". In:

Xie, H., Wang, X., and Liang, T. (2009). "Development and assessment of combined Terra and Aqua snow cover products in Colorado Plateau, USA and northern Xinjiang, China". In: *Journal of Applied Remote Sensing* 3.1, 14pp. DOI: 10.1117/1.3265996.

Yokoyama, R., Shirasawa, M., and Pike, R. J. (2002). "Visualizing topography by openness: a new application of image processing to digital elevation models". In: *Photogrammetric engineering and remote sensing* 68.3, pp. 257–266.

Zappa, M. (2008). "Objective quantitative spatial verification of distributed snow cover simulations—an experiment for the whole of Switzerland". In: *Hydrological Sciences Journal* 53.1, pp. 179–191. DOI: 10.1623/hysj.53.1.179.

Zekollari, H., Fürst, J. J., and Huybrechts, P. (2014). "Modelling the evolution of Vadret da Morteratsch, Switzerland, since the Little Ice Age and into the future". In: *Journal of Glaciology* 60.224, pp. 1155–1168. DOI: 10.3189/2014JoG14J053.

Zhang, W. and Montgomery, D. R. (1994). "Digital Elevation Model Grid Size, Landscape Representation, and Hydrologic Simulations". In: *Water Resources Research* 30.4, pp. 1019–1028. DOI: 10.1029/93WR03553.